# Faces of Gravity: From Classical Cosmology to Quantum Black Holes

**Nico Wintergerst**


München 2014

# Faces of Gravity: From Classical Cosmology to Quantum Black Holes

**Nico Wintergerst**

Dissertation
an der Fakultät für Physik
der Ludwig–Maximilians–Universität
München

vorgelegt von
Nico Wintergerst
aus Göttingen

München, den 19. August 2014

Erstgutachter: Prof. Dr. Georgi Dvali
Zweitgutachter: Prof. Dr. Stefan Hofmann
Tag der mündlichen Prüfung: 10. September 2014

# Contents

**Zusammenfassung** **ix**

**Abstract** **xiii**

**1 Introduction** **1**
1.1 A golden decade for cosmology and high energy physics? . . . 1
1.1.1 This thesis . . . 2
1.2 Gravity, cosmology and phases of accelerated expansion . . . 3
1.2.1 Twenty-one lines of classical gravity . . . 3
1.2.2 Twenty-five lines of quantum gravity . . . 4
1.2.3 A few more lines of cosmology . . . 5
1.2.4 Early accelerated expansion – inflation . . . 6
1.2.5 Late accelerated expansion – dynamical dark energy or a cosmological constant? . . . 11
1.2.6 The formation of large scale structure . . . 15
1.2.7 Modification of gravity . . . 16
1.3 Black Holes and UV completion . . . 18
1.3.1 The no–hair theorem . . . 20
1.3.2 Black hole entropy . . . 20
1.3.3 Hawking evaporation . . . 21
1.3.4 The information paradox . . . 23
1.3.5 Information release and scrambling . . . 25
1.3.6 UV completion in gravity . . . 28
1.3.7 A microscopic model for black holes . . . 32
1.3.8 Non-Wilsonian vs. Wilsonian UV completion in scalar theories - classicalization . . . 35
1.4 Outline . . . 36
1.4.1 Conventions . . . 38

**I Cosmology** **39**

**2 New Higgs Inflation and Planck and BICEP2 data** **41**
2.1 The Higgs boson as the Inflaton . . . . . 41
2.2 Fitting Planck and BICEP2 data with New Higgs Inflation . . 44
2.2.1 Relaxing the tension between Planck and BICEP2 . . . 48
2.3 Unitarity issues: inflationary scale . . . . . 50
2.3.1 The gauge bosons . . . . . 52
2.4 Unitarity issues: post-inflation . . . . . 54
2.5 Summary . . . . . 57

**3 Spherical Collapse and Coupled Dark Energy** **59**
3.1 Introduction . . . . . 59
3.2 Spherical Collapse . . . . . 62
3.2.1 Applications to standard cosmologies . . . . . 63
3.3 Coupled quintessence cosmologies . . . . . 66
3.4 Standard spherical collapse and CQ . . . . . 70
3.4.1 Comparison with relativistic equations . . . . . 71
3.4.2 Lack of the fifth force in spherical collapse . . . . . 73
3.4.3 Inhomogeneity of the scalar field . . . . . 74
3.5 Hydrodynamical spherical collapse . . . . . 75
3.5.1 Methods and initial conditions . . . . . 79
3.5.2 Results . . . . . 80
3.6 Growing neutrinos . . . . . 82
3.6.1 Cosmological model . . . . . 82
3.6.2 Spherical collapse and growing neutrinos . . . . . 84
3.7 Early dark energy . . . . . 86
3.7.1 Cosmological model . . . . . 86
3.7.2 Spherical collapse and EDE . . . . . 87
3.8 Summary . . . . . 88

**4 Massive Spin-2 Theories** **91**
4.1 Introduction . . . . . 91
4.1.1 Helicity decomposition . . . . . 92
4.1.2 The coupling to matter . . . . . 94
4.1.3 The problem of ghost instabilities . . . . . 95
4.2 Massive spin-2 without self-interactions . . . . . 98
4.3 Self-interacting theories . . . . . 101
4.3.1 Boulware-Deser ghost . . . . . 101
4.3.2 Cubic interactions for a massive spin-2 particle . . . . . 103
4.3.3 Resummed theories . . . . . 104

4.4 Summary . . . . . 107

**II Black Holes 109**

**5 Black holes as Bose Condensates of Gravitons 111**
5.1 The black hole quantum portrait . . . . . 111
5.1.1 Quantum corrections . . . . . 115
5.1.2 Hawking evaporation . . . . . 116
5.2 Bose Einstein condensates . . . . . 117
5.2.1 From the BBGKY-hierarchy to Gross-Pitaevskii . . . . 118
5.2.2 Quantum phase transitions and bifurcations . . . . . 119

**6 Quantumness on Macroscopic Scales 121**
6.1 Introduction . . . . . 121
6.2 The 1+1-dimensional Bose gas . . . . . 122
6.2.1 Mean field analysis . . . . . 122
6.2.2 Bogoliubov approximation . . . . . 124
6.2.3 Numerical diagonalization . . . . . 126
6.3 Quantum phase transition in the 1D-Bose gas . . . . . 127
6.3.1 One-particle entanglement . . . . . 128
6.3.2 Ground State Fidelity . . . . . 128
6.4 Fluctuation entanglement . . . . . 130
6.4.1 Calculation in the Bogoliubov approximation . . . . . 131
6.4.2 Homogenous phase . . . . . 131
6.4.3 Solitonic phase . . . . . 132
6.4.4 Numerical treatment . . . . . 132
6.5 Summary . . . . . 134

**7 Scrambling in the Black Hole Portrait 137**
7.1 Introduction . . . . . 137
7.2 Scrambling and quantum break time . . . . . 138
7.2.1 Logarithmic quantum break time . . . . . 139
7.2.2 Chaos and thermalization . . . . . 139
7.3 Quantum break time in BE condensates . . . . . 140
7.3.1 Prototype models . . . . . 140
7.3.2 Quantum breaking in Bose condensates . . . . . 141
7.4 Scrambling and quantumness in BE condensates . . . . . 144
7.5 Numerical Analysis . . . . . 144
7.5.1 Quantum break time of one dimensional condensates . 144
7.5.2 3D condensates and connection with black hole . . . . 148

7.6 Summary and Outlook . . . . . 149

**8 Collapse and Evaporation of a Relativistic Scalar Field 151**
8.1 From gravity to prototype . . . . . 151
8.2 Schwinger-Keldysh formalism . . . . . 153
8.3 Effective action . . . . . 156
8.4 Variational approach . . . . . 158
8.4.1 Equations of motion . . . . . 159
8.4.2 Slow collapse . . . . . 160
8.5 Evaporation . . . . . 161
8.6 Solutions . . . . . 162
8.6.1 Stability . . . . . 163
8.7 Summary . . . . . 164

**9 RG Flows in Scalar O(N) Models with Shift Symmetry 167**
9.1 Introduction . . . . . 167
9.1.1 The physics of the RG scale . . . . . 170
9.2 Scalar O(N) model with shift symmetry . . . . . 172
9.3 Flow equation . . . . . 173
9.4 Taylor expansion . . . . . 176
9.5 A differential equation for a fixed point action . . . . . 179
9.6 Summary . . . . . 181

**10 Conclusions and Outlook 183**

**A Quantum Equivalence of Jordan and Einstein frame 187**
A.1 Scalar field theory . . . . . 187
A.2 Gravity . . . . . 189

**Acknowledgements 221**

# Zusammenfassung

In dieser Dissertation untersuchen wir eine Vielzahl von Themen aus dem Bereich der Kosmologie und der Gravitation. Insbesondere behandeln wir Fragestellungen aus der Inflationstheorie, der Strukturbildung im neuzeitlichen Universum und massiver Gravitation, sowie Quantenaspekte schwarzer Löcher und Eigenschaften bestimmter skalare Theorien bei sehr hohen Energien.

Im sogenannten "New Higgs Inflation"-Modell spielt das Higgs-Boson die Rolle des Inflaton-Felds. Das Modell ist kompatibel mit Messungen der Higgs-Masse, weil das Higgs-Boson nichtminimal an den Einstein-Tensor gekoppelt wird. Wir untersuchen das Modell in Hinblick auf die kürzlich veröffentlichten Resultate der BICEP2- und Planck-Experimente und finden eine hervorragende Übereinstimmung mit den gemessenen Daten. Desweiteren zeigen wir auf, dass die scheinbaren Widersprüche zwischen Planck- und BICEP2-Daten dank eines negativ laufenden Spektralindex verschwinden. Wir untersuchen außerdem die Unitaritätseigenschaften der Theorie und befinden, dass es während der gesamten Entwicklung des Universums nicht zu Unitaritätsverletzung kommt. Während der Dauer der inflationären Phase sind Kopplungen in den Higgs-Higgs und Higgs-Graviton-Sektoren durch eine großen feldabhängige Skala unterdrückt. Die W- und Z-Bosonen hingegen entkoppeln aufgrund ihrer sehr großen Masse. Wir zeigen eine Möglichkeit auf, die es erlaubt die Eichbosonen als Teil der Niederenergietheorie zu behalten. Dies wird erreicht durch eine gravitationsabhängige nichtminimale Kopplung des Higgs-Felds an die Eichbosonen.

Im nächsten Abschnitt konzentrieren wir uns auf das neuzeitliche Universum. Wir untersuchen den sogenannten sphärischen Kollaps in Modellen gekoppelter dunkler Energie. Insbesondere leiten wir eine Formulierung des sphärischen Kollaps her, die auf den nichtlinearen Navier-Stokes-Gleichungen basiert. Im Gegensatz zu bekannten Beispielen aus der Literatur fließen alle wichtigen Fifth-Force Effekte in die Entwicklung ein. Wir zeigen, dass unsere Methode einfachen Einblick in viele Subtilitäten erlaubt, die auftreten wenn die dunkle Energie als inhomogen angenommen wird.

Es folgt eine Einleitung in die Theorien von massiven Spin-2 Teilchen. Hier erklären wir die Schwierigkeiten der Formulierung einer nichtlinearen, wechselwirkenden Theorie. Wir betrachten das bekannte Problem des Boulware-Deser-Geists und zeigen zwei Wege auf, dieses No-Go-Theorem zu vermeiden. Insbesondere konstruieren wir die eindeutige Theorie eines wechselwirkenden massiven Spin-2 Teilchens, die auf kubischer Ordnung trunkiert werden kann, ohne dass sie zu Geist-Instabilitäten führt.

Der zweite Teil dieser Arbeit widmet sich bekannten Problemen der Physik schwarzer Löcher. Hier liegt unser Fokus auf der Idee, das schwarze Löcher als Bose-Kondensate von Gravitonen aufgefasst werden können. Abweichungen von semiklassischem Verhalten sind Resultat von starken Quanteneffekten die aufgrund einer kollektiven starken Kopplung auftreten. Diese starke Kopplung führt in bekannten Systemen zu einem Quantenphasenübergang oder einer Bifurkation. Die quantenmechanischen Effekte könnten der Schlüssel zur Auflösung lang existierender Probleme in der Physik schwarzer Löcher sein. Dies umschließt zum Beispiel das Informationsparadox und das "No-Hair"-Theorem. Außerdem könnten sie wertvolle Einblicke in die Vermutung liefern, dass schwarze Löcher die Systeme sind, die Informationen am schnellsten verschlüsseln.

Als Modell für ein schwarzes Loch studieren wir ein System von ultrakalten Bosonen auf einem Ring. Dieses System ist bekannt als eines, dass einen Quantenkritischen Punkt besitzt. Wir demonstrieren, dass am kritischen Punkt Quanteneffekte sogar für sehr große Besetzungszahlen wichtig sein können. Hierzu definieren wir die Fluktuationsverschränkung, die angibt, wie sehr verschiedene Impulsmoden miteinander verschränkt sind. Die Fluktuationsverschränkung ist maximal am kritischen Punkt und ist dominiert von sehr langwelligen Fluktuationen. Wir finden daher Resultate die unabhängig von der Physik im ultravioletten sind.

Im weiteren Verlauf besprechen wir die Informationsverarbeitung von schwarzen Löchern. Insbesondere das Zusammenspiel von Quantenkritikalität und Instabilität kann für ein sehr schnelles Wachstum von Ein-Teilchen-Verschränkung sorgen. Dementsprechend zeigen wir, dass die sogenannte "Quantum Break Time", welche angibt wie schnell sich die exakte Zeitentwicklung von der semiklassischen entfernt, wie $\log N$ wächst. Hier beschreibt $N$ die Anzahl der Konstituenten. Im Falle eines Gravitonkondensats gibt $N$ ein Maß für die Entropie des schwarzen Lochs an. Dementsprechend interpretieren wir unsere Erkenntnisse als einen starken Hinweis, dass das Verschlüsseln von Informationen in schwarzen Löchern denselben Ursprung haben könnte.

Das Verdampfen von schwarzen Löchern beruht in unserem Bild auf zwei Effekten. Kohärente Anregungen der tachyonischen radialen Mode führen

zum Kollaps des Kondensats, während sich die inkohärente Streuung von Gravitonen für die Hawking-Strahlung verantwortlich zeigt. Hierfür konstruieren wir einen Prototyp, der einen bosonischen Freiheitsgrades mit impulsabhängigen Wechselwirkungen beschreibt. Im Schwinger-Keldysh-Formalismus untersuchen wir die Echtzeit-Evolution des Kondensats und zeigen, dass der Kollaps und die damit einhergehende Evaporation auf selbst-ähnliche Weise verläuft. In diesem Fall ist das Kondensat während des gesamten Kollapses an einem kritischen Punkt. Desweiteren zeigen wir Lösungen, die an einem instabilen Punkt leben, und daher schnelle Verschränkung erzeugen könnten.

Der finale Teil der Arbeit befasst sich mit Renormierungsgruppenflüssen in skalaren Theorien mit impulsabhängigen Wechselwirkungen. Wer leiten die Flussgleichung für eine Theorie, die nur eine Funktion des kinetischen Terms enthält her. Hier zeigen wir die Existenz von Fixpunkten in einer Taylor-Entwicklung der Funktion auf. Wir diskutieren, inwiefern unsere Analyse für Einblick in allgemeinere Theorien mit Ableitungswechselwirkungen sorgen kann. Dies beinhaltet zum Beispiel Gravitation.

# Abstract

This thesis covers various aspects of cosmology and gravity. In particular, we focus on issues in inflation, structure formation, massive gravity, black hole physics, and ultraviolet completion in certain scalar theories.

We commence by considering the model of New Higgs Inflation, where the Higgs boson is kinetically non-minimally coupled to the Einstein tensor. We address the recent results of BICEP2 and Planck and demonstrate that the model is in perfect agreement with the data. We further show how the apparent tension between the Planck and BICEP2 data can be relieved by considering a negative running of the spectral index. We visit the issue of unitarity violation in the model and argue that it is unitary throughout the evolution of the Universe. During inflation, couplings in the Higgs-Higgs and Higgs-graviton sector are suppressed by a large field dependent cutoff, while the W and Z gauge bosons acquire a very large mass and decouple. We point out how one can avoid this decoupling through a gravity dependent nonminimal coupling of the gauge bosons to the Higgs.

We then focus on more recent cosmology and consider the spherical collapse model in coupled dark energy models. We derive a formulation of the spherical collapse that is based on the nonlinear hydrodynamical Navier-Stokes equations. Contrary to previous results in the literature, it takes all fifth forces into account properly. Our method can also be used to gain insight on subtleties that arise when inhomogeneities of the scalar field are considered. We apply our approach to various models of dark energy. This includes models with couplings to cold dark matter and neutrinos, as well as uncoupled models. In particular, we check past results for early dark energy parametrizations.

Next, we give an introduction to massive spin-two theories and the problem of their non-linear completion. We review the Boulware-Deser ghost problem and point out the two ways to circumvent classic no-go theorems. In particular, we construct the unique theory of a massive spin-two particle that does not suffer from ghost instabilities when truncated at the cubic order.

The second part of this dissertation is dedicated to problems in black hole physics. In particular, we focus on the proposal that black holes can be understood as quantum bound states of soft gravitons. Deviations from semiclassicality are due to strong quantum effects that arise because of a collective strong coupling, equivalent to a quantum phase transition or bifurcation. These deviations may hold the key to the resolution of long standing problems in black hole physics, such as the information paradox and the no hair theorem. They could also provide insights into the conjecture that black holes are the fastest information scramblers in nature.

As a toy model for black holes, we study a model of ultracold bosons in one spatial dimension which is known to undergo a quantum phase transition. We demonstrate that at the critical point, quantum effects are important even for a macroscopic number of particles. To this end, we propose the notion of fluctuation entanglement, which measures the entanglement between different momentum modes. We observe the entanglement to be maximal at the critical point, and show that it is dominated by long wavelength modes. It is thus independent of ultraviolet physics.

Further, we address the question of information processing in black holes. We point out that the combination of quantum criticality and instability can provide for fast growth of one-particle entanglement. In particular, we show that the quantum break time in a simple Bose-Einstein prototype scales like $\log N$, where $N$ is the number of constituents. By noting that in the case of graviton condensates, $N$ provides a measure for the black hole entropy, we take our result as as a strong hint that scrambling in black holes may originate in the same physics.

In our picture, the evaporation of the black hole is due to two intertwined effects. Coherent excitation of the tachyonic breathing mode collapses the condensate, while incoherent scattering of gravitons leads to Hawking radiation. To explore this, we construct a toy model of a single bosonic degree of freedom with derivative self-interactions. In the Schwinger-Keldysh formalism, we consider the real-time evolution and show that evaporation and collapse occur in a self-similar manner. The condensate is at a critical point throughout the collapse. Moreover, we discover solutions that are stuck at an unstable point and may thus exhibit fast generation of entanglement.

The final chapter of this thesis is dedicated to renormalization group (RG) flows in scalar theories with derivative couplings. We derive the exact flow equation for a theory that depends on a function of only the kinetic term. We demonstrate the existence of fixed points in a Taylor series expansion of the Lagrangian and discuss how our studies can provide insight into RG flows in more general theories with derivative couplings, for example gravity.

# Chapter 1

# Introduction

## 1.1 A golden decade for cosmology and high energy physics?

The past fifteen years have seen numerous groundbreaking discoveries in cosmology and high energy physics. Three of the last eight Nobel Prizes in physics have been awarded for discoveries directly related to recent experiments. The Large Hadron Collider in Geneva has tested the Standard Model (SM) of particle physics with unprecedented precision; the almost certain discovery of the Higgs boson to date being its most prominent achievement [Chatrchyan et al., 2012, Aad et al., 2012]. At the same time, satellite missions such as Planck [Ade et al., 2013] and WMAP [Komatsu et al., 2011] have mapped the Cosmic Microwave Background (CMB) to extraordinary detail, providing striking evidence for the cosmological standard model, supplemented with a cosmological constant that can explain the late time acceleration of the Universe' expansion that has been discovered roughly fifteen years ago [Riess et al., 1998, Perlmutter et al., 1999].

Just very recently the BICEP2 team have announced the first discovery of quantum gravity [Ade et al., 2014b], albeit indirectly through evidence for primordial gravitational waves in measurements of the polarization of B-modes in the CMB.

In particular the LHC and the Planck mission have raised interest also through the lack of novel discoveries. No hint at physics beyond the Standard Model has been discovered so far. In the CMB mapped by Planck, there are no signs for non-Gaussianities or isocurvature perturbations.

It is the combination of the discoveries and null results that raises a series of important and puzzling theoretical questions.

The accordance of the cosmological constant with experimental data is

striking; the corresponding value, however, may be called a quantum field theorist's nightmare. Deviating from its "technically natural" ['t Hooft, 1980] value by some 120 orders of magnitude, it presents an example of extreme finetuning; in fact, already corrections from the electron yield a discrepancy of 36 orders of magnitude. A finetuning at the level of "only" 17 orders of magnitude is required by the measured value of the Higgs mass; in particular the absence of signatures of supersymmetry or signs of strong gravity at the LHC to date appears to disfavor appealing solutions for the latter. Here, it will be exciting to see new results once the LHC is back running at its design energies [CERN, 2014].

The BICEP2 results signal a very high scale of inflation, of the order of the grand unified scale of $10^{16}$ GeV. Moreover, a detection of primordial gravitational waves indicates inflaton excursions that exceed the Planck scale – a serious issue in an effective field theory of gravity. The ultimate judgment on this fact is crucially dependent on a better understanding of gravity in the deep ultraviolet (UV).

The understanding of gravity at the largest and smallest scales thus provides the key to almost all these problems. Let us note here that the finetuning of the cosmological constant is technically a UV issue; in absence of a satisfactory understanding of even the electroweak corrections it may however prove more promising to focus on the behavior of GR in the far infrared (IR).

Gravity in the deep UV is intrinsically tied to the quantum mechanical properties of black holes. Their formation in high energy scatterings can serve to limit the momentum transfer in gravitational processes and thereby unitarize amplitudes [Dvali and Gomez, 2010]. Any attempt to UV complete gravity has to address the formation of black holes. Ultimately, a better understanding of the black hole quantum mechanics is imperative. By now, it is widely accepted that the evaporation of black holes is a unitary process; Hawking has conceded his famous bet with John Preskill already in 2004 [Hawking, 2005]. Nonetheless, no existing model for black holes can provide a satisfactory resolution to the semiclassical unitarity violation.

All this points to the persistence of the two arguably most important problems in modern high energy physics - the origin and magnitude of the cosmological constant, and the understanding of quantum gravity and its ultraviolet completion.

### 1.1.1 This thesis

Within this dissertation, we will present research in the fields of cosmology, field theory and black hole physics. The first chapter provides an introduction

into the basic concepts. Naturally, it will not be entirely self-contained. We will refer to more extensive reviews of the subjects whenever necessary.

The rest of the thesis is original work. Chapters 2 – 7 are to large extent ad verbatim reproductions of the publications [Wintergerst and Pettorino, 2010, Folkerts et al., 2011, Flassig et al., 2013, Dvali et al., 2013, Folkerts et al., 2014, Germani et al., 2014]; chapters 8 and 9 are based on work in progress and not published elsewhere yet [Floerchinger and Wintergerst, 2014, Foit et al., 2014, Wintergerst, 2014].

## 1.2 Gravity, cosmology and phases of accelerated expansion

Part I of this work is dedicated to problems in cosmology. Chapter 2 is based on a model of inflation in which the Higgs boson plays the role of the inflaton. We lay particular focus on the model's compatibility with the BICEP2 results [Ade et al., 2014a]. Chapter 3 then focuses on late time acceleration, introducing a formalism that allows for semi-analytic analysis of nonlinear structure formation in fifth-force models. Finally, in chapter 4 we focus on modifications of gravity that give a mass to the graviton. We point out potential issues and introduce a theory that is ghost free at the cubic order.

### 1.2.1 Twenty-one lines of classical gravity

The starting point of any overview over the history of the Universe from the viewpoint of modern theoretical physics should be the field equations for Einstein's theory of relativity [Einstein, 1916] - equations so fundamental to all discoveries in cosmology that they deserve the exposed spot in the beginning of any extended work that covers the subject.

$$G_{\mu\nu} \equiv R_{\mu\nu} - \frac{1}{2} R g_{\mu\nu} = 8\pi G_N T_{\mu\nu} \,, \tag{1.1}$$

where we have defined the Einstein tensor $G_{\mu\nu}$ and introduced the Ricci tensor $R_{\mu\nu}$, the Ricci scalar $R$, the metric $g_{\mu\nu}$, Newton's constant $G_N$ and the energy momentum tensor $T_{\mu\nu}$. The field equations can be derived from the Einstein Hilbert action

$$S_{EH} = \frac{1}{16\pi G_N} \int d^d x \sqrt{-g} R + \int d^d x \sqrt{-g} \mathcal{L}_m \,, \tag{1.2}$$

using the metric determinant $g = \det g_{\mu\nu}$ and the definition of the energy momentum tensor

$$T_{\mu\nu} = \frac{2}{\sqrt{-g}} \frac{\delta(\sqrt{-g}\mathcal{L}_m)}{\delta g^{\mu\nu}} \,. \tag{1.3}$$

Supplied with appropriate matter models, these equations describe the evolution of the Universe with marvelous accuracy – nevertheless there is a limit to their regime of validity. Their correctness at the smallest and the largest scales is in doubt, issues that we will both address later in this chapter. Furthermore, there have been many attempts to go beyond the simple Einstein Hilbert action and *modify gravity*. We will also recollect some of these attempts in the following.

### 1.2.2 Twenty-five lines of quantum gravity

The Einstein Hilbert action may equally well be understood as the action of a quantum theory. When expanding around a background configuration, one obtains an infinite tower of interactions of a two-tensor $h_{\mu\nu}$. On a Poincaré invariant background, it only propagates the mass zero, spin two irreducible representation of the Poincaré group - the graviton. In the low momentum limit, it is in fact the unique theory that does so [Weinberg, 1964, 1965, Deser, 1970]. This is essentially due to the little group of the massless spin-two field being $ISO(D-2)$, which includes gauge transformations. The corresponding gauge group of gravity is the group of diffeomorphisms and the structure of the action is determined completely by requiring gauge (or Lorentz) invariance. It ensures that in $D$ dimensions, only $D(D-3)/2$ degrees of freedom[1] propagate[2].

All interaction vertices in Einstein theory contain two derivatives. As a consequence, all couplings have a negative mass dimension, namely different powers of the Planck mass $M_p = (8\pi G_N)^{-1}$. Gravity as a quantum theory is nonrenormalizable. There is an infinite number of genuinely divergent diagrams and therefore an infinite number of coupling constants are required in order to renormalize the theory[3].

[1] On Minkowski, those are precisely the $D(D-3)/2$ components of the helicity two $(2, 0, ..., 0)$ irrep of the short little group $SO(D-2)$.

[2] Note that due to the gauge transformations corresponding to diffeomorphisms, time reparametrizations are part of the gauge transformations. As a consequence, the Hamiltonian in GR is zero. This, however, has a very straightforward interpretation: Gravity responds to an energetic source by creating a gravitational field (or curving spacetime). This gravitational field compensates the energy of the source; the total energy is zero.

[3] Nonetheless, gravity is curious also in this regard. Due to diffeomorphism invariance, the form of counterterms is restricted to curvature invariants. At one loop, the only term

Nevertheless, it can still be used as an effective quantum theory with the cut-off $M_p$. Loop corrections to the Einstein Hilbert action, due to the restriction of diffeomorphism invariance, can (and will) only appear in the form of higher curvature invariants and therefore additional derivatives. At scales $L \gg \ell_p$, these will only give rise to subleading corrections. Only when energies are of the order of the *strong coupling scale* $M_p$, the effective theory breaks down and loses predictivity.

### 1.2.3 A few more lines of cosmology

The next section contains an introduction into homogeneous cosmology and assumes basic background knowledge of the subject. For more details, we refer to [Mukhanov, 2005].

The physics of the Universe at earliest times is still not understood. This is partly due to the lack of data that provide an accurate picture of this time. But more so because curvatures are of order of the Planck scale. In that regime, GR can no longer be used as an effective theory; no meaningful statements can be made about the physics without establishing an ultraviolet completion of gravity.

The currently established standard model of cosmology is based on the assumptions of spatial homogeneity and isotropy. These isometries define a preferred foliation and allow the most general compatible line element to be cast in the Friedmann-Lemaitre-Robertson-Walker (FLRW) form[4]

$$ds^2 = g_{\mu\nu}dx^\mu dx^\nu = dt^2 - a^2(t)\left(\frac{dr^2}{1-kr^2} + r^2 d\Omega^2\right), \tag{1.4}$$

where $a(t)$ is the so called scale factor, $d\Omega^2$ is the spherical volume element and $k = -1,\ 0,\ 1$ is the spatial curvature. Inserting (1.4) into the Einstein equations (1.1) together with a perfect fluid ansatz[5] for the energy momen-

that is generated is the Gauss-Bonnet term $R^2 - 4R^{\mu\nu}R_{\mu\nu} + R^{\mu\nu\rho\sigma}R_{\mu\nu\rho\sigma}$, which is a surface term in 4D. GR is one-loop finite. However, its nonrenormalizable nature is revealed at the next loop order. There are speculations that one can construct a finite model of gravity by enlargening the particle content to the extent that $\mathcal{N} = 8$ supergravity is realized. Current results indicate finiteness at seven-loop order (e.g. [Green et al., 2007, Bern et al., 2009, Beisert et al., 2010, Kallosh, 2012]); nontrivial counterterms may be required at eight loop. Due to the large supersymmetry, phenomenological applicability is however limited.

[4]Note that in the following we ignore all possible modifications of gravity, as is the case in the standard model of cosmology.

[5]$T_{\mu\nu} = \mathrm{diag}(\rho, p, p, p)$

tum tensor gives rise to the Friedmann equations

$$H^2(t) = \frac{\dot{a}^2}{a^2} = \frac{8\pi G_N \rho}{3} - \frac{k}{a^2}\,, \tag{1.5a}$$

$$\frac{\ddot{a}}{a} = -\frac{4\pi G_N}{3}\left(\rho + 3p\right)\,. \tag{1.5b}$$

Here, $\rho$ and $p$ are the matter energy density and pressure, respectively. Note that we have included the cosmological constant in the matter part for notational simplicity.

For later reference, we shall at this point introduce the possible horizons in an FRW spacetime. The particle horizon denotes the largest distance that, in the past, could have been in causal contact with an observer. It is roughly given by the size of the past lightcone of an observer at initial times; its exact expression in an FRW spacetime is given in Eq. (1.6a). The event horizon, on the other hand, is the largest distance that an observer *will* ever be in causal contact with. It is given by the size of the past lightcone of the asymptotic worldline of an observer on the current time slice, and defined in Eq.(1.6b). The presence of the horizon will be important in our discussions of inflation and of structure formation. The comoving distances to the horizon are given by

$$h_p(t) = \int_{t_0}^{t} \frac{dt'}{a(t')}\,, \tag{1.6a}$$

$$h_e(t) = \int_{t}^{\infty} \frac{dt'}{a(t')}\,. \tag{1.6b}$$

Size and existence of the respective horizons of course depends on the solution under consideration.

The Friedmann equations (1.5) are supplemented by the conservation equation for the energy momentum tensor which follows from the Einstein equations by virtue of the Bianchi identities. The dependence of $\rho$ and $p$ on $a(t)$ then depends on the equation of state $\omega = p/\rho$. For example, a pressureless component generically scales like $\sim a^{-3}(t)$, while a relativistic fluid with constant $\omega = 1/3$ scales like $a^{-4}(t)$.

### 1.2.4 Early accelerated expansion – inflation

As preperation for chapter 2, this section contains a glimpse at the subject of inflation. For more details, we refer to the many excellent reviews on the subject, e.g. [Linde, 1984, Brandenberger, 1985, Olive, 1990, Mukhanov et al., 1992, Lyth and Riotto, 1999, Bassett et al., 2006]

Our history of the Universe starts with inflation, an early phase of accelerated expansion [Starobinsky, 1980, Guth, 1981, Kazanas, 1980, Sato, 1981, Mukhanov and Chibisov, 1981, Linde, 1982]. A quick inspection of (1.5b) shows that such a phase requires a dominant component with an equation of state $\omega < -1/3$. In the context of inflation, this is usually achieved with help of one or more scalar fields with at least one flat direction, dubbed inflaton. In the slow-roll inflation scenario, the energy density is dominated by the potential energy density $V(\phi)$ of the inflaton $\phi$:

$$M_p^2 H^2 \sim \rho_\phi \approx V(\phi)\,. \tag{1.7}$$

In the limit of an inflaton at rest, one obtains $\rho_\phi = -p_\phi$. Deviations from this de Sitter limit are usually measured in terms of the slow roll parameters

$$\epsilon \equiv -\frac{\dot{H}}{H^2} \approx \frac{1}{2}\left(\frac{V' M_p}{V}\right)^2\,, \tag{1.8a}$$

$$\eta \equiv -\frac{1}{2}\frac{\ddot{H}}{\dot{H}H} \approx \frac{M_p^2 V''}{V}\,, \tag{1.8b}$$

where the second equality is valid to first order in slow roll.

The success of the inflation as the current paradigm for the earliest stages can be attributed to numerous factors. It provides natural solutions to fine-tuning and coincidence problems. The first is related to the spatial curvature. Observational evidence constrains the spatial curvature to be extremely close to zero. However, from Eq.(1.5a) it is clear that curvature decreases slower than the energy density of either matter or radiation. This seems to indicate substantial fine tuning of the initial curvature. Inflation resolves this because during the phase of accelerated expansion, almost the entire energy density is stored in the inflating component whose energy density is almost constant. If inflation lasts sufficiently long, the spatial curvature can be washed out almost completely. After the end of inflation, the universe reheats [Linde, 1979, Starobinsky, 1980, Guth, 1981, Kofman et al., 1994]. Through appropriate couplings, the energy that was previously stored in a scalar field component is transferred to thermal radiation, thus the name reheating. An epoch of radiation dominance ensues, with spatial curvature being zero for all practical purposes.

The second issue is the homogeneity of the Universe on the largest of scales. A quick inspection of Eq.(1.6a) shows that the particle horizon grows monotonically with time in an expanding universe. Scales that enter our particle horizon now could not have been in causal contact before. An estimate of the particle horizon under the assumption of only matter and radiation

domination in the past yields a particle horizon $d_p \sim H^{-1}$. Homogeneity on the largest observable scales appears like a miraculous coincidences. The obvious resolution to this is that the actual particle horizon is much larger than the naive estimate[6]. This is the case if at early times $a(t)$ was much smaller than what could be inferred from matter or radiation domination. It turns out that an exponential decrease of the scale factor towards early times will do the trick[7].

There are other issues that appear to call for a phase of exponential expansion; the monopole and domain wall problem, for example. Details on this are beyond the scope of this introduction and can be found, e.g., in [Linde, 1984].

The preceding issues become void once we assume an initial epoch of exponential expansion lasted sufficiently long. It turns out that this requires a number of $e$-foldings $\mathcal{N} = \ln(a/a_i) \sim 60$.

#### 1.2.4.1 Scalar perturbations

There are other proposals that can resolve the preceding issues (albeit usually suffering from consistency issues, such as being strongly coupled or requiring to violate energy conditions). The arguably most convincing feature of inflation, however, is the generation of density perturbations [Mukhanov and Chibisov, 1981].

Within the inflationary paradigm, this is achieved through the materialization of quantum fluctuations of the inflaton $\phi$. The metric (1.4) only possesses a timelike Killing vector field if $H$ is constant; only if it is zero, this Killing vector can be global. A phase of accelerated expansion can be well approximated by a quasi-de Sitter universe. In this case, a timelike Killing vector can be chosen within a given Hubble volume. However, at scales larger than this, the Killing vector becomes null and then spacelike; there are no global timelike Killing vectors in de Sitter. This is a situation that we will discuss in more detail later, in relation to black holes.

Important here is the consequence: no matter the choice of spatial slicing, there is no notion of conserved energy. Therefore, the choice of "vacuum" state is somewhat arbitrary. Furthermore, a light scalar field ($m_\phi < H$) in de Sitter is tachyonic; the notion of a lowest energy state can only exist for subhorizon modes. In the context of inflation, the conventional choice is the *Bunch-Davies* vacuum. It corresponds to the lowest energy state of modes

[6] This estimate is sometimes referred to as the *apparent horizon*.

[7] The physical picture behind this is simple. During a phase of exponential expansion, scales may lose causal contact. In other words, during inflation, scales exit the horizon and reenter at late times.

that are contained well within the horizon. During evolution, a given mode stretches and eventually exits the horizon.

Once a mode has stretched beyond the horizon, the corresponding Hamiltonian is no longer positive definite. As a consequence, it makes little sense to view the Bunch-Davies state as an excited state of the instantaneous vacuum at those times, since the latter simply does not exist. Instead of evaluating the physical density of particles, one therefore focuses on the magnitude of quantum fluctuations. One can show that if both are calculable, they give quantitatively very similar results.

In exact de Sitter, for a massless scalar field, the spectrum of quantum fluctuations is scale invariant on superhorizon scales. One obtains

$$P(k) \sim k^3 \int d^3x \langle \phi(x)\phi(0)\rangle e^{ikx} \sim \hbar H^2 \,, \tag{1.9}$$

where we have introduced the power spectrum $P(k)$ and used the isotropy and homogeneity of the Bunch-Davies vacuum. The result (1.9) could have been guessed from the outset; the Hubble scale is the only infrared scale left in exact de Sitter and $m_\phi = 0$.

Exact de Sitter would inflate endlessly; in reality, inflationary cosmologies correspond to a quasi de Sitter phase. In that case, the power spectrum receives corrections due to differences in the Hubble parameter between the times that different modes cross the horizon. This can be quantified using the spectral index $n_s$, which we define below. The spectral index turns out to be observable, and like all observables it better be defined in a gauge invariant way. One therefore introduces the gauge invariant comoving curvature perturbation $\mathcal{R} = \psi + H\frac{\delta\phi}{\dot\phi}$, which is furthermore almost conserved on superhorizon scales. The spectral index is then defined via

$$n_s - 1 \equiv \frac{d\ln P_{\mathcal{R}}(k)}{d\ln k} \,. \tag{1.10}$$

The near-conservation of $\mathcal{R}$ demonstrates nicely that the deviations from a flat spectrum originate from the difference in Hubble scales at horizon crossing. Using the definitions (1.8a), the superhorizon power spectrum of $\mathcal{R}$ becomes in the slow roll approximation

$$P_{\mathcal{R}} \sim \hbar G_N \frac{H^2}{\epsilon} \,, \tag{1.11}$$

where all time dependent quantities are to be evaluated at horizon exit.

#### 1.2.4.2 Tensor perturbations and the Lyth bound

Not only scalar perturbations are generated during inflation, but also gravitational waves. Their origin is exactly the same, only that they are not due to the quantization, and vacuum ambiguence, of a scalar, but of metric perturbations. It turns out that they also follow a nearly scale invariant spectrum, with an amplitude given by [Starobinsky, 1979]

$$P_{\mathcal{T}} \sim \hbar G_N H^2 \,. \tag{1.12}$$

Observation of primordial gravitational waves thus presents a direct measurement of the scale of inflation. The ratio of tensor to scalar perturbation is, after restoration of numerical factors, given by

$$r \equiv \frac{P_{\mathcal{T}}}{P_{\mathcal{R}}} = 16\epsilon \,. \tag{1.13}$$

From Eq.(1.13), we can infer that a measurement of primordial gravitational waves implies for slow roll inflation an inflaton excursion that is trans-Planckian. This has come to be known as the Lyth bound [Lyth, 1997] and can be seen by considering the number of $e$-foldings

$$\mathcal{N} = \int_{t_i}^{t_f} dt H \approx -\int_{\phi_i}^{\phi_f} d\phi \frac{3H^2}{V'} \approx \text{sign}(V') \int_{\phi_i}^{\phi_f} \frac{d\phi}{M_p} \frac{1}{\sqrt{\epsilon}} \sim \frac{\Delta\phi}{M_p \sqrt{\epsilon}} \,, \tag{1.14}$$

where all approximations are to first order in the slow roll parameters. For $\mathcal{N} \sim 60$ and a measurable gravitational wave spectrum $\epsilon \gtrsim 10^{-4}$, we obtain

$$\Delta\phi \gtrsim M_p \,. \tag{1.15}$$

This can present a serious issue for inflationary model building. In usual effective field theory reasoning, trans-Planckian field excursions are beyond the realm of validity of the effective theory and are therefore not predictive. However, the issue is still not well understood. Quantum corrections to the inflaton potential $V(\phi)$ due to scalar loops are, at one loop, proportional to $V''(\phi)^2$. For sufficiently low curvature, they may therefore be suppressed even for large field values. On the other hand, the graviton contributions to the effective potential will have to be proportional to the parameter that controls the breaking of shift symmetry. It is therefore often argued that graviton loops will only induce corrections proportional to $V(\phi)$ [Linde, 1990], which may be small for sub-Planckian potentials. Note, however, that these claims cannot be made without additional assumptions on the ultraviolet completion of gravity. Only if couplings to heavy degrees of freedom are sufficiently

suppressed, one can expect the corresponding *renormalization group* flow to be sufficiently stable. In other words, one relies on an approximate shift symmetry in the ultraviolet. Without the construction of explicit models, this remains an arguable assumption.

The story could be different if gravity is self-complete and unitarizes due to black holes. This possibility will be discussed in a broader extent below. Here, we only remark that in that case the influence of the UV on the scalar potential is argued to be suppressed because the high energy contributions come from large action objects and are therefore exponentially suppressed [Dvali and Gomez, 2014].

In chapter (2), we will consider a particular model of inflation that generates a gravitational wave spectrum compatible with BICEP2, $r \gtrsim 0.11$. There, the inflaton corresponds to the Higgs boson that is non-minimally coupled to the Einstein tensor. There, we will comment further on the issue of trans-Planckian field values.

Let us end this section with a remark on the relation between the quantum fluctuations generated during inflation and the classical perturbations that we observe today. If it were not for the tachyonic nature of the inflaton fluctuations, we could simply expand the Bunch Davies vacuum in terms of number eigenstates of late time creation and annihilation operators. We would then observe the creation of a large number of particles, which we could then call a classical background. Since it does not quite work like that, we rely on *decoherence* (see e.g. [Zurek, 2003] for a review) as the catalyst for classicalization. There, one assumes that interactions lead to a time evolution in which the Bunch Davies vacuum effectively decoheres and one can rightfully speak of classical perturbations.

### 1.2.5 Late accelerated expansion – dynamical dark energy or a cosmological constant?

Chapter 3 will be concerned with the problem of non-linear structure formation in models of dark energy that include fifth-force effects. The relevant concepts will be introduced now. For comprehensive reviews, we refer for example to [Peebles and Ratra, 2003, Copeland et al., 2006].

In 2011, the Nobel Prize in physics was awarded to Saul Perlmutter, Brian P. Schmidt and Adam G. Riess "for the discovery of the accelerating expansion of the Universe through observations of distant supernovae" [Nobel Media, Web, 2011]. In 1998, they were the leaders of the two research groups [Riess et al., 1998, Perlmutter et al., 1999] that independently discovered that the luminosity distance - redshift relation inferred from the measurements of

light curves of type Ia supernovae implies late acceleration of the universe. In combination with the spatial flatness of the universe that can be inferred from measurements of the Cosmic Microwave Background, as well as the failure of dark matter to provide for the critical density of the universe, one arrives at the conclusion that about 70% of the critical density appears to be due to "dark energy".

Just as in inflation, the late time acceleration can be caused by a fluid with negative pressure $p < -1/3\rho$. The most obvious candidate is a cosmological constant[8]. The observational signatures can be reproduced with a cosmological constant $\Lambda \sim \rho_0$, where $\rho_0$ denotes the critical energy density today. This implies $\Lambda \sim 10^{-120} M_p^4$. It is this number which often leads to uneasiness. We will show why in the next section.

The earliest alternatives to a cosmological constant were the so called quint-essence models [Wetterich, 1988, Ratra and Peebles, 1988]. In this case, the negative pressure is provided by a slowly rolling scalar field. This can be an exciting possibility in case a time variation of the equation of state is detected. Furthermore, it is often argued that a rolling scalar field can alleviate some of the finetuning associated with a cosmological constant. We will comment on this in 1.2.5.2.

#### 1.2.5.1 The cosmological constant problem

The simplest candidate for a cosmological constant is vacuum energy. In free quantum field theory, vacuum energy is due to normal ordering of the Hamiltonian; once interactions are introduced one can construct vacuum bubbles with nontrivial topology which will receive contributions from contractions at different points. These vacuum-vacuum diagrams are typically quartically divergent (in 3+1d) and are therefore completely dominated by the ultraviolet. In other words, the vacuum contributions to the cosmological constant are extremely ultraviolet sensitive.

So what does that mean in practice? At first sight, these polynomial contributions appear like any other ultraviolet divergence in QFT that can be renormalized. So why not just add a counterterm (or choose a renormalization scheme that does so automatically), fix it to today's observed value and walk away happily?

The problem that is now widely known as the cosmological constant problem [Weinberg, 1989] is in the end not due to the infinities - it is the finite contributions that lead to such a finetuning problem. In order to see that, it is useful to rephrase the problem in terms of the renormalization group

[8]Note that this possibility was excluded in the case of inflation because a cosmological constant implies an asymptotically de Sitter universe.

[Wilson and Kogut, 1974, Polchinski, 1984, Wetterich, 1993a]. Being a coupling with mass dimension four, the cosmological constant term is the most *infrared relevant* operator one can construct. Let us assume now that one finds a Wilsonian UV completion of gravity. In that case, the cosmological constant would be fixed by matching at the Planck scale. Furthermore we assume a trajectory in the space of couplings that connects the given matching value with today's observed value at some lower scale $M$[9]. If we now expand the RG flow around this solution, we will find that generically the cosmological constant will depend very sensitively on the initial conditions chosen at $M_p$. Moreover, the sensitivity will be enhanced by factors $M_p/M$. As a consequence, only a slight variation of the initial conditions implies a huge deviation in the predicted value of the cosmological constant $\Lambda$. This is the cosmological constant problem, and is solely due to the fact that $\Lambda$ is a relevant operator[10]. Let us reiterate here that this problem is not only a Planck scale problem. Even operator matching at the scale of the electron mass already implies a finetuning of 36 orders of magnitude. For this reason, the cosmological constant problem cannot be solved by typical approaches to the hierarchy problem, such as supersymmetry (SUSY) or large extra dimensions. Even in the most optimistic scenarios with new physics below the TeV scale, we obtain for the ratio between the corresponding scale $\Lambda/M^4_{\text{new}} \lessapprox 10^{-60}$.

So what about theories that do not possess a Wilsonian UV completion? Frankly, we do not know. An alternative to a Wilsonian UV completion of gravity is unitarization by black holes, which we will address in more detail below. In that case, the contributions of massive states at the Planck mass, namely Planck size black holes, to the RG flow are not yet understood. It is however likely that a similar problem exists.

In absence of an explanation of the RG flow of the cosmological constant, one may attempt to modify gravity in the infrared to render the large scale solutions of GR largely insensitive to its exact value. This idea can be summarized under the name of degravitation [Dvali et al., 2007] (see e.g. [Dvali et al., 2000, de Rham et al., 2008] for attempts at particular realizations). However, so far no consistent degravitating model has been constructed.

[9] Note that this does not imply a physical running of the cosmological constant; it only measures how its value changes if more and more quantum fluctuations are taken into account. The map between renormalization group scale and physical scale strongly depends on the process, on the operator under consideration and on the vertices in the theory.

[10] This is also the underlying reason for the hierarchy problem.

#### 1.2.5.2 Fine tuning in quintessence models

The smallness of the cosmological constant troubles any model of dark energy. Without deeper knowledge of the behavior of gravity in the deep UV, and corresponding understanding of the RG flows, the vacuum energy will be fine tuned. This is also the case for quintessence models, which we consider in this section. While they cannot solve the cosmological constant problem, they are interesting dark energy candidates in case the equation of state of dark energy is found to be time dependent.

A generic quintessence model assumes a light scalar field $\phi$ with a nearly flat potential, minimally coupled to gravity. By this we include all models that can be brought into such form, e.g. $f(R)$ theories or scalar tensor theories. Hence we work exclusively in the Einstein frame[11].

By definition, quintessence models possess another relevant operator that is usually finetuned, namely the scalar mass. Just like in the discussion above, this mass will generically receive large corrections from the ultraviolet, which can spoil the flatness of the potential. Note that this problem also exists in inflation. There, however, the finetuning is (arguably) not very severe[12], since $m_{\text{inflaton}}/M_p \gtrsim 10^{-5}$. In contrast, to provide for late acceleration, one generically obtains $m_\phi/M_p \sim H_0/M_p \sim 10^{-60}$. The only way to circumvent this finetuning is by assuming a UV completion that respects certain symmetries, e.g. a shift or dilatation symmetry in the scalar sector. This way, the small mass could be protected from corrections.

In some quintessence models, there are additional fine tuning problems, related to initial conditions and/or the transition from a matter dominated to a dark energy dominated universe. These, however, are not as bad. For example, the problem of initial conditions may be solved by considering models that allow for tracking solutions, e.g. potentials of the exponential form [Wetterich, 1988, 1995]. The problem of engineering the transition can be alleviated through appropriate couplings [Wetterich, 1995, Amendola, 2000]; in particular a coupling to relic neutrinos could provide an explanation to the so-called cosmic coincidence problem [Amendola et al., 2008, Wetterich, 2007, Mota et al., 2008b, Wintergerst et al., 2010, Pettorino et al., 2010][13].

[11] We will address some issues that are related to viewing theories in the Jordan frame in Appendix A.

[12] In fact, if nature were supersymmetric, it could even be turned off completely, since the scale of inflation is higher than the supersymmetry breaking scale $M_{\text{SUSY}}$ in most models. The mass is then protected by the usual nonrenormalization theorems for the superpotential. This mechanism, however, cannot be used for quintessence, since $m_\phi \ll M_{\text{SUSY}}$ for any phenomenologically viable model. This is exactly the same as for the cosmological constant.

[13] At the quantum level, however, these couplings will a priori introduce new finetuning

Coupling a scalar field to other matter will introduce fifth forces that fall off with distance as $r^{-1}\exp(-m_\phi r)$; for light scalars these will lead to observable effects, as they influence the large scale structure formation[14].

### 1.2.6 The formation of large scale structure

After the inflationary density perturbations have materialized, they begin to evolve again once they reenter the horizon. From then on, they grow due to the attractive nature of gravity. The entire theory of linear cosmological perturbations, including all aspects of the gauge symmetries, has been studied in numerous works. For some of the earliest papers on the subject, see for example [Bardeen, 1980, Kodama and Sasaki, 1984].

What is important here is that the details of structure growth strongly depend on both the background cosmology and, of course, on the component under consideration. Depending on the behavior of the Hubble constant, fluctuations grow differently. For adiabatic perturbations of a pressureless component, e.g. cold dark matter, one can draw the following generic picture. As suggested above, fluctuations are constant as long as they are superhorizon. Subhorizon fluctuations oscillate during the radiation dominated era, and grow during matter domination. Finally, in the limiting case of de Sitter, they are frozen. One defines the growth factor

$$D_+(a) \equiv \frac{\delta(a)}{\delta_i}\,, \tag{1.16}$$

using the density contrast $\delta \equiv \delta\rho/\rho$ and the scale factor $a$. One obtains $D_+(a) \sim a$ during matter domination and $D_+(a) \to$ const for asymptotically de Sitter.

At sufficiently large scales $k^{-1} \gtrsim 100Mpc$, structures are still linear today. On these scales, one can propagate the primordial power spectrum to late times using linear perturbation theory. On smaller scales, however, the growth of structure during the matter dominated era has led to structures being nonlinear. In this case, the measured power spectrum can only be predicted through the full nonlinear evolution of the fluctuations.

issues that again call for a better understanding of ultraviolet physics.

[14]Depending on the strength of couplings, they can also spoil solar system physics. In this case, there exist attempts to save local gravity through shielding mechanisms. This includes, for example, the chameleon [Khoury and Weltman, 2004], the symmetron [Hinterbichler and Khoury, 2010], or the Vainshtein [Vainshtein, 1972, Nicolis et al., 2009] mechanisms. However, it can be quite generically proven that the unification of the screening and acceleration properties induce a strong coupling at scales of $(m_\phi^2 M_p)^{1/3} \sim (1000\text{km})^{-1}$.

Solutions to the nonlinear perturbation equations are notoriously hard to find. An easy and computationally cheap approximation to nonlinear structure formation is the so-called spherical collapse model [Peebles, 1967, Gunn and Gott, 1972]. There, nonlinear fluctuations are approximated as obeying a top-hat profile. This top-hat is then treated as a closed Friedmann universe which first expands with the background but eventually collapses. This allows to find a close estimate for the timescale from nonlinearity to cluster formation which in turn can be used to estimate cluster counts, e.g. using the Press-Schechter formalism [Press and Schechter, 1974].

The spherical collapse model relies crucially on the validity of Birkhoff's theorem [Jebsen, 1921, Birkhoff and Langer, 1923]. Already the presence of quintessence in principle leads to corrections, which however can be shown to be small [Mota and van de Bruck, 2004, Maor and Lahav, 2005, Wang, 2006]. The story is different when a fifth force is present. In that case, a traditional spherical collapse ansatz misses precisely the fifth force effects. In chapter 3), we derive an improved formulation of the spherical collapse that includes these effects.

By measuring the large scale structure at different scales and different redshifts, structure growth may be compared with predictions from different models. This way, one can ultimately decide whether, for example, the dark energy equation of state differs from $-1$, whether there is time dependence involved, or whether additional fifth forces are present.

### 1.2.7 Modification of gravity

The final chapter of our excursion into cosmology focuses on a specific class of modified gravity theories, namely massive gravity. We shall address the consistency of nonlinear theories of massive gravity and show under which circumstances the appearance of additional ghost-like degrees of freedom can be avoided. In particular we give a novel construction a model of a massive spin-two particle that can be truncated at the cubic order. For more information on the subject, see for example [de Rham, 2014, Hinterbichler, 2012]

In the literature, modified gravity theories usually include a large class of theories that can be reduced to Einstein gravity with an additional scalar field through appropriate field redefinitions, $S = S_{\rm EH} + S_{\rm add}$, where $S_{\rm add}$ contains only minimal couplings to gravity. As indicated above, we will use a slightly different definition of modified gravity. For us, a modification of gravity is a model that *cannot be brought to the form above.* In these models, one finds a genuine modification of the graviton propagator at least on some length scales. Under this definition fall for example theories with extra dimensions

(e.g. [Arkani-Hamed et al., 1998, Randall and Sundrum, 1999], in the context of late time acceleration for example [Dvali et al., 2000, 2007]) or theories of massive gravity [Fierz and Pauli, 1939]. We will now introduce the latter.

#### 1.2.7.1 Massive gravity

The question of a graviton mass dates back to 1939. In their seminal paper [Fierz and Pauli, 1939], Fierz and Pauli showed that there exists one unique extension of the linearized Einstein-Hilbert action that lends a mass to the graviton without introducing spurious degrees of freedom, the corresponding mass term being

$$\mathcal{L}_m = \frac{1}{2}m^2(h_{\mu\nu}^2 - h^2)\,, \tag{1.17}$$

where $h_{\mu\nu}$ is the symmetric tensor that describes the linearized graviton and $h \equiv \eta^{\mu\nu}h_{\mu\nu}$ its trace. The reason for the restrictiveness is simple. In $3+1$ dimensions, the little group of a massive particle is $SO(3)$; the symmetric tensor representation of the Lorentz group decomposes into the angular momentum representations $\mathbf{0} \oplus \mathbf{0} \oplus \mathbf{1} \oplus \mathbf{2}$. In order for the theory to only propagate a massive spin two particle, the spin zero and one parts have to be projected out. The unique action that does so is the Fierz-Pauli action. Note that a different form for either mass or kinetic term not only implies additional degrees of freedom, but inevitably leads to the appearance of ghost instabilities. Roughly, the reason is related to the Lorentzian signature of the metric. By allowing for the propagation of additional spins, at least one will always carry negative energy.

In terms of massless representations, the symmetric tensor splits differently. In particular, the $\mathbf{2}$ representation under $SO(3)$ splits into $\mathbf{0} \oplus \mathbf{1} \oplus \mathbf{2}$ under the short little group $SO(2)$. When taking the massless limit of the theory, the additional graviton polarizations do not generically decouple. As a consequence, predictions of any massive gravity theory in a first linear approximation differ from massless general relativity (GR) by numerical factors [van Dam and Veltman, 1970, Zakharov, 1970]. However, it has been pointed out in [Vainshtein, 1972] that this so-called van Dam-Veltman-Zakharov (vDVZ) discontinuity may disappear when correctly taking nonlinearities into account, with nonlinearities growing with decreasing graviton mass as $m^{-4}$. Later, in [Deffayet et al., 2002] this nonperturbatively continuous behavior has been demonstrated for a specific model of massive gravity.

However, non-linearities in massive gravity generically introduce a different problem: that of ghost instabilities. Crudely, self-interactions usually spoil the structure that ensures that all other Poincaré irreps are projected out. Simple addition of the Fierz-Pauli mass term to the Einstein Hilbert

action indeed leads to the propagation of an additional, ghost-like scalar degree of freedom [Boulware and Deser, 1972, Deffayet et al., 2002, Arkani-Hamed et al., 2003]. The responsible leading singularity of the graviton vertex can be cancelled by appropriately adding non-derivative interactions to the action [Arkani-Hamed et al., 2003, Creminelli et al., 2005]. However, it remained unsettled if other operators could spoil the stability of the theory. Since then, massive gravity has enjoyed a massive resurgence. In a number of papers [de Rham et al., 2011b, Hassan and Rosen, 2012b,a], it was shown that one can construct a nonlinear action that reduces to the Fierz-Pauli form on the quadratic level and propagates only five degrees of freedom. Nonetheless, it is yet to be understood whether this is enough to render the theory both consistent and phenomenologically viable. Numerous papers have discovered superluminal propagation and causality violation [Dubovsky et al., 2006, Gruzinov, 2011, Burrage et al., 2012, de Fromont et al., 2013, Deser and Waldron, 2013, Deser et al., 2013a,b], while others have discovered instabilities of certain backgrounds, for example in [Tasinato et al., 2013, De Felice et al., 2012, Kuhnel, 2013, Babichev and Fabbri, 2013], which can even be of the ghost type. Moreover, the leading interactions in the model become strong on scales $\Lambda_3 \equiv (m^2 M_p)^{1/3}$. For $m$ chosen such that the model describes Einsteinian dynamics on sub-Hubble scales, this is as low as $(1000\text{km})^{-1}$. Whether this necessarily implies the breakdown of the effective field theory on solar system scales is subject of ongoing research [Hinterbichler et al., 2010, de Rham et al., 2011a, de Paula Netto and Shapiro, 2012, Codello et al., 2013, de Rham et al., 2013a,b, Brouzakis et al., 2013].

When considering general theories of massive spin-2 fields, an Einsteinian derivative structure is not preferred. For $m = 0$ it is known that Poincaré invariance, locality and unitarity alone pin down general relativity as the unique theory with self-interactions [Weinberg, 1964, 1965, Ogievetsky and Polubarinov, 1965, Deser, 1970]. For $m \neq 0$ these arguments cannot be generalized. We build on this in chapter 4 and construct a ghost-free cubic theory of a massive spin-2 field by only requiring the self-interactions to be Lorentz-invariant and to involve at most two derivatives. A priori, all coupling parameters are arbitrary and can be adjusted model dependently.

## 1.3 Black Holes and UV completion

The second part of this thesis considers various problems in black hole physics. In particular, we collect evidence for a microscopic description of black holes in terms of a Bose condensate of gravitons. Here, we provide

a basic introduction into the physics of black holes. We review the current state of affairs and motivate why a microscopic picture for black holes is of fundamental importance for the understanding of various properties of gravity. More details on the classic results can in this case be found, for example, in [Strominger, 1994, Wald, 2001, Mathur, 2005].

Discussions of black holes date back to the times in which gravitation was still entirely Newtonian. The assumptions that light is affected by gravitation and that it propagates with a finite speed inevitably lead to the realization that one may find objects that gravitate so strongly that not even light can escape [Michell, 1784].

In the framework of General Relativity, published only a few months prior [Einstein, 1916], the first black hole solution was found by Karl Schwarzschild in 1916. The now famous Schwarzschild spacetime is a solution to Einstein's field equations (1.1) with a point source

$$T_{\mu\nu} = M\delta^{(3)}(r)g_{\mu 0}g_{\nu 0}\,. \tag{1.18}$$

Here, $G^{\mu\nu}$ is the Einstein tensor, $R^{\mu\nu}$ the Ricci tensor and $R$ and $G_N$ as above. $M$ is the mass of the source. Essentially by virtue of Gauss' law for General Relativity, we may evaluate the total mass of the configuration that corresponds to the solution of (1.18). With little surprise, this total mass is given by $M$, which will lead us to refer to $M$ as the mass of the black hole.

The solutions to Eq. (1.18) is most famously known in the Schwarzschild coordinates; arguably the most natural for an observer at spatial infinity. The line element takes on the form

$$ds^2 = g_{\mu\nu}dx^\mu dx^\nu = \left(1-\frac{r_s}{r}\right)dt^2 - \left(1-\frac{r_s}{r}\right)^{-1}dr^2 - r^2 d\Omega^2\,, \tag{1.19}$$

where we have introduced the Schwarzschild radius $r_s = 2G_N M$.

In 3+1 dimensions, the metric (1.19) possesses a total of four Killing vector fields, corresponding to three spatial rotations and translations along the $t$-direction[15]. For $r > r_s$ the Killing field $\partial_t$ is timelike. Consequently, the generator of these translations is nothing but the (conserved) Hamiltonian. The spacetime is stationary.

At $r = r_s$, the norm of the Killing field $\partial_t$ vanishes:

$$g(\partial_t, \partial_t)|_{r=r_s} = \left(1-\frac{r_s}{r}\right)|_{r=r_s} = 0\,. \tag{1.20}$$

[15]Of course, the former is a consequence of the spherically symmetric setup, while the latter is just a manifestation of Birkhoff's theorem [Jebsen, 1921, Birkhoff and Langer, 1923]

The codimension-two hypersurface $r = r_s$ is therefore a Killing horizon. It is a null surface, generated by the null vectors that are tangent to outgoing null geodesics[16].

Note that at this point, we have not been completely honest. In the Schwarz-schild coordinates, the metric (1.19) is singular at $r = r_s$ and the entire spacetime is strictly speaking not covered by the Schwarzschild patches. Instead, one should revert to maps that extend across this surface, for example Kruskal coordinates. However, all conclusions remain unaltered.

Within the Schwarzschild radius, we may again work with the metric in Schwarzschild coordinates. Within this region, the Killing vector $\partial_t$ is no longer timelike. Instead, its corresponding Noether charge is now a spatial momentum. On the other hand, time translations are generated by $\partial_r$, which does not generate an isometry. Consequently, the Hamiltonian is no longer conserved. This will have dramatic consequences, as we will soon see.

### 1.3.1 The no–hair theorem

Generalizations of the Schwarzschild metric introduce rotating and charged black holes. In fact, it has been shown that classically, the most general black hole solution can be described by a handful parameters o only, namely the mass $M$, the angular momentum $L$ and charges $Q$ corresponding to gauged symmetries, whose conservation at infinity is guaranteed either by the existence of a Gauss' law or by topology[Misner and Wheeler, 1973]. All deformations that may be decribed by other parameters correspond to excitations of the quasi-normal modes [Vishveshwara, 1970, Press, 1971] of the black hole and will thus decay in time. This observation has led many to postulate that conserved global charges cannot exist in quantum gravity. While the non-existence of global symmetries e.g. in perturbative string theory strengthens this point of view, there exists no proof that global symmetries are anomalous in any theory of quantum gravity. However, it seems likely that if quantum gravity respects the conservation of global charges, the interpretation of the horizon has to be altered, as well as the understanding of the black hole interior. We will discuss this in more detail below.

### 1.3.2 Black hole entropy

Before we enter the issues of Hawking evaporation, let us address another important black hole property that originates from the realms of classical

[16]In the extended Schwarzschild spacetime, there is another Killing horizon generated by the tangent vectors of incoming null geodesics. Furthermore, one has a *bifurcate* Killing horizon where these surfaces intersect.

physics but has proven to be a particular obstacle in any attempt of a quantum description of black holes.

The fact that black holes carry entropy follows from a simple gedanken-experiment [Bekenstein, 1972]. Any object carrying entropy that enters the black hole leads to a decrease in entropy of the outer Schwarzschild region. If one assumes that the object simply disappears into the singularity, this appears to imply a violation of the second law of thermodynamics.

Of course, this cannot be the end of the story. The foundation for the resolution of the puzzle was set in the observation, that classically, the horizon area of a black hole can never decrease [Hawking, 1973] and in this regard mimics the behavior of entropy. This, in combination with a number of thermodynamic arguments, has led Bekenstein to postulate the area law for the black hole entropy [Bekenstein, 1973]

$$S = \frac{A_{\rm BH}}{4\ell_p^2} = \frac{\pi r_s^2}{\hbar G_N}\,, \tag{1.21}$$

where we have introduced the Planck length $\ell_p = \sqrt{\hbar G_N}$ and included all factors of $\hbar$ for later convenience.

### 1.3.3 Hawking evaporation

The main physical reason for the existence of Hawking evaporation [Hawking, 1974, 1975] is the absence of a global timelike Killing vector field, as remarked above. There exist a plethora of calculations that lead to the observation that black holes emit radiation; they are all founded on the mapping of the vacuum of the distant past to that of the distant future. We will here present a rather heuristic derivation that nevertheless contains the important physical ingredients.

The spatial slices of the Schwarzschild spacetime that are orthogonal to the timelike Killing vector do not cover the entire Schwarzschild manifold. This is intuitively clear - Schwarzschild time becomes infinite at the horizon and the Schwarzschild coordinates do not extend beyond the horizon. As discussed above, this is only a problem of the coordinate choice. There are no obstacles to choosing a spatial slicing of the entire Schwarzschild manifold. However, these slices inevitably have the two following properties. (i) There exists some distance $\delta$ s.t. for $r < r_s + \delta$, the spatial slices are not orthogonal to $\partial_t$. (ii) The Hamiltonian that generates the time translations of the slices in the BH interior is not conserved. In order to neglect high curvature effects as long as possible, we may choose this slicing to be "nice". This simply means that the slicing is chosen s.t. in the interior, the timelike distance between two given slices is much smaller than in the exterior (see Fig. 1.1).

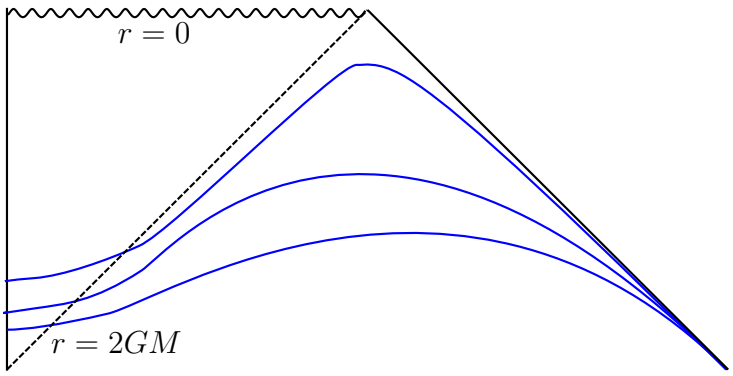


Figure 1.1: Time slicing of (the relevant part of eternal) Schwarzschild spacetime into a set of "nice" slices. The horizon is given by the dashed line at $r = 2G_N M$, while the spacelike singularity is the wiggly line at $r = 0$.

Due to its nonconservation, the Hamiltonian at different times does not commute[17]. A set of eigenmodes that diagonalizes it at some initial time no longer serves to do so at later times[18]. Consequently, the initial vacuum corresponds to an eigenstate from the point of view of the eigenmodes at some later time – we have particle production.

In his original work [Hawking, 1974, 1975], Hawking related the eigenmodes of an observer at past null infinity to those of an observer at future null infinity in the spacetime of a collapsing star. He concluded that for the future observer, the initial vacuum appears like a thermal state[19] at temperature

$$T = \frac{\hbar}{4\pi r_s} \,. \tag{1.22}$$

Hawking quanta are produced in the near horizon region. This resonates with the intuition that they are quantum fluctuations that can materialize if one quantum is in the interior region and the other outside, since in that case there is no objection due to energy conservation. This, in turn, seems to indicate that for sufficiently large black holes, Hawking evaporation is an infrared phenomenon.

Up to the time this dissertation was written, there exists no calculation that consistently takes into account the backreaction of the emitted radiation on the background spacetime. In other words, the calculation is carried out

[17] Strictly speaking, the above conditions are not sufficient to draw this conclusion. It is however true in the present case.

[18] The eigenmodes are related via a so-called Bogolyubov transformation [Bogolyubov, 1947]. We will discuss these at length in chapter 6.

[19] That is, the spectrum of out-particles $\langle 0_i | b_k^\dagger b_k | 0_i \rangle$ is thermally distributed.

in the limit in which the background spacetime decouples, which corresponds to the double scaling limit

$$G_N \to 0,\ M \to \infty,\ r_s = 2G_N M \text{ fixed.} \tag{1.23}$$

Only in this limit can the radiation emitted by a black hole be exactly thermal[20]. Otherwise trivial deviations from thermality would already arise because different times correspond to different Schwarzschild radii and therefore different temperatures. However, backreaction effects are not only important because they lead to an *effective* time dependent black hole. The build-up of two point correlations of the metric and other quantum fields can invalidate the applicability of the classical field equations. Once a large number of quanta has been emitted, it is by no means clear that the spacetime still follows any kind of classical evolution. Note that this can already happen when the black hole is still half its original size and thus in a regime in which quantum gravity effects are usually assumed to be completely subdominant. This issue is one of the central points of the second part of this thesis.

Let us conclude this section by briefly revisiting the question of conserved global charges. As long as the (semi-)classical description of black holes is valid, we expect the horizon not to depend on any global charge, see above. However, the Hawking evaporation appears to originate from a region just outside the horizon, which due to locality is therefore also independent of said global charge. This seems to forbid the release of global charge until the semiclassical approximation breaks down. Therefore, a theory of quantum gravity that allows for global symmetries has to violate some of the above assumptions. In this thesis, we will consider a model that circumnavigates this issue in two ways. First, it predicts a breakdown of the semiclassical approximation that occurs far earlier than naively expected. Second, since it models black holes as a quantum mechanical bound state, the release of the information on a global charge is a mere matter of probability. While it can be strongly suppressed at initial stages of the evaporation, it will be released eventually[21].

### 1.3.4 The information paradox

The evaporation process as described above appears as a vacuum process. Hawking quanta are emitted solely due to the time dependence of the background spacetime. As such, they cannot carry more information than what is contained in said background. However, in classical gravity, the background

[20] It is also the origin of the divergence of the integrated energy of the emitted quanta.

[21] Of course, this holds only if there is no other source of an anomaly.

metric of a Schwarzschild black hole can carry only very limited information, as we have discussed above. In particular, any (collapsing) initial state of given mass will evolve into the same Schwarzschild black hole and as such evaporate into the same final state. This is irreconcilable with one of the fundamental principles of quantum mechanics, namely the unitarity of time evolution[22]:

$$\begin{aligned} U(t,t_0)\,|\psi_1\rangle = U(t,t_0)\,|\psi_2\rangle \;\text{ and }\; |\psi_1\rangle \neq |\psi_2\rangle \\ \Rightarrow U(t,t_0) \text{ not invertible } \Rightarrow \left\langle \psi \,\middle|\, U^\dagger(t,t_0)U(t,t_0) \,\middle|\, \psi \right\rangle \neq 1\,. \end{aligned} \tag{1.24}$$

Probabilities are not conserved! [Hawking, 1976]

There is another formulation of the information paradox that is worth mentioning [Hawking, 1976]. One can interpret the evaporation process as particles being created just inside and outside of the horizon. In other words, the Hamiltonian mixes modes, or more precisely wavepackets of modes, that live in- and outside the horizon, respectively. In terms of the eigenmodes, the initial vacuum then looks like a squeezed state on top of their vacuum:

$$|0_i\rangle \sim e^{\int a_k^\dagger b_k^\dagger}\,|0\rangle\;, \tag{1.25}$$

where $a_k$ and $b_k$ are creation and annihilation operators of wavepackets that live just inside and outside the horizon. $|0_i\rangle$ is obviously not a product state in terms of $a$ and $b$. Tracing over the black hole interior, in this case the $b$'s, will result in a mixed state for $a$. This is not surprising. The black hole interior becomes entangled with the Hawking radiation. However, if the infalling particle vanishes in the singularity, it will not be reemitted even if the black hole evaporates completely. Then, at the end of the evaporation process, the state of the spacetime is described by a density matrix, although it was in a pure state initially. Again, violation of unitarity is guaranteed. Reverting to Planck scale corrections to the metric that eliminates the singularity does not solve the problem. Remember that the particle production is expected to occur right at the horizon, which is only subject to Planck scale corrections at the very latest stages of the collapse. By then, however, the black hole does no longer contain enough particles to purify the state of the Hawking radiation [Page, 1993b].

By now, it has widely been accepted that the above points do not tell the entire the story. To many, the realization that information is preserved

[22] If the black hole were stable, the fact that all initial states evolve into the same Schwarzschild metric were of little consequence. Since the core of the black hole is inaccessible to an outside observer, the loss of unitarity is simply due to a certain form of dissipation. For an evaporating black hole, the system is assumed to be closed. Unitarity loss is therefore fatal.

throughout the evaporation process has been triggered by the dual description using the AdS/CFT correspondence [Maldacena, 1998, Witten, 1998]. Since the conformal field theory is perfectly unitary, the same should be expected on the gravity side.

For a quantum physicist, this may have been clear from the outset. The above obstacles rely, in the end, on classical arguments. The first one is easily dismantled. It merely means that a full quantum black hole carries additional quantum numbers that do not survive the classical limit.

The second argument, however, is difficult to counter. It requires a drastic modification of our understanding of Hawking evaporation. Quantum effects must somehow be able to ensure that the entangled partners can already be released at relatively early stages of the evaporation. This implies that the picture of localized wave packets that, in the interior, move away from the horizon has to be given up. Alternatively, it could imply that the evaporation is not due to some localized process. Irrespective of the precise dynamics, one thing is clear: the notion of a classical spacetime within the black hole horizon can only make sense for a very limited amount of time.

### 1.3.5 Information release and scrambling

In chapter 7, we focus on the way that a black processes information and generates entanglement if described as a Bose condensate. Here, we review classic results which include the release of information and the conjectured fast scrambling property of black holes.

Once one accepts that black holes release information eventually, the details of this process become issues of interest. We will here again revert to observations that rely to large parts on the classical geometry, despite our above objections. This is merely due to the fact that the majority of literature on the topic considers precisely this setup.

It has been noted relatively early ['t Hooft, 1985, Susskind et al., 1993] that the superposition of unitarity and the equivalence principle can lead to apparent inconsistencies. Let us illuminate this with help of a simple Gedankenexperiment. Imagine two observers, A and B, where A hovers at some fixed Schwarzschild coordinate $r$ and B falls into the black hole. Any information that B carries will eventually be carried by the Hawking evaporation. At the same time, according to the equivalence principle, B will only notice troublesome effects once tidal forces become strong. Before, it will happily hold on to its piece of information long after it crossed the horizon. In a "nice" slicing of the Schwarzschild spacetime (Fig. 1.1), this implies that the Hawking evaporation may be observed before B is in any way affected. This seems to imply the cloning of quantum states – both

A and B can at the same time hold on to the *same* piece of information. This again violates unitarity. The proposed resolution has been dubbed "complementarity principle". It suggests that while both A and B observe the same quantum state, neither of them will ever know[23], since there is no way of communication between the two observers after B has fallen into the black hole[24]. The precise realization of this phenomenon on the Hilbert space is of no particular importance to us.

Concerning the process of information release, Don Page has introduced concepts [Page, 1993a] that apply generically to any evaporating substance. Before applying them to the black hole case, let us briefly make the notion of entanglement entropy precise. Consider a two particle quantum system that is not in a product state, i.e. is entangled with respect to the individual particles. For example, we could consider two qubits in the state

$$|\psi\rangle = \frac{1}{\sqrt{2}} \left( |\uparrow\rangle_A |\downarrow\rangle_B + |\downarrow\rangle_A |\uparrow\rangle_B \right) \tag{1.26}$$

and define its density matrix as

$$\rho_{AB} = |\psi\rangle \langle\psi| \ . \tag{1.27}$$

A notion of purity of a given state is given by the so called entanglement entropy. It is the von Neumann entropy of the density matrix and thus defined as

$$S \equiv - \operatorname{tr} \rho \log \rho \, . \tag{1.28}$$

It vanishes for the density matrix $\rho_{AB}$ since the whole system is in a pure state. We may now trace over $B$ to obtain the quantum state of $A$ alone. We obtain

$$\rho_A = \operatorname*{tr}_B \rho_{AB} = \frac{1}{2} \left( |\uparrow\rangle_A \langle\uparrow|_A + |\downarrow\rangle_A \langle\downarrow|_A \right) \, , \tag{1.29}$$

and, consequently

$$S_A = - \operatorname{tr} \rho_A \log \rho_A = \log 2 \, . \tag{1.30}$$

[23]The precise wording of the complementarity principle introduces the notion of a stretched horizon that is a surface slightly away from the event horizon. According to A, B never reaches the event horizon. Instead, the information is spread around the stretched horizon and eventually released as Hawking evaporation. To B instead, the information enters the horizon at a localized point. Neither will be able to observe both phenomena.

[24]There exists a carefully designed Gedankenexperiment that could lead to communication between the two observers. It has come to be known as the *firewall paradox* [Almheiri et al., 2013], and, according to its inventors, requires the existence of a firewall just inside the horizon that ensures that B cannot hold on to the information. We will not go into more detail here.

We see from Eq. (1.29) that the subsystem $A$ is in a mixed state. Correspondingly, its entanglement entropy is nonvanishing. $A$ and $B$ are entangled. For us, the important properties of the entanglement entropy are

(i) $0 \leq S(\rho) \leq \dim\mathcal{H}$, where $\mathcal{H}$ is the Hilbert space under consideration. The equalities hold for $\rho$ representing a pure and a maximally mixed state, respectively.

(ii) For subsystems $A$ and $B$, $|S_A - S_B| \leq S_{AB}$. In particular if $AB$ is in a pure state, $S_A = S_B$. Using (i), we see that in this case, the entropy of either system is given by that of the smaller one.

Complementary to the entanglement entropy is the amount of information. It is defined via

$$I \equiv \log\left(\dim\mathcal{H}\right) - S\,. \tag{1.31}$$

We can now recapitulate Page's analysis of the evaporation process [Page, 1993b].

- During the early stages of evaporation, the entanglement entropy of the radiation increases. In fact, the Hawking radiation is maximally entangled with the interior of the black hole. At this point, no information is released.

- Once the evaporation crosses the halfway point, the entanglement entropy of the radiation turns around and decreases. Now the black hole, being the smaller subsystem, is maximally entangled with the radiation. Information will start to be released and will do so continuously. The time it takes until this time is commonly referred to as *Page's time*.

- At the endpoint of evaporation, the entanglement entropy vanishes. The radiation is purified and the entire information has been released.

In the limit of a large dimension of the relevant Hilbert space, we may quantify the above statements. We obtain

$$S_{\rm rad} \simeq N_{\rm rad} - \frac{1}{2}e^{N_{\rm rad}-N_{\rm BH}}\,,\;\; I_{\rm rad} \simeq \frac{1}{2}e^{N_{\rm rad}-N_{\rm BH}} \tag{1.32}$$

for the *average* entropy and information before the halfway point. Here we have introduced the "number" of radiation and black hole constituents as $N_i = \log\left(\dim\mathcal{H}_i\right)$. The equations are valid as long as $N_i \gg 1$. After crossing we have

$$S_{\rm rad} \simeq N_{\rm BH} - \frac{1}{2}e^{N_{\rm BH}-N_{\rm rad}}\,,\;\; I_{\rm rad} \simeq N_{\rm rad} - N_{\rm BH} + \frac{1}{2}e^{N_{\rm BH}-N_{\rm rad}}\,. \tag{1.33}$$

Thus, before half of the black hole is evaporated, very little information is contained in its Hawking radiation. After the halfway point, however, $N_{\text{rad}} > N_{\text{BH}}$ and information starts to leak out. At the end of the evaporation process, $N_{\text{BH}} = 0$ and $I_{\text{rad}} = N_{\text{rad}}$. Note that these derivations are only valid if the Hilbert space of the black hole really decreases during evaporation. This, however, seems inevitable if the black hole can evaporate completely. Furthermore, this can be deduced from Bekenstein's entropy formula, since the dimension of the Hilbert space $\mathcal{N} \sim \exp(S)$.

Using basic ingredients of quantum information processing, it can be shown that once a black hole is older than Page's time, it acts as a quantum mirror and releases information almost instantaneously [Hayden and Preskill, 2007]. This is due to the fact that after this time, the black hole is maximally entangled with an observer that controls the Hawking radiation. The main assumption that leads to the immediate release of information is that the information processing by the black hole can be modeled as a unitary process. The only delay in the emission process is then due to this processing of information. The corresponding timescale is dubbed the *scrambling* or thermalization time. Note that thermalization here refers to the spreading of information within the black hole. The system is thermalized, or scrambled, once from the point of view of almost any subspace, it appears as a thermal state. Of course the entire quantum state of inside, outside and the additional information is still pure.

Hayden and Preskill realized that the only way to save the complementarity principle is that the scrambling time has a lower bound

$$t_{\text{sc}} \geq r_s \log \frac{r_s}{l_p} \,. \tag{1.34}$$

Shortly thereafter, it was suggested that the scrambling time indeed saturates the bound [Sekino and Susskind, 2008] and that black holes are the fastest information scramblers in nature. The main motivation for this *fast scrambling conjecture* was taken from the observation that classically the field of a charge spreads around the stretched horizon in logarithmic time. That fast scrambling occurs in a quantum mechanical model of the black hole is far from proven. In this thesis, we present a mechanism that naturally leads to a weaker form of fast scrambling.

### 1.3.6 UV completion in gravity

Black holes are not only fascinating objects themselves. They may also hold the key to the long-sought ultraviolet completion of gravity ['t Hooft, 1987,

Banks and Fischler, 1999, Eardley and Giddings, 2002, Dvali and Gomez, 2010].

The motivation for this section is twofold. For one, it provides another viewpoint to the dire need for a microscopic model of black holes. Second, the final chapter of the thesis attempts to provide insights into ultraviolet properties of derivatively coupled scalar theories. These are conjectured to possess very similar properties to those considered below.

Be reminded that as a quantum theory, the Einstein Hilbert action can only be taken as an effective description at energies far below the Planck scale. Due to its nonrenormalizable[25] nature, predictions can at best be made with corrections that can be organized in a power series in $E/M_p$. Once this ratio becomes of order unity, the corrections to the low energy form (1.1) are no longer suppressed; anything beyond appears to require the measurement of infinitely many coupling constants.

In hand with this effect goes the violation of *perturbative unitarity*. When expanded in terms of the graviton, already the lowest interaction is of dimension 5. The amplitude of graviton-graviton scattering can be straightforwardly estimated; it will be suppressed by two powers of the Planck mass and therefore scale in the $s$-channel like

$$\mathcal{A} \sim \frac{s}{M_p^2}\,. \tag{1.35}$$

The linear growth at high energies violates various unitarity bounds, such as the Froissart [Froissart, 1961] and partial wave unitarity bounds, both originating in the optical theorem. The violation implies that the *perturbative* time evolution cannot be described by a unitary operator. Let us mention here again that not the energies themselves are the problem. Instead, only the interaction and the corresponding momentum transfer lead to the apparent unitarity violation.

We will distinguish between two possible ways towards a resolution of this issue: Wilsonian and non-Wilsonian UV-completion.

The Wilsonian way towards the ultraviolet essentially relies on the existence of a renormalization group fixed point. This could be a non-interacting, Gaussian, fixed point. In this case, it is usually the integration of new degrees of freedom that softens the amplitude. The perturbative description that leads to expression (1.35) breaks down; the full amplitude that includes the new, weakly coupled degrees of freedom remains below the unitarity bound. Note that in this picture there could also be an intermediate regime

[25] Strictly speaking, the proof of nonrenormalizability of gravity relies on perturbative arguments. However, there are strong indications that also a nonperturbative renormalization is unattainable. The reason for this will be outlined in the text.

of genuine strong coupling, much like in QCD. The UV theory may also be described by an interacting fixed point. This possibility usually goes under the name of asymptotic safety (AS)[Weinberg, 1976, 1979]. This corresponds in part to the weakening of couplings due to loop effects. In contrast, however, it does not rely on a perturbative expansion and therefore on the smallness of a coupling constant. In this case, the appropriate ultraviolet degrees of freedom are unknown.

We will now argue that the above cases are in fact unlikely to be applicable to gravity due to the formation of black holes. We further make the case that it is precisely this which could provide a *non-Wilsonian* UV completion of gravity.

The argument is twofold. The first part relies on the observation that gravity can never be weakened in the perturbative regime. There, loop corrections to the interaction vertices are due to graviton loops. These, however, cannot induce a running of the corresponding coupling. Let us illustrate this at the example of the three point function. The coupling is given by $p^2\ell_P$. A loop that can give rise to running needs to be proportional to the operator itself. However, since only nonrenormalizable vertices are at our disposal, each vertex will contribute at least one additional power of $\ell_P$. In order to give the right mass dimension, these have to be eaten by appropriate powers of either momenta, or the cut-off of loop integrals. This, however, prevents the appearance of a term $\log p^2 p^2\ell_P$; at best, we will be able to produce $\Lambda^k p^2\ell_P^{1+k}$. This contribution can be simply renormalized away. The coupling does not run[26]. This is quite a generic result for nonrenormalizable theories: An irrelevant coupling can never induce a running of itself. We will address this issue in more detail in section 1.3.8 and chapter 9.

Now, if loop effects cannot weaken gravity in the weakly coupled regime, how about the inclusion of additional degrees of freedom? It turns out that also this is impossible. The argument [Dvali et al., 2011a] is simple and relies on the spectral decomposition of the graviton propagator in the full theory. Unless negative energy states are introduced into the theory, the spectral densities are constrained to be positive; since gravity is always attractive, this implies that it can only become stronger (see also [Dvali, 2006, Dvali et al., 2008, Brustein et al., 2009]).

This implies that renormalization effects can only kick in close to the Planck scale[27]. In this case, however, they are likely shielded by the formation of black holes[28]

[26]Instead, one may think that we can renormalize higher order operators using the low order couplings. This, however, is forbidden by gauge invariance.

[27]The IR Planck scale, to be precise.

[28]There are other arguments that challenge the existence of a nontrivial fixed point in

The idea of black hole formation as a way to unitarize scattering amplitudes in gravity has been around for almost 30 years ['t Hooft, 1987]. The idea is as simple as it is alluring. If a quantum analog of Thorne's hoop conjecture [Thorne, 1972] exists, a black hole will inevitably form in any scattering in which the impact parameter $b$ and center of mass energy $\sqrt{s}$ are such that at some time the energy is localized within its corresponding Schwarzschild radius. Noticing that the corresponding $r_s$ is given roughly by $\sqrt{s}/M_p^2$, we conclude that a black hole will form for $b \leq \sqrt{s}/M_p^2$; the momentum transfer $t$ is limited by $t \sim b^{-1} \leq M_p^2/\sqrt{s}$. One may attempt to draw a very crude picture of the consequence in terms of Feynman diagrams. The diagram of Fig.1.2a that describes (1.35) effectively opens up; the actual process is described by diagrams of the form of Fig.1.2b. For sufficiently small momentum transfer, this process corresponds to the product of $t$-channel diagrams (Fig. 1.2c), whose scaling is proportional to $b^{-1}$. We obtain

$$\mathcal{A} \sim M_p^{2+k} s^{-k} \text{ for } k \gg 0\,, \tag{1.36}$$

and the process is unitarized. Moreover, it turns out that $2 \to 2$-scattering is strongly suppressed. The dominant channel corresponds to $2 \to N$ scattering – the formation and subsequent evaporation of a black hole.

Note that these findings have immediate implications. For one, they imply that gravity as an effective field theory does not really break down. The counterterms that we have previously dubbed problematic at high energies are now effectively shielded and can not be probed. Albeit being generated by loop corrections, they present no more of an obstruction to the predictivity of the theory at high energies than at low energies.

Moreover, we can infer the existence of the Planck length $\ell_P$ as the smallest measurable length scale. Due to Heisenberg's uncertainty relation, any experiment that would try to probe sub-Planckian distances would require center of mass energies $\sqrt{s} > \ell_P^{-1}$. In that case, however, the corresponding

the UV. By definition, the theory at the fixed point is a conformal field theory (CFT). Conformal field theories, however, are quite constrained. In 2D, thanks to the state-operator map and unimodular invariance of the partition function, entropy of a CFT can be readily evaluated with help of the Cardy formula [Cardy, 1986]; Verlinde has demonstrated that similar expressions hold in higher dimensions [Verlinde, 2000]. Simple estimations demonstrate that this cannot match the Bekenstein Hawking entropy for black holes - gravity appears to have a lot more degenerate states than a conformal field theory can provide [Shomer, 2007]. We can therefore already at this point make the rather robust statement that a Wilsonian UV-completion of quantum gravity is incompatible with many results from black hole physics and string theory. Let us also remind the reader of the generic trouble of defining local operators in a theory of quantum gravity (see e.g. [DeWitt, 1967]; [Arkani-Hamed et al., 2007] contains a nice discussion on the fact that this is due to dynamical gravity).

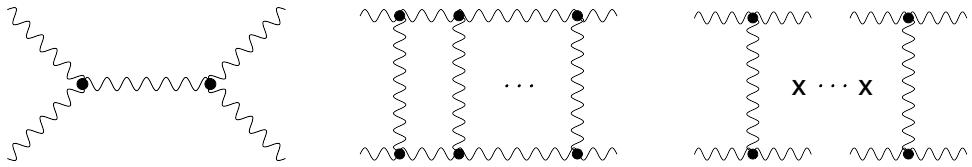


Figure 1.2: (a): Diagram for s-channel graviton-graviton scattering. (b): At energies $\sqrt{s} \gg M_p$, the vertex effectively opens up. (c): Since the corresponding momentum transfer $\sqrt{t} \sim b^{-1} \sim r_s^{-1}$ is small, the amplitude effectively factorizes.

Schwarzschild radius is $r_s \sim \sqrt{s}\ell_P^2 > \ell_P$. Accordingly, the impact parameter is limited to trans-Planckian distances and the short distance behavior is shielded by black hole formation[29].

These ideas are summarized under the notion of *self-completeness* of Einstein gravity [Dvali and Gomez, 2010].

Let us here make a brief comment on the validity of these results. They rely on the relevant energies to be much larger than the Planck scale, i.e. $E \gg M_p$, much like the effective field theory requires $E \ll M_p$. In the intermediate region, these findings do not apply without a better understanding of Planck size black holes. At this point, it is still entirely conceivable that this regime is governed by a different embedding of gravity, for example in string theory.

Finally, we have reached a rather peculiar point. The best chance for a field theoretical UV completion of gravity is due to the formation of black holes. The final process of any scattering will, however, correspond to a completely evaporated black hole. The evaporation process in turn seems to violate almost all we know about quantum mechanics. It is clear that the former problem will never be understood before the latter is under control. A microscopic understanding of black holes is an inevitable step towards the goal of disarming gravity in the ultraviolet.

### 1.3.7 A microscopic model for black holes

As mentioned above, the second part of this thesis is based on a novel approach to black holes that aims precisely to provide such a microscopic model [Dvali and Gomez, 2011, 2012b, 2013a, 2012a,c]. It is based on the observa-

[29]The formation of black holes in high energy scattering experiments can also be understood from the path integral. A large black hole possesses a large Euclidean action $S_E \sim r_s^2/\ell_P^2$, which leads to an exponential suppression factor. This is canceled by the degeneracy factor $\exp S$, where $S \sim r_s^2/\ell_P^2$ is the black hole entropy.

tion that classical solutions in quantum field theory should have a representation in terms of some fundamental quanta of the theory. In other words, localized classical lumps can be interpreted as bound states of a large number $N$ of constituents. Only in the limit of $N \to \infty$ can they be expected to behave truly classically[30].

At finite $N$, on the other hand, there will be corrections to classicality. In some cases, and for some observables, they may scale like $\exp(-N)$. In this case, they can only be resolved on timescales that are exponentially long. On the other hand, corrections can be present that scale like $1/N$. These corrections can then integrate up to $\mathcal{O}(1)$ already on timescales $t \propto N$.

The most famous systems that receive $1/N$ corrections are Bose Einstein condensates [Bose, 1924, Einstein, 1925]. There, these polynomially suppressed corrections manifest themselves as due to the interactions of quasiparticle excitations of the condensate. The foundation of the Dvali-Gomez approach is that black holes are Bose condensates of approximately $N = r_s^2/\ell_p^2$ *long-wavelength* gravitons. Henceforth, physical black holes are, contrary to the naive intuition, very *quantum* objects even for large $N$ [Dvali and Gomez, 2012a,c, Flassig et al., 2013].

Modeled as bound states of a large number of quanta, all seemingly mysterious properties of black holes disappear. Hawking evaporation is due to the depletion of the condensate; incoherent scattering between condensed gravitons leads to the emission of continuum gravitons with wavelengths of order of the Schwarzschild radius. The production of wavelengths very different from $r_s$ is strongly suppressed, leading to a possible explanation of the observed thermal spectrum in terms of combinatoric properties of scattering amplitudes. Of course, black holes modeled as bound states preserve unitarity. No information is lost and the entanglement entropy behaves essentially like in the generic case discussed by Page (see section 1.3.5). Quantum corrections can overcome the semiclassical predictions at timescales that scale maximally as $r_s N$, which corresponds to the Page time, $t_P \propto N^{3/2}$.

Moreover, a bound state of gravitons that fulfills necessary conditions to be a black hole candidate, automatically lies at a point of collective strong coupling. This phenomenon can have important applications for the number of microstates available to a given black hole. Analogies to the physics of quantum phase transitions indicate the appearance of nearly gapless collective modes that are a natural candidate for the origin of black hole entropy. Moreover, their presence is a crucial ingredient for the evident *quantumness*

[30]For example, this resonates with the arguments given in [Witten, 1979], that baryons in large $N$ $SU(N)$ gauge theories can be described by a solitonic solution, the skyrmion [Skyrme, 1961].

of black holes in the quantum portrait.

Naturally, there are also finite $N$ corrections to the no-hair theorem. The picture provided is compatible with conserved global charges. This leads to observable consequences, since black holes can now carry, for example, baryonic hair [Dvali and Gomez, 2013a].

Moreover, the black hole evaporation implies an instability of the condensate. This instability can provide a natural explanation for the conjectured fast scrambling behavior of black holes [Dvali et al., 2013].

The appealing property of this approach is that, for sufficiently large black holes, it relies entirely on long wavelength physics[31]. This has far-reaching implications. All corrections to the classical picture are in principle calculable in the effective theory described by the Einstein Hilbert action. Loop corrections can at best become important for very small black holes.

Furthermore, such a microscopic description carries the potential to complete the picture of self-unitarization of gravity. In the end, gravity amplitudes unitarize because gravity has the property of producing a very large number of soft quanta in high energy collisions and black hole formation is a natural extension of the behavior of scattering in the eikonal approximation.

Despite all these virtues, the understanding of black holes as Bose condensates is still in its infancy. The majority of results so far either relies on rather rough estimates in gravity or precise calculations in low-dimensional prototype models. The transfer of latest results to models that capture more and more properties of actual gravity is an imminent necessity.

In part II, we will take both approaches. We will consider simplified low dimensional models that provide elementary understanding to key concepts such as quantumness and scrambling. At the same time, we aim to extend previous results to more realistic models. Most prominently, this includes the analysis of the evaporation properties of a condensate of a relativistic scalar field with derivative interactions.

We end this section by pointing to a different approach to a bound state description for black holes. The authors of [Hofmann and Rug, 2014, Gruending et al., 2014] consider a setup which is widely known in the context of quantum chromodynamics. There, black holes are modeled through the inclusion of auxiliary currents that act on a nontrivial vacuum and generate states of appropriate quantum numbers[32].

[31] In this respect, this approach sharply differs from previous attempts, such as $D$-brane models for extremal black holes[Strominger and Vafa, 1996], models based on Matrix theory [Banks et al., 1997, 1998a,b] and fuzzballs [Mathur, 2005]. These approaches heavily rely on a particular UV-completion of gravity at short distances, such as string or Planck ($L_p$) length-scales.

[32] Probably the simplest example of the relevant physics are the Goldstone bosons of

### 1.3.8 Non-Wilsonian vs. Wilsonian UV completion in scalar theories - classicalization

It has been conjectured that also certain classes of scalar theories may possess ultraviolet properties similar to gravity [Dvali et al., 2011b]. The idea is based on the following observation: In scalar field theories with self-couplings that come with a sufficient number of derivatives, classical interactions of waves become important at distance scales that are much larger than the inverse cut-off of the theory[33]. Furthermore, the radius at which nonlinearities start taking over grows with the energy of the incident waves. The resemblance to black hole formation has led to the conjecture that the formation of large multi-particle states, here dubbed classicalons, shields the theory from probing short distance physics. At the same time, it could protect the theory from unitarity violation at high energies.

It has been suggested that an essential ingredient to classicalization is the non-existence of a Wilsonian UV-completion [Dvali, 2011, Dvali et al., 2012]. Otherwise the softening of self-interactions at high energies prevents the formation of classicalons. Also this is in close resemblance to gravity; the weakening of $G_N$ at high energies could prevent the formation of black holes in high energy scattering experiments [Basu and Mattingly, 2010].

An often considered example [Dvali et al., 2011c] is the low energy approximation to the Dirac-Born-Infeld (DBI) action, also describing the first interactions of the Goldstone bosons of broken nonlinear symmetries,

$$\mathcal{L} = \frac{1}{2}(\partial_\mu \phi)^2 + \frac{a}{\Lambda^4}(\partial_\mu \phi)^4 \,. \tag{1.37}$$

It can be shown that this model only possesses a Wilsonian UV-completion for $a < 0$. In the other case, there are analyticity obstructions that are related to the possibility of superluminal propagation [Adams et al., 2006]. [34]. In the end, this can be tracked back to a violation of the optical theorem[35].

broken symmetries. Even though both the exact interacting groundstate and the creation and annihilation operators of the Goldstone boson may be unknown, the corresponding state may be modeled as $|\mathrm{gs}\rangle \sim \int d^3x e^{i\mathbf{px}} J_0(x)\,|\Omega\rangle$, where $|\Omega\rangle$ is the nonperturbative groundstate and $J_0(x)$ the current of the broken symmetry.

[33]Note the similarity to the Vainshtein effect in massive gravity, discussed above.

[34]This does not necessarily imply causality violation. Strong background effects can effectively shield the creation of closed timelike curves [Burrage et al., 2012, Dvali et al., 2012]

[35]This observation has in fact also paved the way to the by now widely accepted proof for the so-called $a$-theorem [Komargodski and Schwimmer, 2011]. The $a$-theorem is the extension of Zamolodchikov's $c$-theorem [Zamolodchikov, 1986] to four dimensions and relates the anomaly coefficient $a$ of two CFTs connected by a Wilson flow. It states that

A preparatory remark for our final chapter points again to the concept of asymptotic safety. AS is an attempt to understand the UV properties of gravity through the renormalization group (RG) by looking for a nontrivial fixed point in the RG flow. If such a fixed point exists, and is characterized by a finite number of UV-relevant (i.e. IR-irrelevant) operators, gravity is rendered nonperturbatively renormalizable. Note that in this case, the vanishing of the Wilson coefficients of the infinite set of remaining UV-relevant operators is a prediction.

However, as we have already hinted before, there are strong arguments that disfavor the possibility of UV-completing gravity in this way [Dvali et al., 2011a]. This is related, most prominently, to the previously mentioned observation that the UV fixed point, if it exists, likely lies in a regime in which gravity is strongly coupled. As mentioned before, this regime may be expected to be shielded by the formation of black holes.

Nevertheless, the E(xact) RG flow of gravity exhibits nontrivial behavior. This raises several questions. What is the physical meaning of a fixed point if it is really shielded by black holes? Could the latter possibly show up in the RG flow, e.g. as composite operators? How are renormalization group scale and the physical scales related?

In the final chapter of this thesis, we attempt to address these questions in terms of the renormalization group by generalizing the Goldstone model (1.37) to an arbitrary function of the kinetic term; $\mathcal{L} = F\left(X = (\partial_\mu \phi)^2\right)$. There, exactly the same questions arise. In a perturbative treatment, none of the given operators run with momentum; as above this is due to the fact that their logarithmic divergences can only be countered by operators with a higher number of derivatives per field. Nevertheless, their functional renormalization group equations are non-trivial. If a nontrivial fixed point at large renormalization scales is found, this can help to provide an understanding of the physical meaning of the existing results in asymptotic safety. In particular it can shed some light on the mapping between the renormalization group scale and physical momenta in these kind of theories, and therefore potentially also in gravity.

## 1.4 Outline

Let us end this first chapter with a more detailed account of what will be found in the remainder of this work.

$a_{\mathrm{UV}} > a_{\mathrm{IR}}$, i.e. the number of degrees of freedom decreases along a flow towards the infrared.

In this dissertation, we consider various aspects of gravity, cosmology and quantum field theory. The thesis is divided into three major parts. The first part focuses on problems in cosmology.

We begin by considering a particular model of inflation with a nonminimal coupling between the inflaton and gravity. We inspect this model in light of the recent BICEP2 results and demonstrate that the nonminimal coupling naturally leads to a sufficiently high tensor to scalar ratio. We then address the question of quantum stability and argue under which circumstances the model could be protected from large quantum corrections even for trans-Planckian field values.

In the second chapter, we take a phenomenological approach to dark energy. In case of a time varying equation of state of the dark energy component, a scalar field could play its role. We consider scenarios in which this scalar field is coupled to a second component, e.g. dark matter. We demonstrate that previous approaches to nonlinear structure formation in these models miss key components that lead to differences from uncoupled models. We then derive a formalism that includes these fifth force effects, and subsequently apply it to various models. We conclude this chapter with a few general remarks on the quantum stability of coupled dark energy models. We also clarify the role that certain symmetries may play in protecting the models from large quantum corrections. In particular, we remark that a path integral quantization in the Jordan frame can lead to erroneous conclusions.

Finally we build a bridge towards quantum physics by considering theories of massive spin-2 particles. We revisit the issue of constructing nonlinearities and demonstrate in a helicity decomposition that almost all interaction terms lead to higher derivatives on the helicities, therefore signaling the presence of ghosts. We point out two possible ways out from this problem. First, interaction terms can be constructed that rely on redundancies of certain interactions. This requires a nonlinear completion that cannot be truncated consistently. Second, we construct the unique interaction term that does not require this kind of nonlinear completion but is instead ghost free as cubic theory. We point out possible phenomenological applications.

The second part of the thesis is dedicated to the understanding of quantum mechanical properties of black holes. We address long-standing paradoxa in the framework of a constituency picture in which black holes are described as bound states of long-wavelength gravitons. In the first chapter, we demonstrate that such a bound state, albeit containing a macroscopic number of particles, can be very quantum mechanical. This is done by analyzing quantumness properties of a one-dimensional Bose gas that can undergo a quantum phase transition. In particular, we define the quantity of "fluctuation entanglement", which measures the entanglement between different

momentum modes. We prove that this quantity is maximal at the quantum critical point both in the Bogolyubov approximation and through the exact diagonalization of the corresponding Hamiltonian.

In the second chapter, we show that the generation of strong quantum correlations in such a bound state can be attributed to an instability. This could provide a simple explanation for the conjectured fast scrambling property of black holes, since black holes are unstable towards collapse, going in hand with their evaporation. We provide an explicit study of a Bose condensate at an unstable point and demonstrate that one-particle entanglement is generated on a time scale that grows logarithmically with the number of constituents.

Finally, we consider the problem of black hole evaporation in the quantum portrait. We construct an appropriate prototype model by stripping the Hamiltonian of gravity of all but one polarization and number violating vertices. In the Schwinger-Keldysh formalism, we then study the real-time evolution of a quantum state that corresponds to a localized state of these bosons that tends to collapse due to attractive interactions. We demonstrate that incoherent scattering of condensed particles leads to evaporation. We prove the existence of scaling solutions in which the number of constituents tracks the width of the condensate. Amongst these solution, of particular interest may be those which are at a point of instability throughout the collapse, and those which lie at a bifurcation point. The existence of either class of solution is shown.

In the final chapter, we move towards the question of ultraviolet completion of effective theories. We briefly introduce the concept of classicalization. We then present an RG analysis of an $O(N)$ symmetric scalar field theory with just derivative interactions. We construct the exact flow equations and initiate the investigation of possible fixed points. This could provide valuable insight into the physical meaning of the nontriviality of RG flows in quantum gravity.

### 1.4.1 Conventions

For the major parts of the thesis, we use natural units

$$\hbar = c = 1\,. \tag{1.38}$$

In the chapters on the quantum black hole portrait, $\hbar$ is explicitly restored.

Unless otherwise stated, the metric signature used is $(+,-,-,-)$.

# Part I

# Cosmology

# Chapter 2

# New Higgs Inflation and Planck and BICEP2 data

## 2.1 The Higgs boson as the Inflaton

Recently, there have been three extremely important discoveries:

- The Standard Model (SM) Higgs boson has been observed in the Large Hadron Collider (LHC) of Geneva [Chatrchyan et al., 2012, Aad et al., 2012]. In the same experiment, no new particles, beyond the SM, have been discovered so far.

- The European Planck satellite has measured, with unprecedented precision, the primordial spectrum of scalar (temperature) perturbations, showing no trace of non-gaussianities and isocurvature perturbations [Ade et al., 2013].

- The USA BICEP2 experiment has measured the polarization of the B-modes in the Cosmic Microwave Background (CMB), thus providing the first evidence for primordial gravitational waves [Ade et al., 2014a].

If the results of Planck and BICEP2 are confirmed, they provide striking evidence for the existence of an inflationary stage in our Universe.

The null observation of isocurvature and non-gaussian modes in the CMB point to the simplest model of inflation, the one generated by a single scalar field, the inflaton. At the same time, the large spectrum of gravitational waves, as now apparently measured by BICEP2, singles out chaotic type models of inflation [Linde, 1983], where the (canonically normalized) inflaton ranges over trans-Planckian values. Historically, this fact has always been matter of debate. Naively one would indeed expect Planck suppressed

operators (from quantum gravity) correcting the inflationary potential. However, these corrections will be suppressed if they only appear as expansions in powers of the potential itself, which is always way below the Planck scale [Linde, 1990] (see also [Kehagias and Riotto, 2014]).

With the LHC discovery, it is tempting to consider the very minimal scenario where the Higgs boson not only accounts for the masses of the SM particles, but also for inflation.

In absence of gravity, the Higgs boson Lagrangian is

$$\mathcal{L}_{\mathcal{H}} = -\mathcal{D}_\mu \mathcal{H}^\dagger \mathcal{D}^\mu \mathcal{H} - \lambda \left(\mathcal{H}^\dagger \mathcal{H} - v^2\right)^2 \ , \tag{2.1}$$

where $\mathcal{D}_\mu = \partial_\mu - igW_\mu^a \tau^a - i\frac{g'}{2}B_\mu$ is the covariant derivative related to the $SU(2)$ gauge bosons $W_\mu^a$ with generator $\tau^a$ and the $U(1)_Y$ gauge boson $B_\mu$. The Higgs boson is a complex doublet of SU(2) (charged under $U(1)_Y$). The scale $v \sim 246$ GeV is very low compared to the Higgs background during inflation, we can therefore safely neglect it.

Forgetting for a moment the contributions of the gauge sectors of the SM, and focusing only on the radial part of the Higgs boson $\phi \sim \sqrt{2\mathcal{H}^\dagger \mathcal{H}}$, we reduce to the following Lagrangian

$$\mathcal{L}_\phi = -\frac{1}{2}\partial_\mu \phi \partial^\mu \phi - \frac{\lambda}{4}\phi^4 \ . \tag{2.2}$$

Defining the slow-roll parameters that parametrize how close the the system is evolving to a de Sitter background [Mukhanov, 2005]

$$\epsilon_V \equiv \frac{V'^2 M_p^2}{2V^2} \text{ and } \eta_V \equiv \frac{V'' M_p^2}{V} \ , \tag{2.3}$$

where we considered a generic potential $V$ for the inflaton ($\phi$) and $V' = dV/d\phi$, one finds that the power spectrum of primordial perturbations, quantum mechanically generated by the inflaton during inflation, is

$$\mathcal{P} \simeq \frac{H^2}{8\pi^2 \epsilon_V M_p^2} \ , \tag{2.4}$$

and the spectral index

$$n_s = 1 - 6\epsilon_V + 2\eta_V \ . \tag{2.5}$$

Planck data constrains $\mathcal{P} \sim 10^{-9}$ and $n_s \sim 0.96$. This requires the Higgs self coupling to run to an extremely small value for $\lambda \sim 10^{-12}$, which would in turn imply an extreme fine tuning for the top quark mass [Degrassi et al., 2012].

This fine tuning can be alleviated by considering a non-SM Higgs boson potential, interpolating from the low energy quartic SM coupling, to a high-energy flatter potential. However, in this case the pure Higgs sector of the SM must pass through a strong coupling below the inflationary and above the LHC scales. This automatically requires a UV completion by other degrees of freedom at intermediate scale (see for example [Kehagias et al., 2014]). Therefore, in those cases, this "Higgs" potential cannot be directly connected to the SM Higgs potential (for latest examples see [Bezrukov and Shaposhnikov, 2008, Nakayama and Takahashi, 2014]).

It is interesting to mention that one of the most popular example of Higgs inflation of this class of models, the one of [Bezrukov and Shaposhnikov, 2008], is now ruled out by BICEP2. In the Higgs inflation of [Bezrukov and Shaposhnikov, 2008] a conformal coupling of the Higgs boson to the Ricci scalar of the form $\xi\phi^2 R$ effectively introduces an exponentially flat potential which now predicts a too low gravitational wave spectrum.

An alternative to consider a new potential for the Higgs boson has been introduced in [Germani and Kehagias, 2010b]. In the New Higgs Inflationary scenario of [Germani and Kehagias, 2010b], the Higgs boson kinetic term is (uniquely) non-minimally coupled to the Einstein tensor as follows

$$\mathcal{L}_{kin} = -\frac{1}{2}\left(g^{\alpha\beta} - \frac{G^{\alpha\beta}}{M^2}\right)\partial_\alpha\phi\partial_\beta\phi \ . \tag{2.6}$$

The above coupling does not introduce any new degrees of freedom other than the graviton and the Higgs boson and, in particular, no higher derivative terms. Interesting enough, this kind of non-minimal coupling can also be obtained in supergravity [Farakos et al., 2012, Dalianis and Farakos, 2014]. Finally, the mass scale $M$ must be determined experimentally.

For a sufficiently low scale $M$, but much bigger than LHC scales [Germani and Kehagias, 2010a, Germani and Watanabe, 2011], the non-minimal coupling of the Higgs boson to gravity introduces an enhanced friction acting on the scalar $\phi$ making $\phi$ slowly rolling even for large (e.g. $\lambda \sim 0.1$) values [Germani and Watanabe, 2011, Germani, 2012c]. In the same regime, the New Higgs inflation scenario is able to match observational data (for previous results in compatibility with WMAP [Komatsu et al., 2011], see [Germani and Watanabe, 2011]). The interesting point is that, since in this case the quartic Higgs coupling can assume any value, the fine tuning of the top quark mass afflicting the General Relativistic (GR) case is removed.

In addition, the New Higgs inflation, being a chaotic-like inflationary model, conversely to previous attempts [Bezrukov and Shaposhnikov, 2008] also produces a gravitational wave spectrum which is simultaneously compatible with Planck and BICEP2, as we shall show in the following.

## 2.2 Fitting Planck and BICEP2 data with New Higgs Inflation

As announced before, we shall consider a generic inflationary Lagrangian of gravity and a scalar field kinetically coupled to gravity in the following form:

$$\mathcal{L} = \sqrt{-g}\left[\frac{1}{2}M_p^2 R - \frac{1}{2}\left(g^{\mu\nu} - \frac{G^{\mu\nu}}{M^2}\right)\partial_\mu\phi\partial_\nu\phi - V(\phi)\right], \tag{2.7}$$

where the sign of the kinetic gravitational coupling was chosen to avoid appearance of ghost instabilities in perturbations [Germani and Kehagias, 2010b,a, Germani and Watanabe, 2011].[1] In the Arnowitt-Deser-Misner (ADM) formalism with a metric $ds^2 = -N^2dt^2 + h_{ij}(N^i dt + dx^i)(N^j dt + dx^j)$, all geometrical quantities are described by defining a spatial covariant derivative $D_i$, a three-dimensional curvature scalar ${}^{(3)}R$ and extrinsic curvature $K_{ij} = E_{ij}/N$ all constructed from $h_{ij}$. The Lagrangian (2.7) then reads

$$\begin{aligned}
\mathcal{L} &= \sqrt{h}\frac{M_p^2}{2}\left[{}^{(3)}R\left(N + \frac{\dot\phi^2}{2NM^2M_p^2}\right)\right. \\
&\quad \left. +(E_{ij}E^{ij} - E^2)\left(\frac{1}{N} - \frac{\dot\phi^2}{2N^3M^2M_p^2}\right) + \frac{\dot\phi^2}{NM_p^2} - \frac{2NV}{M_p^2}\right], \\
E_{ij} &= \frac{1}{2}(\dot h_{ij} - D_iN_j - D_jN_i), \quad E = h^{ij}E_{ij},
\end{aligned} \tag{2.8}$$

where the unitary gauge $\phi(x,t) = \phi(t)$ has been chosen. We further assume an almost flat Friedmann universe with a metric

$$N = 1 + \alpha, \quad N_i = \partial_i\beta, \quad h_{ij} = a^2e^{2\zeta}(\delta_{ij} + \gamma_{ij} + \gamma_{il}\gamma_{lj}/2) \tag{2.9}$$

to second order, where $\zeta$ is the curvature perturbation and $\gamma_{ij}$ are gravitational waves with transverse-traceless conditions $D^i\gamma_{ij} = 0$ and $h^{ij}\gamma_{ij} = 0$.

Varying the Lagrangian (2.8) with respect to the lapse $N$, we find the

[1] It is known that this model is equivalent to another form: [Kobayashi et al., 2011]

$$\mathcal{L} = \sqrt{-g}\left[\frac{1}{2}M_p^2R - \frac{1}{2}g^{\mu\nu}\partial_\mu\phi\partial_\nu\phi + \frac{1}{2M^2}\left(-\frac{1}{2}(\partial_\mu\phi)^2R + (\Box\phi)^2 - (\nabla_\mu\nabla_\nu\phi)^2\right) - V(\phi)\right],$$

where integration by parts has been done. See also [Kamada et al., 2012] for studies of Higgs inflation in the context of the most general single-field model.

Hamiltonian constraint equation

$$ {}^{(3)}R\left(N^2-\frac{\dot\phi^2}{2M^2M_p^2}\right)-(E_{ij}E^{ij}-E^2)\left(1-\frac{3\dot\phi^2}{2N^2M^2M_p^2}\right) - \frac{\dot\phi^2}{M_p^2}-\frac{2N^2V}{M_p^2}=0. \quad (2.10) $$

This equation to zeroth order gives the Friedmann equation

$$ H^2=\frac{1}{3M_p^2}\left[\frac{\dot\phi^2}{2}\left(1+\frac{9H^2}{M^2}\right)+V\right], \quad (2.11) $$

where we have used $\bar{E}_{ij}\bar{E}^{ij}-\bar{E}^2=-6H^2$ and ${}^{(3)}\bar{R}=0$. Varying the Lagrangian (2.8) with respect to $\phi(t)$, we find the background equation of motion for $\phi$ as

$$ \frac{1}{a^3}\frac{d}{dt}\left[a^3\dot\phi\left(1+\frac{3H^2}{M^2}\right)\right]+V'=0. \quad (2.12) $$

Varying the Lagrangian (2.8) with respect to $a(t)$ and combining with (2.11), we get another useful background relation

$$ -\frac{\dot H}{H^2}\left(1-\frac{\dot\phi^2}{2M^2M_p^2}\right)=\frac{\dot\phi^2}{2H^2M_p^2}\left(1+\frac{3H^2}{M^2}\right)-\frac{\ddot\phi\dot\phi}{HM^2M_p^2}. \quad (2.13) $$

Varying the Lagrangian (2.8) with respect to the shift $N_j$, we find the momentum constraint equation

$$ D^i\left[\left(\frac{1}{N}-\frac{\dot\phi^2}{2N^3M^2M_p^2}\right)(E_{ij}-h_{ij}E)\right]=0, \quad (2.14) $$

whose solution to first order is given by [Germani and Watanabe, 2011]

$$ \alpha=\frac{\Gamma}{H}\dot\zeta, \quad \Gamma\equiv\frac{1-\frac{\dot\phi^2}{2M^2M_p^2}}{1-\frac{3\dot\phi^2}{2M^2M_p^2}}. \quad (2.15) $$

To first order in (2.10) we get

$$ \begin{aligned} \delta^{(3)}R\left(1-\frac{\dot\phi^2}{2M^2M_p^2}\right) &- \delta(E_{ij}E^{ij}-E^2)\left(1-\frac{\dot\phi^2}{2M^2M_p^2}\right) \\ &+\frac{18H^2\dot\phi^2\alpha}{M^2M_p^2}-\frac{4V\alpha}{M_p^2}=0, \\ \delta^{(3)}R &= -4D^2\zeta, \\ \delta(E_{ij}E^{ij}-E^2) &= -12H\dot\zeta+4HD^2\beta, \end{aligned} \quad (2.16) $$

whose solution is given by [Germani and Watanabe, 2011]

$$\begin{aligned}\beta &= -\frac{\Gamma}{H}\zeta + \chi, \quad \partial_i^2\chi = \frac{a^2\Gamma^2\Sigma}{H^2\left(1-\frac{\dot\phi^2}{2M^2M_p^2}\right)}\dot\zeta, \\ \Sigma &\equiv \frac{\dot\phi^2}{2M_p^2}\left[1+\frac{3H^2(1+\frac{3\dot\phi^2}{M^2M_p^2})}{M^2(1-\frac{\dot\phi^2}{2M^2M_p^2})}\right],\end{aligned} \tag{2.17}$$

where the Friedmann equation (2.11) and the lapse (2.15) have been used to get the shift.

To second order in the Lagrangian (2.8), scalar and tensor modes decouple. We obtain the quadratic Lagrangian in $\zeta$ after a few integration by parts:

$$\begin{aligned}\mathcal{L}_{\zeta^2} &= a^3M_p^2\left[\frac{\Gamma^2\Sigma}{H^2}\dot\zeta^2 - \frac{\epsilon_s}{a^2}(\partial_i\zeta)^2\right], \\ \epsilon_s &\equiv \frac{1}{a}\frac{d}{dt}\left[\frac{a\Gamma}{H}\left(1-\frac{\dot\phi^2}{2M^2M_p^2}\right)\right] - \left(1+\frac{\dot\phi^2}{2M^2M_p^2}\right),\end{aligned} \tag{2.18}$$

where we have used background and first-order equations (2.11), (2.13), (2.15) and (2.17). From the Friedmann equation (2.11), $0 < \dot\phi^2/(M^2M_p^2) < 2/3$, and thus the positive-definite coefficient of $\dot\zeta^2$ is guaranteed in the quadratic action, i.e. $\Gamma^2\Sigma/H^2 > 0$; this indicates that the curvature perturbation cannot be ghost-like in the Friedmann background with $V \geq 0$. Note that $\zeta$ is ill-defined when $\dot\phi = 0$, and we have to choose another gauge (or variable) to describe perturbations. We will stretch this point later on in connection to the unitarity issues of our theory.

A gradient instability can be avoided if $\epsilon_s > 0$, which is true as long as

$$\epsilon \equiv -\frac{\dot H}{H^2} < \frac{11}{6} + \frac{5M^2}{6H^2} + \frac{M^4}{12H^4}, \tag{2.19}$$

where we have used (2.13).

The coefficients of the quadratic Lagrangian, $\Gamma^2\Sigma/H^2$ and $\epsilon_s$, are governed by background equations (2.11), (2.12) and (2.13). During slow rolling of $\phi$, we obtain a quasi-DeSitter background universe that is described by

$$H^2 \simeq \frac{V}{3M_p^2}, \quad \dot\phi \simeq -\frac{V'}{3H\left(1+\frac{3H^2}{M^2}\right)}, \quad \epsilon = -\frac{\dot H}{H^2} \simeq \frac{\dot\phi^2}{2H^2M_p^2}\left(1+\frac{3H^2}{M^2}\right) \tag{2.20}$$

where $\epsilon \ll 1$ and $\delta \equiv \ddot\phi/(H\dot\phi) \ll 1$. Under this approximation, relations such that $\Gamma^2\Sigma/H^2 \simeq \epsilon_s \simeq \epsilon$ hold.

In order to evaluate the primordial power spectrum from inflation, we canonically quantize $\zeta$ by using conformal time $\tau$ and the Mukhanov-Sasaki variable $v = z\zeta$ [Mukhanov, 2005], where $z = aM_p\Gamma\sqrt{2\Sigma}/H \simeq aM_p\sqrt{2\epsilon}$. Since background quantities ($\dot{\phi}$, $H$ and $\Sigma$) are changing slowly during inflation, a non-decaying solution for $\zeta_k$ can be found on super-horizon scales. These modes stay constant until the horizon re-entry. The power spectrum of primordial curvature perturbations is then given by [Germani and Watanabe, 2011]

$$\mathcal{P}_\zeta = \frac{k^3}{2\pi^2}|\zeta_k|^2 \simeq \frac{H^2}{8\pi^2\epsilon_s c_s M_p^2}, \quad c_s^2 = \frac{H^2\epsilon_s}{\Gamma^2\Sigma}, \tag{2.21}$$

where the Hubble scale has been evaluated at the sound horizon exit, $c_s k = aH$. Note that in the limit $3H^2 \ll M^2$ (conventional general relativity limit), $c_s^2 \simeq 1$ and in the other limit $3H^2 \gg M^2$ (gravitationally enhanced friction limit), $c_s^2 \simeq 1 - 8\epsilon/3$. Although these limits have no impact on the amplitude of curvature perturbation, they do on its spectral index and change theoretical predictions. The scalar spectral index is given by

$$n_s - 1 \simeq -2\epsilon - \frac{\dot{\epsilon}_s}{\epsilon_s H} = -4\epsilon\left(1 - \frac{3H^2}{2M^2(1+\frac{3H^2}{M^2})}\right) - 2\delta. \tag{2.22}$$

In a similar manner, gravitational waves can be canonically quantized and described by the Mukhanov-Sasaki equation with

$$\begin{aligned} v_t &= z_t\gamma_\lambda\,, \\ z_t &= aM_p\sqrt{1-\dot{\phi}^2/(2M^2M_p^2)} \simeq aM_p\,, \\ c_t^2 &= [1+\dot{\phi}^2/(2M^2M_p^2)]/[1-\dot{\phi}^2/(2M^2M_p^2)] \simeq 1\,, \end{aligned} \tag{2.23}$$

as in the scalar modes. The tensor power spectrum is given by [Germani and Watanabe, 2011]

$$\mathcal{P}_\gamma = \frac{k^3}{2\pi^2}\sum_{\lambda=+,\times}|\gamma_\lambda(k)e_{ij}^\lambda(k)|^2 \simeq \frac{2H^2}{\pi^2 c_t M_p^2(1+\frac{\dot{\phi}^2}{2M^2M_p^2})}, \tag{2.24}$$

which has been evaluated at the tensor horizon exit, $c_t k = aH$. The tensor spectral index is given by

$$n_t \simeq -2\epsilon. \tag{2.25}$$

From (2.21) and (2.24), the tensor-to-scalar-ratio is given by

$$r \simeq 16\epsilon, \tag{2.26}$$

which yields a consistency relation

$$r \simeq -8n_t. \tag{2.27}$$

In Fig. 2.1, we numerically solve the slow-roll equations (2.20) and show a sample of possible matchings of the New Higgs Inflation predictions with the combined Planck and BICEP2 data sets chosen by the BICEP2 team [Ade et al., 2014a]. In particular one finds that, for any value of $\lambda$, the quartic Higgs coupling, there is always a value for $M$ such to fit the combined Planck and BICEP2 data within 2-$\sigma$. The central value in Fig. 2.1, fitting the data within 1-$\sigma$, is for a hybrid case in which the enhanced friction due to the non-minimal coupling $\sim H \times \frac{3H^2}{M^2}$, is comparable to the GR friction $\sim H$. In this case though, the Higgs quartic coupling has to run to order $10^{-9}$ at the inflationary scale. Whether this is the case or not, can only be known after a better measure of the top-quark mass and Yukawa coupling in collider experiments.

### 2.2.1 Relaxing the tension between Planck and BICEP2

The tensor-to-scalar-ratio $r$ measured by BICEP2 is in mild tension with the best value of $r$ found by the Planck team. As it has been suggested already by the BICEP2 team, a possible resolution to this tension is to relax some of the assumption used in the data analysis performed by the Planck team.

One obvious possibility is to allow for a running of the scalar spectral index. Although other explanations of this tension are also possible, such as a better measure of the optic depth, it is intriguing to see that the New Higgs inflationary model can provide a non-trivial negative running of the spectral index relaxing the tension between Planck and BICEP2. We will be very quantitative here.

In gravitationally enhanced friction (GEF) limit $3H^2 \gg M^2$, we get the scalar spectral index from (2.22)

$$n_s - 1 = -2\epsilon - 2\delta = (-8\epsilon_V + 2\eta_V)\frac{M^2}{3H^2}, \tag{2.28}$$

which is different from the GR one, $n_s - 1 = -4\epsilon - 2\delta = -6\epsilon_V + 2\eta_V$ in the other limit; the difference indeed makes the $\lambda\phi^4/4$ potential (or other non-flat potentials [Germani and Watanabe, 2011, Tsujikawa, 2012]) compatible with the Planck and BICEP2 observations since a relevant quantity is not $\epsilon_V$ but $\epsilon = \epsilon_V M^2/(3H^2)$ (in the GEF limit). The running of the spectral index

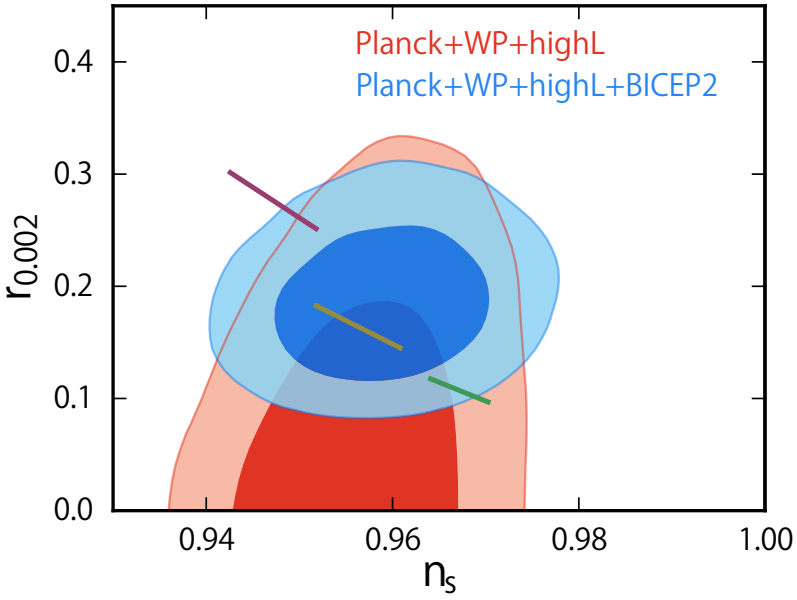


Figure 2.1: The contours show $1\sigma$ and $2\sigma$ constraints on $n_s$ and $r$, taken from Fig. 13 of [Ade et al., 2014a]. The lines show predictions of New Higgs inflation with $N_* = 50 - 60$ and different values of a theoretical parameter, $\lambda M_p^2/M^2$. The highest value corresponds to the GR limit, the lowest to the high friction limit $H^2/M^2 = \mathcal{O}(10^5)$ and the middle to the best value of $\lambda M_p^2/M^2 = 2.2 \times 10^{-4}$. The latter, *does not* describe an inflating background in the high friction limit. It is numerically found for $H^2/M^2 = \mathcal{O}(10)$, here $\lambda = \mathcal{O}(10^{-9})$.

in the GEF limit is given by

$$\left.\frac{dn_s}{d\ln k}\right|_{c_s k = aH} = -6\epsilon\delta - 2\delta\delta' + 2\delta^2 = (24\epsilon_V\eta_V - 48\epsilon_V^2 - 2\xi_V^2)\frac{M^4}{9H^4}, \quad (2.29)$$

where $\delta' \equiv \dddot{\phi}/(\ddot{\phi}H)$ and $\xi_V^2 \equiv V'''V'M_p^4/V^2$.

According to the above equations, the New Higgs inflation predicts

$$n_s \;-\; 1 = -5\epsilon, \quad r = 16\epsilon, \quad \frac{dn_s}{d\ln k} = -15\epsilon^2, \quad (2.30)$$

and

$$\begin{aligned}
\frac{\phi_*}{M_p} &= 0.037\left(\frac{\mathcal{P}_\zeta}{2\times 10^{-9}}\right)^{1/4}\left(\frac{\epsilon}{\lambda}\right)^{1/4}, \\
\frac{M}{M_p} &= 9.0\times 10^{-6}\left(\frac{\mathcal{P}_\zeta}{2\times 10^{-9}}\right)^{3/4}\frac{\epsilon^{5/4}}{\lambda^{1/4}}, \\
\frac{H}{M_p} &= 4.0\times 10^{-4}\left(\frac{\mathcal{P}_\zeta}{2\times 10^{-9}}\right)^{1/2}\sqrt{\epsilon}, \quad \epsilon = \frac{1}{3N_*+1},
\end{aligned} \tag{2.31}$$

where $N_*$ is the number of e-folds at the CMB scale.

In Planck Collaboration (2013) XXII [Ade et al., 2013], the constraints on the parameters for $\Lambda\mathrm{CDM} + r + dn_s/d\ln k$ model are given from Planck combined with other data sets. In the data set Planck+WP+BAO, $n_s = 0.9607 \pm 0.0126$, $r < 0.25$ and $dn_s/d\ln k = -0.021^{+0.024}_{-0.020}$ all at $2\sigma$. In the data set Planck+WP+high-$\ell$, $n_s = 0.9570 \pm 0.0150$, $r < 0.23$ and $dn_s/d\ln k = -0.022^{+0.022}_{-0.020}$ all at $2\sigma$, though BICEP2 team [Ade et al., 2014a] cited a slightly different upper bound for the running as $dn_s/d\ln k = -0.022 \pm 0.020$. If we allow the non-vanishing running, the New Higgs inflation's predictions can be well within the constraints from Planck and BICEP2. The New Higgs inflation generically predicts $dn_s/d\ln k \sim -10^3$ slightly larger than that from other simple chaotic inflation models.

Specifically we have the following predictions compatible with the Planck and BICEP2 data

$$n_s = 0.95, \quad r = 0.16, \quad \frac{dn_s}{d\ln k} = -0.0015, \tag{2.32}$$

with $N_* = 33$. Compared with minimal gravity (GR), the reported $r$ is a few times smaller and the running is a few times larger, for the same $n_s$.

## 2.3 Unitarity issues: inflationary scale

In this section we complete the previous analysis of [Germani and Kehagias, 2010b] by showing that the New Higgs inflation is weakly coupled during the whole inflationary evolution.

We will initially focus on the scalar sector of the theory. The introduction of a non-minimal kinetic term for the Higgs boson introduces a new non-renormalizable interaction to the SM

$$\mathcal{L}_{\rm nr} = \frac{1}{2}\frac{G^{\alpha\beta}}{M^2}\partial_\alpha\phi\partial_\beta\phi \ . \tag{2.33}$$

The question is then what is the tree-level unitarity violating scale of this system, and whether our inflating background is safely below this scale, as to be able to trust our semiclassical calculations.

During inflation, and in the high friction regime, the perturbed Lagrangian around the inflating background, up to cubic order, is

$$\begin{aligned}\mathcal{L}_{\delta\phi,h} &= -\frac{M_p^2}{2}h^{\alpha\beta}\mathcal{E}_{\alpha\beta} - \frac{3H^2}{2M^2}\partial_\mu\delta\phi\partial^\mu\delta\phi + \frac{\mathcal{E}^{\alpha t}}{M^2}\dot{\phi}_0\partial_\alpha\delta\phi + \frac{\mathcal{E}^{\alpha\beta}}{2M^2}\partial_\alpha\delta\phi\partial_\beta\delta\phi + \\ &+ h^{\alpha t}\dot{\phi}_0\partial_\alpha\delta\phi + \frac{1}{2}h^{\alpha\beta}\partial_\alpha\delta\phi\partial_\beta\delta\phi + \dots \ . \end{aligned} \tag{2.34}$$

In the above Lagrangian the Higgs boson has been split as $\phi = \phi_0 + \delta\phi$ where $\phi_0$ is the background value and $\delta\phi$ the perturbation. The metric has been expanded as $g_{\alpha\beta} = g^{(0)}_{\alpha\beta} + h_{\alpha\beta}$ where $g^{(0)}_{\alpha\beta}$ is the background metric and $h_{\alpha\beta}$ is the metric perturbation. Finally, $\mathcal{E}_{\alpha\beta}$ is the linearized Einstein tensor on the inflating background.

By looking at the Lagrangian (2.34), it is clear that neither the graviton nor the Higgs boson are canonically normalized, and in fact also mix. The canonical normalizations of these fields are

$$\begin{aligned}\bar{h}_{\alpha\beta} &= M_p h_{\alpha\beta} \\ \bar{\phi} &= \frac{\sqrt{3}H}{M}\delta\phi \ . \end{aligned}$$

Thus we have

$$\mathcal{L}_{\delta\phi,h} = -\frac{1}{2}\bar{h}^{\alpha\beta}\mathcal{E}(\bar{h})_{\alpha\beta} - \frac{1}{2}\partial_\mu\bar{\phi}\partial^\mu\bar{\phi} + \frac{\mathcal{E}(\bar{h})^{\alpha\beta}}{2H^2M_p}\partial_\alpha\bar{\phi}\partial_\beta\bar{\phi} + \text{mixings}\dots \tag{2.35}$$

It would then seem that the strong coupling scale of this theory is given by $\Lambda_H \sim (H^2M_p)^{1/3} \ll M_p$.

However, as we shall see, the scale $\Lambda_H$ will be removed by diagonalization of the scalar-graviton system. The easy way to do that is to use the the diffeomorphism invariance of the theory and go in what is usually called the unitary gauge [Maldacena, 2003a].

Allowing the freedom of time reparameterization, in an inflating background we have

$$\phi(t+\delta t, x) = \phi_0(t) + \delta\phi + \dot{\phi}_0\delta t + \dots \ . \tag{2.36}$$

Now it is clear that one can always reabsorb the scalar fluctuations by choosing

$$\delta t = -\frac{\delta\phi}{\dot{\phi}_0} \ . \tag{2.37}$$

This is a very well known fact in cosmological perturbations (see for example [Maldacena, 2003a] for a heavy use of this).

In this gauge, we see that all interactions of the scalar $\bar{\phi}$ to the longitudinal graviton are gauged away and the strong coupling scale of the theory becomes $M_p$. This is of course true only at leading order in slow-roll. As shown by the explicit computations of [Germani and Watanabe, 2011], the scalar (longitudinal graviton) interactions during inflation are indeed governed by the strong coupling scale

$$\Lambda = M_p \sqrt{1 - \frac{\dot{\phi}^2}{2M^2 M_p^2}} \ , \tag{2.38}$$

which, at leading order in slow roll, is $\Lambda \simeq M_p$, as mentioned before.

It is curious to see that in a Friedmann background the strong coupling scale is bounded by $M_p\sqrt{\frac{2}{3}}$. This can be seen from the Friedmann equations (2.11)

$$H^2 = \frac{\dot{\phi}^2}{6M_p^2}\left(1 + \frac{9H^2}{M^2}\right) + \frac{V}{3M_p^2} \ . \tag{2.39}$$

For a positive definite potential we have the following bound

$$\frac{3\dot{\phi}^2}{2M^2 M_p^2} \leq 1 \ , \tag{2.40}$$

which sets the smallest strong coupling scale to be $M_p\sqrt{\frac{2}{3}}$.

### 2.3.1 The gauge bosons

If the Higgs boson was just a real scalar field, the discussion before about the strong scale would be exhaustive. However, the Higgs boson is *not* a real scalar field. The Higgs boson being a complex doublet of the SU(2) and charged under $U(1)_Y$, will couple to the SM gauge bosons as well. In order to keep gauge invariance, the coupling must be of the form

$$\mathcal{L}_{gauge} = -\left(g^{\alpha\beta} - \frac{G^{\alpha\beta}}{M^2}\right)\mathcal{D}_\alpha \mathcal{H}^\dagger \mathcal{D}_\beta \mathcal{H} \ . \tag{2.41}$$

On a background for the Higgs, the gauge fields obtain masses proportional to the Higgs vev via the Higgs mechanism. In the unitary gauge, in which the Higgs boson is only parameterized by $\phi$, the Goldstone bosons are eaten

up by the gauge vectors. During inflation it is then easy to see that the gauge vectors W and Z will become heavy with a mass $m_{W,Z} = g_{W,Z}\phi_0 \frac{\sqrt{3}H}{M} > M_p$. In any theory of gravity, particles with masses larger than $M_p$ can be considered as Black Holes [Dvali et al., 2011a] (note that Black Holes in this theory are the same as in GR [Germani et al., 2012]). In this case, one could think to abandon the elementary particle description of the gauge bosons and integrate them out as if they were extended objects, i.e. Black Holes. In this case, practically, we could forget about this sector, as mentioned in [Germani and Kehagias, 2010b].

After inflation, but still in the high friction regime, the vector masses are sub-Planckian. However, the W and Z bosons are heavier than the tree-level cut off scale of the scalar-vector interactions $\sim \Lambda_M^3/(g^2\phi_0^2)$, as read off from the tree-level coupling in (2.41). Here $\Lambda_M = (M^2 M_p)^{1/3}$ is the cut-off scale on a Minkowski background.

The assumption usually taken in the literature would be to consider the bosons to be decoupled from our effective "low energy" theory. This might indeed be the easiest way to treat the gauge bosons.

Here we will also consider an additional approach. We will introduce a mechanism that brings the bosons masses below the vector-scalar cut-off, and in particular below the Hubble scale. In this way we can still treat the bosons as propagating degrees of freedom throughout the evolution of the Universe. We do so by introducing to our theory a non-minimal kinetic coupling of the gauge bosons to the Higgs. This serves to enhance the kinetic term of the vectors, thereby reducing both their mass and their effective coupling to gravity. We consider the interaction

$$\mathcal{L}_{\rm nm} = -\frac{1}{4}\left(g^{\alpha\mu}g^{\beta\nu} + M_p\frac{\xi^2|\mathcal{H}|^2}{\Lambda_M^5}{}^{**}R^{\mu\nu\alpha\beta}\right)F_{\alpha\beta}F_{\mu\nu}, \qquad (2.42)$$

where ${}^{**}R^{\mu\nu\alpha\beta}$ is the double dual of the Riemann tensor and $\xi$ is a constant to be fixed by experiment[2]. Note that this interaction is unique in the sense that it introduces neither ghosts, via higher derivatives, nor new degrees of freedom in the gauge-gravity sector [Germani, 2012b].

By expanding into the graviton and vector, again in the gauge $\delta\phi = 0$, one easily finds that the cut-off scale of this interaction is $\Lambda_H$, exactly the scale that we were able to gauge away in the scalar-scalar interactions, via a diagonalization of the graviton-Higgs system.

[2]Note that we choose the interaction (2.42) by the requirement that on flat space, the coupling becomes strong at $\Lambda_M$. This forbids more minimal interaction, such as a direct coupling without the double dual Riemann tensor. There, a sufficient decrease of the mass would imply a flat-space strong coupling scale of order $M$.

During the high friction regime, the gauge bosons will be canonically normalized as

$$\bar{A}_\mu = \xi\phi\sqrt{\frac{\Lambda_H^3}{\Lambda_M^5}}A_\mu, \tag{2.43}$$

with $\Lambda_H^3 = H^2 M_p$, changing their effective mass to

$$m_{\text{eff}}^2 = \frac{3g^2}{\xi^2}\Lambda_M^2 \ . \tag{2.44}$$

It is easy to convince ourselves that $m_{\text{eff}} \ll \Lambda_H$ for any reasonable value for $\xi$, in particular $\xi = \mathcal{O}(1)$. Therefore, as announced, the coupling (2.42) brings back the vectors to the low energy theory during inflation.

The interaction between the graviton and the vectors in the Higgs covariant derivative coupling (2.41) is instead suppressed by a scale $\sim \frac{\xi^2}{g^2}\frac{\Lambda_H^3}{\Lambda_M^2} \gg \Lambda_H$.

After the end of inflation, the vector masses reduce to the known values, $m^2 \sim g^2\phi^2$, while the strong coupling scale becomes $\Lambda_M$.

## 2.4 Unitarity issues: post-inflation

Although the New Higgs inflation might be completely unitary during inflation, one may ask whether an inflationary background can be consistently obtained from the Higgs boson, starting from a Minkowski background, without the necessity of integrating-in any new degree of freedom at low energies.

Let us re-discuss the gauge choice for scalar fluctuations. Up to second order in the fluctuations, we have

$$\phi(t+\delta t, x) = \phi_0 + \delta\phi + \dot{\phi}_0\delta t + \delta\dot{\phi}\delta t + \frac{1}{2}\ddot{\phi}_0\delta t^2 + \dots \ . \tag{2.45}$$

Truncating this series at the first order would mean

$$\dot{\phi}_0\delta t \gg \delta\dot{\phi}\delta t \ , \tag{2.46}$$

or

$$\dot{\phi}_0 \gg \delta\dot{\phi} \ . \tag{2.47}$$

When the time derivative of the scalar is too small, a linear truncation in (2.45) will be inconsistent and so the expansion in $\delta t$ would no longer be useful. In other words, at these low energies, the fluctuations of the field

cannot be re-absorbed into a *linear* coordinate re-definition, i.e. into a longitudinal linear graviton. From a particle physics language, this just means that there is effectively no mixing between the graviton and the scalar in flat background.

The easier way to treat the system in this regime is thus to "integrate out" gravity as in [Germani, 2012a]. In that case, the non-minimal gravitational interaction appears as a non-trivial self-derivative coupling of the Higgs boson. The structure will be the one of a quartic Galileon [Nicolis et al., 2009, Germani, 2012a].

Ignoring the gauge bosons and considering scales much larger than the electroweak, thus also ignoring $v$, we have that in the decoupling limit $M_p \to \infty$ but $\Lambda_M^3 = M^2 M_p < \infty$ [Germani, 2012a]

$$\mathcal{L}_{\rm dec} = -\frac{1}{2}\partial_\mu\phi\partial^\mu\phi\left[1+\frac{(\Box\phi)^2-\partial_{\mu\nu}\phi\partial^{\mu\nu}\phi}{2\Lambda_M^6}\right]-\frac{\lambda}{4}\phi^4\ . \tag{2.48}$$

The precise question is now whether we could create a background with Hamiltonian energy density larger than $\Lambda_M^4$.

Before answering this question, let us see why this *would not* be possible in a theory with a non-renormalizable potential. Let us take for example a potential $V = \frac{\phi^6}{\Lambda^2}$. The Hamiltonian of the system would be

$$\mathscr{H} = \frac{\pi^2}{2}+\frac{1}{2}\partial_i\phi\partial^i\phi+\frac{\phi^6}{\Lambda^2}\ , \tag{2.49}$$

where the momentum is defined in the standard way to be $\pi \equiv \frac{\delta\mathcal{L}_{\rm dec}}{\delta\dot\phi}$.

Suppose we want to have a large homogeneous background with $\mathscr{H} \gg \Lambda^4$, i.e. a background formed by a large number of particles with very large wavelength. This can only be realized by taking $\phi \gg \Lambda$. However, a quick inspection of quantum corrections reveals the (expected) inconsistency. The one-loop correction to the effective potential, renormalized at the scale $\mu$, takes the form

$$V_{\text{1-loop}} \sim \frac{\phi^8}{\Lambda^4}\log\frac{\phi}{\mu}+\text{counter-terms}, \tag{2.50}$$

The problem of large logarithms may be avoided by integrating the corresponding renormalization group equations. This, however, reveals the generation of additional couplings $\phi^8/\Lambda^4, ...$, with coefficients that are not generically small when going towards the UV.

Of course, this is nothing but the incarnation of the non-renormalizability of the potential; when interested in processes at high energies, the theory

requires a measurement of infinitely many coupling constant and loses predictivity. Therefore, no statements can be made without specifying the UV completion of the theory.

Let us now instead consider our theory, a quartic galileon. After a lengthy but straightforward calculation, one obtains that

$$\mathscr{H} = \frac{1}{2}\frac{\pi^2}{1+3\Delta} + \frac{1}{2}\partial_i\phi\partial^i\phi(1+\Delta) + \frac{\lambda\phi^4}{4} \ , \tag{2.51}$$

where

$$\Delta = \frac{1}{\Lambda_M^6}\left[(\partial_i\partial^i\phi)^2 - \partial_{ij}\phi\partial^{ij}\phi\right] \ . \tag{2.52}$$

In passing, we note that all Galilean theories are quadratic in momenta and, therefore, path integral integration of momenta can be readily performed. Thus, Galilean theories can be generically quantized in the Lagrangian path integral.

If we now consider a homogeneous field $\phi$ which is large in amplitude, $\phi \gg \Lambda_M$, but small in spatial momenta $\frac{\partial_i\partial^i\phi}{\phi} \ll \Lambda_M^2$, we would *not* encounter the above strong coupling problem. In other words, in this case, we would be allowed to consider a homogeneous background field formed by a large number of quanta and very large wavelength. This is precisely what we need for inflation, as also explained in [Dvali and Gomez, 2013b]. In other words, zero-momentum quantum corrections are under control also for large field values, as our potential is renormalizable. This is due to the famous non-renormalization theorem of the Galilean couplings [Luty et al., 2003b, Nicolis and Rattazzi, 2004]. Although the shift symmetry is broken by the potential, no contributions to the effective potential involving the scale $\Lambda_M$ can be generated at the one loop level. Any loop containing the Galilean vertex vanishes in the zero-momentum limit[3]. This theory also has another interesting property: it may allow fluctuations (or scatterings) with center of mass energy larger than $\Lambda_M$ without encountering unitarity problems. In fact, as the theory is self-derivatively coupled it enters into the realm of classicalizing theories [Dvali et al., 2011b][4].

Finally, we would like to comment on the fact that, similarly to the gravitational progenitor, this theory has a background dependent cut-off. On an inhomogeneous background, quantum corrections to Galilean theories are

[3] A thorough analysis of this issue at higher loops is postponed for future work.

[4] If, instead, one insists on a Wilsonian UV-completion, the above analysis relies on the implicit, but reasonable, assumption that couplings to new degrees of freedom respect an approximate shift symmetry.

suppressed by a scale that increases with increasing inhomogeneities [Nicolis and Rattazzi, 2004, Hinterbichler et al., 2010, de Rham et al., 2011a, de Paula Netto and Shapiro, 2012, Codello et al., 2013, de Rham et al., 2013a,b, Brouzakis et al., 2013].

Whenever the energy of the potential energy overcomes the scale $\sqrt{MM_p}$, where gravity will be reintegrated-in, the strong coupling scale of the system will start to grow with the homogeneous Friedmann background. As explained before, this is due to the non-trivial re-canonicalization of the Higgs boson.

## 2.5 Summary

The discovery of polarized B-modes in the CMB by BICEP2 has completely changed our prospective of inflation since the release of the Planck results. With this new data, if inflation ever occurred, it must be chaotic-type, i.e. the excursion of the canonically normalized inflaton must be trans-Planckian. With the discovery of the Higgs boson at the LHC, it is very tempting to seriously consider the minimal scenario in which the Higgs boson is the inflaton. Here we showed that this would be compatible with Planck and BICEP2 data if the Higgs boson is non-minimally kinetically coupled to curvatures, as in the New Higgs Inflationary scenario of [Germani and Kehagias, 2010b]. In particular, we show that the mild tension between Planck and BICEP2 data can be released by a negative running of the New Higgs inflation spectral index.

Finally, we have argued that our model is unitary throughout the whole evolution of the Universe. In particular, in the original model of Higgs inflation the gauge sector can be considered decoupled from the low energy effective theory.

A non-minimal interaction of the gauge bosons to the Higgs and the double-dual Riemann tensor will, on the other hand, significantly lower the gauge boson masses during inflation. In this case, we showed that the gauge bosons can be treated within our effective field theory even during inflation.

# Chapter 3

# Spherical Collapse and Coupled Dark Energy

## 3.1 Introduction

A wide variety of theoretical cosmological models can be challenged and discriminated thanks to predictions on structure formation. At the nonlinear level the behavior of ΛCDM cosmologies, in which the role of dark energy (DE) is played by a cosmological constant, can significantly differ from dynamical dark energy models. In more realistic scenarios, these allow for DE couplings to other species. Interacting dark energy cosmologies include: coupled quintessence (DE evolution is coupled to dark matter) [Amendola, 2000, G. Mangano and Pettorino, 2003, Amendola and Quercellini, 2003, Amendola, 2004, Wang et al., 2007, Pettorino and Baccigalupi, 2008, Quartin et al., 2008, Boehmer et al., 2008, Bean et al., 2008, La Vacca et al., 2009]; growing neutrino cosmologies [Amendola et al., 2008, Wetterich, 2007, Mota et al., 2008b] and MaVaNs ([Fardon et al., 2004, Afshordi et al., 2005, Bjaelde et al., 2008, Brookfield et al., 2006b,a, Takahashi and Tanimoto, 2006] and references therein) (DE is interacting with neutrinos); so-called modified gravity theories such as scalar-tensor theories, including F(R) and extended quintessence [Hwang, 1990a,b, Wetterich, 1995, Uzan, 1999, Faraoni, 2000, Riazuelo and Uzan, 2002, Perrotta et al., 1999, Boisseau et al., 2000, Perrotta and Baccigalupi, 2002, Pettorino et al., 2005]. In all these cosmologies a fifth force is present, acting on species whose evolution is coupled to the DE evolution. The presence of a fifth force, mediated by the DE scalar field (the cosmon, seen as the mediator of a cosmological interaction) can modify structure formation in a significant way [Baldi et al., 2010, Maccio et al., 2004], in particular at large scales [Wintergerst et al., 2010]. In view of fu-

ture data, it is therefore important to understand how these theories behave when density perturbations reach nonlinearity.

While up to now N-body simulations represent the best way to numerically evolve structures, other semi-analytical methods have been used to follow perturbations into the nonlinear regime, either using spherical collapse [Peebles, 1967, Gunn and Gott, 1972, Padmanabhan, 1993, Peacock, 1999, Bilic et al., 2004, Pace et al., 2010] or other alternative methods [Peacock and Dodds, 1996, Pietroni, 2008, Angrick and Bartelmann, 2010]. In particular, spherical collapse has been used in several occasions in literature for ΛCDM [Padmanabhan, 1993, Peacock, 1999, Engineer et al., 2000], minimally coupled quintessence models [Wang and Steinhardt, 1998, Mainini et al., 2003, Mota and van de Bruck, 2004, Maor and Lahav, 2005, Wang, 2006, Dutta and Maor, 2007, Mota et al., 2008a, Abramo et al., 2007, Creminelli et al., 2010], coupled quintessence [Mainini and Bonometto, 2006, Nunes and Mota, 2006] and when parametrizing early dark energy contributions [Bartelmann et al., 2006, Sadeh et al., 2007, Francis et al., 2008].

In this chapter we give a detailed description of the spherical collapse method and clarify some tricky issues in its applications. We lay particular focus on the calculation of the extrapolated linear density contrast at collapse $\delta_c$, a quantity of major interest within a spherical collapse description, often used in a Press-Schechter [Press and Schechter, 1974] approach to estimate dark matter halo mass distributions.

After reviewing results for standard cosmologies like ΛCDM, we consider the case in which a fifth force is present in addition to standard gravitational attraction, as in the case of all the interacting dark energy models mentioned above. The inclusion of the fifth force within the spherical collapse picture requires particular attention. Spherical collapse is intrinsically based on gravitational attraction only and cannot account for other external forces unless it is suitably modified. The dynamics in the spherical collapse model are governed by Friedmann equations. Hence, only gravitational forces determine the evolution of the different scale factors and, in turn, of the density contrast.

A detailed comparison between the linearized spherical collapse picture and the linear relativistic equations allows us to first identify the presence (or absence), in the spherical collapse picture, of terms which are a direct signature of the coupling already at the linear level. We show how spherical collapse necessitates to be suitably modified whenever an additional force other than gravity is present and is big enough to influence the collapse. We use this comparison also to show that a standard treatment of spherical collapse may lead to problems even in the uncoupled case when treating inhomogeneities in the scalar field.

A modification of the spherical collapse picture is indeed possible, via a nonlinear analysis of the model. We derive the set of second order differential equations for the density contrast from the nonlinear Navier-Stokes equations described in [Wintergerst et al., 2010], extending an idea from [Wintergerst, 2009]. We show how $\delta_c$ can be evaluated directly from these equations and how they can serve as a starting point for a reformulation of spherical collapse. Our results match the numerical solution of the nonlinear hydrodynamical equations solved as described in [Wintergerst et al., 2010, Wintergerst, 2009].

We apply our method to coupled quintessence scenarios where a coupling is present among dark matter particles, comparing our results with alternative methods presented in the past [Mainini and Bonometto, 2006, Nunes and Mota, 2006]. As a further application of our method, we consider for the first time spherical collapse within growing neutrino models, where an interaction is active among neutrinos: in this case we obtain an extrapolated linear density at collapse $\delta_c$ which shows an oscillating behavior, a characteristic feature of the interaction.

Finally we confirm results found in [Francis et al., 2008] on spherical collapse and early dark energy (EDE).

In Sec. 3.2 we recall the spherical collapse model and its applications to standard cosmologies (Sec. 3.2.1). In Sec. 3.3 we focus on spherical collapse in presence of a fifth force, taking the case of coupled quintessence as an example of fifth force cosmologies. In Sec. 3.4, we demonstrate that the standard spherical collapse leads to wrong results when applied to coupled quintessence: indeed, by comparing with full relativistic equations (Sec.3.4.1) we demontrate that the spherical collapse equations lack terms that are essential in the presence of a fifth force (Sec.3.4.2) and can lead to incorrect results when an inhomogeneous DE scalar field is included within this framework (Sec. 3.4.3). Consequently, in Sec. 3.5, we illustrate how the spherical collapse can be correctly reformulated in coupled scenarios by basing it on the full nonlinear Navier-Stokes equations for the respective model. We further comment on the careful choice of initial conditions in Sec. 3.5.1. We apply the derived formalism to give results for coupled quintessence (Sec. 3.5.2) and growing neutrinos (Sec. 3.6). Finally, we use the described framework to confirm results found in [Francis et al., 2008] for uncoupled early dark energy.

## 3.2 Spherical Collapse

Consider a cold dark matter density perturbation within a homogeneous background Universe. Under the effect of gravitational attraction the perturbation grows, possibly entering the nonlinear regime, depending on the scale of the perturbation. A popular method often used to follow the evolution of cold dark matter (CDM) structures during the first stages of the nonlinear regime is the spherical collapse model. In its original applications [Peebles, 1967, Gunn and Gott, 1972, Peacock, 1999, Padmanabhan, 1993], it is assumed that the initial overdensity obeys a top hat profile

$$\delta\rho_{\rm in}(t,s) \equiv \delta\rho_0(t)\Theta(r(t)-s) \quad , \tag{3.1}$$

where $r(t)$ specifies the radius of the top hat and $s$ is the spherical coordinate indicating the distance from the center of the perturbation. $\Theta(r(t)-s)$ is the top hat function, equal to 1 for $s \leq r(t)$ and 0 otherwise. The amplitude of the top hat is given by $\delta\rho_0$ and is evolving in time. As a consequence of Birkhoff's theorem of General Relativity, which ensures that the dynamics of the radius $r(t)$ are governed only by the enclosed mass, the top hat "bubble" is conveniently described as a closed Universe where the total density $\rho = \rho_{crit} + \delta\rho_m$ exceeds the critical density $\rho_{crit}$ due to the presence of CDM density perturbation.

Hence, all densities and geometric quantities are treated according to the Friedmann equations:

$$H^2 \equiv \left(\frac{\dot{r}}{r}\right)^2 = \frac{1}{3}\sum_\alpha \rho_\alpha - \frac{K}{r^2} \quad , \tag{3.2}$$

$$\frac{\ddot{r}}{r} = -\frac{1}{6}\sum_\alpha \left[\rho_\alpha(1+3w_\alpha)\right] \quad . \tag{3.3}$$

Here the "scale factor" is given by the radius of the bubble $r(t)$, commonly normalized to match the background scale factor $a(t_i)$ at some initial time $t_i$. The corresponding Hubble function of the bubble is indicated by $H$. Eq. (3.2) explicitly contains a curvature term $K$; Eq. (3.3), albeit the lack of an explicit curvature term, is still describing a closed Universe as the sum of the densities on the right hand side exceeds the critical one. Note that throughout this work densities have been normalized in units of the square of the reduced Planck mass $M^2 = (8\pi G_N)^{-1}$.

The bubble is embedded in a homogeneous Friedmann-Robertson-Walker (FRW) background characterized by a scale factor $a(t)$ and a corresponding Hubble function $\bar{H} \equiv \dot{a}/a$. We use a bar to indicate background quantities.

For clarity, we recall the Friedmann equations describing the homogeneous and flat background Universe:

$$\bar{H}^2 \equiv \left(\frac{\dot{a}}{a}\right)^2 = \frac{1}{3}\sum_\alpha \bar{\rho}_\alpha \quad , \tag{3.4}$$

$$\frac{\ddot{a}}{a} = -\frac{1}{6}\sum_\alpha \left[\bar{\rho}_\alpha(1+3\bar{w}_\alpha)\right] \quad . \tag{3.5}$$

Note that throughout this work we neglect baryonic components. For simpler notation we refer to CDM by a subscript $m$.

### 3.2.1 Applications to standard cosmologies

Spherical collapse can be safely applied to the case of Einstein de Sitter (EdS) cosmologies (in which $\Omega_m = 1$), and to ΛCDM models. In this case, the energy density of matter $\rho_m$, appearing on the right hand side of Eq. (3.3) and (3.5), is conserved both inside and outside the overdensity:

$$\dot{\rho}_m = -3H(1+w_m)\rho_m \quad , \tag{3.6}$$

$$\dot{\bar{\rho}}_m = -3\bar{H}(1+\bar{w}_m)\bar{\rho}_m \quad . \tag{3.7}$$

The nonlinear density contrast is defined by $1+\delta_m \equiv \rho_m/\bar{\rho}_m$ and is determined by the above equations. The linear density contrast evolves according to well known linear perturbation theory [Kodama and Sasaki, 1984, Ma and Bertschinger, 1995] and satisfies the linear equation:

$$\ddot{\delta}_{m,L} + 2H\dot{\delta}_{m,L} - \frac{3}{2}H^2\Omega_m\delta_{m,L} = 0 \quad , \tag{3.8}$$

Equations (3.3) - (3.8) can be integrated numerically. We start the integration at some initial time $t_{\rm in}$ in which the total energy density in the bubble is higher than the critical energy density, due to the presence of the CDM overdensity $\delta_m$. Equation (3.3) provides $r(z)$, which is shown in Fig.3.1 for a ΛCDM model with $\Omega_\Lambda = 0.7$ and for three different overdensities ($\delta_{\rm in} = 1\cdot10^{-3}, 2\cdot10^{-3}, 3\cdot10^{-3}$ for $z_{\rm in} = 10^4$): $r(z)$ first increases as the bubble expands with the background; then, it reaches a maximum value (turnaround) in which comoving velocities become zero; finally, the bubble collapses, the radius tends to zero and the nonlinear density contrast $\delta_m$ increases rapidly. The redshift of collapse depends on the amplitude of the initial perturbation. The higher this is, the earlier the overdense region will collapse. The corresponding value of the linear density contrast extrapolated

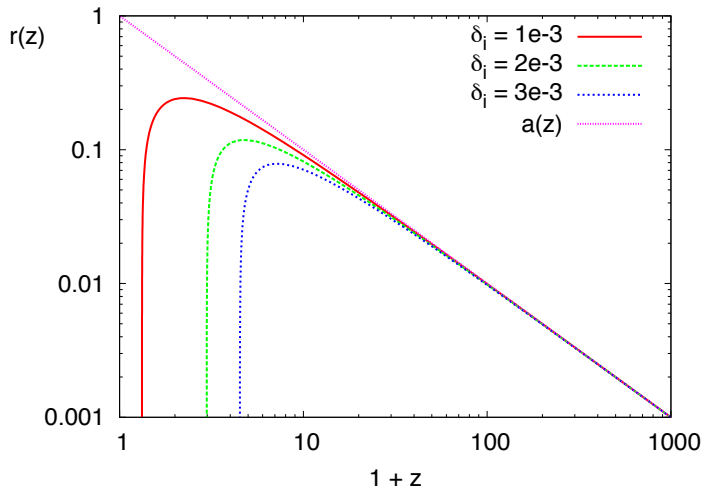


Figure 3.1: Evolution of radial parameter $r(z)$ for different initial overdensities in a ΛCDM model with $\Omega_m = 0.3$, $\Omega_\Lambda = 0.7$, as used throughout this work. For comparison, we have included the background scale factor $a$ (dotted, pink).

at the time of collapse is usually referred to as $\delta_c$ and represents one of the key ingredients for a Press-Schechter analysis, which gives statistical estimates of the cluster distribution in space. We will not go into the Press-Schechter procedure here; instead, we will focus on the calculation of $\delta_c$ within the spherical collapse analysis, putting in evidence how this calculation has to be carefully performed depending on the underlying theoretical model.

In an Einstein de Sitter model the linear density contrast at collapse can be calculated analytically [Padmanabhan, 1993, Peacock, 1999]: it is equal to a constant value independent of the redshift of collapse $z_c$

$$\delta_c = (3/20)\,(12\pi)^{2/3} \simeq 1.686 \quad . \tag{3.9}$$

Note that we define $z_c$ as the redshift at which $r \to 0$. In a ΛCDM model one expects this value to decrease for late collapse times [Padmanabhan, 1993, Peacock, 1999], when dark energy dominates over matter and leads to cosmic acceleration, slowing down structure formation. In Fig. 3.2 we plot $\delta_c(z_c)$ for both EdS and ΛCDM.

It is also common to analyze the (nonlinear) density contrast at virialization. From the virial theorem one may deduce [Padmanabhan, 1993, Peacock, 1999, Engineer et al., 2000, Maor and Lahav, 2005] that a given

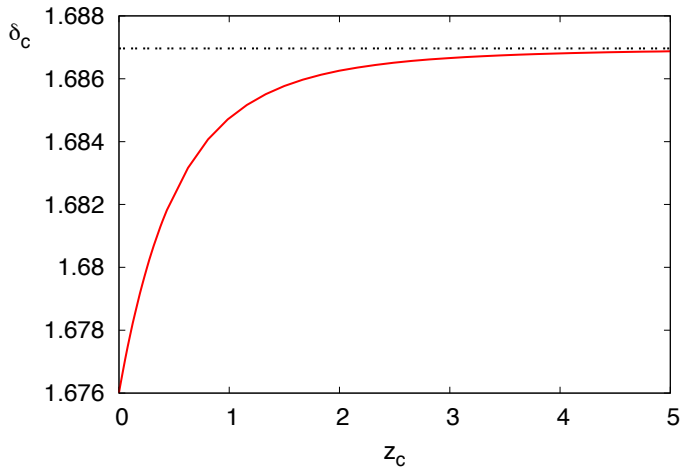


Figure 3.2: Extrapolated linear density contrast at collapse $\delta_c$ vs. redshift at collapse $z_c$ for a ΛCDM (solid, red) and an EdS (double-dashed, black) model.

bubble virializes whenever it has collapsed to half its turnaround radius. In an EdS Universe, the density contrast at virialization is analytically found to be $\delta_{\rm vir} = (9\pi + 6)^2 / 8 \simeq 146.8$. For the ΛCDM model, an increase is observed for late collapse times. This corresponds to the fact that, in presence of dark energy, it takes longer for structures to virialize, with a corresponding higher value of $\delta_{\rm vir}$, as shown in Fig.3.3.

To better illustrate the effect of Λ on both $\delta_{\rm vir}$ and $\delta_c$, we have plotted $\delta_{m,L}$ and $\delta_{m,NL}$ in Fig.3.4, as well as the radius $r$ for a fixed initial overdensity in both an EdS and a ΛCDM Universe. It can be seen that the later virialization in ΛCDM leads to an increase in $\delta_{vir}$. On the other hand, the smaller linear growth rate reduces the extrapolated linear density contrast $\delta_c$ in ΛCDM.

Alternatively to a cosmological constant, dark energy can be described by a dynamical energy component, such as a quintessence scalar field rolling down a potential [Wetterich, 1988, Ratra and Peebles, 1988]. A meaningful quintessence model should naturally explain why dark energy dominates over cold dark matter only at recent times; this happens to be difficult to achieve within minimally coupled quintessence models, which are often fine-tuned as much as a ΛCDM model [Matarrese et al., 2004]. Viable models in this direction often involve the presence of a coupling between the dark energy scalar field, referred to as "cosmon" or "quintessence", and other components in

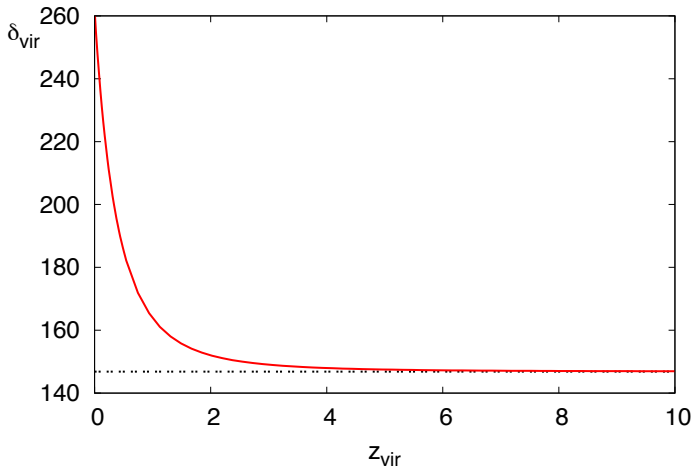


Figure 3.3: Nonlinear density contrast at virialization for a ΛCDM (solid, red) and an EdS (double-dashed, black) model.

the Universe such as cold dark matter [Wetterich, 1995, Amendola, 2000] or neutrinos [Fardon et al., 2004, Amendola et al., 2008, Wetterich, 2007, Mota et al., 2008b, Wintergerst et al., 2010]. The presence of an interaction that couples the cosmon dynamics to another species introduces a new force. This "fifth force" is acting between particles (CDM or neutrinos in the examples mentioned) and is mediated by dark energy fluctuations. Whenever such a coupling is existent, spherical collapse, whose concept is based on gravitational attraction, has to be suitably modified. In the following sections we will present some examples of quintessence models in presence of a fifth force and show how the latter can be taken into account.

## 3.3 Coupled quintessence cosmologies

The first set of cosmologies in presence of a fifth force that we consider is known as coupled quintessence (CQ): here the evolution of the quintessence scalar field (from hereon we refer to it as the "cosmon" [Wetterich, 1988]) is coupled to CDM [Wetterich, 1995, Amendola, 2000, 2004, Pettorino and Baccigalupi, 2008, Baldi et al., 2010]. The cosmon $\bar{\phi}$ interacts with CDM particles whose mass $m(\bar{\phi})$ changes with $\bar{\phi}$. This set of cosmologies is described by the Lagrangian:

$$\mathcal{L} = -\frac{1}{2}\partial^\mu\bar{\phi}\partial_\mu\bar{\phi} - U(\bar{\phi}) - m(\bar{\phi})\bar{\psi}\psi + \mathcal{L}_{\rm kin}[\psi]\,, \tag{3.10}$$

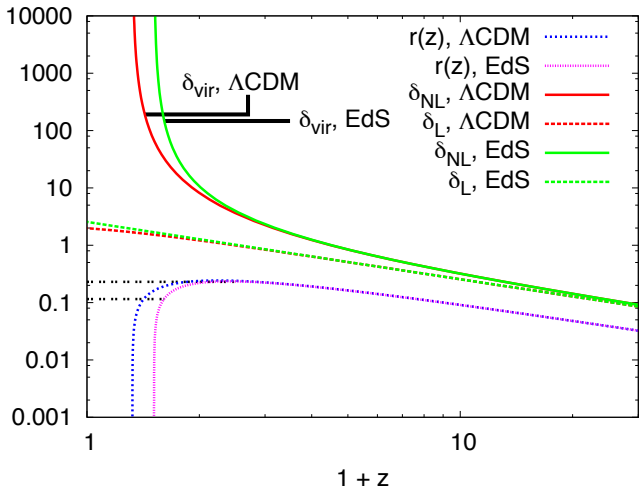


Figure 3.4: Linear and nonlinear density contrasts in ΛCDM (red) and EdS (green) models, as well as the corresponding radius functions (blue, short-dashed and pink, dotted, respectively). The upper double-dashed black line marks the turn around radius $r_{\rm ta}$, the lower one $r_{\rm ta}/2$. The later virialization time in ΛCDM ($r_{\rm ta}/2$ is reached substantially later, when the blue dotted line and the lower black double-dashed lines intersect) leads to an increase of $\delta_{\rm vir}$. The overdensities collapse when the radii go to zero and $\delta_c$ is given by the value reached by the linear curves at this redshift. Although collapse happens later for ΛCDM, the linear growth is suppressed at late times (red dashed line in comparison to green dashed line). This leads to a decrease in $\delta_c$.

in which the mass of matter fields $\psi$ coupled to DE is a function of the scalar field $\bar{\phi}$.

The homogeneous flat background follows the set of equations described in [Amendola, 2000, Mota et al., 2008b]. The Universe evolves in time according to the Friedmann and acceleration equations:

$$\bar{H}^2 \equiv \left(\frac{\dot{a}}{a}\right)^2 = \frac{1}{3}\sum_\alpha \bar{\rho}_\alpha \tag{3.11}$$

and

$$\frac{\ddot{a}}{a} = -\frac{1}{6}\sum_\alpha \left[\bar{\rho}_\alpha(1+3\bar{w}_\alpha)\right] \tag{3.12}$$

where the sum is taken over all components $\alpha$ in the Universe. A crucial ingredient is the dependence of CDM mass on the cosmon field $\bar{\phi}$, as encoded

in the dimensionless cosmon-CDM coupling $\beta$,

$$\beta \equiv -\frac{d\ln m}{d\bar{\phi}} \quad . \tag{3.13}$$

For increasing $\bar{\phi}$ and $\beta > 0$ the mass of CDM particles decreases with time

$$m = \bar{m} e^{-\beta\bar{\phi}} \quad , \tag{3.14}$$

where $\bar{m}$ is a constant and $\beta$ is also fixed to be a constant in the simplest coupling case. The cosmon field $\bar{\phi}$ is normalized in units of the reduced Planck mass $M = (8\pi G_N)^{-1/2}$, and $\beta \sim 1$ corresponds to a cosmon-mediated interaction for CDM particles of roughly gravitational strength.

For a given cosmological model with a set time dependence of $\bar{\phi}$, one can determine the time evolution of the mass $m(t)$. The dynamics of the cosmon can be inferred from the Klein Gordon equation, now including an extra source due to the coupling to CDM:

$$\ddot{\bar{\phi}} + 3\bar{H}\dot{\bar{\phi}} + \frac{dU}{d\bar{\phi}} = \beta\bar{\rho}_m \quad . \tag{3.15}$$

We choose an exponential potential [Wetterich, 1988, Ratra and Peebles, 1988, Ferreira and Joyce, 1998, Barreiro et al., 2000]:

$$V(\bar{\phi}) = M^2 U(\bar{\phi}) = M^4 e^{-\alpha\bar{\phi}} \quad , \tag{3.16}$$

where the constant $\alpha$ is one of the free parameters of our model. Note that our analysis, however, is more general and can be applied in presence of any quintessence potential.

The homogeneous energy density and pressure of the scalar field $\bar{\phi}$ are defined in the usual way as

$$\bar{\rho}_\phi = \frac{\dot{\bar{\phi}}^2}{2} + U(\bar{\phi}) \quad , \quad \bar{p}_\phi = \frac{\dot{\bar{\phi}}^2}{2} - U(\bar{\phi}) \quad , \quad \bar{w}_\phi = \frac{\bar{p}_\phi}{\bar{\rho}_\phi} \quad . \tag{3.17}$$

Finally, we can express the conservation equations for dark energy and coupled matter as follows [Wetterich, 1995, Amendola, 2000]:

$$\begin{aligned} \dot{\bar{\rho}}_\phi &= -3\bar{H}(1+\bar{w}_\phi)\bar{\rho}_\phi + \beta\dot{\bar{\phi}}\bar{\rho}_m \quad , \\ \dot{\bar{\rho}}_m &= -3\bar{H}\bar{\rho}_m - \beta\dot{\bar{\phi}}\bar{\rho}_m \quad . \end{aligned} \tag{3.18}$$

The sum of the energy momentum tensors for CDM and the cosmon is conserved, but not the separate parts. We neglect a possible cosmon coupling to baryons ($b$) or neutrinos ($\nu$), so that $\dot{\bar{\rho}}_{b,\nu} = -3\bar{H}(1+\bar{w}_{b,\nu})\bar{\rho}_{b,\nu}$.

For a given potential (3.16) the evolution equations for the different species can be numerically integrated, giving the background evolution shown in Fig.3.5 (for constant $\beta$). For a detailed description of attractor solutions in this context see [Wetterich, 1995, Copeland et al., 1998, Amendola, 2000]

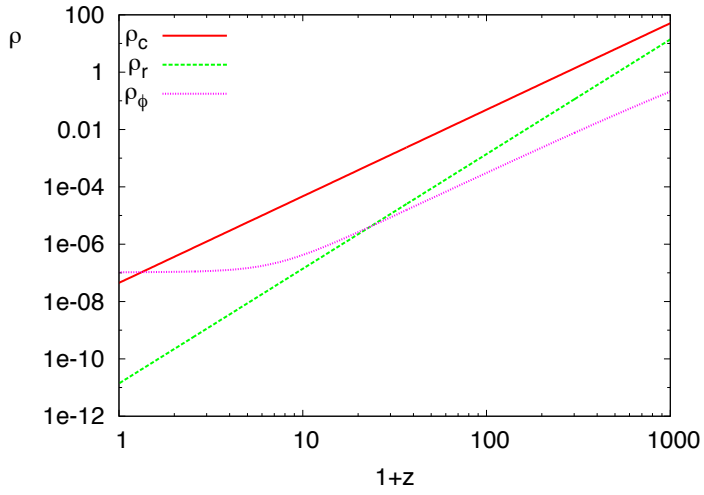


Figure 3.5: Energy densities of cold dark matter (solid), dark energy (dotted) and radiation (long dashed) are plotted vs redshift. We take a constant $\beta = 0.1$, with $\alpha = 0.1$.

It will later prove useful to understand the evolution of perturbations within coupled models in the linear regime. The relativistic calculation in coupled quintessence is described in detail in [Amendola, 2004, Mota et al., 2008b, Wintergerst et al., 2010]. Here we just recall the resulting second order equations (in Fourier space) for $\delta_{m,L}$ and the perturbation of the scalar field $\delta\phi$ in Newtonian gauge (in which the nondiagonal metric perturbations are fixed to zero):

$$\begin{aligned}\ddot{\delta}_{m,L} &= -2\bar{\bar{H}}\left(\dot{\delta}_{m,L} + \beta\,\delta\dot{\phi}\right) + (k/a)^2\left(\Phi + \beta\,\delta\phi\right) \\ &\quad +\beta\,\dot{\bar{\phi}}\left(\dot{\delta}_{m,L} + \beta\,\delta\dot{\phi}\right) - 3\dot{\Phi}\left(2\bar{\bar{H}} - \beta\,\dot{\bar{\phi}}\right) \\ &\quad -3\ddot{\Phi} - \beta\,\delta\ddot{\phi} \quad , \end{aligned} \tag{3.19}$$

$$\begin{aligned}\delta\ddot{\phi} &= -3\bar{\bar{H}}\delta\dot{\phi} - U_{,\phi\phi}\,\delta\phi + \beta\bar{\rho}_m\left(\delta_{m,L} + 2\Phi\right) \\ &\quad -(k/a)^2\delta\phi - 2\Phi U_{,\phi\phi} + 4\dot{\bar{\phi}}\dot{\Phi} \quad . \end{aligned} \tag{3.20}$$

Since the spherical collapse is intended to model the nonlinear evolution in the Newtonian limit, we are interested in the case in which $k \gg a\bar{H}$. Following [Amendola, 2004, Pettorino and Baccigalupi, 2008], we obtain

$$\ddot{\delta}_m = (\beta\dot{\bar{\phi}} - 2\bar{H})\dot{\delta}_m + (k/a)^2(1+2\beta^2)\Phi \quad , \tag{3.21}$$

$$k^2\delta\phi \sim \beta\, a^2\bar{\rho}_m\delta_m \quad . \tag{3.22}$$

and the gravitational potential is approximately given by

$$k^2\Phi \sim \frac{1}{2}a^2\sum_{\alpha\neq\phi}\bar{\rho}_\alpha\delta_\alpha \quad , \tag{3.23}$$

where we have assumed that no anisotropic stress is present, so that $\Phi = -\Psi$. We can then define an effective gravitational potential as

$$\Phi_{\rm eff} \equiv \Phi + \beta\delta\phi \quad . \tag{3.24}$$

In real space (comoving spatial coordinates) and after substituting the expressions for $\Phi$ [Eq. (3.23)] and for $\delta\phi$ [Eq. (3.22)], we get the modified Poisson equation:

$$\Delta\Phi_{\rm eff} = -\frac{a^2}{2}\bar{\rho}_m\delta_m\left(1+2\beta^2\right) \quad . \tag{3.25}$$

Cold dark matter then feels an effective gravitational constant

$$\tilde{G}_{\rm eff} = G_N[1+2\beta^2] \quad , \tag{3.26}$$

where $G_N$ is the usual Newton's constant.

The first term on the right hand side of Eq.(3.21) includes the expansion damping, modified by the velocity dependent term $\beta\dot{\bar{\phi}}$, which accounts for momentum conservation; the last term on the right hand side specifies the presence of the fifth force.

## 3.4 Standard spherical collapse and CQ

We will now apply the framework described in Sec. 3.2 as it is to CQ. This approach has been used, for example, in [Nunes and Mota, 2006]. We will show, by comparison with the perturbation equations recalled in Sec.3.3, that this does not correctly model the evolution of nonlinear structures in coupled quintessence.

For this purpose, consider the standard spherical collapse equations (3.2) and (3.3), in which the densities on the right hand side satisfy the coupled conservation equations:

$$\dot{\rho}_r = -4H\rho_r + \Gamma_r \quad , \tag{3.27}$$

$$\dot{\rho}_m = -3H\rho_m - \beta\dot{\phi}\rho_m \quad , \tag{3.28}$$

$$\dot{\rho}_\phi = -3H(\rho_\phi + p_\phi) + \beta\dot{\phi}\rho_{cdm} + \Gamma_\phi \quad , \tag{3.29}$$

or equivalently the Klein-Gordon equation:

$$\ddot{\phi} + 3H\,\dot{\phi} + U_{,\phi} = \beta\rho_m + \frac{\Gamma_\phi}{\dot{\phi}} \quad . \tag{3.30}$$

Here additional source terms $\Gamma_r$ and $\Gamma_\phi$ may account for possible differences between the bubble and the background components for radiation and the scalar field, respectively [Mota and van de Bruck, 2004, Maor and Lahav, 2005, Wang, 2006, Nunes and Mota, 2006]. In case of clustering dark energy and/or radiation, both source terms are set to zero:

$$\Gamma_r \equiv 0 \quad , \tag{3.31}$$

$$\Gamma_\phi \equiv 0 \quad . \tag{3.32}$$

If both radiation and the scalar field are to be homogenous, i.e. they behave in the bubble as in the background, the source terms are defined as:

$$\Gamma_r \equiv 4(H - \bar{H})\rho_r \quad , \tag{3.33}$$

$$\Gamma_\phi \equiv 3(H - \bar{H})\,(\rho_\phi - p_\phi) + \beta\,(\dot{\phi} - \dot{\bar{\phi}}) \quad . \tag{3.34}$$

In order to account for a fractional outflow of dark energy or radiation, one may suitably interpolate between the two values [Mota and van de Bruck, 2004, Maor and Lahav, 2005, Wang, 2006, Nunes and Mota, 2006].

### 3.4.1 Comparison with relativistic equations

We will now show that the approach described by Eqs. (3.3) and (3.5) together with (3.27 - 3.34) is incorrect. The actual fifth force term is entirely missing from the equations.

As a starting point, we remark that Eq.(3.18) for the background CDM density and (3.28) for the bubble CDM density can be directly integrated [Amendola, 2000] to yield

$$\bar{\rho}_m = \bar{\rho}_{m,\mathrm{in}}\, e^{\beta\,\bar{\phi}_{\mathrm{in}}} \left(\frac{a}{a_{\mathrm{in}}}\right)^{-3} e^{-\beta\,\bar{\phi}} \quad , \tag{3.35}$$

$$\rho_m = \rho_{m,\mathrm{in}}\, e^{\beta\,\phi_{\mathrm{in}}} \left(\frac{r}{r_{\mathrm{in}}}\right)^{-3} e^{-\beta\,\phi} \quad . \tag{3.36}$$

The density contrast $\delta_m$ is then given by

$$\begin{aligned} 1 \;+\; \delta_m &\equiv \frac{\rho_m}{\bar{\rho}_m} \\ &= (1+\delta_{m,\mathrm{in}})\, e^{\beta\,\delta\phi_{\mathrm{in}}} \left(\frac{r_{\mathrm{in}}}{a_{\mathrm{in}}}\right)^3 \left(\frac{a}{r}\right)^3 e^{-\beta\,\delta\phi} \quad , \end{aligned} \tag{3.37}$$

where we have introduced $\delta\phi \equiv \phi - \bar{\phi}$. The first and second time derivatives of $\delta_m$ read

$$\dot{\delta}_m = 3\,(1+\delta_m)\left(\bar{H}-H\right) - \beta\,\delta\dot{\phi}\,(1+\delta_m) \quad , \tag{3.38}$$

$$\begin{aligned} \ddot{\delta}_m &= \frac{\dot{\delta}_m^2}{1+\delta_m} + 3\,(1+\delta_m)\left(\dot{\bar{H}}-\dot{H}\right) \\ &\quad -\beta\,\delta\ddot{\phi}\,(1+\delta_m) \quad . \end{aligned} \tag{3.39}$$

We can substitute $\left(\bar{H}-H\right)$ and $\left(\dot{\bar{H}}-\dot{H}\right)$ using Eqs. (3.5) and (3.3). Taking the square of Eq. (3.38) and inserting it into Eq. (3.39) we obtain:

$$\begin{aligned} \ddot{\delta}_m &= -2\bar{H}\left(\dot{\delta}_m + \beta\,\delta\dot{\phi}\,(1+\delta_m)\right) \\ &+ \frac{1}{2}\,(1+\delta_m)\sum_\alpha (\delta\rho_\alpha + 3\delta p_\alpha) + \frac{4}{3}\,\frac{\dot{\delta}_m^2}{1+\delta_m} \\ &+ \frac{2}{3}\beta\,\delta\dot{\phi}\,\dot{\delta}_m + \frac{1}{3}\,(1+\delta_m)\,\beta^2\,\delta\dot{\phi}^2 \\ &- \beta\,\delta\ddot{\phi}\,(1+\delta_m) \end{aligned} \tag{3.40}$$

This is the evolution equation for the density contrast $\delta_m$, as derived directly from spherical collapse applied to coupled quintessence. Usually, one considers only cold components to actually cluster, reducing the sum in Eq. (3.40) to one over CDM only. For the moment we still allow for an inhomogenous scalar field and therefore also for nonvanishing $\delta\rho_\phi$ and $\delta p_\phi$.

The evolution of $\delta\phi = \phi - \bar{\phi}$ is determined by combining the Klein-Gordon equations for the bubble (3.30) with that of the FRW background (3.15):

$$\begin{aligned} \delta\ddot{\phi} &= -3\bar{H}\,\delta\dot{\phi} + \left(\frac{\dot{\delta}_m}{1+\delta_m} + \beta\,\delta\dot{\phi}\right)(\dot{\bar{\phi}} + \delta\dot{\phi}) \\ &- \left(U_{,\phi}|_{\phi} - U_{,\phi}|_{\bar{\phi}}\right) + \beta\,\delta\rho_m + \frac{\Gamma_\phi}{\dot{\bar{\phi}} + \delta\dot{\phi}} \end{aligned} \tag{3.41}$$

Again, we remark that Eqs. (3.40) and (3.41) are obtained by applying standard spherical collapse equations (3.3) and (3.5) to coupled quintessence simply by adding a coupling in the conservation equations (3.27) - (3.34).

If linearized, Eqs. (3.40) and (3.41) read as shown in the left column of Table 3.1.

In Table 3.1 we compare the equations found for $\ddot{\delta}_m$ and $\delta\ddot{\phi}$ obtained from standard spherical collapse to Eqs. (3.19) and (3.20) obtained from the fully relativistic theory in Newtonian gauge and shown in the central column of Table 3.1. In the right column we display the relativistic equations within the Newtonian limit, corresponding to Eqs. (3.22) and (3.21). Some remarkable problems become evident.

Note that we have chosen to display the relatistic equations in Newtonian gauge to analyze time derivatives of $\delta\phi$ in the spherical collapse equations, as well as to weigh the importance of different terms in the Klein-Gordon equation when going to small scales. One should keep in mind that at large scales, these equations are gauge dependent.

### 3.4.2 Lack of the fifth force in spherical collapse

As compared to both the Newtonian and relativistic equations, major terms are missing in the standard spherical collapse scenario:

- Comparing (a) to (b) and (c) in Table 3.1, no term proportional to $\beta\dot{\bar{\phi}}$ appears. Depending on the strength of the coupling $\beta$, this term, originating in momentum conservation, can be of great relevance. For $\beta \sim 1$, it can significantly alter structure formation when correctly considered in the vectorial velocity equations, as shown in [Baldi et al., 2010]. For large couplings, as e.g. in a growing neutrino scenario we will discuss later, it is less important, since the cosmon $\bar{\phi}$ is almost constant at late times. Comparing (g) to (h) and (i), one notices a sign reversal in front of a friction-like term. This will also lead to wrong results.

- Comparing (a) to (b) and (c), as well as (g) to (h), in Table 3.1, terms proportional to $\beta k^2\delta\phi$ are absent in the spherical collapse equations; this term is exactly what provides the fifth force. Its absence in (g) leads to a sign reversal of $\beta^2\,\delta\rho_{m,L}$ as compared to (i), thus yielding an incorrect effective Newton's constant.

- Comparing (d) to (e) and (f) in Table 3.1, terms proportional to $k^2\delta\phi$ are absent in the spherical collapse equations; remarkably, this term does not depend on $\beta$ and is therefore missing even in the uncoupled quintessence scenario.

The lack of terms proportional to $\beta k^2 \delta\phi$ leads to a description which does not correspond to the desired coupled quintessence scenario: indeed, these are exactly the terms responsible for the fifth force, originating in (3.22) and leading to an effective gravitational force as in Eq. (3.26). In other words, we point out that the standard spherical collapse, as used for example in [Nunes and Mota, 2006] does not include the main ingredient of coupled quintessence. A fifth attractive force acting between CDM particles and mediated by the cosmon is absent, although densities are indeed coupled to each other as in (3.28) - (3.30). The reason for this can be seen as follows: spherical collapse is by construction based on gravitational dynamics and cannot account for other external forces unless appropriately modified. The dynamics in the spherical collapse models are governed by the usual Friedmann equations, which are particular formulations of Einstein's field equations. Hence, only gravitational forces determine the evolution of the different scale factors and, in turn, of the density contrast. We note that, though in the limit of small couplings the difference can be small, for strongly coupled scenarios a completely different evolution is obtained. This is simply connected to the fact that for small couplings gravity is still the crucial ingredient to fuel the collapse.

### 3.4.3 Inhomogeneity of the scalar field

The issue of whether the scalar field should be considered to be homogeneous (with the cosmon inside the top hat given by the homogeneous background field) or not has also been addressed in literature. In particular, one could try to compare a homogenous scalar field $\phi$ to an inhomogeneous one by appropriately fixing $\Gamma_\phi$ in Eq.(3.30) to the expression (3.34) and (3.32) respectively. This comparison led, for example, [Nunes and Mota, 2006] to find differences between the homogenous and inhomogeneous cases.

The difference found following such procedure is, however, not caused by the fifth force, which, as shown, is not present. Even without any fifth force or coupling, we have noticed in Table 3.1, comparing (d) to (e), that terms proportional to $k^2\delta\phi$ are absent in the spherical collapse equations.

Evaluating the clustering $\delta\phi$ using a spherical collapse scenario as given by (d) in Table 3.1, leads to effects which do not correspond to the relativistic behavior. In fact, in absence of the term $-k^2\delta\phi$, spherical collapse overestimates the time dependence of the scalar field perturbations as soon as $\delta\phi$ is assumed to be different from zero: if, for example, $\delta\phi_{\rm in} > 0$ initially, the $\delta\ddot{\phi}$ obtained from the bottom left equation (d) in Table 3.1, is bigger than it would be if the term $-k^2\delta\phi$ appearing in the relativistic equations was actually present. Hence, within spherical collapse, all time derivatives of the

cosmon are overestimated and, as a consequence, $\ddot{\delta}_m$ is incorrectly reduced.

We remark that this reasoning also applies to ordinary, uncoupled quintessence. Here the question of (in)homogeneities in the scalar field was addressed in various works, e.g. [Mota and van de Bruck, 2004, Maor and Lahav, 2005, Wang, 2006, Dutta and Maor, 2007, Mota et al., 2008a]. Also in this case, one may gain some insight by considering the equations in Table 3.1, now for $\beta = 0$. In the relativistic description, scalar field perturbations will decay due to the presence of the term $-(k/a)^2\delta\phi$, until the latter may eventually be countered by gravitational contributions. In the spherical collapse, however, this decay is only driven by the scalar mass term $-U_{,\phi\phi}\delta\phi$. For a light scalar field and/or sufficiently small scales, this term is smaller than the missing term $-(k/a)^2\delta\phi$ and therefore scalar field inhomogeneities are incorrectly overestimated. The error may be substantially reduced if heavy scalar fields are considered. In this case, the presence of the large mass term $V''(\phi)\delta\phi$ in the perturbed Klein-Gordon equation may make up for the lack of spatial gradients.

In conclusion, we have shown that applying the spherical collapse equations to coupled quintessence by merely modifying the conservation equations can lead to results which do not correspond to the wanted cosmological scenario: this procedure in fact not describe the nonlinear evolution in CQ. It is, however, possible to amend the above model to properly include the fifth force whenever a coupling is present. In order to illustrate and justify that, we consider the nonlinear hydrodynamical evolution equations within coupled quintessence scenarios.

## 3.5 Hydrodynamical spherical collapse

In uncoupled, purely gravitational cosmologies the spherical collapse can be derived from the hydrodynamical Navier-Stokes equations. This is a consequence of the fact that the Friedmann equations in presence of nonrelativistic components can be derived from Newtonian gravity. We will demonstrate now that this is also possible in the presence of external forces.

In order to derive the correct formulation in coupled quintessence, we consider the full nonlinear evolution equations in coupled cosmologies within

the Newtonian limit:

$$\begin{aligned}
\dot{\delta}_m &= -\mathbf{v}_m \nabla\delta_m - (1+\delta_m)\,\nabla\cdot\mathbf{v}_m && (3.42)\\
\dot{\mathbf{v}}_m &= -(2\bar{H} - \beta\,\dot{\bar{\phi}})\,\mathbf{v}_m - (\mathbf{v}_m\nabla)\mathbf{v}_m \\
&\quad -a^{-2}\,\nabla(\Phi - \beta\,\delta\phi) && (3.43)\\
\Delta\delta\phi &= -\beta\,a^2\,\delta\rho_m && (3.44)\\
\Delta\Phi &= -\frac{a^2}{2}\sum_\alpha \delta\rho_\alpha && (3.45)
\end{aligned}$$

These equations can be derived both from the nonrelativistic Navier-Stokes equations and from the Bianchi identities in the appropriate limit in presence of an external source [Kodama and Sasaki, 1984].

$$\nabla_\gamma T^\gamma_\mu = Q_\mu = -\beta T^\gamma_\gamma \partial_\mu\phi \quad , \tag{3.46}$$

where $T^\gamma_\mu$ is the stress energy tensor of the dark matter fluid. They are valid for arbitrary quintessence potentials as long as the scalar field is sufficiently light, i.e. $m^2_\phi\delta\phi = V''(\phi)\delta\phi \ll \Delta\delta\phi$ for the scales under consideration. For a more detailed discussion of the equations, see [Wintergerst et al., 2010, Wintergerst, 2009]. We are working in comoving spatial coordinates $\mathbf{x}$ and cosmic time $t$. The sign in Eq. (3.45) was chosen to match Eq. (3.25). Note that $\mathbf{v}_m$ is the comoving velocity, related to the peculiar velocities by $\mathbf{v}_m = \mathbf{v}_{pec}/a$. The sum in Eq.(3.45) is to be taken over all clustering components; as an important consequence of the Newtonian limit, the cosmon is explicitly excluded.

In order to obtain a correct description of the spherical collapse model, we are interested in the evolution of a top hat, spherically symmetric around $\mathbf{x} = 0$. We note that the below derivation is not limited to a top hat but holds for the amplitude at $\mathbf{x} = 0$ for generic spherically symmetric profiles. From simple symmetric arguments we may infer

$$\nabla\delta_m|_{\mathbf{x}=0} = \mathbf{v_m}(0,t) = 0 \quad , \tag{3.47}$$

which changes (3.42) to

$$\dot{\delta}_m\Big|_{\mathbf{x}=0} = -\left[(1+\delta_m)\,\nabla\cdot\mathbf{v}_m\right]|_{\mathbf{x}=0} \quad . \tag{3.48}$$

We now want to relate Eqs. (3.42)-(3.45) to the spherical infall: it is therefore useful to combine (3.42) and (3.43) to give a second order equation for $\delta_m$, taken at $\mathbf{x} = 0$

$$\ddot{\delta}_m\Big|_{\mathbf{x}=0} = \left.\frac{\dot{\delta}^2_m}{1+\delta_m}\right|_{\mathbf{x}=0} - \left[(1+\delta_m)\,\nabla\cdot\dot{\mathbf{v}}_m\right]|_{\mathbf{x}=0} \quad , \tag{3.49}$$

where we have used (3.47) and (3.48). Inserting the divergence of (3.43) yields

$$\begin{aligned}\ddot{\delta}_m\Big|_{\mathbf{x}=0} &= -(2\bar{H}-\beta\,\dot{\bar{\phi}})\,\dot{\delta}_m\Big|_{\mathbf{x}=0} \\ &+ \left[\frac{\dot{\delta}_m^2}{1+\delta_m}+\frac{1+\delta_m}{a^2}\,\Delta\Phi_{\rm eff}\right]\Bigg|_{\mathbf{x}=0} \\ &+ (1+\delta_m)\nabla(\mathbf{v}_m\,\nabla)\mathbf{v}_m|_{\mathbf{x}=0} \quad . \end{aligned} \tag{3.50}$$

Note that $\Phi_{\rm eff}$ is defined as in (3.24) and obeys the Laplace equation (3.25), as can be seen by combining (3.44) and (3.45). The first three terms in (3.50) can be evaluated straightforwardly at $\mathbf{x}=0$. To rewrite the last term we use the identity

$$\begin{aligned}\nabla(\mathbf{v}_m\,\nabla)\mathbf{v}_m|_{\mathbf{x}=0} &= \frac{1}{3}\,(\nabla\cdot\mathbf{v}_m)^2\big|_{\mathbf{x}=0} \\ &= \frac{1}{3}\,\frac{\dot{\delta}_m^2}{(1+\delta_m)^2}\Bigg|_{\mathbf{x}=0}\end{aligned} \tag{3.51}$$

which holds for spherically symmetric situations and is rederived in the Appendix. Inserting this into expression (3.50) yields the final expression for the evolution of the top hat density amplitude (writing $\delta$ instead of $\delta|_{\mathbf{x}=0}$)

$$\begin{aligned}\ddot{\delta}_m &= -(2\bar{H}-\beta\,\dot{\bar{\phi}})\,\dot{\delta}_m \\ &+ \frac{4}{3}\frac{\dot{\delta}_m^2}{1+\delta_m}+\frac{1+\delta_m}{a^2}\,\Delta\Phi_{\rm eff} \quad . \end{aligned} \tag{3.52}$$

Linearization leads to:

$$\ddot{\delta}_{m,L} = -(2\bar{H}-\beta\,\dot{\bar{\phi}})\,\dot{\delta}_{m,L}+a^{-2}\,\Delta\Phi_{\rm eff} \quad , \tag{3.53}$$

which corresponds to the relativistic equation (3.21). Here we recall that the effective gravitational potential, given by (3.24), follows the modified Poisson equation (3.25) which we rewrite here for convenience:

$$\Delta\Phi_{\rm eff} = -\frac{a^2}{2}\bar{\rho}_m\delta_m\left(1+2\beta^2\right) \quad . \tag{3.54}$$

Equations (3.52) and (3.53) are the two main equations which correctly describe the nonlinear and linear evolution for a coupled dark energy model. They describe the dynamics of a spherical top hat as it follows from relativistic perturbation theory in the Newtonian regime and they can be used,

among other things, for estimating the extrapolated linear density contrast at collapse $\delta_c$ in the presence of a fifth force. To our knowledge it is the first time that the second order equations (3.52) and (3.53) are presented in this way.

We will now demonstrate that we may easily reformulate Eqs. (3.52) and (3.53) into an effective spherical collapse: we can combine them to derive an equation for the radius $r$ which extends Eq.(3.3) to the case of coupled dark energy. To do so, we consider a spherical bubble of radius $r$ containing the CDM overdensity $\delta_m$. Particle number conservation yields

$$1 + \delta_{n,m} = (1 + \delta_{n,m,\mathrm{in}}) \left(\frac{r_{\mathrm{in}}}{a_{\mathrm{in}}}\right)^3 \left(\frac{a}{r}\right)^3 \quad , \tag{3.55}$$

where $n$ is the number density of CDM particles and $\delta_n \equiv \delta n/n$.

We demand the scale factors $r$ and $a$ to be equal initially, i.e. $a_{\mathrm{in}} = r_{\mathrm{in}}$. Further, we assume that the mass of CDM particles is the same inside the bubble and in the background. Note that this is not a limitation, but merely a prescription that we have employed in order to obtain an equation for the scale factor $r$ in a form which is analogous to the original Friedmann equation (3.3). We obtain

$$1 + \delta_m = (1 + \delta_{m,\mathrm{in}}) \left(\frac{a}{r}\right)^3 \quad . \tag{3.56}$$

The first and second time derivatives of $\delta_m$ then read

$$\dot{\delta}_m = 3\,(1+\delta_m)\left(\frac{\dot{a}}{a} - \frac{\dot{r}}{r}\right) \quad , \tag{3.57}$$

$$\begin{aligned} \ddot{\delta}_m &= 3\,(1+\delta_m)\left(\frac{\ddot{a}}{a} - \frac{\ddot{r}}{r} + \left(\frac{\dot{r}}{r}\right)^2 - \left(\frac{\dot{a}}{a}\right)^2\right) \\ &\quad + \frac{\dot{\delta}_m^2}{1+\delta_m} \quad , \end{aligned} \tag{3.58}$$

which we can combine appropriately to yield

$$\ddot{\delta}_m = -2\bar{H}\,\dot{\delta}_m + \frac{4}{3}\,\frac{\dot{\delta}_m^2}{1+\delta_m} + 3(1+\delta_m)\left(\frac{\ddot{a}}{a} - \frac{\ddot{r}}{r}\right) \quad . \tag{3.59}$$

Comparison to (3.52) and insertion of the background Friedmann equation (3.2) gives the evolution equation for the bubble radius

$$\begin{aligned} \frac{\ddot{r}}{r} &= -\beta\,\dot{\bar{\phi}}\left(\bar{H} - \frac{\dot{r}}{r}\right) - \frac{1}{6}\sum_\alpha \left[\bar{\rho}_\alpha(1+3\bar{w}_\alpha)\right] \\ &\quad - \frac{1}{3}\,\beta^2\,\delta\rho_m \quad . \end{aligned} \tag{3.60}$$

Equation (3.60), equivalent to the one used in [Mainini and Bonometto, 2006], describes the general evolution of the radius of a spherical overdense region within coupled quintessence. Comparing with the Friedmann equation (3.3) we notice the presence of two additional terms: a friction term and the coupling term $\beta^2\,\delta\rho_m$; the latter is precisely the term responsible for the additional attractive fifth force. Note that the "friction" term is velocity dependent and its effects on collapse depend, more realistically, on the direction of the velocity [Baldi et al., 2010], information which is not contained within a *spherical* collapse picture.

We conclude that one may indeed apply the spherical collapse model to coupled dark energy scenarios. However, it is crucial to include the additional force term in the equations.

Note that the outlined procedure can easily be generalized to include uncoupled components, for example baryons. In this case, the corresponding evolution equation for $\delta_b$, will be fed by $\Phi_{\rm eff} = \Phi$. This yields an evolution equation for the uncoupled scale factor $r_{uc}$ that is equivalent to the regular Friedmann equation (3.3).

### 3.5.1 Methods and initial conditions

To provide maximum stability and to rule out a dependence on initial conditions, we directly integrate Eqs. (3.52) and (3.53) for the nonlinear and linear density contrasts, together with the corresponding background equations and the Klein-Gordon equation (3.15) for the scalar field. The radial parameter $r(z)$ may equivalently be obtained by integrating Eq. (3.60) or by directly applying the relation (3.56). The following initial conditions at the initial redshift $z_{\rm in}$ were imposed:

- $\delta_{m,{\rm in}} = \delta_{m,L,{\rm in}}$
- $\dot{\delta}_{m,L,{\rm in}} = 3(1+\delta_{m,L,{\rm in}})(\bar{H}_{\rm in} - H_{\rm in}) = 0$, as initially the Hubble functions of background and overdensity evaluate to the same value.

The value of the extrapolated linear density contrast at collapse $\delta_c$ can be obtained by stopping the evolution of Eq.(3.53) when $\delta_m$ as obtained from (3.52) goes to infinity, i.e. the overdensity collapses. If we then vary the initial conditions, leading to different collapse redshifts $z_c$, we arrive at a redshift dependent expression for this critical density, $\delta_c = \delta_c(z_c)$. Equivalently, one may vary the initial redshift $z_{\rm in}$, keeping $\delta_{m,{\rm in}}$ fixed. To be sure of starting the integration when densities are still linear, we find that it is necessary to work in a range of initial overdensities with $\delta_{m,{\rm in}} < 10^{-3}$.

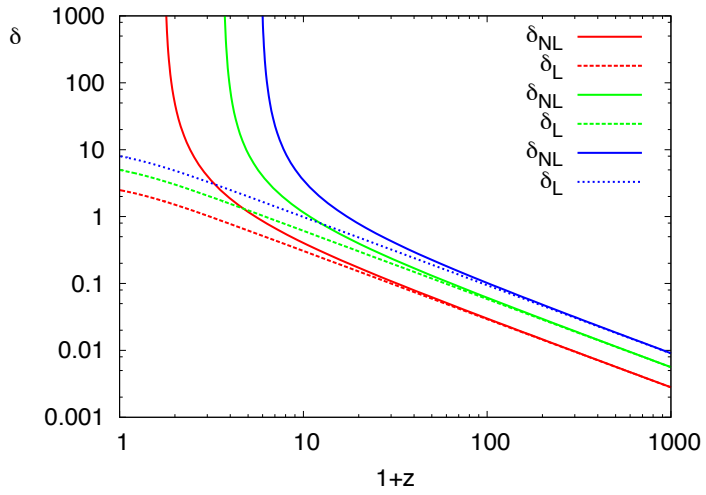


Figure 3.6: CDM linear and nonlinear perturbations for different initial conditions.

### 3.5.2 Results

We depict the evolution of $\delta_m(z)$ and $\delta_{m,L}(z)$ for different initial redshifts in Fig. 3.6. For this plot, we used sample parameters $\alpha = 0.1$ and $\beta = 0.1$. We have also plotted the linear density contrast at collapse $\delta_c(z_c)$ for three coupled quintessence models with $\alpha = 0.1$ and $\beta = 0.05$, 0.1 and 0.15 in Fig. 3.7. We note that these as well as all subsequent results are valid under the hypothesis in which the linear extrapolation traces the nonlinear behavior when a fifth force is present.

As opposed to the results found in [Nunes and Mota, 2006], no oscillations are seen in $\delta_c(z_c)$. Furthermore, the effect of the coupling on the extrapolated linear density contrast at collapse is smaller, though we observe an increase of $\delta_c$ with increasing coupling strength $\beta$, as depicted in Fig.3.8 for two collapse redshifts $z_c = 0$ and $z_c = 5$. A coupling $\beta = 0$ corresponds to a $\Lambda$CDM cosmology, hence the observed $\delta_c$ is given by $\delta_c = 1.686$ for z $z_c = 5$ and by the accordingly reduced value for $z_c = 0$. An increase of $\beta$ results in an increase of $\delta_c$ for both redshifts. The reason for this increase is quite simple. In Eqs.(3.52) and (3.53) two terms lead to an enhanced growth: the fifth force term in the effective potential and the reduction of the damping $-\beta\dot{\phi}$. In the linear equation, they are always of comparable strength. In Eq.(3.52), however, the damping will be negligible once $\delta_m \sim 1$ as it only enters the equation linearly. The enhancement of growth is then weaker than in the

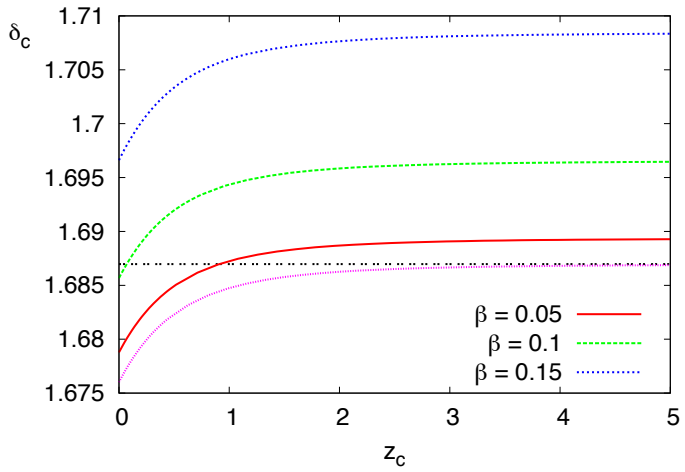


Figure 3.7: Extrapolated linear density contrast at collapse for coupled quintessence models with different coupling strength $\beta$. For all plots we use a constant $\alpha = 0.1$. We also depict $\delta_c$ for reference $\Lambda$CDM (dotted, pink) and EdS (double-dashed, black) models.

linear equation and $\delta_c$ grows with increasing $\beta$.

For small $\beta \lessapprox 0.4$, $\delta_c(\beta)$ at $z_c \geq 5$ is well described by a simple quadratic fitting formula,

$$\delta_c(\beta) = 1.686(1 + a\beta^2)\,, a = 0.556 \quad . \tag{3.61}$$

For larger $\beta \leq 1$ a fit requires an additional correction and reads

$$\delta_c(\beta) = 1.686(1 + a\beta^2 - b\beta^4),\ a = 0.556,\ b = 0.107 \quad . \tag{3.62}$$

It is worth noting that our values of $\delta_c$ were obtained under the assumption that baryonic contributions may be neglected, in order to be able to relate the results to the simple Einstein de Sitter scenario. Indeed, a numerical analysis under inclusion of a baryonic component shows a quite significant increase of the critical density contrast $\delta_c$, leading to values close to those found in [Mainini and Bonometto, 2006].

Also note that we have limited our analysis to the critical density contrast at collapse. Other works [Angrick and Bartelmann, 2010] have rather focused on the respective quantities at virialization. Since there are no fundamental differences, these may as easily be evaluated within our formalism.

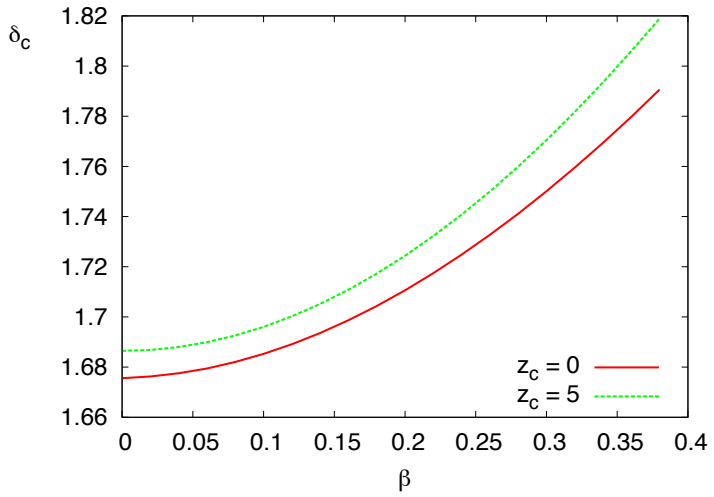


Figure 3.8: Extrapolated linear density contrast at collapse $\delta_c$ for coupled quintessence models as a function of coupling strength $\beta$, evaluated for two different collapse redshifts $z_c = 0$ (solid, red) and $z_c = 5$ (long-dashed, green).

## 3.6 Growing neutrinos

Another interesting framework, analogous to coupled quintessence, in which a fifth force is present, is the growing neutrinos scenario [Amendola et al., 2008, Wetterich, 2007]. Here, relic neutrinos obtain a growing, cosmon dependent mass, implemented by a large, negative coupling $\beta$. In this context, dark energy domination and the late acceleration of the Universe can be naturally explained by relating it to a "trigger event", the recent transition of neutrinos to the nonrelativistic regime.

### 3.6.1 Cosmological model

As neutrinos have been relativistic particles through most of the history of the Universe, Eqs. (3.15), (3.18) and (3.18) are appropriately altered to include neutrino pressure

$$\dot{\bar{\rho}}_\phi = -3\bar{H}(1+\bar{w}_\phi)\bar{\rho}_\phi + \beta\,\dot{\bar{\phi}}\,(1-3\bar{w}_\nu)\bar{\rho}_\nu \tag{3.63}$$

$$\dot{\bar{\rho}}_\nu = -3\bar{H}(1+\bar{w}_\nu)\bar{\rho}_\nu - \beta\,\dot{\bar{\phi}}\,(1-3\bar{w}_\nu)\bar{\rho}_\nu \tag{3.64}$$

$$\ddot{\bar{\phi}} = -3\bar{H}\dot{\bar{\phi}} - \frac{dU}{d\bar{\phi}} + \beta(1-3\bar{w}_\nu)\bar{\rho}_\nu \quad . \tag{3.65}$$

As opposed to the models of coupled CDM discussed above, the constant $\beta$ is now negative and its modulus much larger than one. Bounds for the couplings $\alpha$ and $\beta$ have been discussed in [Doran et al., 2007, Amendola et al., 2008]. For the following analysis we choose $\alpha = 10$ and several values for the coupling $\beta = -52$, $-112$ and $-560$. Note that the couplings may be related to the present neutrino mass via

$$m_\nu(t_0) = -\frac{\alpha}{\beta}\,\Omega_\phi(t_0)\,16\text{ eV} \quad , \tag{3.66}$$

where $\Omega_\phi$ is the dark energy density fraction today.

A numerical integration of (3.63) - (3.65) and the appropriate equations for radiation and CDM leads to the background evolution depicted in Fig. 3.9. While the cosmon is on the matter (radiation) attractor at early times, the transition of neutrinos to the nonrelativistic regime almost stops the evolution of the cosmon. The dark energy density is able to overcome all other components and dominates the Universe at $t = t_0$. As the kinetic contribution to the cosmon energy density is greatly reduced, the latter is dominated by the potential $V(\bar{\phi})$, successfully mimicking the behavior of a cosmological constant.

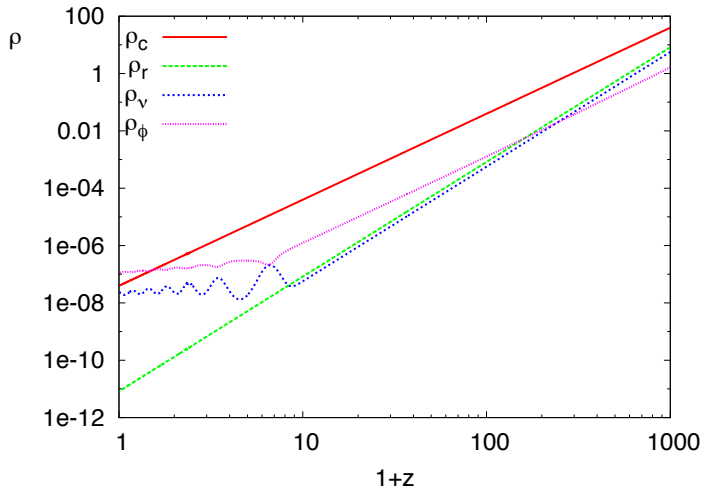


Figure 3.9: Energy densities of neutrinos (solid, red), cold dark matter (long dashed, green), dark energy (dot-dashed, blue) and photons (short dashed, black) are plotted vs redshift. We use a sample model with constant $\beta = -52$, $\alpha = 10$ and a large average neutrino mass $m_\nu = 2.11$ eV.

### 3.6.2 Spherical collapse and growing neutrinos

We have applied our method to the case of growing neutrino quintessence. To our knowledge this is the first time that spherical collapse is performed on this class of models.

Because of the strong cosmon-mediated attractive force between neutrinos, bound neutrino structures may form within these models [Brouzakis et al., 2008]. It was shown in [Mota et al., 2008b] that their formation will only start after neutrinos become nonrelativistic. A nonlinear treatment of the evolution of neutrino densities is thus only required for very late times, and one may safely neglect neutrino pressure as compared to their density, which substantially simplifies the scenario. All calculations of the previous sections are thus equally valid for the growing neutrinos scenario; we can straightforwardly apply the evolution equations (3.52) and (3.53) for the nonlinear and linear neutrino density contrast.

In Fig.3.10 we plot the evolution of the nonlinear density contrast as obtained from numerically solving Eq. (3.52) for a model with $\beta = -52$. The linear density contrast, solution of Eq. (3.53), is also shown. For comparison, we have also included the linear density contrast resulting from the full relativistic equations as given in [Mota et al., 2008b]. The results of the linearized spherical collapse and the relativistic theory can be seen to agree remarkably well. Comparison with the full hydrodynamic results from Ref.[Wintergerst et al., 2010] also yields a one-to-one agreement, as expected since the latter is the basis for the present work. The slight deviation around redshift $z \sim 1.5$ can be accounted for by a short recuperation of neutrino pressure at this time. However, no significant impact on the extrapolated linear density contrast $\delta_c$ was found.

In order to illustrate the dependence of the growth of the overdensity on the coupling $\beta$, we show the evolution of $\delta_\nu(z)$ and $\delta_{\nu,L}(z)$ in Fig. 3.11 for the three given couplings $\beta = -52$, $-112$, $-560$ and $\alpha = 10$. Given a fixed self-interaction $\alpha$, a larger $\beta$ corresponds to a smaller present neutrino mass; as a consequence, neutrinos become nonrelativistic at smaller redshifts $z_{\rm NR}$. In the relativistic regime, no growth of neutrino perturbations is observed in the linear regime. To comply with this, we only start the integration of the spherical collapse equations once the transition to the nonrelativistic regime is observed at redshift $z_{\rm NR}(\beta)$. It can be observed in Fig.3.11 that a higher $\beta$ leads to a strongly enhanced growth of the density contrast. On the other hand, because of the later transition to the nonrelativistic regime, perturbations start to grow at much lower redshifts.

The extrapolated linear density at collapse $\delta_c$ for growing neutrino quintessence reflects in all respects the characteristic features of this model and

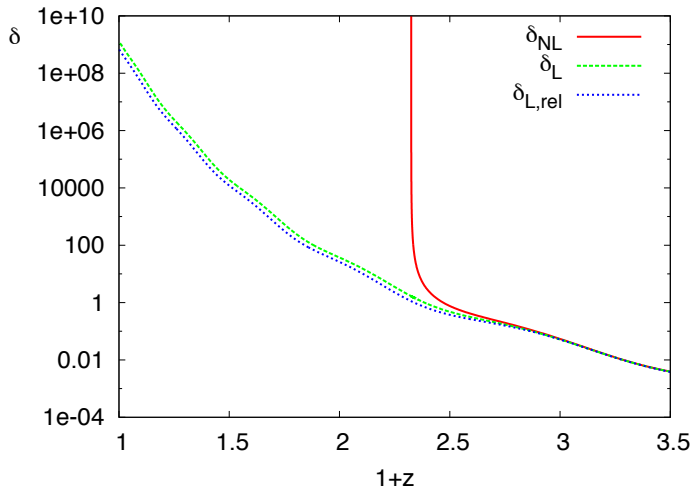


Figure 3.10: Evolution of neutrino nonlinear (solid, red) and linear (long-dashed, green) density contrast. For comparison, we have also included the relativistic linear density contrast including pressure terms (short-dashed, blue).

result in a $\delta_c$ which looks quite different from standard dark energy cosmologies. We have plotted the dependence of $\delta_c$ on the collapse redshift $z_c$ in Fig.3.12 for all three couplings.

The oscillations seen are the result of the oscillations of the neutrino mass caused by the coupling to the scalar field: the latter has characteristic oscillations as it approaches the minimum of the effective potential in which it rolls, given by a combination of the self-interaction potential $U(\phi)$ and the coupling contribution $\beta(1-3\bar{w}_\nu)\bar{\rho}_\nu$. Furthermore, due to the strong coupling $\beta$, the average value of $\delta_c$ is found to be substantially higher than 1.686. Such an effect can have a strong impact on structure formation and $\delta_c$ can then be used within a Press-Schechter formalism.

For the strongly coupled models, corresponding to a low present day neutrino mass $m_\nu(t_0)$, the critical density at collapse is only available for $z_c \lesssim 0.2$, 1 for $\beta = -560$, $-112$, respectively. This is again a reflection of the late transition to the nonrelativistic regime.

A full nonlinear investigation of single lumps within growing neutrino quint-essence was performed in [Wintergerst et al., 2010].

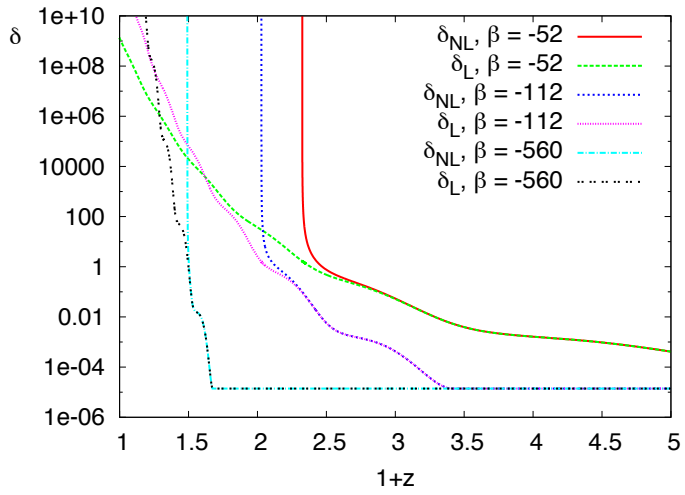


Figure 3.11: Evolution of neutrino nonlinear / linear density contrast for $\alpha = 10$ and $\beta = -52$ (solid, red / long-dashed, green), $\beta = -112$ (short-dashed, blue / dotted, pink) and $\beta = -560$ (dot-dashed, light blue / double-dashed, black). The chosen couplings correspond to a present average neutrino mass of $m_\nu(t_0) = 2.1$ eV, 1 eV and 0.2 eV, respectively.

## 3.7 Early dark energy

### 3.7.1 Cosmological model

A convenient way to parametrize the presence of a nonnegligible homogenous dark energy component at early times (from now on labeled as EDE) was presented in [Wetterich, 2004]. Here, the dark energy density is

$$\bar{\rho}_{\mathrm{DE}}(z) = \bar{\rho}_{\mathrm{DE},0}\,(1+z)^{3(1+\bar{w}_h(z))} \quad , \tag{3.67}$$

with

$$\bar{\rho}_{\mathrm{DE},0} = \bar{\rho}_{crit,0}\,\Omega_{\mathrm{DE},0} = 3\bar{H}_0^2\,(1-\Omega_{m,0}) \tag{3.68}$$

and the equations of state parametrized by:

$$\bar{w}_h(z) = \frac{\bar{w}_0}{1+b\ln(1+z)} \quad , \tag{3.69}$$

where $b$ is a constant related to the amount of dark energy present at early times

$$b = -\frac{3\bar{w}_0}{\ln\frac{1-\Omega_{\mathrm{DE},e}}{\Omega_{\mathrm{DE},e}} + \ln\frac{1-\Omega_{m,0}}{\Omega_{m,0}}} \quad . \tag{3.70}$$

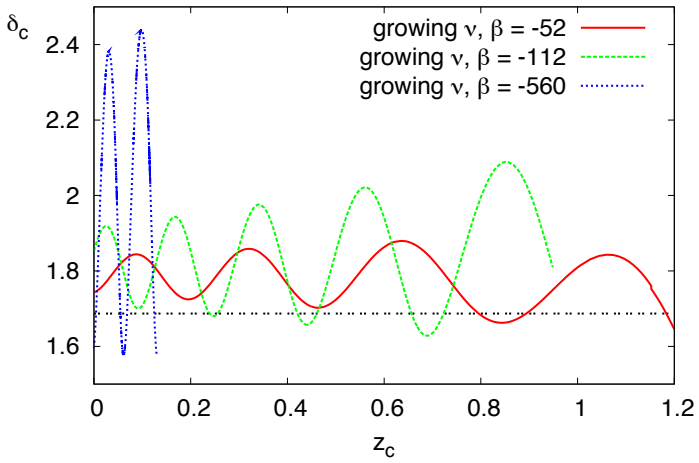


Figure 3.12: Extrapolated linear density contrast at collapse $\delta_c$ vs. collapse redshift $z_c$ for growing neutrinos with $\beta = -52$ (solid, red), $\beta = -112$ (long-dashed, green) and $\beta = -560$ (short-dashed, blue). A reference EdS model (double-dashed. black) is also shown.

Here the subscripts "0" and "$e$" refer to quantities calculated today or early times, respectively. Dark energy pressure is given by $p_{\rm DE}(z) = \bar{w}_h(z)\,\bar{\rho}_{\rm DE}(z)$. If we specify the spherical collapse equations for this case, the nonlinear evolution of the density contrast follows the evolution equations (3.52) and (3.53) without the terms related to the coupling:

$$\ddot{\delta}_m = -2\bar{H}\dot{\delta}_m + \frac{4}{3}\frac{\dot{\delta}_m^2}{1+\delta_m} + \frac{1}{2}\delta_m(1+\delta_m)\bar{\rho}_m \quad , \tag{3.71}$$

$$\ddot{\delta}_{m,L} = -2\bar{H}\dot{\delta}_{m,L} + \frac{1}{2}\delta_{m,L}\,\bar{\rho}_m \quad . \tag{3.72}$$

As before, we assume relativistic components to remain homogenous.

### 3.7.2 Spherical collapse and EDE

In the following we present our results for two models of early dark energy, namely model I and II from [Bartelmann et al., 2006]. Model I is given by the set of parameters

$$\Omega_{m,0} = 0.332\,, \quad w_0 = -0.93\,, \quad \Omega_{{\rm DE},e} = 2\cdot 10^{-4} \quad , \tag{3.73}$$

whereas model II is parametrized by

$$\Omega_{m,0} = 0.314\,, \quad w_0 = -0.99\,, \quad \Omega_{\mathrm{DE},e} = 8 \cdot 10^{-4} \quad . \tag{3.74}$$

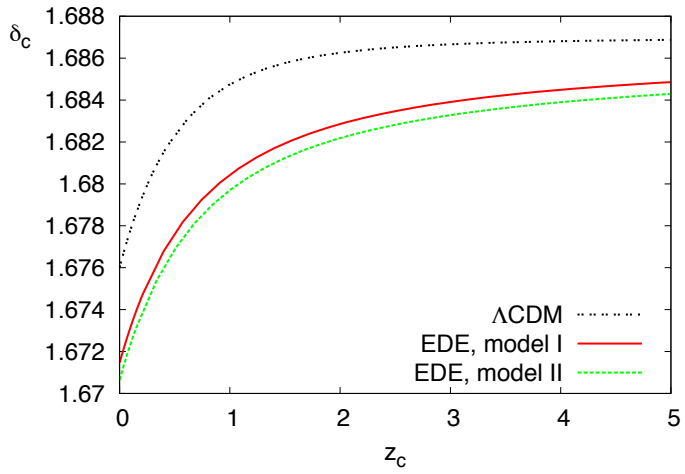


Figure 3.13: Extrapolated linear density contrast at collapse $\delta_c$ vs. collapse redshift $z_c$ for EDE models I (solid, red) and II (long-dashed, green), as well as ΛCDM (double-dashed, black).

Our results for $\delta_c$ in both EDE models are plotted in Fig. 3.13, together with $\delta_c$ in ΛCDM. Coherent with the results of [Francis et al., 2008], we find a suppression of $\delta_c$ as compared to ΛCDM that is much lower than in the original paper [Bartelmann et al., 2006]. More precisely, while the latter found $\delta_c(z_c = 5) \sim 1.62$ for model I, corresponding to a relative change of $\sim 4\%$, we obtain $\delta_c(z_c = 5) \sim 1.685$ ($\sim 5 \cdot 10^{-2}\%$).

## 3.8 Summary

Spherical collapse is a semi analytical method often used to estimate the nonlinear evolution of structures without reverting to complex numerical methods like N-body simulations.

After reviewing its application to standard cosmologies, we have considered the case of coupled dark energy cosmologies, in which a fifth force other than gravity modifies the collapse.

We have shown that the inclusion of the fifth force within the spherical collapse picture deserves particular caution. As spherical collapse is intrinsically based on gravitational attraction via the Friedmann equations, it does not account for other external forces unless it is suitably modified.

We have presented a detailed comparison between the linearized standard spherical collapse picture and the linear relativistic equations, whose results are summarized in Table 3.1. Applying standard spherical collapse equations to coupled dark energy by adding a coupling in the conservation equations is insufficient to describe the coupled dark energy scenario, as the fifth force is still missing entirely from the evolution of the density contrast $\delta$. Results in Table 3.1 also show that a standard treatment of spherical collapse may lead to problems even in the uncoupled case, whenever the scalar field is treated as inhomogeneous.

We have illustrated in detail how a modification of the spherical collapse picture which correctly accounts for the presence of a fifth force is still possible. We have derived the set of second order differential equations for the density contrast from the fully nonlinear Navier-Stokes equations. We have then shown how $\delta_c$ can be evaluate directly from these equations and how the spherical collapse formalism can be reformulated starting from them. Most importantly, we have further checked that our results match the numerical resolution of the nonlinear hydrodynamical equations performed as described in [Wintergerst et al., 2010, Wintergerst, 2009].

We have applied our procedure to coupled quintessence scenarios, evaluating the extrapolated linear density at collapse for this class of cosmologies and showing how it depends on the coupling $\beta$. Furthermore, we have for the first time applied the spherical collapse to the case of growing neutrino quintessence, where neutrinos feel a fifth force interaction that can lead them to cluster at very large scales. In this case, we demonstrate how the extrapolated linear density at collapse shows a characteristic oscillating behavior, different from standard dark energy models. In future work, this result could be used within a Press-Schechter [Press and Schechter, 1974] formalism to estimate neutrino halo mass distributions. We have further commented on the choice of initial conditions, whose choice has to be made with careful attention when dealing with the extrapolated linear density at collapse. Finally we have used our approach to verify results found in [Francis et al., 2008] on spherical collapse and early dark energy (EDE).

| **Spherical collapse** | **Relativistic linear** | **Newtonian linear** |
|---|---|---|
| $\ddot{\delta}_{m,L} = -2\bar{H}\left(\dot{\delta}_{m,L} + \beta\,\delta\dot{\phi}\right) + \frac{1}{2}\sum_{\alpha}(\delta\rho_\alpha + 3\delta p_\alpha) - \beta\delta\ddot{\phi}$ | $\ddot{\delta}_{m,L} = -2\bar{H}\left(\dot{\delta}_{m,L} + \beta\,\delta\dot{\phi}\right) + (k/a)^2\,(\Phi + \beta\,\delta\phi) + \beta\,\dot{\phi}\left(\dot{\delta}_{m,L} + \beta\,\delta\dot{\phi}\right) - 3\dot{\Phi}\left(2\bar{H} - \beta\,\dot{\phi}\right) - 3\ddot{\Phi} - \beta\,\delta\ddot{\phi}$ | $\ddot{\delta}_{m,L} = \left(\beta\,\dot{\phi} - 2\bar{H}\right)\dot{\delta}_{m,L} + (k/a)^2\,(\Phi + \beta\,\delta\phi)$ |
| (a) | (b) | (c) |
| $\delta\ddot{\phi} = -3\bar{H}\delta\dot{\phi} - U_{,\phi\phi}\,\delta\phi + \beta\delta\rho_{m,L} + (\dot{\delta}_{m,L} + \beta\,\delta\dot{\phi})\,\dot{\phi}$ | $\delta\ddot{\phi} = -3\bar{H}\delta\dot{\phi} - U_{,\phi\phi}\,\delta\phi + 4\dot{\phi}\dot{\Phi} + \beta\rho_m\,(\delta_{m,L} + 2\Phi) - (k/a)^2\delta\phi - 2\Phi U_{,\phi\phi}$ | $k^2\,\delta\phi = a^2\,\beta\,\delta\rho_{m,L}$ |
| (d) | (e) | (f) |
| $\ddot{\delta}_{m,L} = \left(-2\bar{H} - \beta\dot{\phi}\right)\dot{\delta}_{m,L} + \bar{H}\beta\,\delta\dot{\phi} - \beta^2\delta\rho_{m,L} + \frac{1}{2}\sum_{\alpha}(\delta\rho_\alpha + 3\delta p_\alpha) - \beta^2\delta\dot{\phi}\dot{\phi} + U_{,\phi\phi}\beta\,\delta\phi$ | $\ddot{\delta}_{m,L} = \left(-2\bar{H} + \beta\dot{\phi}\right)\dot{\delta}_{m,L} + \bar{H}\beta\,\delta\dot{\phi} + (k/a)^2\Phi + 2(k/a)^2\beta\,\delta\phi - \beta^2\delta\rho_{m,L} + \beta^2\,\delta\dot{\phi}\,\dot{\phi} + U_{,\phi\phi}\beta\delta\phi - 3\dot{\Phi}\left(2\bar{H} - \beta\,\dot{\phi}\right) - 3\ddot{\Phi} + 2\beta\Phi U_{,\phi\phi} - 4\beta\dot{\phi}\dot{\Phi}$ | $\ddot{\delta}_{m,L} = \left(\beta\,\dot{\phi} - 2\bar{H}\right)\dot{\delta}_{m,L} + \frac{1}{2}\sum_{\alpha}\delta\rho_\alpha + \beta^2\delta\rho_{m,L}$ |
| (g) | (h) | (i) |

Table 3.1: Comparison between linearized SC and relativistic linear evolution. The third row is a combination of the first two rows.

# Chapter 4

# Massive Spin-2 Theories

## 4.1 Introduction

Massive representations of the $4D$-Poincaré algebra can be labeled by the eigenvalues of the quartic Casimir $W_\mu^2$, where $W_\mu = \epsilon_{\mu\nu\alpha\beta} P^\nu M^{\alpha\beta}$ is the Pauli-Lubanski pseudovector. Here, $P^\mu$ generates the four-dimensional translations and $M^{\alpha\beta}$ are the generators of the Lorentz algebra $\mathfrak{so}(3,1)$. In the rest frame of a massive one-particle state, $W_\mu = (P^0)^2 S_i^2$, where $S_i = \epsilon_{ijk} M_{jk}|_{P_i=0}$ is the spin operator. The eigenvalues of $W_\mu^2$ thus correspond to eigenvalues of the spin and are labeled by integers[1] $s$, with the eigenvalues being $m^2 s(s+1)$.

In the massless limit, the above representation is no longer irreducible. Instead, the representation $s$ decomposes into the irreps $\mathbf{s} \oplus (\mathbf{s-1}) \oplus ... \oplus \mathbf{0}$, where the integers now label the *helicity* of the corresponding massless particles.

One can use this property to construct a simple picture for highly boosted one particle states of massive spin $s$ particles, i.e. $|s, \mathbf{k}\rangle$ with $|\mathbf{k}| \gg \mathbf{m}$. In this high momentum limit, the mixing between helicity eigenstates is suppressed by $m/|\mathbf{k}|$. One can therefore understand the high momentum properties in terms of helicity eigenstates.

Within this chapter, we will make use of this property in order to understand stability, consistency and uniqueness properties of massive spin-2 theories.

A Poincaré invariant consistent theory of massless spin-2, at least at the lowest momentum expansion, must be Einstein's theory [Weinberg, 1964, Ogievetsky and Polubarinov, 1965, Deser, 1970]. Therefore, at least in the low momentum limit, a massless spin-2 theory is unique. Similarly, the lin-

[1] Ignoring the fact that the algebra $\mathfrak{so}(3)$ is isomorphic to $\mathfrak{su}(2)$ and the little group therefore possesses spinorial representations.

earized action of a massive spin-2 field obeys a uniqueness theorem. Only if the mass term is given by the Fierz-Pauli form [Fierz and Pauli, 1939], does the theory consistently describe the propagation of a single massive spin-2 field. It is then natural to ask whether this property survives the addition of self-interactions. As we will see, this is not the case. Instead, we obtain the following picture for massive spin-2 theories:

(i) Generic self-interactions of the massive spin-2 field introduce an additional ghost mode into the theory. This mode is often referred to as the Boulware-Deser ghost.

(ii) In the language of helicities, the ghost mode is manifest in higher derivative interactions of the helicity-0 mode. This presents two possible resolutions to this problem. One can tune the interaction in such a way that higher derivatives are absent. There is a unique way to do so, and the corresponding theory was discovered in [Folkerts et al., 2011]. Or one may introduce a nonlinear structure in such a way that the higher derivatives are in fact redundant and do not lead to instabilities of the Hamiltonian. This is the approach taken in [de Rham et al., 2011b].

### 4.1.1 Helicity decomposition

Before we enter the specifics of massive spin-2 theories, let us make the notion of a helicity decomposition more precise at hand of an example. Let $A_\mu$ be a massive spin one field, described by the Proca Lagrangian

$$\mathcal{L} = -\frac{1}{4}F_{\mu\nu}^2 + \frac{1}{2}A_\mu^2 \,. \tag{4.1}$$

In Fourier space, $A$ can be decomposed as

$$A_\mu = \sum_{\lambda=1}^{3} d^3k \epsilon_{\mathbf{k},\lambda}^\mu A_{\mathbf{k}} \,, \tag{4.2}$$

where the sum extends over the three polarizations defined by the conditions

$$\begin{aligned} \mathbf{k}_\mu \epsilon_{\mathbf{k},\lambda}^\mu &= 0 \ , \\ \epsilon_{\mu;\mathbf{k},\lambda}\epsilon_{\mathbf{k},\lambda}^\mu &= 1 \ . \end{aligned} \tag{4.3}$$

The spatial part of the longitudinal polarization is defined to be parallel to the three-momentum, i.e. $\epsilon_{\mathbf{k},3}^i \propto \mathbf{k}^i$. Explicitly, it takes on the form

$$\epsilon_{\mathbf{k},3}^\mu = \left(\frac{|\mathbf{k}|}{m}, \frac{\mathbf{k}}{|\mathbf{k}|}\frac{E_{\mathbf{k}}}{m}\right) \tag{4.4}$$

For large $|\mathbf{k}|$,

$$\epsilon^{\mu}_{\mathbf{k},3} \approx \frac{1}{m} k^{\mu} \,. \tag{4.5}$$

We can construct one particle states by defining creation and annihilation operators $a^{\lambda}_{\mathbf{k}}$, generating the eigenstates of the non-interacting Hamiltonian. We write

$$A^{\lambda}_{\mu} = \int \frac{d^3k}{\sqrt{2E_{\mathbf{k}}}} \epsilon^{\lambda}_{\mu}(\mathbf{k}) \left( a^{\lambda}_{\mathbf{k}} e^{i\mathbf{k}\cdot\mathbf{x}} + a^{\dagger\lambda}_{\mathbf{k}} e^{-i\mathbf{k}\cdot\mathbf{x}} \right) \,. \tag{4.6}$$

At the same time we can define a new scalar field $\phi$ as

$$\phi = \int \frac{d^3k}{\sqrt{2E_{\mathbf{k}}}} \left[ \left( i a^{(3)}_{\mathbf{k}} \right) e^{i\mathbf{k}\cdot\mathbf{x}} + \left( i a^{(3)}_{\mathbf{k}} \right)^{\dagger} e^{-i\mathbf{k}\cdot\mathbf{x}} \right] \,. \tag{4.7}$$

On an asymptotic state $|\mathbf{k}\rangle$ of four-momentum $k^{\mu}$ one has

$$\partial_{\mu}\phi |\mathbf{k}\rangle = \frac{1}{\sqrt{2E_{\mathbf{k}}}} k_{\mu} \left( a^{(3)}_{\mathbf{k}} e^{i\mathbf{k}\cdot\mathbf{x}} + a^{\dagger(3)}_{\mathbf{k}} e^{-i\mathbf{k}\cdot\mathbf{x}} \right) |\mathbf{k}\rangle \,. \tag{4.8}$$

Henceforth

$$\left( A^{(3)}_{\mu} - \frac{1}{m} \partial_{\mu}\phi \right) |\mathbf{k}\rangle \underset{\mathbf{k}\gg m}{\sim} \frac{m}{|\mathbf{k}|} \hat{k}_{\mu} a^{(3)}_{\mathbf{k}} |\mathbf{k}\rangle \underset{\mathbf{k}\to\infty}{\to} 0 \,. \tag{4.9}$$

Here, $\hat{k}_{\mu}$ is the unit vector pointing in the direction of $\mathbf{k}$. We thus see that the longitudinal polarization in the high energy limit is well described by a scalar field up to corrections $\mathcal{O}\left(\frac{m}{\mathbf{k}}\right)$. This is the essence of the helicity decomposition of the massive vector.

One can understand the scalar as the re-incarnation of the gauge direction of the massless case. To be precise, in the massless case the action is invariant under the gauge transformation

$$A_{\mu} \to A_{\mu} + \frac{\partial_{\mu}\phi}{m} \,, \tag{4.10}$$

for any $\phi$ and some mass scale $m$. In the massive case however $\phi$ represents the extra polarization at high energies as in (4.9). In this case, we can decompose

$$A_{\mu} = \tilde{A}_{\mu} + \frac{\partial_{\mu}\phi}{m} \,. \tag{4.11}$$

As a consequence, $A_{\mu}$, and hence any action constructed from it, is invariant under transformations of $\tilde{A}_{\mu}$ of the type (4.10) (U(1)) if the change is absorbed by a shift in the scalar $\phi$.

Let us now consider a massive spin 2 field $h_{\alpha\beta}$. Similar to the massive vector field discussed above, the properties of this theory can also be investigated

through a helicity or *linear* Stückelberg decomposition. The decomposition in complete analogy to the massive vector. For high energies the helicity-1 component (or vectorial polarizations) can be described by the derivative of a Lorentz vector ($A_\mu$), whereas the helicity-0 component (or longitudinal polarization) can be described by a scalar field $\chi$.The helicity-2 component (the transverse polarizations) is described by a tensor $\tilde{h}_{\mu\nu}$.

One thus decomposes the massive spin-2 field as

$$h_{\mu\nu} = \tilde{h}_{\mu\nu} + \frac{\partial_{(\mu}A_{\nu)}}{m} + \frac{1}{3}\left(\frac{\partial_\mu\partial_\nu\chi}{m^2} + \frac{1}{2}\eta_{\mu\nu}\chi\right) . \tag{4.12}$$

Here we used the symmetrization convention $a_{(\mu}b_{\nu)} = \frac{1}{2}(a_\mu b_\nu + a_\nu b_\mu)$.

### 4.1.2 The coupling to matter

According to the decomposition Eq. (4.11), the longitudinal mode of a Proca field only couples derivatively to sources. In particular, this implies that the massless limit of a Proca field describes *exactly* the same physics as that of a massless vector, iff $A_\mu$ couples only to conserved sources $\partial_\mu J^\mu = 0$. In that case, the helicity-0 mode simply decouples.

The coupling of the longitudinal polarization $\chi$ of a massive spin-2 particle to external sources survives in the massless limit, even if coupled to a conserved energy momentum tensor $\partial_\mu T^{\mu\nu} = 0$ (to lowest order). In terms of helicities, one obtains

$$\frac{1}{M_p}h_{\mu\nu}T^{\mu\nu} = \frac{1}{M_p}\tilde{h}_{\mu\nu}T^{\mu\nu} + \frac{1}{6}\frac{\chi}{M_p}T\,. \tag{4.13}$$

The strength of the source coupling is fixed by demanding that the predictions for light bending in the massless limit are indistinguishable from General Relativity. Since $T_\gamma = 0$, sources couple with strength $1/M_p$.

Now consider the potential between two static probe sources of mass $m_1$ and $m_2$ at sufficiently large distances $r$ in the Born approximation:

$$\begin{aligned} V_{\mathrm{mGR}}(r) &= G_N m_1 m_2 \int d^3p \left(\frac{1}{2}\frac{1}{p^2-m^2} + \frac{1}{6}\frac{1}{p^2-m^2}\right) e^{i\mathbf{pr}} \\ &= \frac{4}{3}G_N m_1 m_2 \frac{e^{-mr}}{r} \\ &\xrightarrow[m\to 0]{} \frac{4}{3}\frac{G_N m_1 m_2}{r}\,. \end{aligned} \tag{4.14}$$

Comparing this with the prediction of GR

$$V_{\mathrm{GR}}(r) = \frac{G_N m_1 m_2}{r}\,, \tag{4.15}$$

we see that, in the linear approximation, the gravitational attraction between two static bodies is stronger than in GR no matter how small the mass, unless one gives up the correct predictions for light bending. This property is known as the vDVZ discontinuity [van Dam and Veltman, 1970, Zakharov, 1970][2]. However, it was realized that the linear approximation breaks down at a distance from the source proportional to the inverse mass, the so-called Vainshtein radius. In turn, taking nonlinearities into account yields an effective source-source coupling which can be phenomenologically acceptable [Vainshtein, 1972]. In terms of $h_{\mu\nu}$, this can be understood from the $m^{-2}$ and $m^{-4}$ contributions to the propagator from the longitudinal mode (cf. Eq.(4.5)) [Deffayet et al., 2002]. In terms of helicities, it can be associated to the nonlinearities of $\chi$ that become strong at the Vainshtein radius [Arkani-Hamed et al., 2003]. The precise mechanism that suppresses the fifth force on sufficiently small scales depends on the theory at hand. It may be due to the exchange of a ghost mode [Deffayet and Rombouts, 2005] or due to an enhancement of the kinetic term on the induced background. There, canonically normalizing its fluctuations leads to suppression of the coupling to the source [Luty et al., 2003a]. More on the Vainshtein mechanism, its application and viability in massive gravity theories and matching of solutions can be found, for example, in [Hinterbichler, 2012, Babichev and Deffayet, 2013] (see also references therein).

### 4.1.3 The problem of ghost instabilities

Before entering into details of free and interacting massive spin-2 theories, let us briefly review the problem of ghost instabilities.

Ghosts are fields that enter the action with a wrong sign kinetic term. In canonical quantization, they appear in the Hamiltonian with a negative sign in front of their according number operator:

$$\hat{H}_{\text{ghost}} \sim \int d^3k \, (-E_{\mathbf{k}}) \, a^\dagger_{\mathbf{k}} a_{\mathbf{k}} \tag{4.16}$$

where we have suppressed all possible labels but the momenta and assumed the existence of positive energy contributions to the Hamiltonian. Otherwise, one could simply reverse the sign. If one now defines the vacuum state the usual way, via $a_{\mathbf{k}} |0\rangle = 0$, one obtains for number eigenstates $\hat{H} |N_{\mathbf{k}}\rangle \sim -N_{\mathbf{k}} E_{\mathbf{k}} |N_{\mathbf{k}}\rangle$. The energy can be lowered arbitrarily and the previously defined vacuum state is not the lowest energy state! In fact, a lowest

[2]Note that this problem does not persist in asymptotically de Sitter or Anti-de Sitter space. For a nonvanishing cosmological constant, the limit is indeed smooth [Kogan et al., 2001, Porrati, 2001].

energy does not exist; the Hamiltonian is unbounded. Of course, in a free theory, $|0\rangle$ is still an energy eigenstate. Upon introduction of interactions, however, it will become hopelessly unstable.

One could try to make the Hamiltonian positive definite by interchanging the role of creation and annihilation operators. This amounts to changing the canonical commutation relations to

$$[a_{\mathbf{k}}, a^{\dagger}_{\mathbf{k}'}] \sim -\delta(\mathbf{k}-\mathbf{k}')\,. \tag{4.17}$$

Consequently, $a^{\dagger}_{\mathbf{k}} a_{\mathbf{k}} |N_{\mathbf{k}}\rangle = -N_{\mathbf{k}} |N_{\mathbf{k}}\rangle$ and therefore $\hat{H}|N_{\mathbf{k}}\rangle \sim N_{\mathbf{k}} E_{\mathbf{k}} |N_{\mathbf{k}}\rangle$ is positive.

But as we know, messing with the commutation relations is rarely a good idea. In fact, we immediately obtain

$$\langle 0|a_{\mathbf{k}} a^{\dagger}_{\mathbf{k}'}|0\rangle = -\delta(\mathbf{k}-\mathbf{k}')\,, \tag{4.18}$$

for a normalized vacuum state $|0\rangle$. We have rendered the Hamiltonian positive at the expense of creating states with negative norm. If we tried to cure the latter problem, we would end up with a nonnormalizable vacuum state. Either way, the theory is inconsistent!

As discussed, preserving the metric structure of the Hilbert space implies unboundedness of the Hamiltonian. Once the negative and positive energy sectors of the theory are coupled, the vacuum will decay infinitely fast (owing to the infinite phase space for the decay). We may also see this in terms of the path integral. When performing the integral, negative eigenvalues of the kinetic operator induce an imaginary part of the vacuum persistence amplitude. As long as the positive and negative sectors are uncoupled, one may be saved through an appropriate redefinition. Once a coupling is present, however, the effective action picks up an infinite imaginary part

$$\mathrm{Im}(\Gamma) \sim \int d^4k\,, \tag{4.19}$$

owing to the infinite number of negative eigenvalues.

#### 4.1.3.1 Ghosts from higher derivatives

The realization that ghosts are present in higher derivative theories is due to Ostrogradski [Ostrogradski, 1850]. His proof is related to the fact, that in order to Legendre transform to find the Hamiltonian in presence of higher time derivatives, one needs to introduce the notion of generalized momenta. Consider a Lagrangian system of the form

$$L = f\left(q, \dot{q}, ..., \frac{d^n q}{dt^n}\right)\,. \tag{4.20}$$

The Hamiltonian may be constructed by appropriately extending the phase space via defining

$$Q^{(i)} = \frac{d^i q}{dt^i}\,, \quad P^{(i)} = \frac{\delta L}{\delta \dot{Q}^{(i)}}\,. \tag{4.21}$$

If the Lagrangian is nondegenerate, that is $\frac{d^n q}{dt^n}$ can be expressed in terms of $P^{(n)}$, the Hamiltonian will necessarily contain linear instabilities

$$H = \sum_i P^{(i)}\dot{Q}^{(i)} - L = \sum_i P^{(i)}Q^{(i+1)} + P^{(n)}\frac{d^n q}{dt^n}\left(P^{(n)}\right) - L\,. \tag{4.22}$$

There is a way around Ostrogradski's theorem. Precisely if the Lagrangian is degenerate, the Hamiltonian cannot be defined without previous redefinitions of the canonical variables. If the degeneracy is appropriate, the Lagrangian is void of higher time derivatives after the redefinitions, although it may (but does not have to) contain extra variables that were not previously manifest.

The most famous example are $F(R)$ theories. In that case, any nonlinear function of the Ricci scalar $R$ will induce higher derivatives on the graviton, since, to linear order, $R \sim \partial^2 h$. However, the corresponding Lagrangian is degenerate. It can be shown that the appropriate field redefinition introduces an extra degree of freedom; the action is equivalent to an action of gravity with an additional scalar field. In appropriate regions of parameter space, no ghostlike instabilities exist.

We shall see that something similar happens in the case of nonlinear massive gravity. In a helicity decomposition, the nonlinear action of [de Rham et al., 2011b] contains higher derivatives. However, the corresponding Hamiltonian cannot be defined without a previous field redefinition. The appropriate field redefinition eliminates all higher derivatives. The degeneracy, however, relies crucially on the full nonlinear structure and is lost upon truncation at any finite order. We will discuss this in detail below.

#### 4.1.3.2 Nonlinear ghosts

Ghostly degrees of freedom may also show up in interactions. Around a vanishing background they are then infinitely massive. However, they still have an effect. If the total Hamiltonian is unbounded, a vacuum state is still non-existent. One then has to carefully investigate the stability properties of the chosen perturbative vacuum. The effective action will still obtain an imaginary part, which is not generated perturbatively but instead on nontrivial saddle points.

Moreover, on said background configurations, the ghost may start to propagate. The background is perturbatively unstable with an infinitely short instability timescale.

## 4.2 Massive spin-2 without self-interactions

The action of a free massive spin-2 particle is given by what is commonly called the Fierz-Pauli action and is unique [Fierz and Pauli, 1939].

Its construction can be understood most easily by considering the aforementioned helicity or Stückelberg decomposition. Demanding the absence of higher derivatives, which signal the appearance of new degrees of freedom, removes all arbitrariness in the action; only the Fierz-Pauli form allows for this property. It is given by

$$\begin{aligned} S = \int d^4x \mathcal{L} &= \int d^4x \left( \partial_\mu h^{\mu\nu} \partial_\nu h - \partial_\mu h^{\rho\sigma} \partial_\rho h^\mu_\sigma + \frac{1}{2} \partial_\mu h^{\rho\sigma} \partial^\mu h_{\rho\sigma} - \frac{1}{2} \partial_\mu h \partial^\mu h \right. \\ &\quad \left. - \frac{1}{2} m^2 (h^{\mu\nu} h_{\mu\nu} - h^2) \right), \end{aligned} \tag{4.23}$$

where $h \equiv h^\mu_\mu$.

Inserting (4.12) into the quadratic action (4.23) leads to

$$\begin{aligned} \mathcal{L}_{\mathrm{PF}} &= \tilde{h}^{\mu\nu} \mathcal{E}^{\rho\sigma}_{\mu\nu} \tilde{h}_{\rho\sigma} - \frac{1}{8} F_{\mu\nu} F^{\mu\nu} + \frac{1}{12} \chi \Box \chi - \frac{1}{2} m^2 \left( \tilde{h}^{\mu\nu} \tilde{h}_{\mu\nu} - \tilde{h}^2 \right) + \frac{1}{6} m^2 \chi^2 \\ &\quad + \frac{1}{2} m^2 \chi \tilde{h} + m \left( \tilde{h} \partial_\mu A^\mu - \tilde{h}^{\mu\nu} \partial_\mu A_\nu \right) + \frac{m}{2} \chi \partial_\mu A^\mu \,, \end{aligned} \tag{4.24}$$

where $\tilde{h}^{\mu\nu} \mathcal{E}^{\rho\sigma}_{\mu\nu} \tilde{h}_{\rho\sigma} = \partial_\mu \tilde{h}^{\mu\nu} \partial_\nu \tilde{h} - \partial_\mu \tilde{h}^{\rho\sigma} \partial_\rho \tilde{h}^\mu_\sigma + \frac{1}{2} \partial_\mu \tilde{h}^{\rho\sigma} \partial^\mu \tilde{h}_{\rho\sigma} - \frac{1}{2} \partial_\mu \tilde{h} \partial^\mu \tilde{h}$ describes the linear part of the Einstein action. For $k^2 \gg m^2$, the action becomes diagonal in field space. The individual kinetic terms for $\tilde{h}_{\mu\nu}$ and $A_\mu$ correspond to massless linearized Einstein and Maxwell theory, respectively. Thus, in the limit where the mixing of the individual fields can be neglected, $\tilde{h}_{\mu\nu}$ carries precisely the two helicity-2, $A_\mu$ the two helicity-1 and $\chi$ the single helicity-0 degrees of freedom.

Note that requiring the diagonalization of the kinetic term fixes the relative factor of $1/2$ between the $\chi$-terms in (4.12). Similarly, the factors of $m$ in (4.12) normalize the kinetic terms. The coefficient of the kinetic term for $\chi$ is determined by the coupling of $h_{\mu\nu}$ to sources: $\int d^4x T^{\mu\nu} h_{\mu\nu}$. The propagator of a massive spin-2 field $h_{\mu\nu}$ between two conserved sources $T_{\mu\nu}$ and $\tau_{\mu\nu}$ is given by

$$\begin{aligned} T^{\mu\nu} D_{\mu\nu,\rho\sigma} \tau^{\rho\sigma} &= \frac{1}{2} T^{\mu\nu} \frac{\left(\eta_{\mu\rho}\eta_{\nu\sigma} + \eta_{\mu\sigma}\eta_{\nu\rho} - \frac{2}{3}\eta_{\mu\nu}\eta_{\rho\sigma}\right)}{p^2 - m^2} \tau^{\rho\sigma} \\ &= \frac{1}{2} T^{\mu\nu} \frac{\left(\eta_{\mu\rho}\eta_{\nu\sigma} + \eta_{\mu\sigma}\eta_{\nu\rho} - \eta_{\mu\nu}\eta_{\rho\sigma}\right)}{p^2 - m^2} \tau^{\rho\sigma} + T^{\mu\nu} \frac{1}{6} \frac{\eta_{\mu\nu}\eta_{\rho\sigma}}{p^2 - m^2} \chi^{\rho\sigma} \end{aligned} \tag{4.25}$$

The first term in the last line corresponds to the helicity-2 state $\tilde{h}_{\mu\nu}$. The second term is an additional interaction from the extra scalar degree of freedom $\chi$ and fixes the overall normalization of it in our helicity decomposition. By considering non-conserved sources one can accordingly fix the normalization of $A_\mu$ in (4.12).

For $m = 0$, the action (4.23) describes linearized Einstein gravity and is invariant under linearized diffeomorphisms,

$$h_{\mu\nu} \to h_{\mu\nu} + \frac{1}{2}(\partial_\mu \xi_\nu + \partial_\nu \xi_\mu) \ , \tag{4.26}$$

where $\xi_\mu(x)$ defines the linear coordinate transformation. The gauge redundancy fixes the relative coefficients of the two-derivative terms. Since both vector and scalar appear with derivatives in the Stückelberg decomposition, the only way for their equations of motion to be second order is for these derivative terms to drop out from the two-derivative kinetic term for $h_{\mu\nu}$. In other words, we impose on the kinetic part of the Lagrangian the condition

$$\mathcal{L}(h_{\mu\nu}) = \mathcal{L}(h_{\mu\nu} + \partial_{(\mu}\tilde{A}_{\nu)} + \partial_{\mu\nu}\tilde{\chi}) + \text{boundaries} \ , \tag{4.27}$$

where $\tilde{A}_\mu$ and $\tilde{\chi}$ are respectively a vector and a scalar. This is equivalent to the gauge invariance (4.26) for a specific $\xi_\mu$.

The uniqueness of said structure can also be understood from a Hamiltonian analysis. Let us first examine the kinetic term. After having integrated by parts such that $h_{00}$ and $h_{0i}$ do not appear with time derivatives, the canonical momenta of the Lagrangian (4.23) are

$$\pi_{ij} = \frac{\partial \mathcal{L}}{\partial \dot{h}_{ij}} = \dot{h}_{ij} - \dot{h}_{ii}\delta_{ij} - 2\partial_{(i}h_{j)0}. \tag{4.28}$$

The other canonical momenta ($\pi_{00}$ and $\pi_{0i}$) are zero due to the absence of their time derivatives. Inverting (4.28), one obtains

$$\dot{h}_{ij} = \pi_{ij} - \pi_{kk}\delta_{ij} + 2\partial_{(i}h_{j)0}. \tag{4.29}$$

Performing the Legendre transformation and rewriting the Lagrangian in terms of the canonical momenta yields

$$\mathcal{L} = \pi_{ij}\dot{h}_{ij} - \mathcal{H} + 2h_{0i}\partial_j \pi_{ij} + h_{00}(\nabla^2 h_{ii} - \partial_i \partial_j h_{ij}) \ , \tag{4.30}$$

where

$$\mathcal{H} = \frac{1}{2}\pi_{ij}^2 - \frac{1}{4}\pi_{ii}^2 + \frac{1}{2}\partial_k h_{ij}\partial_k h_{ij} - \partial_i h_{jk}\partial_j h_{ik} + \partial_i h_{ij}\partial_j h_{kk} - \frac{1}{2}\partial_i h_{jj}\partial_i h_{kk}.$$

The canonical momenta for $h_{00}$ and $h_{0i}$ are zero and the variables themselves appear only linearly in terms without time-derivatives. They are Lagrange multipliers which give the constraint equations $\nabla^2 h_{ii} - \partial_i\partial_j h_{ij} = 0$ and $\partial_j \pi_{ij} = 0$. All these constraints commute, in the sense of Poisson brackets, with each other. Hence, the constraints are first class (for an introduction to constrained systems see for example [Henneaux and Teitelboim, 1992, Dirac, 2001]). This is characteristic for theories with a gauge symmetry. The constraints together with the gauge transformations reduce the physical phase space to a four dimensional hypersurface, which is described by the canonical coordinates of the two physical polarizations of the massless spin-2 graviton and their conjugate momenta.

Adding a mass term to the analysis changes the Hamiltonian and the Lagrangian of (4.30) in the following way

$$\mathcal{L} = \pi_{ij}\dot{h}_{ij} - \mathcal{H} + m^2 h_{0i}^2 + 2h_{0i}\partial_j \pi_{ij} + h_{00}(\nabla^2 h_{ii} - \partial_i\partial_j h_{ij} - m^2 h_{ii}) \ , \quad (4.31)$$

where

$$\begin{aligned}\mathcal{H} \ &= \ \frac{1}{2}\pi_{ij}^2 - \frac{1}{4}\pi_{ii}^2 + \frac{1}{2}\partial_k h_{ij}\partial_k h_{ij} - \partial_i h_{jk}\partial_j h_{ik} + \partial_i h_{ij}\partial_j h_{kk} \\ &\quad -\frac{1}{2}\partial_i h_{jj}\partial_i h_{kk} + \frac{1}{2}(h_{ij}h_{ij} - h_{ii}^2).\end{aligned}$$

Note that the conjugate momenta are unchanged by the additional mass term. However, the structure of the Lagrangian is different and $h_{0i}$ is no longer a Lagrange multiplier. Nevertheless, it is still non-dynamical and its equation of motion yields the algebraic relation

$$h_{0i} = -\frac{1}{m^2}\partial_i \pi_{ij}. \quad (4.32)$$

$h_{00}$ still is a Lagrange multiplier and it enforces the constraint

$$\nabla^2 h_{ii} - \partial_i\partial_j h_{ij} - m^2 h_{ii} = 0 \quad (4.33)$$

which is now of second class. Requiring that the constraint is conserved in time, i.e. that it commutes with the Hamiltonian, gives rise to a secondary constraint. Since $h_{0i}$ is determined by (4.32) and $h_{00}$ gives two second class constraints (one primary and one secondary), the resulting physical phase

space is then ten dimensional describing the five physical polarizations of the massive spin-2 particle and their conjugate momenta. Departing from the Fierz-Pauli mass term introduces nonlinearities in $h_{00}$ and the constraint which fixes the trace $h_{ii}$ to zero is lost resulting in either a tachyonic or ghost-like sixth degree of freedom [Boulware and Deser, 1972, Van Nieuwenhuizen, 1973].

Let us briefly mention coupling to sources. Adding a source term to the Lagrangian (4.23) of the form $h_{\mu\nu}T^{\mu\nu}$ does not change the linear constraint analysis. No matter whether the source is conserved, $\partial_\mu T^{\mu\nu} = 0$, or not, the source coupling will only introduce $h_{00}$ and $h_{0i}$ linearly and without time derivatives and therefore it will not affect the number of constraints. Note that this holds true for any linear coupling of $h_{\mu\nu}$ to sources.

## 4.3 Self-interacting theories

We now focus on the question of self-interactions in massive spin-2 theories. We address subtleties in the construction and inquire whether uniqueness theorems can exist similar to the case of the Einstein theory for a massless spin-2 field.

### 4.3.1 Boulware-Deser ghost

Boulware and Deser (BD) argued in [Boulware and Deser, 1972] that simply introducing a mass term for the full nonlinear theory of general relativity reintroduces the sixth degree of freedom which could be tuned away in the Fierz-Pauli theory. Although this result turned out to be not generic, it is instructive to see their reasoning.

Let us first consider pure general relativity. Using the ADM formalism [Arnowitt et al., 1960, 2008] in which a general metric can be re-written as

$$ds^2 = g_{\alpha\beta}dx^\alpha dx^\beta = -N^2dt^2 + \gamma_{ij}\left(dx^i + N^i dt\right)\left(dx^j + N^j dt\right) \ , \qquad (4.34)$$

where $\gamma_{ij} \equiv g_{ij}$, $N \equiv (-g^{00})^{-\frac{1}{2}}$ (lapse), $N_i \equiv g_{0i}$ (shift). The full action reads (for simplicity we set the Planck mass to one)

$$S = \int d^4x\sqrt{-g}\ R = \int d^4x(\pi_{ij}\dot{\gamma}_{ij} - NR^{(0)} - N_iR^i - 2(\pi^{ij}N_j - \frac{1}{2}\pi N^i + N^{|i}\sqrt{\gamma})_{|j}), \qquad (4.35)$$

All curvatures are functions of $\gamma_{ij}$ and $\pi_{ij}$, but do not depend on $N$ or $N_i$. R is the four dimensional Ricci scalar and $-R^{(0)} \equiv {}^3R + \gamma^{-\frac{1}{2}}(\frac{1}{2}\pi^2 - \pi_{ij}\pi^{ij})$ and ${}^3R$ is the three dimensional Ricci scalar with respect to the metric $\gamma_{ij}$.

$R^i = -2\pi^{ij}_{|j}$, where the bar "$|$" denotes covariant differentiation with respect to the spatial metric $\gamma_{ij}$.

In the massless theory, $N$ and $N_i$ are Lagrange multiplier which enforce first class constraints on the system, thereby eliminating four (and correspondingly eight phase space) degrees of freedom yielding 2 propagating helicities of the massless spin-2 particle. We now introduce the Minkowski background by expanding

$$g_{\alpha\beta} = \eta_{\alpha\beta} + h_{\alpha\beta} \ , \tag{4.36}$$

where $\eta_{\alpha\beta}$ is the Minkowski metric and $h_{\alpha\beta}$ is a tensor on the flat background. Its indices are consequently raised and lowered by the Minkowski metric. The inverse metric $g^{\alpha\beta}$ is given by an infinite series of $h_{\alpha\beta}$ and can be obtained from $g^{\alpha\mu}g_{\mu\beta} = \delta^\alpha_\mu$. At linear order $N = 1 - \frac{1}{2}h_{00}$ and $N_i = h_{0i}$ and one recovers the result of the previous section. At nonlinear order, however,

$$N^2 = (1 - h_{00}) - h_{0i}h_{0j}g^{ij} \ , \tag{4.37}$$

whereas $N_i$ remains unchanged.

The Fierz-Pauli mass term $f = (h_{\mu\nu}h^{\mu\nu} - h^2)$ can nevertheless easily be expressed in terms of $N_i$ and the nonlinear $N$ [Boulware and Deser, 1972],

$$f = h_{ij}^2 - h_{ii}^2 - 2N_i^2 + 2h_{ii}(1 - N^2 - N_iN^i). \tag{4.38}$$

In contrast to the linear case, here $N$ (which to linear order is equivalent to $h_{00}$) appears quadratically in the mass term although still appearing linearly in the full non-linear derivative (Einstein) structure of the theory. Therefore now neither $N$ nor $N_i$ are Lagrange multipliers.

Thus, at the full non-linear level, the trace $h_{ii}$ is no longer constrained since the constraint was related to the fact that $N$ was a Lagrange multiplier. Therefore, there are six degrees of freedom propagating: The so-called Bouleware-Deser ghost propagates on top of the five degrees of freedom of the Fierz-Pauli massive spin-2. We will see that this conclusion, although correct generically, can be avoided for specific theories.

The simplest example is the free Fierz-Pauli theory discussed above. There, since the expansion is truncated at the linear level we have that $N = 1 - \frac{1}{2}h_{00}$ and the mass term in the Lagrangian is

$$f = h_{ij}^2 - h_{ii}^2 - 2N_i^2 + 2h_{ii}(1 - 2N). \tag{4.39}$$

Thus, as in the derivative part of the action (the linearized Einstein-Hilbert Lagrangian), $N$ only appears linearly. In other words, the lapse is here again a Lagrange multiplier, as in General Relativity.

The philosophy of avoiding the BD ghost will be the same for interacting theories: we will search for theories that can be written in terms of a linear lapse function acting as a Lagrange multiplier. In order to do that and to avoid the BD conclusions, we will have to either deform the derivative structure of the massless theory and/or the non-derivative structure.

### 4.3.2 Cubic interactions for a massive spin-2 particle

We will start by considering the simplest possible interaction, a cubic interaction as described in [Folkerts et al., 2011].

There, the idea was to consider a cubic interaction that keeps the structure of the *linear* Fierz-Pauli action. In other words, by deviating from the Einsteinian derivative structure at the cubic order, $N = 1 - \frac{1}{2}h_{00}$ remains a Lagrange multiplier also in the nonlinear theory. Non-derivative interactions can then be constructed that preserve this property.

This construction can straightforwardly be achieved by considering the most general cubic interaction with at most two derivatives on $h_{\mu\nu}$. Demanding linearity in $h_{00}$ fixes all coefficients besides respective prefactors of the zero- and two-derivative terms.

The unique structure is found to be [Folkerts et al., 2011]

$$\begin{aligned}\mathcal{L}^{(3)} = \frac{1}{\Lambda_a}\big(&h^{\alpha\beta}\partial_\alpha h^{\mu\nu}\partial_\beta h_{\mu\nu} - h^{\alpha\beta}\partial_\alpha h\partial_\beta h + 4h^{\alpha\beta}\partial_\beta h\partial_\mu h^\mu_\alpha - 2h^{\mu\nu}\partial_\alpha h\partial^\alpha h_{\mu\nu}\\ &+ h\partial_\mu h\partial^\mu h - 3h^{\mu\nu}\partial_\alpha h^\alpha_\mu\partial_\beta h^\beta_\nu - 4h^{\mu\nu}\partial_\nu h^\alpha_\mu\partial_\beta h^\beta_\alpha + 3h\partial_\mu h^{\mu\nu}\partial_\alpha h^\alpha_\nu\\ &+ 2h^{\mu\nu}\partial^\alpha h_{\mu\nu}\partial_\beta h^\beta_\alpha - 2h\partial_\alpha h\partial_\beta h^{\alpha\beta} + h^{\mu\nu}\partial_\alpha h_{\nu\beta}\partial^\beta h^\alpha_\mu + 2h^{\mu\nu}\partial_\beta h_{\nu\alpha}\partial^\beta h^\alpha_\mu\\ &- h\partial_\alpha h_{\mu\nu}\partial^\nu h^{\mu\alpha} - h\partial_\alpha h^{\mu\nu}\partial^\alpha h_{\mu\nu}\big) + \Lambda_b\big(2h^\mu_\nu h^\nu_\rho h^\rho_\mu - 3hh_{\mu\nu}h^{\mu\nu} + h^3\big)\,. \quad (4.40)\end{aligned}$$

Here, $\Lambda_a$ and $\Lambda_b$ are arbitrary constants of mass dimension 1. Under the assumption $\Lambda_b \ll m \ll \Lambda_a$, which corresponds to to the massive gravity case, they are related to the strong coupling scale $\Lambda$ via $\Lambda^3 \sim \min\{m^2\Lambda_a,\, m^4/\Lambda_b\}$.

In terms of the components of $h_{\mu\nu}$, for example, the non-derivative part is given by

$$\mathcal{L} = \frac{3k_2}{2}h_{00}(h_{ii}^2 - h_{ij}^2) + \text{terms independent of } h_{00}. \quad (4.41)$$

Hence, $h_{00}$ and $h_{0i}$ appear in the same way as in the free action. We do not display the explicit expression for the derivative part because the expression is rather lengthy. Still, one can easily check that also there $h_{0i}$ remains non-dynamical and can be solved for algebraically, yielding 3 constraints on $h_{\mu\nu}$. Furthermore, $h_{00}$ appears as a Lagrange multiplier in (4.40) and accordingly eliminates another two degrees of freedom [Folkerts et al., 2011].

The fact that the action (4.40) propagates five degrees of freedom can also be checked in the helicity decomposition (4.12). Inserting the decomposition into (4.40) reveals that the corresponding equations of motion are free of higher time derivatives on the helicity components.

Indeed, this is in direct correspondence to the Hamiltonian analysis outlined above. The components $h_{00}$ and $h_{0i}$ are exactly those components of $h_{\mu\nu}$ which can introduce higher time derivatives on the equations of motion as, in terms of helicities, these correspond to $\partial_0^2\chi$, $\partial_0 A_0$, $\partial_0\partial_i\chi$ and $\partial_0 A_i$. Therefore, any action free of higher derivatives on the helicities, requires $h_{00}$ to be a Lagrange multiplier and $h_{0i}$ to be nondynamical.

Up to boundary terms, one can rewrite the above Lagrangian in a compact form [Hinterbichler, 2013] as follows

$$\mathcal{L}^{(3)} = \Lambda_a^{-1}\epsilon^{\alpha_1\dots\alpha_4}\epsilon^{\beta_1\dots\beta_4}\partial_{\alpha_1}\partial_{\beta_1}h_{\alpha_2\beta_2}\dots h_{\alpha_4\beta_4} + \Lambda_b\epsilon^{\alpha_1\dots\alpha_3\sigma_4}\epsilon^{\beta_1\dots\beta_3}_{\sigma_4}h_{\alpha 1\beta_1}\dots h_{\alpha_3\beta_3}\,. \tag{4.42}$$

$\epsilon^{\alpha_1\dots\alpha_4}$ denotes the totally antisymmetric four-tensor in four dimension. From its antisymmetry properties it is then simple to conclude that the constraint structure of the free Lagrangian is preserved. If there is one $h_{00}$ in (4.42), then there cannot be any other factor of it in that term. Therefore, $h_{00}$ can only appear as a Lagrange multiplier. Terms with $h_{0i}$ can carry at most one time derivative and one power of $h_{0i}$ or only spatial derivatives and at most two powers of $h_{0i}$; all other terms have spatial indices. Variation with respect to $h_{0i}$, thus, leads to a constraint equation for itself which defines it algebraically in terms of the components $h_{ij}$.

### 4.3.3 Resummed theories

The second possible route to find nonlinear extensions of the Fierz-Pauli theory is to retain the Einsteinian derivative structure and construct a nonlinear extension of the mass term. In this case one searches for a theory preserving a similar constraint structure of the lapse for the full Einstein theory. This approach was taken in [de Rham et al., 2011b].

What we learned from the analysis of BD is that the lapse $N$ cannot be a lagrange multiplier if the the two following assumptions co-exist

- The derivative structure is Einsteinian
- $N$ and $N^i$ are independent variables.

As we are interested in the class of theories that fulfill the former assumption, one needs to relax the latter, thereby keeping $N$ as a Lagrangian multiplier to

eliminate the BD ghost. The theory with this property has been constructed in [de Rham et al., 2011b], the so-called dRGT massive gravity.

In other words, the theory of [de Rham et al., 2011b] is a deformation of General Relativity with non-derivative term such that [Hassan and Rosen, 2012b]

- The derivative structure is Einsteinian.
- $N^i$ can be fully traded by a new variable $n^i(N, N^i, h_{ij})$.
- After the field redefinition, $N$ only appears linearly in the action and without derivatives.

The second condition forces the redefinition to be of type

$$N^i = \left(\delta^i_j + N D^i_j\right) n^j \ , \tag{4.43}$$

where $D^i_j$ is an appropriate matrix independent upon $N$.[3] Of course, any truncation in powers of $h_{ij}$ of this construction would bring back the BD ghost.

For our purposes, we adopt the notation of [Hassan and Rosen, 2012b]. We write the resummed theory of [de Rham et al., 2011b] in terms of the inverse metric $g^{-1}$ and an auxiliary background metric $\eta$. The action of dRGT massive gravity can then be written according to [Hassan and Rosen, 2012b] (here we re-introduce the Planck mass $M_P$)

$$S = M_P^2 \int d^4x\sqrt{-g}\left[R(g) + 2m^2\sum_{n=0}^{2}\beta_n e_n\left(\sqrt{g^{-1}\eta}\right)\right] \ , \tag{4.44}$$

where $m$ is the graviton mass and the $e_n(\mathbb{X})$ are functions of matrix traces given by

$$e_0(\mathbb{X}) = 1 \ , e_1(\mathbb{X}) = [\mathbb{X}], e_2(\mathbb{X}) = \frac{1}{2}([\mathbb{X}]^2 - [\mathbb{X}^2]) \ . \tag{4.45}$$

The square brackets denote the trace and $\beta_0 = 6$, $\beta_1 = -3$ and $\beta_2 = 1$ for dRGT massive gravity [de Rham et al., 2011b, Hassan and Rosen, 2012b]. Note that the coefficients are chosen such that the action describes a flat background without a cosmological constant. The matrix $\sqrt{g^{-1}\eta}$ is defined by $\sqrt{g^{-1}\eta}\sqrt{g^{-1}\eta} = g^{\mu\nu}\eta_{\nu\rho}$. Since $\eta_{\mu\nu}$ transforms as a rank-two tensor, the action (4.44) is invariant under general coordinate transformations.

[3] Note that we would get exactly the same results without the field redefinition. This field redefinition only makes manifest that the lapse is a Lagrange multiplier.

Expanding the action (4.44) to second order in the metric perturbations $g_{\mu\nu} = \eta_{\mu\nu} + h_{\mu\nu}$, one recovers the Fierz-Pauli action (4.23).

As suggested in [de Rham et al., 2011b] and later shown in [Hassan and Rosen, 2012b,a, de Rham et al., 2012, 2011c], the action (4.44) indeed only propagates five degrees of freedom. In order to see this, one can redefine the shift as (4.43). This has been also done for the full nonlinear action in [Hassan and Rosen, 2012b]. We will briefly discuss their findings.

A constraint analysis is most conveniently carried out by using the ADM decomposition [Arnowitt et al., 1960, 2008]. Using (4.34), the Lagrangian (4.44) is given by

$$M_P^{-2}\mathcal{L} = \pi^{ij}\partial_t\gamma_{ij} + NR^0 + R_iN^i + 2m^2\sqrt{\det\gamma}N\sum_{n=0}^{2}\beta_n e_n\left(\sqrt{g^{-1}\eta}\right) \ . \quad (4.46)$$

The mass term includes $N$ in a non-linear way and is, therefore, responsible for the seeming loss of the constraint. However, one can redefine the shift $N_i$ by (4.43) and finds the following Lagrangian [Hassan and Rosen, 2012b,a]

$$M_P^{-2}\mathcal{L} = \pi^{ij}\partial_t\gamma_{ij} - \mathcal{H}_0(\pi^{ij}, \gamma_{ij}, n_j) + N\mathcal{C}(\pi^{ij}, \gamma_{ij}, n_j) \ , \quad (4.47)$$

where $\mathcal{H}_0$ is the Hamiltonian and $\mathcal{C}$ is the additional constraint ensuring that only five of the six components of $\gamma_{ij}$ are propagating. Thus, we have established that there are three independent variables $n_i$ which are not propagating and algebraically determined by their equations of motion and there is one Lagrange multiplier $N$ which yields a constraint equation for $\pi^{ij}$ and $\gamma_{ij}$. Therefore, there are only five propagating independent degrees of freedom which constitute the massive graviton.

It is, however, important to note that the redefinition (4.43) can only be used when considering the full non-linear action (4.44). Whenever truncating the theory, this ceases to be valid and thus one is left with six propagating degrees of freedom.

One might be puzzled by analyzing the action (4.44) in terms of the helicity decomposition (4.12). There, indeed, are higher derivatives (apparently signaling new degrees of freedom) appearing on the equations of motion of, e.g., the scalar helicity $\chi$ for the nonlinear terms [Folkerts et al., 2011]. The lowest suppression scale of these terms is $\Lambda_5 = (m^4 M_P)^{\frac{1}{5}}$. In the full theory, however, this scale is redundant and can be removed by a field redefinition [de Rham et al., 2011c][4]. With this field redefinition also the higher derivative terms disappear. It can be shown that this happens for all scales below

[4]Note that this field redefinition is in fact necessary in order to define a Hamiltonian in terms of the helicities. Without it, the relation between the canonical momenta and time derivatives of fields is not invertible. This reflects the redundancy of the coupling in the full theory.

$\Lambda_3 = (m^2 M_P)^{\frac{1}{3}}$ [de Rham et al., 2011c], such that the theory in terms of the redefined fields is free of higher derivative interactions. Note, however, that when truncating the theory to any finite order this is no longer the case.

In works subsequent to [de Rham et al., 2011b, Hassan and Rosen, 2012b], it was furthermore shown that the absence of the sixth ghostlike degree of freedom can also be confirmed in the Stückelberg language (see for example [de Rham et al., 2012]).

## 4.4 Summary

Within this chapter we have addressed the question whether theories of a single interacting massive-spin 2 field obey similar uniqueness theorems as in the massless case.

For a long time, it was doubtful whether there even exists one consistent theory that describes self-interactions of a massive spin-2 particle. The fact that adding the Fierz-Pauli mass term to the Einstein-Hilbert action introduces nonlinearities in the lapse into the action was taken as the basis of a no-go-theorem for nonlinear extensions of Fierz-Pauli theory. It was argued that any such extension necessarily leads to the appearance of a sixth unphysical and ghost-like polarization in the theory, the Boulware-Deser ghost.

We have reviewed two possible ways to circumvent this apparent theorem. The first one is to sacrifice the Einsteinian derivative structure, such that the (00)-component of the tensor field $h_{\mu\nu}$ enters the action only linearly even when self-interactions are added. This ensures that only five degrees of freedom are propagating. We have shown that this property can equivalently be checked in a helicity decomposition of the massive tensor. The found action is characterized by the absence of higher derivatives on the helicity components. It is the unique theory with this property.

The second route is to leave the derivative structure untouched, but instead adding a potential for the massive spin-2 field in such a way that guarantees the presence of a Lagrange multiplier in the system. By casting the action into an appropriate form, this Lagrange multiplier is once again given by the lapse.

The latter approach, since it relies on redundancies of the full action, requires a full resummation of the theory. Any truncation to finite order appears to propagate more than five degrees of freedom. However, the scale at which this additional degree of freedom appears coincides with the scale at which nonlinearities become important. Henceforth, conclusions can only be drawn from the resummed theory.

We have further addressed the issue of higher derivatives in the helicity

decomposition in the latter class of theories. While these are present, the fact that redundancies are present prevents one from constructing a Hamiltonian. A field redefinition is necessary in order to be able to invert the canonical momenta; after this redefinition, no more higher derivatives are present. The Hamiltonian of the theory does not suffer from an Ostrogradski linear instability.

The experimental viability of either theory is unknown. The former deviates from the well probed Einsteinian cubic vertex and is therefore not viable as a massive graviton. The latter has the correct vertex structure. However, choosing its mass to be of the order of the Hubble scale leads to a strong coupling already at very low energies, $\Lambda_s = (m^2 M_P)^{1/3} \sim (1000 \text{ km})^{-1}$.

Let us also note here that the absence of the sixth polarization does not automatically guarantee that the theory is stable and consistent. The theory discovered in [Folkerts et al., 2011] is cubic, and thus inherently unstable. The theory of [de Rham et al., 2011b], on the other hand, may propagate superluminal modes and violate causality [Dubovsky et al., 2006, Gruzinov, 2011, Burrage et al., 2012, de Fromont et al., 2013, Deser and Waldron, 2013, Deser et al., 2013a,b]. Moreover, large classes of backgrounds have been found to suffer from instabilities [Tasinato et al., 2013, De Felice et al., 2012, Kuhnel, 2013, Babichev and Fabbri, 2013], which can even be of the ghost type.

Cosmological applications of either theory are therefore still under investigation. Nevertheless, they could in principle describe self-interactions of a massive spin-2 meson and hence be of different phenomenological interest.

# Part II

# Black Holes

# Chapter 5

# Black holes as Bose Condensates of Gravitons

## 5.1 The black hole quantum portrait

In section 1.3, we have given an introduction into the mysteries that surround black hole physics, but have also discovered the great opportunities that black holes may have to offer for the understanding of gravity. On one hand, there is the search for microstates that can possibly account for the Bekenstein-Hawking entropy; there is the question of the dynamics that underlie Hawking evaporation and render it unitary. Or the question whether global charges are necessary anomalous in any quantum theory of gravitation. On the other hand, black holes may themselves hold the answer to the arguably most pressing question in quantum gravity - the formation of black holes could unitarize gravity in the ultraviolet.

Obviously, it is impossible to disentangle the two issues. Unitarization through black hole formation is by definition only possible if the evaporation of the black hole itself is a unitary process. Therefore, UV completion of gravity through black hole production crucially relies on a microscopic understanding of black holes and their radiation.

In a recent series of papers [Dvali and Gomez, 2011, 2012b, 2013a, 2012a,c], Dvali and Gomez have proposed a new conceptual framework for the understanding of black hole physics. The first of two key claims is that the black hole is a bound state or condensate of many weakly interacting (i.e. long-wavelength) gravitons whose interaction strength is completely determined from the perturbative vertices in Einstein gravity. Secondly, it was suggested that this condensate is at a quantum critical point and therefore exhibits properties that are not apparent in the traditional description in

terms of (semi-)classical general relativity. Most importantly, the underlying quantum physics could be able to resolve the mysteries of the information paradox. Hawking evaporation is described as the depletion and evaporation of the condensate and its purification is thus a natural result. To the same extent, black holes could carry quantum hair [Dvali and Gomez, 2013a]. These effects are not visible in the semiclassical approximation, since this limit corresponds to an infinite number of black hole constituents.

Since the black hole is modeled as a bound state of long-wavelength gravitons $\lambda \sim r_s$, the physics of sufficiently large black holes is almost independent from the ultraviolet physics. Instead, all seemingly mysterious properties must be due to quantum collective effects of the infrared constituents.

Let us begin our review of the black hole quantum portrait with a motivation for a description of black holes in terms of long wavelength constituents. We will consider black hole formation in two regimes: One is the classical regime in which a black hole is formed through gravitational collapse; the other the quantum regime in which a black hole is a long lived intermediate state in a high energy scattering experiment.

Consider an unstable spherical body of radius $R$ and mass $M$, for simplicity taken homogeneous, that eventually collapses into a black hole. As long as $R \gg r_s = 2G_N M$, the gravitational field is essentially Newtonian and given by a $\Phi(r) \sim 1/r$ outside and and $\Phi(r) \sim r^2$ inside the sphere. It is a simple exercise to check that the energy is dominated by the Fourier components with $k \sim 1/R$. Ascribing to the classical field configuration an interpretation in terms of quanta, we see that the gravitational energy is carried by *longitudinal* gravitons with approximate wavelength $1/R$. We can easily estimate their number to be

$$N \sim RE_{\rm grav} \sim M^2/M_p^2\,, \tag{5.1}$$

which is independent of the radius of the body and therefore the same for any spherical object of mass $M$!

Extending this analysis until the radius of the sphere crosses its Schwarzschild radius, we see that just after the formation of the black hole, the energy is dominated by gravitons of wavelength $\lambda \sim r_s$.

In gravitational high energy scattering, there are three major regimes to distinguish as one lowers the impact parameter $b$ of colliding particles with center of mass energy $\sqrt{s} \gg M_p$ [Giddings, 2011]. In the (i) Born regime, the scattering is completely Newtonian and mediated by one-graviton exchange. Scattering angles are small and the relevant momentum transfer $\sqrt{t} \sim b^{-1}$. As the impact parameter is lowered, one enters the (ii) eikonal regime. Even though the total momentum transfer can become large, $\sqrt{t} \gg M_p$, it is caused

by the repeated exchange of soft gravitons. Individual momentum transfer will still be of the order $b^{-1}$. Finally, once $b \simeq r_s$ one will enter a regime in which (iii) black hole formation is possible. Although strictly speaking, the eikonal approximation loses its validity before, it appears likely that for $b \sim r_s$, the relevant processes are still those involving an enormous number of *soft gravitons*.

The foundation of the black hole quantum portrait now lies in the following observation: The relevant number of gravitons in either of the two preceding scenarios was $N \sim r_s^2/\ell_p^2$; the corresponding wavelengths are of order $\lambda \sim r_s$. Correspondingly, one finds for the dimensionless gravitational coupling

$$\alpha_{\rm GR} \equiv G_N/\lambda^2 \sim 1/N\,. \tag{5.2}$$

While individual couplings are extremely weak, one immediate sees that the collective coupling of the gravitons, $\alpha N$ is of order unity once the wavelength decreases down to the Schwarzschild radius. There is a phenomenon of *collective strong coupling*!

So what does this imply? In bosonic condensed matter systems, such a phenomenon of collective strong coupling often indicates non-trivial changes in the (local) ground state. These, in turn, are a signal of a quantum phase transition or bifurcation; $\alpha N \sim 1$ corresponds to a quantum critical point (QCP). QCPs, in turn, can exhibit very quantum mechanical behavior even for a macroscopic number of particles $N$. It appears that no matter the size of the black hole, quantum mechanical effects can be of crucial importance.

This immediately brings us to the main postulate of the black hole quantum portrait: If a black hole, upon formation, can encode very non-classical behavior, there is no reason to expect the classical solution for the interior to remain meaningful. Instead, it may be that a singularity never forms and a black hole is described by long wavelength physics until the very latest stages of its evolution. This is what has been proposed in [Dvali and Gomez, 2011] and sets the ground for the remaining part of this thesis.

The idea of a black hole as a Bose condensate of gravitons can also be motivated in a bottom-up approach. As gravitons are self interacting, they can potentially form a self sustained bound state. The properties of such a bound state can be estimated via the virial theorem,

$$\langle E_{\rm kin}\rangle \sim \langle V\rangle\,. \tag{5.3}$$

The kinetic energy $E_{\rm kin}$ of $N$ gravitons of wavelength $\lambda$ is given by

$$\langle E_{\rm kin}\rangle = N\frac{\hbar}{\lambda}\,, \tag{5.4}$$

while a naive estimate of the potential energy of the configuration of size $R$ is

$$\langle V \rangle \sim N^2 \frac{G_N \hbar^2}{\lambda^2 R} \,. \tag{5.5}$$

Assuming the size to be of the order of the wavelength, $R \sim \lambda$, one obtains

$$\lambda \sim \sqrt{N} L_p \,. \tag{5.6}$$

It is easily verified that this relation is nothing but Eq. (5.1).

The fact that the system lies at a critical point turns out to be of crucial importance. The implications are numerous:

(a) Since $\alpha \sim 1/N$, $M \sim M_p\sqrt{N}$ and $r_s \sim \ell_p\sqrt{N}$, the system can be described entirely by only one parameter, the occupation number $N$. Note that the former relations also imply $S_{\rm BH} \sim N$ and $T_{\rm BH} \sim M_p\sqrt{N}$.

(b) At a bifurcation point, the spectrum of the theory is characterized by nearly gapless excitations of mass $\sim 1/N$. It is known that tangent bifurcations go in hand with real solutions becoming complex [Kuś et al., 1993]. Close to the bifurcation point, deformations in the direction of the complex solutions appear as nearly gapless Bogoliubov modes[1]. These can be responsible for the Bekenstein Hawking entropy of black holes ($S \sim N$).

(c) If the energy of one of the Bogoliubov directions becomes imaginary, the solution is unstable and the system tends to collapse. This, due to the lightness of excitations, goes in hand with efficient depletion of the condensate. Incoherent scattering between condensed atoms leads to evaporation. This is the physical picture for Hawking radiation. The system decreases its size, while at the same time reducing the number of constituents. This happens self-similarly, s.t. $r_s \sim \ell_p\sqrt{N}$ throughout the evolution. Moreover, since the evaporation is not a vacuum process but instead the decay of an excited state, it happens perfectly unitarily.

(d) At the bifurcation point, the system is characterized by significant quantum fluctuations, which can explain the apparent deviation from classicality even for large black holes. Generically, quantum corrections scale as $1/N$ and will therefore necessarily become important over the lifetime of the black hole. Moreover, the presence of an instability can be responsible for very efficient scrambling of information inside the black hole on a logarithmic timescale.

[1] This somewhat resonates with previous arguments given in [Maldacena, 2003b, Hawking, 2005], albeit phrased in rather different terms.

### 5.1.1 Quantum corrections

One of the most important outputs of the black hole $N$-quantum portrait is to allow us to identify important quantum corrections that are not resolvable within the standard semi-classical approximation. In the semi-classical picture one works with the notion of classical metric. Irrespectively whether the metric is derived from the loop-corrected effective action, it is an intrinsically classical entity and its quantum constituents are not resolved. The only non-perturbative quantum corrections that one can visualise in this limit for a black hole of action $S$ are of the form $e^{-\frac{S}{\hbar}}$. These sort of corrections take into the account only the total black hole action and are blind to any form of microscopic constituency. Such corrections, for instance, can measure the transition amplitudes between black hole and thermal topologies [Maldacena, 2003b, Hawking, 2005].

On the other hand there exist more important quantum corrections that scale as $\hbar/S$, but they are unaccountable in the semi-classical treatment. The key problem lies in unveiling their *microscopic meaning* as well as in understanding under what conditions these quantum corrections can effectively lead to order-one effects for macroscopic black holes. In the quantum $N$-portrait these corrections naturally appear as $1/N$ corrections, since the occupation number of gravitons measures the black hole action (as well as the entropy),

$$N = \frac{S}{\hbar}\,. \tag{5.7}$$

Thus, the quantity $1/N$ is a measure of quantum effects that are much more important then the $e^{-N}$-type effects captured by the semi-classical analysis. In particular, it was shown that $1/N$-corrections account for the deviations from thermality of black hole radiation [Dvali and Gomez, 2011] as well as for the quantum hair of black holes [Dvali and Gomez, 2013a]. Existence of these corrections was also confirmed for the string holes [Veneziano, 2013].[2] These $1/N$-corrections are the key for resolving the black hole "information paradox", since over the black hole half-lifetime they give order-one effect for arbitrarily-large black holes $N \gg 1$ [Dvali and Gomez, 2012c].

[2]The similarly large corrections are also indicated in a different treatment in which one prescribes a wave-function to the horizon [Brustein and Medved, 2013a,b, Casadio and Scardigli, 2014], This approach differs from ours since the metric is still treated semi-classically and its quantum constituents are not resolved. Nevertheless the largeness of the corrections is in a qualitative agreement.

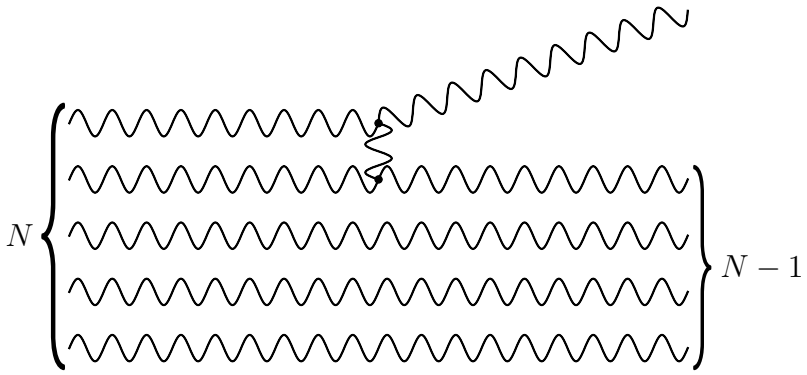


Figure 5.1: Leading order process responsible for evaporation of the black hole.

### 5.1.2 Hawking evaporation

As hinted above, we can parametrize the collapse and evaporation process as a self-similar decrease of $N$,

$$\frac{dN}{dt} = -\frac{1}{\sqrt{N}L_P}\,. \tag{5.8}$$

Note that this instability survives in the semi-classical limit ($L_P \to 0, N \to \infty, \sqrt{N}L_P =$ fixed), which corresponds to the Gross-Pitaevskii limit of the graviton condensate.

The above expression relies on a simple estimate. A constituent may escape the condensate when its energy exceeds the collective binding energy

$$E_{\text{escape}} = N\alpha\frac{\hbar}{\ell} = \frac{\hbar}{\ell} = \frac{\hbar}{\ell_P\sqrt{N}}, \tag{5.9}$$

which is the characteristic energy scale for evaporation. The leading contribution for evaporation is due to two-graviton scatterings, as shown in Fig. 5.1.

The decay rate is approximately given by

$$\Gamma_{\text{escape}} = \frac{1}{N^2}N^2\frac{\hbar}{\ell_P\sqrt{N}} + \mathcal{O}(N^{-3/2})\,. \tag{5.10}$$

The first factor is the squared amplitude of the scattering of two gravitons which is $\sim 1/N$. The second one is a combinatoric factor, since there are $N^2$ possibilities to pick two gravitons. As these factors cancel, the rate is determined by the characteristic energy of the evaporation process. The

leakage of particles is approximated by

$$\dot{N} = -\frac{\Gamma_{\text{escape}}}{\hbar} = -\frac{1}{\ell_P\sqrt{N}} + \mathcal{O}(N^{-3/2}), \tag{5.11}$$

or in terms of the black hole mass

$$\dot{M} = -\frac{\hbar}{\ell}\frac{\Gamma_{\text{escape}}}{\hbar} = -\frac{\hbar}{\ell_P^2 N} + \mathcal{O}(N^{-2}). \tag{5.12}$$

In the large $N$ limit, this corresponds to the mass loss that is obtained semi-classically for a black hole of temperature $T_H = \frac{\hbar}{\ell_P\sqrt{N}}$ [Dvali and Gomez, 2011]. Note that the form of the spectrum can also be understood from diagrams similar to Fig. 5.1. The emission of high energy particles requires the annihilation of a large number of gravitons. The combination of combinatoric and kinematic factors may thus be responsible for the exponential tail of the distribution.

## 5.2 Bose Einstein condensates

Let us end this introduction to the black hole quantum portrait by introducing the prerequisites from the physics of cold atoms that set the foundation of the model. We will focus solely on the zero temperature case and are not interested in the condensation dynamics; details on this can be found in any comprehensive review on Bose Einstein condensation, for example [Dalfovo et al., 1999, Stringari, 2005, Dalfovo et al., 2006].

Let us consider a system of $N$ identical (and therefore indistinguishable) bosons, which we will for simplicity assume to be in a pure state $|\psi\rangle$, although all definitions below apply to mixed states as well. The notion of a Bose condensate is most easily made precise using the (reduced) density matrix. Recalling the definition of a reduced density matrix as a density matrix that is traced over a subsystem[3], see Eq.(1.29), we define the *one-particle reduced* density matrix via

$$\rho_{1P} = \operatorname*{tr}_{N-1} \rho\,, \tag{5.13}$$

where we have introduced the density matrix of the full system $\rho = |\psi\rangle\langle\psi|$ and the trace is taken over all other particles. It can be shown that the

[3]We point here to the fact that the reduced density matrix is not a linear operator on a subspace in the strict sense. Since we are dealing with indistinguishable bosons, and are restricting ourselves to the $N$-particle Fock space, the symmetrization property forbids this. We will not let this be an obstacle for us.

elements of the one-particle reduced density matrix are given by

$$(\rho_{1P})_{ij} = \frac{1}{N} \operatorname{tr}\left(\rho \hat{a}_i^\dagger \hat{a}_j\right) = \langle\psi|\hat{a}_i^\dagger \hat{a}_j|\psi\rangle \ . \tag{5.14}$$

Here, $\hat{a}_i$, $\hat{a}_i^\dagger$ are the annihilation and creation operators that generate the multiparticle Fock space and we have normalized the density matrix $\rho_{1P}$ to one: $\operatorname{tr}\rho_{1P} = 1$.

Using these prerequisites, one defines a Bose Einstein condensate as a system, whose one-particle reduced density matrix contains one dominating eigenvalue of order 1, while all other eigenvalues at least suppressed by $1/N$. In other words, the system is very close to a product state; almost all bosons occupy the same mode.

Note that this definition is independent of the dynamics of the system. In particular, if the state $\psi$ is not the ground state, the system will usually evolve away from the condensed state. In case the ground state is very close to the condensed state, one may treat the system as an approximate condensate. In that case, the phenomenon of finding noncondensed particles in the ground state is referred to as depletion.

### 5.2.1 From the BBGKY-hierarchy to Gross-Pitaevskii

For a given many-body system, there is a systematic way of studying the many-body Schrödinger equation using the so-called BBGKY-hierarchy [Bogoliubov, 1946, Yvon, 1935, Kirkwood, 1946, 1947, Born and Green, 1946].

It amounts to a set of coupled differential equations for the $k$-particle density matrices $\hat{\rho}_{kP}$, depending on the $k+1$-particle density matrix $\hat{\rho}_{(k+1)P}$, respectively. In order to close this set of equations, one needs an expression of $\hat{\rho}_{kP}$ in terms of $\hat{\rho}_{(k+1)P}$. For $k = 1$, this could for example be the factorization property $\hat{\rho}_{2P} \sim \hat{\rho}_{1P}^2$, which we will assume in the following. This relation corresponds to the first part of a mean field approximation, since it postulates higher order correlators to be expressible in terms of two-point functions. We expect it to be exact in the limit $N \to \infty$.

Let us assume that the many body Hamiltonian takes on the form

$$H\psi(x_1, ..., x_N) = \left(\sum_{j=1}^{N} \frac{\nabla_j^2}{2m} + \frac{\lambda}{N} \sum \delta(x_j - x_k)\right) \psi(x_1, ..., x_N)\,, \tag{5.15}$$

where $\lambda$ is a coupling constant and $\psi(x_1, ..., x_N)$ is the many particle wavefunction in position space. There, we have $\rho_{1P}(x, x') = \langle x|\hat{\rho}_{1P}|x'\rangle$ and obtain

the equation of motion

$$i\hbar\partial_t\rho_{1P}(x,x') = \left(\frac{\nabla^2}{2m} - \frac{\nabla'^2}{2m}\right)\rho_{1P}(x,x') + \lambda\left(\rho_{1P}(x,x) - \rho_{1P}(x',x')\right)\rho_{1P}(x,x')\,. \quad (5.16)$$

If we further assume that the system is a Bose condensate, we have

$$\rho_{1P}(x,x') = \psi(x)\psi(x') \quad (5.17)$$

for the one-particle wave function $\psi$. In that case, $\psi$ obeys the Gross Pitaevskii equation

$$i\hbar\partial_t\psi(x) = \left(\frac{\nabla^2}{2m} + \lambda|\psi(x)|^2\right)\psi(x)\,. \quad (5.18)$$

This is an example of a Hartree type equation and becomes exact for a Bose condensate in the limit $N \to \infty$, $\lambda \to 0$, $\lambda N$ fixed. For finite $N$, depleted particles will backreact on the condensate. The factorization property (5.17) no longer upholds.

To lowest order, we may model this effect by assuming that the corrections to the factorization are small. This is the so-called Bogoliubov approximation. In it, the quantum fields are expanded around the lowest energy solution of the classical Gross Pitaevskii equation. The Hamiltonian is then diagonalized with respect to quadratic fluctations around the background. The corresponding transformations are Bogoliubov transformations and relate a set of creation and annihilation operators to a different one. The nontrivial information is contained in the mode-mode coupling due to the interactions.

Proper diagonalization yields corrections to the ground state energy [Lee and Yang, 1957, Lee et al., 1957] and the excitation spectrum around nontrivial backgrounds, the Bogoliubov modes. Moreover, it allows to quantify the amount of nontrivial correlations in the ground state. We will use this in chapter 6.

### 5.2.2 Quantum phase transitions and bifurcations

Quantum phase transitions are phase transitions at zero temperature and are due to quantum, in contrast to thermal, fluctuations. They are usually induced by changes in coupling constants and characterized by non-analytic changes in ground state properties under variation of the coupling. As in thermodynamics, an actual phase transition[4] relies on the limit $N \to \infty$; one

[4]Barring the possibility that integrability or some extended symmetry properties allow for level crossing even for finite $N$.

therefore defines the rescaled coupling $\tilde{\lambda} = \lambda N$ and sends $\lambda$ to zero such that $\tilde{\lambda}$ remains finite. The quantum critical point usually corresponds to a point where interactions just start to dominate, $\tilde{\lambda} \sim 1$.

At the level of the Gross Pitaevskii equation, quantum phase transitions may be discovered via the observation of crossing of solutions. The stationary Gross Pitaevskii equation can be obtained from extremizing the Hamiltonian; its solutions thus correspond to classical extrema of the Hamiltonian. In particular, they allow us to find the classical lowest energy configuration. At the critical point of a QPT, a given solution is replaced by another.

At the quantum critical point, the correlation length of the system diverges. This turns out to be responsible for significant quantum correlations. Quantum critical points are "maximally" quantum. This is also implied by the appearance of very light modes. For each solution, an almost gapless Bogoliubov mode emerges, its energy being such that the gap closes in the limit $N \to \infty$. This is rather intuitive. In the infinite particle limit, the classical solutions become energy eigenstates. Since they are degenerate at the critical point, the mode that deforms one into the other must become gapless.

In our picture, black holes correspond to unstable condensates of gravitons. They do not correspond to lowest energy states, not even in some superselection sector. Nevertheless, they may underlie similar phenomena under changes of coupling constants. Here, these go under the name of bifurcations. At a bifurcation point, classically stable points may become unstable, solutions can annihilate each other, or new solutions may emerge. Bifurcation points share several points with quantum critical points. Due to the fact that solutions "become close", light modes emerge. Also here the quantum state corresponding to the classical solution becomes maximally quantum.

In the case of black holes, the existence of a bifurcation can hold the key to the black hole entropy. Let us note here that in order to reproduce the Bekenstein Hawking entropy, the appearance of roughly $N$ modes with gap $1/N$ is necessary to provide for the exponential degeneracy $e^N$. The origin of these modes is subject of ongoing research.

# Chapter 6

# Quantumness on Macroscopic Scales

## 6.1 Introduction

We have argued in the previous chapter that in a quantum theory of gravitation, black holes can be described as Bose condensates of gravitons. Due to their peculiar coupling, these condensates lie at a point of collective strong coupling, usually indicative of quantum phase transitions or bifurcations. We have then suggested that due to this property, even very large black holes, consisting of a number of gravitons $N > 10^{70}$, can be very quantum objects.

In this chapter, we will elaborate in more detail why one can expect Bose condensates at a critical point to display qualitatively new phenomena. In particular, we will discuss how quantum physics can be relevant on macroscopic scales in such systems. To this end, we are going to investigate in detail the quantum phase transition of the attractive Bose gas in $1 + 1$ dimensions. The transition in this system was discovered and first studied in [Kanamoto et al., 2003]. We will substantiate the existence of this critical point by studying appropriate characteristics.

We will then focus on the quantum behavior. As a measure of quantumness, we calculate the entanglement of different momentum modes applying analytical as well as numerical techniques. We observe that it becomes maximal at the critical point and for low momentum modes. We interpret this as further evidence that the black hole condensate picture can be successful independent of the ultraviolet physics that completes Einstein theory.

The remainder of the chapter will be organized as follows. In section 2 we will introduce in detail the $1+1$-dimensional attractive Bose gas, remind the reader of mean g and introduce the basis of our numerical studies. Further

evidence for the existence of a quantum critical point is provided in section 3. We will then introduce the fluctuation entanglement as a relevant measure of quantumness and present our results in 4. Finally, in the conclusions, we discuss the qualitative consequences of our findings with regards to the physics of macroscopic black holes.

## 6.2 The 1+1-dimensional Bose gas

Throughout this chapter, we consider a Bose gas on a $1D$-circle of radius $R$ with attractive interactions. The Hamiltonian is given by

$$\hat{H} = \frac{1}{R}\int_0^{2\pi} d\theta \left[ -\frac{\hbar^2}{2m}\hat{\psi}^\dagger(\theta)\partial_\theta^2\hat{\psi}(\theta) - \frac{\hbar^2}{2m}\frac{\pi\alpha R}{2}\hat{\psi}^\dagger(\theta)\hat{\psi}^\dagger(\theta)\hat{\psi}(\theta)\hat{\psi}(\theta)\right] , \quad (6.1)$$

where $\alpha$ is a dimensionless, positive coupling constant. This Hamiltonian can be cast into a more convenient form by decomposing $\hat{\psi}(\theta)$ in terms of annihilation operators:

$$\hat{\psi}(\theta) = \frac{1}{\sqrt{2\pi R}}\sum_{k=-\infty}^{\infty} \hat{a}_k e^{ik\theta} , \quad (6.2)$$

which leads to

$$\hat{H} = \sum_{k=-\infty}^{\infty} k^2 \hat{a}_k^\dagger \hat{a}_k - \frac{\alpha}{4}\sum_{k,l,m=-\infty}^{\infty} \hat{a}_k^\dagger \hat{a}_l^\dagger \hat{a}_{m+k}\hat{a}_{l-m} \quad (6.3)$$

Note that in order to improve readability we have now switched to units $R = \hbar = 2m = 1$. The total number operator is

$$\hat{N} = \int_0^{2\pi} d\theta \hat{\psi}^\dagger(\theta)\hat{\psi}(\theta) = \sum_{k=-\infty}^{\infty} \hat{a}_k^\dagger \hat{a}_k . \quad (6.4)$$

It was first shown in [Kanamoto et al., 2003] that an increase of the effective coupling $\alpha N$ on the ring leads to a transition from a homogenous ground state to a solitonic phase, where the critical point is reached for $\alpha N = 1$.

### 6.2.1 Mean field analysis

A mean field approach to the hamiltonian (6.1) leads to the Gross-Pitaevskii energy functional

$$E[\Psi_{GP}] = \int_0^{2\pi} d\theta \left[ |\partial_\theta \Psi(\theta)|^2 - \frac{\alpha}{2}|\Psi(\theta)|^4 \right] \quad (6.5)$$

The ground state wavefunction $\Psi_0$ is obtained through minimization of the energy functional subject to the constraint $\int d\theta |\Psi(\theta)|^2 = N$. This leads to the time independent Gross-Pitaevskii equation

$$\left[\partial_\theta^2 + \pi\alpha|\Psi_0(\theta)|^2\right]\Psi_0(\theta) = \mu\Psi_0(\theta)\,, \tag{6.6}$$

where $\mu = dE/dN$ is the chemical potential. Solutions to this equation are given by (see e.g. [Carr et al., 2000])[1]

$$\Psi_0(\theta) = \begin{cases} \sqrt{\frac{N}{2\pi}} \\ \sqrt{\frac{NK(m)}{2\pi E(m)}}\mathrm{dn}\left(\frac{E(m)}{\pi}(\theta-\theta_0)|m\right) \end{cases} . \tag{6.7}$$

Here, $\theta_0$ denotes the center of the soliton and $m$ is determined by the equation

$$K(m)E(m) = \left(\frac{\pi}{2}\right)^2 \alpha N\,. \tag{6.8}$$

For small $\alpha N < 1$, (6.5) is minimized by the homogenous wavefunction. On the other hand, for $\alpha N > 1$ the solitonic solution has a lower energy. At $\alpha N = 1$, both configurations are degenerate in energy - a clear indication for a quantum phase transition.

On a side note, one may wonder whether the one-soliton solution is stable for arbitrary $\alpha N > 1$ or if multi-soliton solutions may eventually be energetically favored. This can be checked in a simple argument. A soliton of size $R_s$ has a total energy

$$E \sim \frac{N}{R_s^2} - \alpha\frac{N^2}{R_s}\,. \tag{6.9}$$

Minimization with respect to $R$ yields $R_s = \frac{2}{\alpha N}$ and $E_1 = -\frac{1}{4}\alpha^2 N^3$. A split into two stable solitons of boson number $rN$ and $(1-r)N$ yields a total energy $E_2 = -\frac{1}{4}\alpha^2 N^3[1-3r(1-r)]$. This is bigger than $E_1$ for any $r < 1$. This can be straightforwardly generalized two multi-soliton solutions; therefore, the single soliton is stable.

Finally, let us note that the apparent spontaneous breaking of translation symmetry in the solitonic phase is in no contradiction to known theorems about the absence of finite volume symmetry breaking. The Gross-Pitaevskii ground state only becomes exact in the $N \to \infty$ limit. In this limit, translated Gross-Pitaevskii states are orthogonal and do not mix under time evolution. Technically, symmetry breaking is made possible because expecation values of composite operators made out of the fields diverge in the large $N$ limit. We comment on this in more detail in the Appendix.

[1]Here, $\mathrm{dn}(u|m)$ is a Jacobi elliptic function and $K(m)$ and $E(m)$ are the complete elliptic integrals of the first and second kind, respectively.

This again emphasizes how the classical limit really emerges as a large $N$ limit from quantum mechanics. Exactly how this argument breaks down at the critical point and what the implications of this breakdown are will be the focus of the remainder of this manuscript.

### 6.2.2 Bogoliubov approximation

The Gross-Pitaevskii equation is the zeroth-order equation in an expansion of the field operator into its mean value and quantum (and, in more general setups, thermal) fluctuations around it:

$$\hat{\psi}(\theta) = \langle\hat{\psi}(\theta)\rangle + \delta\hat{\psi}(\theta)\,. \tag{6.10}$$

The spectrum of these small excitations around the mean field can then be found in the Bogoliubov approximation. Generally, this corresponds to approximating the fluctuation Hamiltonian by its quadratic term and subsequent diagonalization through canonical transformations of the field.

For $\alpha N < 1$, i.e. on the homogeneous background, it is convenient to stick to the momentum decomposition (6.2) and replace $\hat{a}_0 = \hat{a}_0^\dagger = \sqrt{N_0} \sim \sqrt{N}$. In words, one assumes that the zero mode is macroscopically occupied and all commutators $[\hat{a}_0, \hat{a}_0^\dagger]$ in the Hamiltonian are suppressed by relative powers of $1/N$; the quantum fluctuations of the zero mode may therefore be neglected. This, in combination with taking into account the constraint

$$\hat{N} = N_0 + \sum_{k\neq 0} \hat{a}_k^\dagger \hat{a}_k \tag{6.11}$$

leads to the Hamiltonian

$$\mathcal{H} = \sum_{k\neq 0} \left(k^2 - \alpha N/2\right) a_k^\dagger a_k - \frac{1}{4}\alpha N \sum_{k\neq 0} \left(a_k^\dagger a_{-k}^\dagger + a_k a_{-k}\right) + \mathcal{O}(1/N)\,. \tag{6.12}$$

All interaction terms are suppressed by $1/N$ and go to zero in the double scaling limit $N \to \infty$, $\alpha \to 0$ with $\alpha N$ finite. The Hamiltonian can be diagonalized

$$\mathcal{H} = \sum_{k\neq 0} \epsilon_k b_k^\dagger b_k,\ \epsilon_k = \sqrt{k^2(k^2 - \alpha N)} \tag{6.13}$$

with a Bogoliubov transformation

$$a_k = u_k b_k + v_k^\star b_{-k}^\dagger, \tag{6.14}$$

where the Bogoliubov coefficients are

$$u_k^2 = \frac{1}{2}\left[1 + \frac{k^2 - \frac{\alpha N}{2}}{\epsilon_k}\right], \tag{6.15}$$

$$v_k^2 = \frac{1}{2}\left[-1 + \frac{k^2 - \frac{\alpha N}{2}}{\epsilon_k}\right]. \tag{6.16}$$

The Boguliubov approximation breaks down whenever an $\epsilon_k$ becomes too small. In that case the initial assumption that only the zero mode is macroscopically occupied is no longer justified. Obviously, it is $\epsilon_1$ that first goes to zero, namely when $\alpha N \to 1$. Right at the phase transition, the Boguliubov approximation is never valid. It is worth noting however, that for any finite distance $\delta$ from the critical point, there exists a minimal $N$ for which the approximation is valid. In other words, for any finite $\delta$, the Boguliubov approximation becomes exact in the limit $N \to \infty$. This is due to the fact that both the interaction terms as well as $v_k^2/N$ vanish in this limit for any finite $\delta$. For $\delta = 0$, however, this is never true.

In the $\alpha N > 1$ case, the classical background is not homogenous any more, but is given by the bright soliton solution (6.7). In this case, the background induces an additional nontrivial mixing between momentum eigenmodes of different $|k|$. A decomposition into momentum eigenmodes requires an (unknown) analytic expression for the Fourier components of the soliton and is thus no longer convenient. On the other hand, an analytic Bogoliubov treatment is still possible by directly decomposing $\delta\hat{\psi}$ into normal modes:

$$\delta\hat{\psi}(\theta) = \sum_i \left(u_i(\theta)\hat{b}_i^\dagger + v_i^\star(\theta)\hat{b}_i\right). \tag{6.17}$$

If the mode functions obey the Boguliubov-de Gennes equations

$$\partial_\theta^2 u_j + \alpha\Psi_0^2(2u_j + v_j) + \mu u_j = E_j u_j \tag{6.18}$$

$$\partial_\theta^2 v_j + \alpha\Psi_0^2(2v_j + u_j) + \mu u_j = -E_j u_j \tag{6.19}$$

and are normalized such that they form a complete set and the transformation (6.17) is canonical, the Hamiltonian is diagonalized. The first excited Bogoliubov modes have the form

$$u_1(\theta) = N_1 \mathrm{sn}^2\left(\frac{K(m)}{\pi}(\theta - \theta_0)\middle| m\right) \tag{6.20}$$

$$v_1(\theta) = -N_1 \mathrm{cn}^2\left(\frac{K(m)}{\pi}(\theta - \theta_0)\middle| m\right). \tag{6.21}$$

The coefficient $N_1$ is defined by

$$N_1^2 = \frac{mK(m)}{2\pi\left[(2-m)K(m) - 2E(m)\right]}\,. \tag{6.22}$$

### 6.2.3 Numerical diagonalization

While the Bogoliubov treatment provides an approximative description of the Bose gas deep in the respective phases, it fails, as we have reasoned above, around the critical point.

A complementary method to explore the quantum properties of the system is numerical diagonalization of the Hamiltonian. Of course, numerical techniques are only applicable for sufficiently small Hilbert spaces. The Hamiltonian (6.1) is number conserving. This allows for exact diagonalization of (6.3) by considering a subspace of fixed $N$. However, to make any numerical procedure feasible, we need to limit the allowed momenta. In the spirit of [Kanamoto et al., 2003], we truncate the basis of free states in which we perform the diagonalization to $|l| = 0, 1$. This gives a very good approximation to the low energy spectrum of the theory well beyond the phase transition. Analytically, this can be seen by analyzing the spectrum of the soliton solution (6.7). Only for $\alpha N \gtrsim 1.5$, higher $l$ modes start giving relevant contributions. We have further verified this numerically by allowing for $|l| = 2, 3$; the low energy modes are only marginally affected up until $\alpha N \sim 2$. Our code allowed us to consider particle numbers $N \lesssim 10000$. In order to illustrate scaling properties, all analyses are performed for various particle numbers.

Since the normalized coupling $\alpha N$ is the relevant quantity for a phase transition, one can analyze all interesting properties for a fixed $N$ by varying $\alpha$. The corresponding spectrum of excitations above the ground state as a function of $\alpha N$ is shown in Fig.6.1 for $N = 5000$ and $-1 \leq k \leq 1$. One observes a decrease in the energy gap between the low lying excitations due to the attractive interactions as $\alpha N$ is increased. At the quantum critical point, the spacing between levels reaches its minimum. Its magnitude depends on the particle number $N$; the energy of the lowest lying excitation decreases with $N$. By further increasing the coupling $\alpha$ one reaches the solitonic phase. The spectrum corresponds to that of translations and deformations of a soliton.

Obviously, (6.1) is invariant under translations; since we are considering a finite length ring, the ground state obtained by exact diagonalization can never correspond to a localized soliton. It will instead contain a superposition of solitons centered around arbitrary $\theta$. This problem can be overcome by

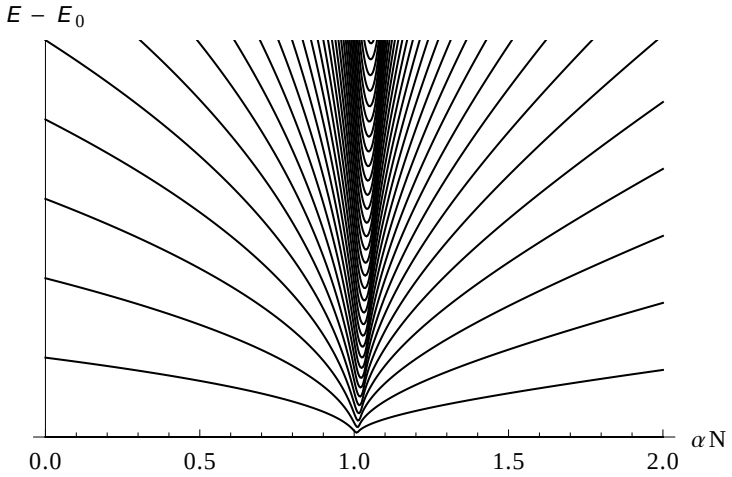


Figure 6.1: Energy spectrum for $N = 5000$ as a function of the effective coupling $\alpha N$

superposing a weak symmetry breaking potential to break the degeneracy between states with a different soliton position:

$$\hat{H}_{sb} = \hat{H} + \hat{V}_\epsilon \tag{6.23}$$

$$\hat{V}_\epsilon = \frac{\epsilon}{N^2} \int d\theta \hat{\psi}^\dagger(\theta) \cos\theta \hat{\psi}(\theta) \,. \tag{6.24}$$

The higher $\epsilon$, the deeper the symmetry breaking potential, and the more localized the soliton will be.

## 6.3 Quantum phase transition in the 1D-Bose gas

The mean field treatment of the attractive 1D Bose gas above has signalled a quantum phase transition. The degeneration of the Bogoliubov modes at $\alpha N = 1$ supports the existence of a critical point. Although, by definition, a phase transition can only occur for infinite $N$, indications for it should already be visible for large but finite $N$. Here we will focus on two observations:

(i) The one-particle entanglement entropy displays a sharp increase close to the critical point.

(ii) The ground state fidelity peaks at the critical point; the height of the peak grows with $N$.

### 6.3.1 One-particle entanglement

The one particle entanglement entropy is defined as the von Neumann entropy $S_1 = \mathrm{tr}[\hat{\rho}_{1\mathrm{p}} \log \hat{\rho}_{1\mathrm{p}}]$ of the one particle density matrix $\hat{\rho}_{1\mathrm{p}}$ of the ground state, obtained by singling out one particle and tracing over all $N-1$ other. As long as the ground state of the system is well described by a Hartree, i.e. product state, $\hat{\rho}_{1\mathrm{p}}$ describes a pure state; the entanglement entropy vanishes. When the critical point is approached, collective effects become important. No longer is the ground state described by a product state; consequently the entanglement entropy increases - a single particle becomes strongly entangled with the rest of the system.

The one particle density matrix is defined via

$$\hat{\rho}_{1\mathrm{p}} = \underset{(N-1)\mathrm{P}}{\mathrm{tr}} \hat{\rho} = \underset{(N-1)\mathrm{p}}{\mathrm{tr}} |0_{GP}\rangle \langle 0_{GP}| \ , \tag{6.25}$$

or, explicitly, in the one particle momentum eigenbasis

$$(\hat{\rho}_{1\mathrm{P}})_{ij} = \delta_{ij} \sum_{\{n_k\}} |\alpha_{\{n_k\}}|^2 \frac{n_i}{N} \, . \tag{6.26}$$

Here, $n_k$ is the occupation number of the $k$-th momentum mode and we have used

$$|0_{GP}\rangle = \sum_{\{n_k\}} \alpha_{\{n_k\}} |\{n_k\}\rangle \ . \tag{6.27}$$

We have plotted the numerically evaluated one particle entanglement as a function of $\alpha N$ for different $N$ in Fig.6.2a. The increase close to the critical point gets profoundly sharper for larger $N$. Independent of $N$, the entropy is bounded by $S_{\max} = \log 3$, due to the truncation of the one-particle Hilbert space to a three level system.

The entanglement entropy becomes maximal for large $\alpha N$. This, as argued before, is due to the fact that the numerical groundstate is given by a superposition of solitons localized at arbitrary positions [Qian et al., 2008].[2]

### 6.3.2 Ground State Fidelity

Ground State Fidelity (GSF) was introduced in [Zanardi and Paunković, 2006] as a characteristic of a QPT. It is defined as the modulus of the overlap of the exact ground states for infinitesimally different effective couplings.

$$F(\alpha N, \alpha N + \delta) = |\langle 0_{\alpha N}| 0_{\alpha N+\delta}\rangle| \tag{6.28}$$

[2]This quantum behavior is not expected to survive in the large $N$ limit if the symmetry breaking potential is turned on. In this case, a vacuum is selected which does not mix with translated states (see Appendix). The entanglement entropy is therefore much smaller.

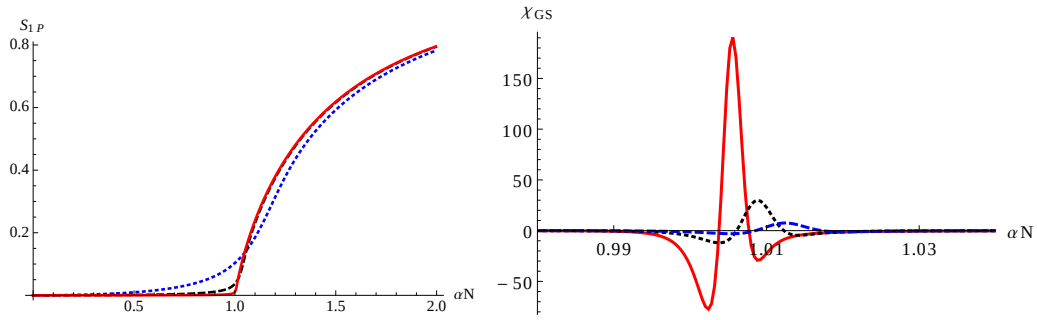


(a) (b)

Figure 6.2: (a): One-particle entanglement entropy for $N = 50$ (blue, dotted), 500 (black, dashed), 5000 (red, solid). (b): Numerical ground state fidelity susceptibility for $N = 3000$ (blue, dashed), $N = 5000$ (black, dotted) and $N = 10000$ (red, solid).

Far away from the critical point, this overlap will be very close to unity. For small $\alpha N$, the ground state is dominated by the homogeneous state, and while coefficients may change slightly, no important effect will be seen. The analogous statement holds deep in the solitonic regime. While the shape of the soliton changes, it will so smoothly; in the infinitesimal limit, the overlap is one. Right at the critical point, however, the ground state changes in a *non-analytic* way. The homogeneous state ceases to be the ground state and becomes an excited state, while the soliton becomes the new ground state. As energy eigenstates with different eigenvalue are orthogonal, the ground state fidelity across the phase transition is exactly zero.

The GSF has the disadvantage of depending on the arbitrary choice of the small parameter $\delta$. This can be cured by introducing the fidelity susceptibility $\chi_{\text{gs}}(\alpha N)$ as the second derivative of the GSF.

$$\chi_{\text{gs}}(\alpha N) = \lim_{\delta \to 0} \frac{F(\alpha N, \alpha N + \delta) - F(\alpha N, \alpha N - \delta)}{\delta^2} \,. \tag{6.29}$$

It has been shown [Yang, 2007] that singular behavior of the fidelity susceptibility directly signals a discontinuity of the first or second derivative of the ground state energy - a quantum phase transition.

The aforementioned behavior is of course idealized for an infinite system, where ground state degeneracy and thus level crossing become an exact property. In the finite $N$ systems we examined numerically, the overlap cannot go to zero, because there is anticrossing which allows the energy levels to degenerate only for $N \to \infty$.

Still we can observe a drop in the fidelity which deepens with $N$ but is

of magnitude much smaller than 1 for all $N$ we were able to simulate. The fidelidy susceptibility as obtained from the exact diagonalization is plotted in Fig.6.2b for different $N$. In the limit $N \to \infty$, we expect a behavior $\chi_{\rm gs} \to -\delta''(\alpha N - 1)$. This tendency can be clearly observed. Both the negative and the positive peak move towards $\alpha N = 1$, they become narrower, and their modulus diverges with growing $N$.

## 6.4 Fluctuation entanglement

We will now consider the entanglement between the fluctuation $\delta\hat{a}_k = \hat{a}_k - a_k^{\rm c}$ of a given original momentum mode and the fluctuations of the rest of the system. The motivation for studying this quantity is twofold. We imagine, that an external observer would couple linearly to the bosonic field (so that the situation has some minimal resamblance with the gravity case). It has been pointed out [Anglin and Zurek, 1996] that for such a coupling, field values (or their Fourier components) will be the environment-selected pointer states[3] and not localized single particle states. This leads us to consider the entanglement of a momentum mode, rather than single-particle entanglement, as a measure of relevant quantum correlations of the given state. Furthermore, the observer couples to the original field $\hat{a}_k$ and hence its fluctuations as opposed to coupling to the Bogoliubov modes $\hat{b}_k$.

More technically speaking, the quantity we calculate is the von Neumann entropy of the reduced density matrix for a given $\delta\hat{a}_k$

$$(\delta\rho_k)_{nm} = \operatorname*{tr}_{\text{modes } k' \neq k} \left[ \rho \, (\delta\hat{a}_k^\dagger)^m |0^{\rm c}\rangle\langle 0^{\rm c}| (\delta\hat{a}_k)^n \right] \tag{6.30}$$

where $|0^{\rm c}\rangle$ denotes the state that would be observed classically.

Fluctuation entanglement provides a measure for the quantum correlations between a single momentum mode with the rest of the system. It hence gives a direct handle of the quantumness of our ground state as measured by an outside observer if coupled linearly to the field. Note also that due to the fact that we are considering a closed system, the fluctuation entanglement is exactly equivalent to the Quantum Discord introduced in works [Henderson and Vedral, 2001] as a measure of quantumness.

[3] Pointer states denote those states that are stable with respect to interactions with the environment and therefore correspond to classically observable states.

### 6.4.1 Calculation in the Bogoliubov approximation

In order to calculate the fluctuation entanglement in the Bogoliubov case, note that the sought-for density matrix is Gaussian[4]. The ground state in terms of $\hat{b}_k$ is Gaussian and the Bogoliubov transformation amounts to squeezing - which leaves a Gaussian state Gaussian. Also integrating out modes in a Gaussian state does not change this property. Hence the reduced density matrix in terms of $\delta\hat{a}_k$ must have the form

$$\rho_k = C_k \exp\Big\{ -\lambda_k\Big(\delta\hat{a}_k^\dagger\delta\hat{a}_k - \frac{1}{2}\tau_k\left[\delta\hat{a}_k^\dagger\delta\hat{a}_k^\dagger + \delta\hat{a}_k\delta\hat{a}_k\right]\Big)\Big\}, \tag{6.31}$$

with real coefficients $\lambda_k$ and $\tau_k$ and normalization $C_k$ such that $\operatorname{tr}\rho_k = 1$. This density matrix has a von Neumann entropy

$$S_k = \frac{\lambda_k\sqrt{1-\tau_k^2}}{2}\left(\coth\frac{\lambda_k\sqrt{1-\tau_k^2}}{2} - 1\right) - \ln\left(1 - e^{-\lambda_k\sqrt{1-\tau_k^2}}\right) \tag{6.32}$$

We can fix the unknown coefficients by imposing

$$\langle\psi|\delta\hat{a}_k^\dagger\delta\hat{a}_k|\psi\rangle = \operatorname{tr}[\rho_k\delta\hat{a}_k^\dagger\delta\hat{a}_k]$$

and

$$\langle\psi|\delta\hat{a}_k\delta\hat{a}_k|\psi\rangle = \operatorname{tr}[\rho_k\delta\hat{a}_k\delta\hat{a}_k]\,, \tag{6.33}$$

where $|\psi\rangle$ is the groundstate of the Bogoliubov modes.

### 6.4.2 Homogenous phase

In the homogenous case, imposing (6.33) and evaluating the left hand side by inserting the Bogoliubov transformation (6.14) leads to

$$\lambda_k = \ln\left(\frac{u_k}{v_k}\right)^2, \qquad \tau_k = 0 \qquad \text{and} \qquad C_k = 1/u_k^2. \tag{6.34}$$

Thus, the fluctuation entanglement entropy is

$$S_k = u_k^2\ln u_k^2 - v_k^2\ln v_k^2. \tag{6.35}$$

The entanglement of the first momentum mode $S_1$ diverges near the critical point $\alpha N = 1-\delta$ as

$$S_1 \approx 1 - \ln(4) - \frac{1}{2}\ln\delta. \tag{6.36}$$

[4]A density matrix is called Gaussian, when its Wigner function $W(\alpha,\alpha^\star) = \frac{1}{\pi^2}\int d^2\beta\exp(-i\beta\alpha^\star - i\beta^\star\alpha)\operatorname{tr}[\rho\exp(i\beta a^\dagger + i\beta^\star a)]$ is Gaussian

A similar divergence of an entanglement entropy has been pointed out in spin chain (and analogous) systems undergoing a phase transition [Vidal et al., 2003]. In contrast to these cases however, where the entanglement is between nearest neighbour sites, the diverging entanglement in our case is between different low-momentum modes and not between localized sites. So one may say, that the entanglement in our case is long-range. Furthermore it should be noted, that the entanglement of the higher modes $|k| > 1$ stays finite near the critical point, showing that the diverging entanglement is an infrared effect, which can be expected to be independent of short distance physics.

### 6.4.3 Solitonic phase

The relevant expectation values in the Bogoliubov ground state are given by

$$\langle\psi|\delta\hat{a}_m^\dagger\delta\hat{a}_n|\psi\rangle = \sum_k \left(\int e^{im\theta}v_k(\theta)d\theta\right)\left(\int e^{-in\theta}v_k(\theta)^\star d\theta\right), \quad (6.37)$$

$$\langle\psi|\delta\hat{a}_m\delta\hat{a}_n|\psi\rangle = \sum_k \left(\int e^{-im\theta}u_k(\theta)d\theta\right)\left(\int e^{-in\theta}v_k(\theta)^\star d\theta\right). \quad (6.38)$$

It can be checked that close to the phase transition the first excited mode gives the leading contribution to the aforementioned entanglement entropy. The quantities $\langle\psi|\delta\hat{a}_1^\dagger\delta\hat{a}_1|\psi\rangle$ and $\langle\psi|\delta\hat{a}_1\delta\hat{a}_1|\psi\rangle$ can be obtained by numerical integration. The parameters $\lambda, \tau$ of the reduced gaussian density matrix can then be determined. The final von Neumann entropy again shows a divergence[5] close to the phase transition. Fig.6.3a shows the fluctuation entanglement obtained in the Bogoliubov approximation on both sides of the phase transition.

### 6.4.4 Numerical treatment

As discussed before, for any given finite size system, the Bogoliubov approximation should not be trusted close to the critical point. Therefore it is important to study the exact behavior of finite size systems numerically, in order to substantiate the claim that the fluctuation entanglement entropy becomes large.

Within an exact treatment this quantity is considerably more difficult to extract, because in contrast to the Bogoliubiv analysis, one does not have direct access to a "classical background" which one could use to disentangle

[5]The shape of the divergence obtained by numeric integration seems to be consistent with a logarithm with a coefficient close to 0.33 near the phase transition.

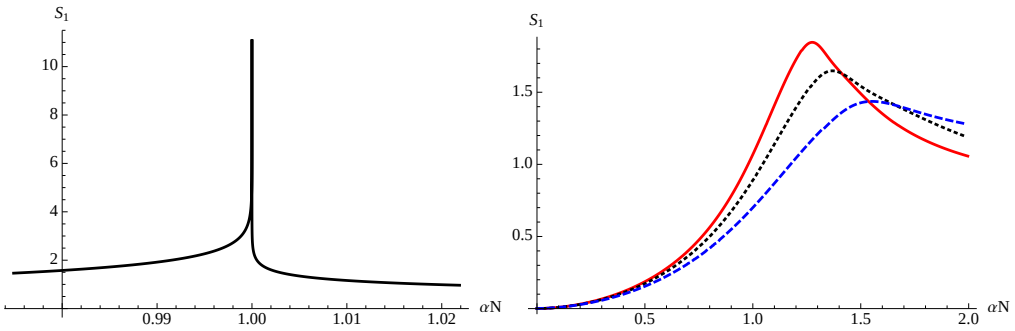


(a) (b)

Figure 6.3: (a): Analytical fluctuation entanglement. (b): Numerical fluctuation entanglement for $N = 15$ (blue, dashed), $N = 20$ (black, dotted) and $N = 25$ (red, solid).

classical correlations. Instead, the seperation can be obtained through the following procedure.

Since all numerical solutions are obtained for a fixed particle number $N$, the field expectation value in the exact ground state $|0_N\rangle$ will necessarily vanish, $\langle 0_N|\,\hat{\psi}(\theta)\,|0_N\rangle = 0$. Obviously, the ground state $|0_N\rangle$ can hence never correspond to the classical (coherent) state with a wave function corresponding to the soliton solution of the Gross-Pitaevskii equation, $\langle\psi_{\rm cl}|\,\hat{\psi}(\theta)\,|\psi_{\rm cl}\rangle = \Psi_{\rm GP}(\theta)$. In order to define a mapping from $|0_N\rangle$ to $|\psi_{\rm cl}\rangle$, we numerically search for the coherent state $|\alpha\rangle$ with maximal overlap with $|0_N\rangle$. This state is expected to be annihilated by the perturbations of the Gross-Pitaevskii ground state,

$$\delta\hat{a}_k\,|\alpha_k\rangle = 0\,, \tag{6.39}$$

where

$$\delta\hat{a}_k = \hat{a}_k - c_k \tag{6.40}$$

and the $c_k$ are the Fourier coefficient of $\Psi_{\rm GP}(\theta)$. From Eq.(6.39) it directly follows that $\alpha_k = c_k$. There is now an obvious measure of correlations which excludes those of the Gross-Pitaevskii background: The entanglement entropy of the $\delta\hat{a}_1$ modes, described by the density matrix

$$(\tilde{\rho}_1)_{kl} = \mathrm{tr}\left[\hat{\rho}\,|\delta l_1\rangle\,\langle\delta k_1|\right]\,. \tag{6.41}$$

Now, $|\delta l_1\rangle$ denotes the eigenstate of $\delta\hat{N}_1 = \delta\hat{a}_1^\dagger\delta\hat{a}_1$ with eigenvalue $\delta l_1$. Eq. (6.41) directly corresponds to the density matrix (6.31) in the Bogoliubov approximation. Using the relations (6.39) and (6.40), it can be directly recast

to take on the form

$$(\tilde{\rho}_1)_{kl} = \mathrm{tr}\left[\hat{\rho}\frac{(\hat{a}_1^\dagger - \alpha_1^*)^l}{\sqrt{l!}}\left|\alpha_1\right\rangle\left\langle\alpha_1\right|\frac{(\hat{a}_1 - \alpha_1)^k}{\sqrt{k!}}\right], \tag{6.42}$$

which, by the definition of a coherent state, can be straightforwardly evaluated.

The resulting fluctuation entanglement is shown in Fig.6.3b for different particle number. It has a clear maximum at the would–be–phase–transition. The maximum value becomes larger and the peak narrower with increasing particle number, so the divergence in the Bogoliubov case seems a plausible limit. The fact that at $\alpha N = 2$, the fluctuation entanglement is still quite high is not surprising. Only in the limit $N \to \infty$ do we expect to see the behavior of the Boguliubov analysis. This is supported by the fact that a decrease is observed for increasing $N$, as well as for stronger localization potentials.

## 6.5 Summary

In this chapter, we have considered properties of the 1+1-dimensional attractive Bose gas around its critical point. By analyzing important indicators for QPTs, we provided further evidence that a tuning of the effective coupling $gN$ leads to a phase transition in the system. More importantly, we have shown that quantum correlations become very important close to the critical point - contrary to the naive intuition that at sufficiently large particle number, systems should behave approximately classical. We have also pointed out that the quantum entanglement of the bosons close to the critical point is "long range" - in contrast to the observations in spin-chain systems that display nearest neighbour entanglement at criticality.

The motivation for our study of this model system, however, was the conjecture that black holes are bound states of a large number of weakly interacting gravitons. It has been claimed that the graviton condensates behave significantly different with respect to the semiclassical black hole analysis due to their being at a quantum critical point. It was argued that criticality allows quantum effects to only be suppressed by the perturbative coupling $\alpha_g \sim 1/N$ as opposed to the usual exponential suppression. If the qualitative insights from our simple toy model are valid for graviton condensates our results can back up several of the claims. We can argue that quantum effects become important for attractive Bose condensates at their critical point - even though the perturbative coupling is very small. Moreover, the entanglement of the true state is long range, consistent with the notion of a con-

densate of gravitons of wavelength comparable to the Schwarzschild radius. This would imply that for a black hole, the semiclassical treatment with a background geometry that obeys classical general relativity and quantization of fields on top of this rigid background becomes invalid much earlier than what the standard lore tells. Although curvature invariants in the horizon region of large Schwarzschild black hole are small, the semiclassical treatment is not applicable. Instead, quantum correlations in the graviton bound state become relevant. Importantly, our results point in the direction that the physics is dominated by large wavelengths. Therefore the description of black holes as graviton condensates has the attractive feature of being independent of the ultraviolet completion of gravity. The only requirement being that the low energy theory resembles perturbatively quantized Einstein theory with a massless spin two graviton.

The 1+1-dimensional Bose gas can indeed capture quite a few of the intriguing features of black holes and their possibly quantum nature. To understand in more detail time dependent features, such as Hawking evaporation, resolutions of the information paradox or scrambling, the implementation of dynamical methods will be amongst the aims of immediate future work. This will then necessarily also address possible couplings to external systems in order to be able to model the evaporation process. Working with more spatial dimensions may prove feasible to model the collapse induced by Hawking evaporation. This could alternatively be achieved by considering couplings that show further resemblance with gravitational self- interactions. Steps in these directions also include generalizations to non-number conserving, and ultimately relativistic theories.

Instabilities can in turn be countered by adding repulsive interactions that dominate at very short scales. Stable configurations of that sort would correspond to extremal black holes. Their properties also provide a vast playground for future investigation.

# Chapter 7

# Scrambling in the Black Hole Portrait

## 7.1 Introduction

In this chapter, we shall discuss how the instability of the Bose Einstein condensate of gravitons is the key for understanding the efficient generation of entanglement and information-scrambling by a black hole in a logarithmic time,

$$t_{\rm scrambling}/R \propto \log N\,. \tag{7.1}$$

Noticing that in our treatment $N$ measures the number of constituents, this result is in full agreement with the semi-classical prediction originally made in [Hayden and Preskill, 2007, Sekino and Susskind, 2008].

One of the most important outputs of the black hole portrait is to allow us to organize quantum corrections in a natural way. For a black hole of action (or entropy) $S = \hbar\, N$ we have non-perturbative corrections that go as $e^{-N}$. These sort of corrections take into the account only the total black hole action and are blind to any form of microscopic constituency. They can for instance measure the transition amplitude between black hole and thermal topologies [Maldacena, 2003b, Hawking, 2005]. On the other hand, any form of quantum back-reaction should be measured in terms of the ratio $1/N \sim \frac{\hbar}{S}$. The key problem however lies in unveiling the *microscopic meaning* of $1/N$-corrections as well as in understanding under what conditions these quantum corrections can effectively become order one for macroscopic black holes with $N \gg 1$.

A Bose-Einstein condensate represents a very natural setup for identifying the physical meaning of $1/N$-corrections. In a nutshell, for BE condensates the small quantum deviations from the mean field Gross-Pitaevskii (GP)

description are $1/N$-corrections, with $1/N$ replacing the role of the Planck constant $\hbar$. Moreover, as we will discuss in this chapter, instabilities of the GP equation can naturally lead to *fast* enhancement of these quantum corrections. More concretely, around instabilities of the GP equation the *quantum break time* (i.e. the time needed to depart significantly ($O(1)$) from the mean field approximation) scales with $N$ as $\log N$. Nicely enough, the BE portrait of black holes implies instabilities of the GP equation. The root of these instabilities lies in the mean-field instability of the condensate at the quantum critical point due to the attractive nature of the interaction. As we will show in this note, the quantum break time for BE condensates fits naturally with the notion of scrambling time for black holes.

## 7.2 Scrambling and quantum break time

The notion of black holes as scramblers was first introduced in [Hayden and Preskill, 2007], where it was realized that perturbed black holes should thermalize in a time $t \geq R \log S_{BH}$ for $S_{BH}$ the black hole entropy and $R$ the black hole radius. In [Sekino and Susskind, 2008] it was then suggested that black holes may saturate this bound, a property that has become known as fast scrambling. The associated timescale is now known as scrambling time.[1]

The concept of scrambling is intimately related to entanglement of subsystems. Consider a quantum mechanical system whose Hilbert space is a direct product $\mathcal{H} = \mathcal{H}_A \otimes \mathcal{H}_B$ in a state described by the density matrix $\rho$. The conventional measure of entanglement between the subsystems is the Von Neumann entropy of the reduced density matrix:

$$S_A = \operatorname*{tr}_A (\rho_A \log \rho_A) \quad \rho_A = \operatorname*{tr}_B \rho \tag{7.2}$$

A system is called a scrambler if it dynamically thermalizes in the sense that, if prepared in an atypical state, it evolves towards typicality. That is, even for an initial state that has little or no entanglement between subsystems, the time evolution is such that the reduced density matrices are finally close to thermal density matrices. The scrambling time is simply the characteristic time scale associated to this process. It can be described as the time it takes for a perturbed system, one that is described by a product state, to evolve back into a strongly entangled state. It can also be interpreted as the time necessary to distribute any information entering the system amongst all its constituents.

[1] For several attempts to understand the physics of scrambling, see [Susskind, 2011, Lashkari et al., 2013, Asplund et al., 2011, Barbon and Magan, 2011].

The quantum meaning of the scrambling time becomes more transparent if we rewrite it as

$$t_{\text{scrambling}} \sim R \log\left(\frac{S}{\hbar}\right) \tag{7.3}$$

with $S$ now denoting the action of the black hole. This is the typical expression for the *quantum break time* provided the system is near an instability, where quantum break time denotes the timescale for the breakdown of the classical (mean field) description. Hence we will identify as a necessary condition for a system to behave as a fast scrambler to have a quantum break time scaling logarithmically with the number of constituents.

### 7.2.1 Logarithmic quantum break time

In the context of quantum chaos, it has long been known that under certain conditions, the classical description breaks down much quicker than the naively expected polynomial quantum break time. Specifically, in the vicinity of an instability for the classical description, i.e. positive local Lyapunov exponent $\lambda$, the quantum break time usually goes as

$$t_{\text{break}} \sim \lambda^{-1} \log \frac{S}{\hbar} \tag{7.4}$$

This exactly resembles the logarithmic scaling of the scrambling time. In fact, the black hole scrambling time coincides with the typical quantum break time if the microscopic description of the black hole contains an instability characterized by a Lyapunov exponent $\lambda \sim 1/R$. The black hole quantum portrait contains such an instability which survives in the semi-classical limit ($L_P = 0$, $N = \infty$, with $\sqrt{N}L_P$ fixed ) and is described by equation (5.8). The characteristic timescale is given by $R = \sqrt{N}L_P$ which classically becomes the black hole radius. Hence we expect the Lyapunov exponent to be set by $1/R$. This is precisely the way we will identify scrambling in the BE portrait of black holes.

In the next section we show specifically for Bose-Einstein condensate systems that they exhibit quantum breaking in the scrambling time. We will also comment on the instability there. In section 7.5, we perform a numerical analysis that confirms this reasoning.

### 7.2.2 Chaos and thermalization

The relation between scrambling and quantum break time is even stronger if the classical limit of the relevant system not only contains a local instability, but also exhibits classical chaos. For such systems it has been claimed - and

checked to some extent - that the time scale of thermalization is of the same order as $t_{\text{break}}$ [Altland and Haake, 2012]. By taking a pure quantum state it was shown that the time evolution not only stretches and folds the quasi-probability distribution, but also smoothens it out. Of course the quantum state stays pure, but it is thermalized in the sense of being smeared out over the accessible classical phase space volume. This would presumably imply scrambling as defined above. Although, at this point we cannot prove that this is indeed how scrambling actually takes place in the graviton condensates of the BH portrait, we do take it as further evidence that the quantum break time is intimately related with scrambling time.

## 7.3 Quantum break time in BE condensates

### 7.3.1 Prototype models

It has been pointed out [Dvali and Gomez, 2011, 2012a,c] that many of the seemingly mysterious properties of black holes can be resolved when considering them as Bose-Einstein condensates of long wavelength gravitons that interact with a critical coupling strength. Indeed, it has been realized that a vast amount of those properties can already be explored in much simpler systems. These systems share the crucial property that they contain bifurcation or quantum critical points.

Within this work we will follow that route and further explore models of attractive cold bosons both in one and three spatial dimensions. We will show that they exhibit a logarithmic quantum break time, again intimately related to the existence of instabilities and quantum critical or bifurcation points.

The explicit models under consideration in d+1 dimensions are described by the Hamiltonian

$$H = \int_V d^d x \left( \frac{\hbar^2}{2m} (\nabla \phi^\dagger)(\nabla \phi) - \frac{g}{2} (\phi^\dagger \phi)^2 \right). \tag{7.5}$$

Here, $\phi$ carries the dimension length$^{-d/2}$, while the coupling constant $g$ carries dimension energy $\times$ length$^d$. The integral is taken over the volume of a $d$-dimensional torus $V$.

Expanding $\phi$ into mean field and quantum fluctuations $\phi = \phi_{\text{mf}} + \delta\phi$ and subsequent minimization of the energy functional leads, at zeroth order, to the Gross-Pitaevskii (GP) equation for stationary solutions:

$$i\hbar \partial_t \phi_{\text{mf}} = \left( \frac{\hbar^2}{2m} \Delta + g |\phi_{\text{mf}}|^2 \right) \phi_{\text{mf}} = \mu \phi_{\text{mf}}. \tag{7.6}$$

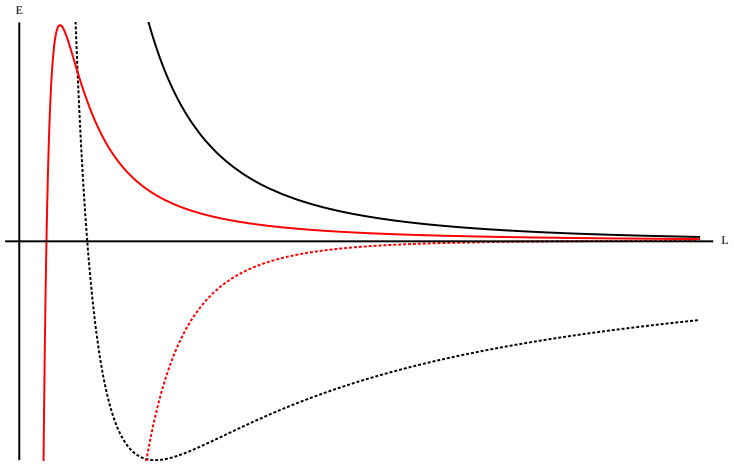


Figure 7.1: Energy as a function of the condensate width for $gN \ll 1$ (solid) and $gN \gg 1$ (dashed) for a condensate in 1 (black) and 3 (red) spatial dimensions.

The chemical potential $\mu$ appears as a Lagrange multiplier that imposes a constraint on the particle number $N$, $\int_V d^d x \phi^\dagger \phi = N$.

An intuitive understanding of the physics of these Bose-Einstein condensates may be gained by considering the behavior of the energy when rescaling the characteristic size of the condensate $R$:

$$E \sim \frac{N}{R^2} - gN\frac{N}{R^d}\,, \tag{7.7}$$

where the coefficients of both terms naturally depend on the shape of the condensate. As illustrated in Fig. 7.1, the behavior depends strongly on the dimension under consideration. For $d = 1$, the energy is always bounded from below. The (stable) ground state solution is given by a homogeneous condensate for $gN < 1$ and a localized soliton for $gN > 1$. A quantum phase transition is observed [Kanamoto et al., 2003] at $gN = 1$. On the other hand, for $d \geq 3$, there is a classically stable homogeneous solution for $gN < 1$, while the condensate is unstable for $gN > 1$.

### 7.3.2 Quantum breaking in Bose condensates

We will now apply the notion of quantum breaking to a Bose-Einstein condensate system of $N$ identical particles. In general, we want to study $k$-particle subsets (although $k$ particles do not form a proper subspace, this technicality will not disturb us much) and use the conventional $k$-particle sub-density

matrices

$$\rho^{(k)}_{mn} = \mathcal{N}\ \mathrm{tr}\left[\rho\left(\prod_l (a_l^\dagger)^{m_l}\right)\left(\prod_l a_l^{n_l}\right)\right] \tag{7.8}$$

where $m$ and $n$ label $k$-particle states, $a_l$ is the annihilation operator for one Boson in the $l$ orbital and $n_l$ is the occupation number in state $n$ of orbital $l$, which satisfy $\sum n_l = k$. The normalization $\mathcal{N}$ is chosen so that $\mathrm{tr}\,\rho^{(1)} = 1$. We would identify a Bose gas as a fast scrambler, *if its time evolution would create a large entropy in each $\rho_k$ for $k \ll N$ on a timescale that scales logarithmically with $N$.*

More precisely, we do not expect generic atomic Bose-Einstein condensates - as available in the laboratory - to be scramblers in the sense of the previous paragraph. We do however identify the scrambling timescale to be the relevant thermalization scale for the quantum time evolution of the system in the following restricted way. If we do not insist on the thermalization of all sub-density matrices, but restrict our attention to $\rho^{(1)}$, then the time in which a state with pure $\rho^{(1)}$ develops a large von Neumann entropy in $\rho^{(1)}$ is exactly the quantum break time. This is because a pure $\rho^{(1)}$ represents a condensate-like state with all bosons in one orbital. This state can be completely described by a classical field representing the wave function of the relevant orbital. Therefore as soon as $\rho^{(1)}$ develops a large entropy, the gas can no longer be expected to have a classical description.

The one-particle density matrix may be diagonalized

$$\rho^{(1)} = \sum_i \lambda_i \left|\Phi_i\right\rangle \left\langle\Phi_i\right| . \tag{7.9}$$

with eigenvectors $|\Phi_i\rangle$, $\lambda_i$ and eigenvalues $\rho^{(1)}(\Psi)$.

A true BE condensate state $|\Psi_{BE}\rangle$ is characterized by possessing one eigenvalue $\lambda_{max} = O(1)$ with the sum of all other eigenvalues suppressed as $1/N$. If a many-body ground state is of this type, we will say that the system is a BE condensate.

In the limit $N \to \infty$ the corresponding reduced one-particle density matrix $\rho^{(1)}$ defines a pure state $|\Phi_{GP}\rangle$ in the one-particle Hilbert space, which is the eigenvector corresponding to the unique maximal eigenvalue. The BE many-body state corresponds to having all the $N$ constituents in the same state $|\Phi_{GP}\rangle$. The wave function $\Phi_{GP}(x,t)$ of this one-particle state is the Gross-Pitaevskii wave function and its evolution is described by the Gross-Pitaevskii equation (7.6).

For finite $N$ and finite $gN$, the Gross-Pitaevskii equation is never exact. In fact, any exact BE condensate state will, by quantum mechanical time evolution, deplete. This is reflected by the fact that the other eigenvalues of

$\rho^{(1)}$ grow. In what follows, we are interested in tracking precisely this growth for some concrete initial conditions, as this allows us to quantify how quickly the Gross-Pitaevskii description breaks down.

Under these conditions the quantum break time $t_b$ appears as the time in which the difference between the exact many-body evolution and the mean field time evolution surpasses a threshold value. Note that the scaling of $t_b$ with $N$ is independent of the choice of threshold value, therefore rendering it effectively arbitrary for our purposes.

Before going into more concrete details let us briefly discuss the physical meaning of this timescale. Let us denote by $\rho^{(1)}(t)$ the exact many-body evolution of the reduced density matrix, whereas by $\rho^{(1)}_{GP}(t)$ we label the mean field GP time evolution for the same initial conditions at $t = 0$. Since $\rho^{(1)}_{GP}(t)$ is a pure state, we can use as a measure of the difference with respect to $\rho^{(1)}(t)$ the entanglement entropy $S(\rho^{(1)}(t))$. We will define $t_b$ as the time needed to reach a certain threshold entropy. This time will generically depend both on the initial condition as well as on the number $N$ of constituents.

The potential growth of the entanglement with time means that the one-particle density matrix is losing *quantum coherence*. On the other hand, and from the point of view of the many body wave function, this loss of quantum coherence is reflected in the form of *quantum depletion*, i.e. in the growth of the number of constituents that are not in the condensate state. Note, that since at the time $t_b$ the number of constituents away from the condensate is significant, this time also sets the limit of applicability of the Bogolyubov approximation.

For regular quantum systems we can expect the time $t_b$ to depend on $N$ as some power [Ehrenfest, 1927]. However, as we will show, some attractive BE condensates exhibit a quantum breaking time scaling with $N$ as $t_b \sim \log N$ i.e., they generate entanglement in a time depending on the effective Planck constant as $\log(1/\hbar)$.

In this sense BE condensates – under those conditions – effectively behave as *fast scramblers*. Hence our task will be, on one side to identify the above conditions and on the other side to relate those fast scrambler BE condensates with the sort of BE condensates we have put forward as microscopic portraits of black holes.

## 7.4 Scrambling and quantumness in BE condensates

A necessary condition for having a quantum break time $t_b$ scaling like $\log N$ for some initial many body state $\Psi_0$ is the exponential growth with time of small fluctuations $\delta\Psi(t)$ where $\Psi = \Psi_0 + \delta\Psi$. In linear approximation the equation controlling $\delta\Psi$ is the Bogolyubov-De-Gennes equation. As discussed above, a significant departure from the mean field approximation as well as generation of entanglement for the reduced one particle density matrix requires a growth in time of the depleted i.e of the non-condensed particles. Nicely enough the equations controlling the growth of depleted particles are the same as the ones controlling the small fluctuations of the Gross-Pitaevskii equation and therefore we can translate the problem of finding a time $t_b$ scaling like $\log N$ into the simpler problem of the *stability of the Gross-Pitaevskii equation*. For a detailed discussion and the related technicalities, see [Castin and Dum, 1998].

We can understand the short break time more concretely if we think about the difference between the exact evolution and the mean field evolution as the addition of a small perturbation to the exact Hamiltonian. Since an unstable system is exponentially sensitive to perturbations of the Hamiltonian then the time for the evolution of states to differ substantially is very short. The instability is controlled by the Lyapunov exponent $\lambda$, while the preexponential factor will depend on the size of the perturbation. The quantum break time is the time when this becomes important, so we can naturally expect it to scale like $t_b \sim \lambda^{-1} \log N$.

## 7.5 Numerical Analysis

### 7.5.1 Quantum break time of one dimensional condensates

In this section we will verify the logarithmic quantum break time numerically for the (1+1)-d Bose condensate.

The theory (7.5) in 1+1 dimensions undergoes a quantum phase transition for $gN = 1$. When surpassing the critical coupling, the homogeneous state becomes dynamically unstable.

As we expect the black hole to lie at such a point of instability, due to its collapse going in hand with Hawking evaporation, we will model the behavior of the black hole by considering the homogeneous state past the point of quantum phase transition.

We consider $gN > 1$ and prepare as initial condition a perfect condensate in the homogeneous one-particle orbital . The linear stability analysis (simply expanding the classical Hamiltonian (7.5) around a the background) at once indicates an instability: the energy of the first Bogolyubov mode becomes imaginary; its magnitude corresponds to $\lambda$, the Lyapunov coefficient for the unstable direction.

Note that this setup may be interpreted as preparing the system in a supercooled phase. Or as the result of a quench across the phase transition, suddenly increasing the coupling from $gN = 0$ to $gN > 1$ (See, for example, [Calabrese and Cardy, 2005, 2006]). The system finds itself in a classically unstable configuration and quantum fluctuations ensure that a rapid depletion of the condensate and simultaneous entanglement generation take place.

Would we evolve the same initial state for $gN < 1$, very little entanglement would be generated (because it overlaps with very few energy eigenstates there) and the relevant timescale of evolution would not scale logarithmically in $N$ (as can be checked by studying the spectrum).

Decomposition of $\phi$ in terms of annihilation and creation operators

$$\hat{\phi} = \frac{1}{\sqrt{L_b}} \sum_{k=-\infty}^{\infty} \hat{a}_k e^{ikx} \,, \tag{7.10}$$

leads to the more convenient form for (7.5)[2]

$$\hat{H} = \sum_{k=-\infty}^{\infty} k^2 \hat{a}_k^\dagger \hat{a}_k - \frac{g}{4} \sum_{k,l,m=-\infty}^{\infty} \hat{a}_k^\dagger \hat{a}_l^\dagger \hat{a}_{m+k} \hat{a}_{l-m} \tag{7.11}$$

Bogolyubov diagonalization around the homogeneous background $\phi_{\text{hom}} = \sqrt{N}$ yields for the energy of the first Bogolyubov mode [Kanamoto et al., 2003, Dvali and Gomez, 2012c, Flassig et al., 2013]

$$\epsilon_1 = \sqrt{1 - gN} \tag{7.12}$$

Parametrizing the effective coupling as $gN = 1 + \delta$, we obtain $\epsilon_1 = i\sqrt{\delta}$. Applying the above argument, we therefore expect the system to break from mean field on a timescale $t_{\text{break}} \sim \Im(\epsilon_1)^{-1} \log N \sim \sqrt{\delta}^{-1} \log N$. The argument of the logarithm is proportional to $N$ because the action of the mean field solution scales as $S \sim N$ for fixed $gN$.

Within this setup, the departure from classical evolution is expected to go in hand with the generation of large entanglement. This allows us to identify the quantum break time directly with the scrambling time.

[2]For improved readability, we have now set $\hbar = 2m = V = 1$

Since we are interested in finite N effects in a regime where we expect semi-classical methods to fail, we will use a method not relying on any kind of perturbation theory. We will diagonalize the Hamiltonian (7.11) explicitly. Then, in order to time evolve the homogeneous Hartree state

$$|\phi_{\text{hom}}\rangle = (\hat{a}_0^\dagger)^N|0\rangle, \tag{7.13}$$

we will project $|\phi_{\text{hom}}\rangle$ onto energy eigenstates and apply the time evolution operator $U(t) = \exp(iHt)$ on the state. Finally, we project the time evolved state onto a k-particle subspace and compute the von Neumann entropy

$$\begin{aligned} S_1 &= -\operatorname{tr}\rho_1 \log \rho_1 \\ (\rho_1)_{ij} &= \langle\phi_{\text{hom}}|\, \hat{a}_i^\dagger \hat{a}_j \,|\phi_{\text{hom}}\rangle \end{aligned} \tag{7.14}$$

as a function of time.

In order to make this task computationally feasible we will make use of several properties of the system [Kanamoto et al., 2003]. Since the Hamiltonian is translationally invariant and number conserving we can restrict ourselves to fixed total momentum and fixed total particle number. In our case, only the total momentum zero sector is relevant, since this contains the homogeneous state. Furthermore, from the Bogolyubov analysis we see that the modes with $k > 2$ have a fairly large gap for $gN$ not much bigger than 1. Therefore, we can truncate the momentum modes $l$ we take into account to $l = -1, 0, 1$.

In Fig. 7.2a we plot $S_1$ as functions of time for different values of N. In order to see the break time, we evaluate the time when $S_1$ is higher than some threshold value $S_{th}$. We plot this time as a function of particle number N in Fig. 7.2b, where the solid line is the result of fitting a logarithm to the data points. This clearly shows a logarithmic break time.

A clearer understanding for the observed behavior emerges if we look at the density of states. In Fig. 7.3a we show a plot of the density of states in the zero-momentum sector for given energy and coupling. It can be clearly observed that there is a large density of states for low energies near the phase transition, which is due to the light Bogolyubov mode appearing at the quantum critical point. Furthermore, we clearly see a band of a high density of states for large couplings. The state we time-evolve in the numerics overlaps only with the modes in this band. We have checked that the density of states in this band varies logarithmically with N, i.e. the gap $\Delta$ between states in this band will typically go as

$$\Delta \sim 1/(\lambda \log N). \tag{7.15}$$

Given that the time scale for the time evolution will be set by this gap we naturally see the logarithmic break time emerging.

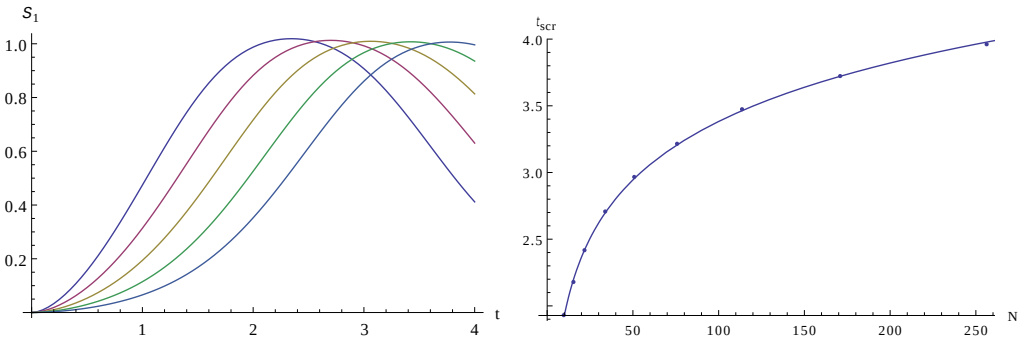


(a) (b)

Figure 7.2: (a): One particle entanglement entropy as a function of time for $N = 16, 32, 64, 128$ and 256. (b): Quantum break time as a function of $N$.

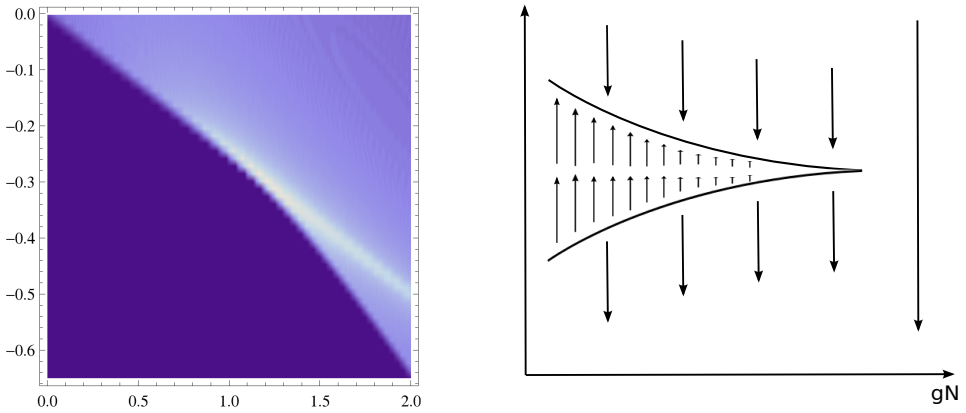


(a) (b)

Figure 7.3: (a): Density of states as a function of $gN$ and $E/N$ for N=1500. (b): Phase diagram for the three-dimensional condensate. For small $gN$ two solutions exist; one is stable while the other one is unstable. At the critical point, both solutions disappear.

### 7.5.2 3D condensates and connection with black hole

In the previous section, we have studied a Bose condensate in one spatial dimension as a prototype model. In that case it was viable to perform numerical simulations of the quantum time evolution. For an attractive Bose condensate, one dimension is special however insofar as the classical GP system has a well defined lowest energy configuration after the phase transition - the bright soliton. In higher dimensions, however, there is no classical solution in the would-be solitonic phase. Instead when increasing the effective coupling $gN$ past 1, the stable lowest energy solution of the Gross-Pitaevskii equation and another (unstable) solution disappear together in a saddle node bifurcation [Pérez-García et al., 1997] (see a sketch of the phase diagram in Fig. 7.3b[3]). Thus, while we willfully prepared an unstable initial state for the $(1+1)-d$ bosons, when a perfectly stable ground state was available, in $(3+1)-d$ it is inevitable to enter the instability when going past the bifurcation point.

It is precisely this instability that we believe to be responsible for the fast scrambling of information in black holes.

There, the relevant coupling controlling the mean field approximation is $gN$ with $g = \frac{L_P^2}{l^2}$ for $l$ the wave length of the constituent gravitons. In the weak coupling regime $gN < 1$ the condensate cannot be self-sustained and we should therefore imagine some external trapping potential that sets the wavelength of the constituent gravitons. The many body wave function is a stretched condensate in the corresponding trap. At the critical point $gN = 1$ the system of gravitons becomes self-sustained in the sense that the quantum pressure compensates the gravitational attraction. However, although at this point we can satisfy the virial condition of self-sustainability, the system is not stable in the mean field approximation and will tend to collapse - reducing its size and consequently decreasing the typical wavelength of the constituent gravitons. As we have elaborated, this mean field picture dramatically changes once we take appropriately into account $1/N$ quantum effects. Based on our prototypes, we expect the quantum evolution to break from mean field in a time $O(R \log N)$. This is reflected in the generation of large entanglement entropy for the corresponding one particle density matrix as a function of $gN$.

The evolution of black holes is different from that of laboratory conden-

[3]This can also be understood intuitively from Fig.7.1 and Eq.(7.7). The two solutions for small $gN$ correspond to the maximum of the energy functional and the infinitely stretched condensate. For large $gN$, no stable points exist. This analysis assumes the presence of a trapping potential. As we will argue below, this is in close analogy to the black hole.

sates because of Hawking evaporation. While collapse usually puts a condensate off the critical point, this is prevented by the decrease of the number of gravitons $N$. As the condition of instability persists along the collapse, we also expect larger-$k$-density matrices to be efficiently scrambled.

## 7.6 Summary and Outlook

The purpose of this chapter was to stress that the properties of unstable Bose-Einstein condensates are crucial in understanding the efficient generation of quantum entanglement and scrambling.

The idea of black holes as maximal scramblers is a very interesting hypothesis. Its verification requires a microscopic quantum theory and the goal of this chapter is to set some ideas in this direction.

The very conservative assumption of our work lies in modeling black holes as many-body quantum systems governed by weakly-coupled IR gravity. The semi-classical one-particle collective behavior appears as a consequence of the many-body system being in a BE condensate state. Quantum fluctuations relative to this state are measured by $1/N$ with $N$ being the number of graviton constituents (and, equivalently, the BH action in Planck units). Some special features of BHs, as, for instance, fast scrambling, are understood in this frame as the reflection of a logarithmic quantum break time.

These observations provide the clue for solving some recalcitrant BH paradoxes. In particular, the assumption of purity of the final evaporation state seems to lead to strong departures from semi-classicality at least in Page's time [Page, 1993b], meaning that a breakdown of semi-classicality takes place after this time irrespective of the size of the black hole. This is very puzzling, since naively one expects the semi-classical approximation to be valid for large macroscopic black holes. The approach to these sort of puzzles that we can extract from the present work lies in identifying the root of this breakdown of semi-classicality in the existence of a logarithmic quantum break time. Because BHs are unstable BECs, the quantum evolution takes over much sooner then what would be naively expected.

Furthermore, we consider the properties of quantum criticality and quantum instability as crucial for fast scrambling. We take the ensuing logarithmic quantum break time as a very encouraging sign. However, we would refrain from making strong statements about implications of additional black hole properties, such as, for example, their age or the embedding spacetime.

Finally, it would be very interesting to study some of the phenomena discussed in this work, in particular the appearance of logarithmic quantum break time, for realistic Bose-Einstein condensates in the laboratory. This

would give an exciting prospect of simulating some aspects of quantum black hole physics in the labs.

# Chapter 8

# Collapse and Evaporation of a Relativistic Scalar Field

In this chapter, we focus on the evaporation of black holes in the condensate picture. Along the lines of the introduction in chapter 5, we develop a toy model that captures some of the essential properties for particle loss in graviton condensates.

## 8.1 From gravity to prototype

In the condensate picture for black holes, the dynamics of collapse and Hawking evaporation are due to two intertwined effects. The coherent excitation of the tachyonic breathing mode of the condensate, leading to a collapse of the black hole. This is a process involving only the gravitons of the condensate. At the same time, incoherent scattering allows for the production of gravitons from the continuum that can escape the black hole. In principle, the former may be accounted for through mean field evolution, while the latter is due to the interaction of the mean field with quantum fluctuations.

In a gauge where the linear[1] graviton obeys the relations

$$h_{0i} = 0,\ h^{\mu}_{\mu} = 0,\ \partial^{\mu} h_{\mu\nu} = 0, \tag{8.1}$$

the corresponding time evolution is generated by a Hamiltonian that in

[1] As usual, we linearize around Minkowski. This also gives us a preferred time slicing.

Fourier space takes the (suggestive) form

$$\hat{H} = \int d^3k \sum_{\lambda=1,2} |\mathbf{k}| \hat{a}^\dagger_{\mathbf{k},\lambda} \hat{a}_{\mathbf{k},\lambda} + \sum_n M_p^{2-n} \int d^3k_1 ... d^3k_n \frac{\mathbf{k}_i \mathbf{k}_j}{\sqrt{\prod_{l=1}^n |\mathbf{k}_l|}} P^{(n)}(\hat{a})\ \delta^{(3)}\left(\sum \mathbf{k}_i\right). \tag{8.2}$$

Here, $\lambda = 1, 2$ corresponds to the two transverse polarizations of the graviton and the $a^\dagger_{\mathbf{k},\lambda}, a_{\mathbf{k},\lambda}$ are creation and annihilation operators of gravitons with polarization $\lambda$. The functions $P^{(n)}$ comprise all possible degree $n$ monomials of said creation and annihilation operators, thereby generating the infinite series of vertices present in an interacting massless spin-2 theory. Note that the interaction term will generically contain also the longitudinal and temporal polarizations of the graviton, depending on the choice of nonlinear gauge.

In our picture, a black hole corresponds to a set of quantum states $|\mathrm{BH}\rangle$ in the interacting theory with a large occupation number of gravitons in a single mode $\hat{c}_{\mathrm{BH}} = \int d^3k c_k \hat{a}_k$. Note that the $\hat{a}_k$ comprise annihilation operators of all possible polarizations, in order for the black hole state to be part of the physical spectrum[2].

In principle, (8.2) contains all the relevant information for the analysis of the non-equilibrium behavior of the states $|\mathrm{BH}\rangle$. However, the corresponding vertices, stemming from a Poincaré invariant field theory, will not conserve particle number. And as if this were not bad enough, we are dealing with the presence of the infinite series of vertices and the ambiquity due to gauge redundancy. An explicit treatment of this theory is virtually impossible. Therefore, we are in dire need of simplifying assumptions.

For us, these will be:

(i) Reduce the number of polarizations to a single mode, thereby also removing the gauge ambiguity.

(ii) Focus on the leading order dynamics of the condensate. We assume that these are due to the two-body interaction. As a consequence, we consider only the quartic vertex.

(iii) Consider only particle number conserving processes.

The latter two assumptions will of course prevent us from learning anything about the actual spectrum of emitted particles. Nevertheless, we will see

[2]In particular, it should be annihilated by the full Hamiltonian, due to the constraint $\mathcal{H} \approx 0$.

that they already allow for very interesting conclusions on the condensate dynamics. Take note here that due to (ii) and (iii), all momenta involved in the leading order collision processes are expected to be of the same order. We will therefore also neglect the momentum dependent prefactor of the quartic interaction term.

With these assumptions, we arrive at the Hamiltonian

$$\hat{H} = \int d^3k |\mathbf{k}| \hat{a}^\dagger_{\mathbf{k}} \hat{a}_{\mathbf{k}} + M_p^{-2} \int d^3k_1 ... d^3k_4 \hat{a}^\dagger_{\mathbf{k}_1} \hat{a}^\dagger_{\mathbf{k}_2} \hat{a}_{\mathbf{k}_3} \hat{a}_{\mathbf{k}_4} \delta^{(3)} \left( \sum \mathbf{k}_i \right). \quad (8.3)$$

Under our assumptions, the difference to previous prototype models for graviton condensates [Dvali and Gomez, 2012a, Flassig et al., 2013, Dvali et al., 2013] reduces to the relativistic dispersion relation. We will see, however, that it is precisely this feature that is responsible for interesting properties. Note also that our Hamiltonian is based on derivative interactions. The difference in the interaction as compared to [Berkhahn et al., 2013] is due to the inherently nonrelativistic nature of the model considered there.

Before we start analyzing the dynamics of (8.3), we utter a word of caution. Of course, the simplified Hamiltonian is void of quite a few important features of gravitation. Besides the simplifications in terms of number conservation, we have eliminated the longitudinal and temporal modes from the dynamics. In GR, it is precisely these modes that are responsible for the gravitational potential. Their presence may in principle be modeled through the inclusion of a trapping potential. This will be left for future work.

## 8.2 Schwinger-Keldysh formalism

The following section provides an introductory review of the Schwinger-Keldysh [Schwinger, 1961, Keldysh, 1965] formalism that will allow for a proper treatment of the real time dynamics of collapse and evaporation[3]. It may be skipped by the experienced reader. Comprehensive introductions may be found, for example, in [Kamenev, 2011]. Our analysis presents a generalization of previous results [Stoof, 1999, Duine and Stoof, 2001, 2002] to systems with a relativistic dispersion relation.

We are interested in the time evolution of an unstable condensate, which is initially describe by a (normalized) density matrix $\hat{\rho}(t_i)$. The expectation

[3]Since we are dealing with a closed system at zero temperature, the full time evolution is in principle also accessible in a regular effective action, or in-out formalism approach. However, for states with a large number of particles, the relevant information is considerably more difficult to retrieve than in the Schwinger-Keldysh approach

value of any observable $\hat{\mathcal{O}}$ is given by

$$\langle \mathcal{O} \rangle (t) = \mathrm{Tr}\left[ U(t_i, t) \hat{\mathcal{O}} U(t, t_i) \hat{\rho} \right] \tag{8.4}$$

$$= \mathrm{Tr}\left[ U(t_i, t_f) U(t_f, t) \hat{\mathcal{O}} U(t, t_i) \hat{\rho} \right], \tag{8.5}$$

where, $U(t_1, t_2) = \exp\left(-iH(t_1 - t_2)\right)$ is the time evolution operator. The second equation has been obtained through an insertion of $U(t_i, t_f)U(t_f, t_i)$ for $t_f$ in the asymptotic future. It has served to extend the integration path from $t_i \to t \to t_i$ to $t_i \to t_f \to t_i$, the so-called Keldysh contour, which we will denote by $\mathcal{C}$.

With use of the Keldysh contour, expectation values can be obtained from a generating functional through the introduction of corresponding sources into the Hamiltonian:

$$H_J^{\pm} = H \pm J(t) \hat{\mathcal{O}}\,, \tag{8.6}$$

$$Z[J] = \mathrm{Tr}\left[ U_J(\mathcal{C}) \hat{\rho} \right], \tag{8.7}$$

$$\langle \mathcal{O} \rangle (t) = \frac{i}{2} \left. \frac{\delta Z[J]}{\delta J(t)} \right|_{J=0}, \; t_i \leq t \leq t_f\,. \tag{8.8}$$

Here, $H^+$ and $H^-$ are the Hamilton operators along the forward and backward contour, respectively.

As usual, (8.7) may be turned into a path integral by introducing at each timestep an appropriate partition of unity. In this case, we use coherent states that are eigenstates of the annihilation operators appearing in (8.3), $\hat{a}_{\mathbf{k}} |\psi\rangle = \psi_{\mathbf{k}} |\psi\rangle$. One obtains

$$Z = \int \mathcal{D}\psi \mathcal{D}\psi^{\dagger} e^{iS[\psi, \psi^{\dagger}]}\,. \tag{8.9}$$

The "action" $S$ is given by

$$S[\psi, \psi^{\dagger}] = \int_{\mathcal{C}} dt \int d^3 k_1 \Bigg\{ i \psi^{\dagger}_{\mathbf{k_1}} \partial_t \psi_{\mathbf{k_1}} - |\mathbf{k_1}| \psi^{\dagger}_{\mathbf{k_1}} \psi_{\mathbf{k_1}} + M_p^{-2} \int d^3 k_2 ... d^3 k_4 \psi^{\dagger}_{\mathbf{k_1}} \psi^{\dagger}_{\mathbf{k_2}} \psi_{\mathbf{k_3}} \psi_{\mathbf{k_4}} \delta^{(3)} \left( \sum \mathbf{k_i} \right) \Bigg\}. \tag{8.10}$$

The information on the initial state is encoded in the correlation of the field on the forward and backward branch. The time integral in (8.10) may be brought into conventional form by introducing forward and backward fields $\psi^{\pm}$ that live on the forward (backward) branch of the Keldysh contour.

Furthermore, we perform a so called Keldysh rotation and introduce the "classical" and "quantum" fields

$$\psi^{\rm cl}_{=}\frac{1}{\sqrt{2}}\left(\psi^{+}+\psi^{-}\right)\ ,\ \psi^{\rm q}_{=}\frac{1}{\sqrt{2}}\left(\psi^{+}-\psi^{-}\right)\ . \tag{8.11}$$

We obtain

$$S[\psi^{\rm cl},\psi^{\rm cl\dagger},\psi^{\rm q},\psi^{\rm q\dagger}]=\int dt\,d^3\mathbf{k}_1 d^3\mathbf{k}_2\Bigg\{i\vec{\psi}^{\dagger}_{\mathbf{k_1}}H(\mathbf{k_1},\mathbf{k_2})\vec{\psi}_{\mathbf{k_2}}$$
$$+M_p^{-2}\int d^3\mathbf{k}_3 d^3\mathbf{k}_4\delta^{(3)}\left(\sum\mathbf{k_i}\right)\left(\psi^{\rm cl\dagger}_{\mathbf{k_1}}\psi^{\rm cl\dagger}_{\mathbf{k_2}}\psi^{\rm cl}_{\mathbf{k_3}}\psi^{\rm q}_{\mathbf{k_4}}+\psi^{\rm q\dagger}_{\mathbf{k_1}}\psi^{\rm q\dagger}_{\mathbf{k_2}}\psi^{\rm q}_{\mathbf{k_3}}\psi^{\rm cl}_{\mathbf{k_4}}\right)\Bigg\}+\text{h.c.}\,, \tag{8.12}$$

where we have introduced $\vec{\psi}_{\mathbf{k}}\equiv(\psi^{\rm cl}_{\mathbf{k}},\psi^{\rm q}_{\mathbf{k}})^t$ and the kinetic matrix $H$ is defined as

$$H(\mathbf{k}_1,\mathbf{k}_2)\equiv\begin{pmatrix}0 & \delta(\mathbf{k}_1-\mathbf{k}_2)(i\partial_t-|\mathbf{k}_1|)\\ \delta(\mathbf{k}_1-\mathbf{k}_2)(i\partial_t-|\mathbf{k}_1|) & \Sigma_K\left(\mathbf{k}_1,\mathbf{k}_2\right)\end{pmatrix} \tag{8.13}$$

We have introduced the Keldysh self-energy $\Sigma_K$, whose precise value depends on the interactions and is of no particular interest to us. Its presence, however, is important, since it contains the information on the correlators of the forward and backward fields and thereby on the initial density matrix. Note that at this point, one may equivalently seek a formulation for the action (8.12) in terms of real fields by expressing $\Psi$ and $\Psi^{\dagger}$ in terms of a real scalar field and its canonical momentum. However, our focus on particle number conserving processes is more straightforwardly implemented in the current language.

The classical mean-field dynamics of the condensate arises from (8.12) as the solution to the saddle-point equations that has $\psi^{\rm q}=0$. In this case, variation of (8.12) with respect to $\psi^{\rm q\dagger}$ yields the equation of motion for the classical field. This is the Gross-Pitaevskii equation that describes the mean-field dynamics of the condensate:

$$i\partial_t\psi^{\rm cl}_{\mathbf{k}}=|\mathbf{k}|\psi^{\rm cl}_{\mathbf{k}}+M_p^{-2}\int d^3\mathbf{k}_1 d^3\mathbf{k}_2 d^3\mathbf{k}_3\left(\mathbf{k}+\mathbf{k}_1-\mathbf{k}_2-\mathbf{k}_3\right)\psi^{\rm cl\dagger}_{\mathbf{k_1}}\psi^{\rm cl}_{\mathbf{k_2}}\psi^{\rm cl}_{\mathbf{k_3}}\,. \tag{8.14}$$

For a condensate with attractive self-interactions, the normalized solutions to this equation will correspond to a collapsing condensate of $N$ particles once $N$ surpasses a critical value [Shuryak, 1996, Stoof, 1997].

The evaporation of the condensate is due to scattering of condensed particles into the quasi-particle cloud. These effects may be taken into account most readily by integrating out the quasi-particles. To this regard, we separate the fields into a condensate part and fluctuations.

$$\psi^{\rm cl} = \phi + \delta\varphi\,,\ \psi^{\rm q} = \phi^q + \delta\varphi^q\,. \tag{8.15}$$

Inserting (8.15) into (8.12) gives rise to a plethora of terms, of which only few have a relevant effect. The reason for this lies in the fact that we are dealing with a condensate with $N \gg 1$ at $T = 0$. Therefore, the quasiparticle occupation is much lower than that of the condensate mode. We may therefore focus on terms that are at most quadratic in the fluctuations. All corrections that arise from higher order terms are proportional to the density of fluctuations and therefore at least $1/N$-suppressed.

The quadratic part of the fluctuation action allows one to read off the quasi-particle spectrum; diagonalization leads to the celebrated Bogoliubov modes [Bogolyubov, 1947]. Note that for us, the relevant physics is not due to the low-lying, collective modes but instead to higher energy particles with a dispersion relation closer to that of an on-shell particle. Moreover, the quadratic action also gives rise to backreaction of the quasi-particle cloud onto the condensate dynamics. This part will be neglected in our analysis, for the reasons described above.

The part that is linear in the fluctuations is what gives rise to the particle loss of the condensate. These terms are only non-vanishing for an inhomogeneous condensate; otherwise they would violate the conservation of energy-momentum.

## 8.3 Effective action

Explicitly, we are therefore concerned with the following expression:

$$\delta S = \int dt\, d^3\mathbf{k}_1 d^3\mathbf{k}_2 \Bigg\{ i\vec{\delta\phi}^\dagger_{\mathbf{k_1}} H(\mathbf{k_1},\mathbf{k_2}) \vec{\delta\phi}_{\mathbf{k_2}} + M_p^{-2} \int d^3\mathbf{k}_3 d^3\mathbf{k}_4 \delta^{(3)}\left(\sum \mathbf{k_i}\right)$$
$$\times \left( 2\delta\phi^{cl\dagger}_{\mathbf{k_1}} \phi^\dagger_{\mathbf{k_2}} \phi_{\mathbf{k_3}} \phi^q_{\mathbf{k_4}} + \delta\phi^{cl}_{\mathbf{k_1}} \phi^\dagger_{\mathbf{k_2}} \phi^\dagger_{\mathbf{k_3}} \phi^q_{\mathbf{k_4}} + \delta\phi^q_{\mathbf{k_1}} \phi^\dagger_{\mathbf{k_2}} \phi^\dagger_{\mathbf{k_3}} \phi_{\mathbf{k_4}} \right) \Bigg\} + \text{h.c.}\,, \tag{8.16}$$

Due to on-shell fluctuations, the diagram shown in Fig.8.1 obtains an imaginary part [Duine and Stoof, 2001]. It gives rise to the following term in the effective action:

$$\delta S = i \int dt d^3\mathbf{k}_1 d^3\mathbf{k}_2 \Gamma(\mathbf{k}_1,\mathbf{k}_2) \left( \phi^{q\dagger}_{\mathbf{k}_1} \phi_{\mathbf{k}_2} - \phi^\dagger_{\mathbf{k}_1} \phi^q_{\mathbf{k}_2} \right)\,, \tag{8.17}$$

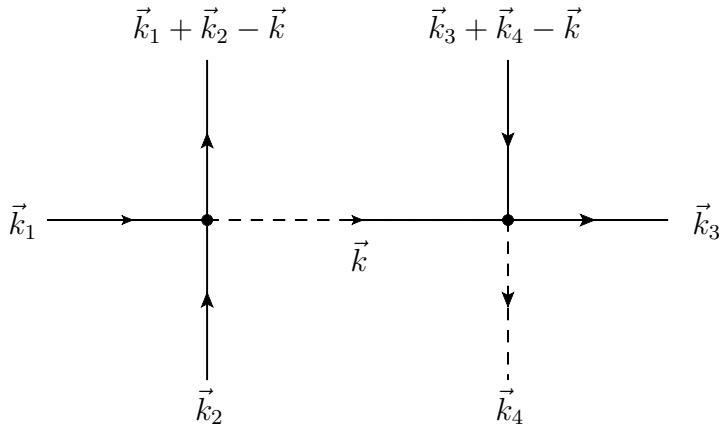


Figure 8.1: Lowest order diagram responsible for the imaginary part of the self-energy. The external lines correspond to condensed particles; solid lines identify $\psi^{\mathrm{cl}\dagger}$ and dashed lines $\psi^{\mathrm{q}\dagger}$. The imaginary part is induced when $\vec{k}$ goes on-shell.

where we have introduced

$$\Gamma(\mathbf{k}_1, \mathbf{k}_2) \equiv \int d^3\mathbf{k} d^3\mathbf{k}_3 d^3\mathbf{k}_4 \delta\left(|\mathbf{k}_1| + |\mathbf{k}_2| - |\mathbf{k}| - |\mathbf{k}_1 + \mathbf{k}_2 - \mathbf{k}|\right) \times \phi^\dagger_{\mathbf{k}_3} \phi_{\mathbf{k}_4} \phi^\dagger_{\mathbf{k}_1+\mathbf{k}_2-\mathbf{k}} \phi_{\mathbf{k}_3+\mathbf{k}_4-\mathbf{k}} \,. \quad (8.18)$$

In turn, this leads to a change in the Gross-Pitaevskii equation, which now reads

$$i\partial_t \phi_{\mathbf{k}} = |\mathbf{k}|\phi_{\mathbf{k}} + M_p^{-2} \int d^3\mathbf{k}_1 d^3\mathbf{k}_2 d^3\mathbf{k}_3 \left(\mathbf{k} + \mathbf{k}_1 - \mathbf{k}_2 - \mathbf{k}_3\right) \phi^\dagger_{\mathbf{k_1}} \phi_{\mathbf{k_2}} \phi_{\mathbf{k_3}} - i \int d^3\mathbf{k}_2 \Gamma(\mathbf{k}, \mathbf{k}_2) \phi_{\mathbf{k}_2} \,. \quad (8.19)$$

From this, we can immediately read off the change in the number of condensed particles

$$\frac{dN_c}{dt} = -\int d^3\mathbf{k}_1 d^3\mathbf{k}_2 \Gamma(\mathbf{k}_1, \mathbf{k}_2) \phi^\dagger_{\mathbf{k}_1} \phi_{\mathbf{k}_2} \quad (8.20)$$

The final step towards an effective action that describes the collapse and evaporation of our condensate is now to integrate out the quantum field $\psi^{\mathrm{q}}$.

We will do this via the introduction of an auxiliary "noise" field $\eta_{\mathbf{k}}(t)$.

$$Z = \int \mathcal{D}\phi\, \mathcal{D}\phi^q\, \mathcal{D}\phi^\dagger\, \mathcal{D}\phi^{q\dagger}\, \mathcal{D}\eta\, e^{iS_\eta[\phi,\phi^\dagger]}\,, \tag{8.21}$$

$$S_\eta[\phi,\phi^\dagger] = \int dt d^3\mathbf{k} \frac{1}{\Sigma_{\mathbf{k}}} \phi^{q\dagger}\left(\mathcal{E}_{\mathbf{k}}(\phi,\phi^\dagger) - \eta_{\mathbf{k}}\right) + \text{h.c.}\,, \tag{8.22}$$

where $\mathcal{E}$ is the operator corresponding to the Gross Pitaevskii equation (8.19). Integrating out $\psi^{\rm q}$ now constrains the classical field $\psi^{\rm cl}$ to obey a Langevin equation with gaussian noise $\eta$:

$$\mathcal{E}_{\mathbf{k}}(\phi,\phi^\dagger) = \eta_{\mathbf{k}}\,. \tag{8.23}$$

The dynamics described by (8.23) may in principle be obtained numerically. Instead, we will here take a different route and seek a variational solution to the *averaged* Gross-Pitaevskii equation. Taking note that the dissipative equation (8.23) does not directly follow from a variational principle, we proceed by dividing the variational approach into two steps. First, we shall look for a variational solution to the simpler problem without the dissipative term. This will provide us with an equation for the condensate size. Second, we supplement this with Eq.(8.20) in order to take into account the loss of particles.

## 8.4 Variational approach

Without the dissipative term, Eq. (8.23) can be obtained as the stationary point of the following Lagrangian.

$$\begin{aligned}\mathcal{L}_{\mathbf{k}} = {} & \frac{i}{2}\left(\phi^*_{\mathbf{k}}\dot{\phi}_{\mathbf{k}} - i\phi_{\mathbf{k}}\dot{\phi}^*_{\mathbf{k}}\right) - |\mathbf{k}||\phi_{\mathbf{k}}|^2 \\ & + M_p^{-2}\int d^3\mathbf{k}_1 d^3\mathbf{k}_2 d^3\mathbf{k}_3 \delta^{(3)}\left(\sum \mathbf{k_i}\right)\left(\phi^\dagger_{\mathbf{k}}\phi^\dagger_{\mathbf{k}_1}\phi_{\mathbf{k}_2}\phi_{\mathbf{k}_3}\right) + \text{h.c.}\,,\end{aligned} \tag{8.24}$$

We extremize Eq.(8.24) with respect to a set of spherically symmetric trial functions. In our case, the choice of trial function is somewhat arbitrary. For a nonrelativistic harmonically trapped condensate, the ground state wavefunction can be well approximated by a Gaussian even in the presence of interactions [Pérez-García et al., 1997, Dalfovo et al., 1999]. We take this as a motivation to choose the spherically symmetric ansatz of the following form in real space

$$\phi(r,t) = A(t)\left(\frac{3}{4q(t)}\right)^{\frac{3}{2}} e^{-\frac{\pi}{2}\left(\frac{3}{4}\right)^2\left(\frac{r^2}{q(t)^2} - ir^2 b(t)\right)}. \tag{8.25}$$

$A(t)$ is the complex amplitude, $q(t)$ the real width of the condensate and $r$ the radial coordinate. The function $b(t)$ can later be identified with the velocity of the collapse. The normalization of $\phi$ is chosen such that $|A(t)|^2 = N$ and the numerical factors simplify the calculation.

By plugging Eq. (8.25) into Eq. (8.24), we obtain the averaged Lagrangian density $L = \int \mathrm{d}^3k\tilde{\mathcal{L}}$

$$L = -\frac{1}{2}i(A^*\dot{A} - A\dot{A}^*) - \frac{3}{4}|A|^2q^2\dot{b} - \frac{3|A|^2}{2q}\sqrt{1+b^2q^4} + \frac{27|A|^4}{128\sqrt{2}M_p^2q^3}\,. \quad (8.26)$$

We can now understand the collapse dynamics as a variational problem of the time dependent parameters $s = \{A, A^*, q, b\}$, which obey the equations of motion

$$\frac{\mathrm{d}}{\mathrm{d}t}\left(\frac{\partial L}{\partial \dot{s}_i}\right) - \frac{\partial L}{\partial s_i} = 0. \quad (8.27)$$

### 8.4.1 Equations of motion

The equations of motion for the amplitude simplifies to particle number conservation

$$\frac{\mathrm{d}}{\mathrm{d}t}|A|^2 = 0, \quad (8.28)$$

or in other words $\dot{N} = 0$.

Next, we can relate $b$ to the collapse velocity $\dot{q}$ by varying for $b$ and using Eq. (8.28)

$$b = \frac{\dot{q}}{q^2\sqrt{1-\dot{q}^2}} \quad (8.29)$$

This equation thus completely determines the function $b$ in terms of $q$ and $\dot{q}$.

The expression for the condensate width is obtained by variation with respect to $q$. After substitution of Eq. (8.28) and (8.29), one obtains

$$\ddot{q} = \frac{1}{q^3}\left(1-\dot{q}^2\right)\left(q^2 - \frac{28\sqrt{2}}{128}\frac{N}{M_p^2}\sqrt{1-\dot{q}^2}\right)\,. \quad (8.30)$$

Note the Lagrangian after integrating out $b$:

$$L = -\frac{3N}{2q}\sqrt{1-\dot{q}^2} + \frac{27}{128\sqrt{2}}\frac{N^2}{M_p^2q^3}\,. \quad (8.31)$$

We recognize it as the Lagrangian of relativistic point particle with a mass that depends on $q$.

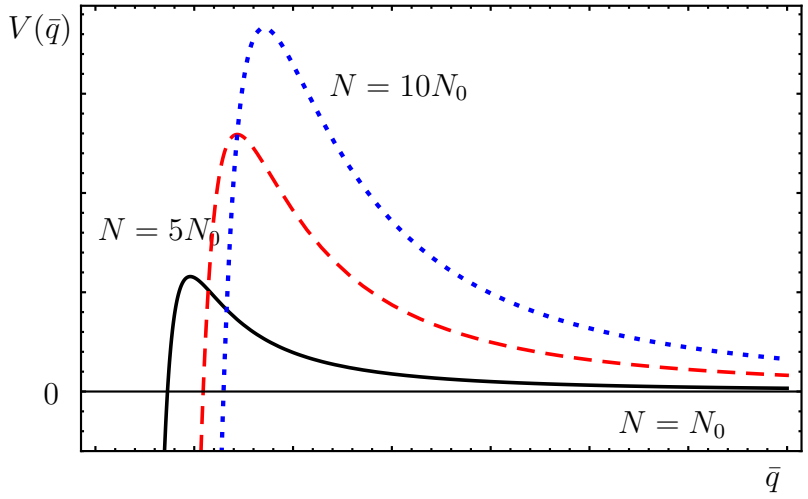


Figure 8.2: Effective potential for various values of $N$. The value $N_0$ is arbitrary.

### 8.4.2 Slow collapse

It is instructive to first consider the case of small collapse velocities, as this corresponds to a nonrelativistic limit and allows us to qualitatively compare our expressions with existing results from the literature.

In the limit of small velocities and small acceleration, Eq.(8.30) reads

$$\ddot{q} \approx \frac{1}{q} + \frac{\dot{q}^2}{2q} - \frac{27}{64\sqrt{2}} \frac{N}{M_p^2 q^3} \,. \tag{8.32}$$

The first term in Eq.(8.32) corresponds to the outward force due to the kinetic energy of the bosons; its scaling with inverse $q$ is dictated by Heisenberg's uncertainty principle. The third term is due to the attractive interactions and can, for sufficiently large $N$, overcome the repulsive force. In that case, the condensate collapses. In comparison with known results in the literature (e.g. [Pérez-García et al., 1997, Duine and Stoof, 2001]), the second term corresponds to corrections due to the relativistic dispersion relation.

#### 8.4.2.1 Effective Potentials

In the small velocity limit, the Lagrangian (8.31) may be canonically normalized. The corresponding equation of motion will then give us a simple picture of the time evolution of the width as the motion of a particle $m\ddot{q} = -\frac{\mathrm{d}}{\mathrm{d}q} V(q, N)$ in a one dimensional potential. To see this, let us take

the small velocity limit also in the Lagrangian (8.31):

$$L \approx \frac{3}{4} N \frac{\dot{q}^2}{q} - \frac{3N}{2q} + \frac{27}{128\sqrt{2}} \frac{N^2}{M_p^2 q^3} \,. \tag{8.33}$$

We may canonically normalize the kinetic term through the redefinition $q = \bar{q}^2$. From the canonical Lagrangian

$$L = 3N\dot{\bar{q}}^2 - \frac{3N}{2\bar{q}^2} + \frac{27}{128\sqrt{2}} \frac{N^2}{M_p^2 \bar{q}^6} \,, \tag{8.34}$$

we can conclude that the motion corresponds to that of a particle with mass $m = 6N$ in the effective potential

$$V(\bar{q}) = \frac{3N}{2\bar{q}^2} - \frac{27}{128\sqrt{2}} \frac{N^2}{M_p^2 \bar{q}^6} \,. \tag{8.35}$$

We plot the effective potential in Fig. 8.2.

The potential $V(\bar{q})$ possesses a maximum, located at

$$\bar{q}_+^2 = q_+ \sim \ell_P \sqrt{N} \,. \tag{8.36}$$

It turns out that for $q \sim q_+$, the criticality condition is fulfilled:

$$\alpha_{\rm gr} N \sim \frac{\ell_P^2}{q^2} N \sim 1 \,. \tag{8.37}$$

Finally note that the runaway behavior for large $q$ is due to the fact that we have not included an external trapping potential for the condensate.

## 8.5 Evaporation

The decay rate of the condensate according to Eq. (8.20) can be evaluated for a spherically symmetric collapse using the ansatz Eq. (8.25) which yields

$$\dot{N} = -\frac{c}{M_p^4} \frac{N^3}{q^5} . \tag{8.38}$$

Here, c is a dimensionless constant of order $\mathcal{O}(10^{-2})$, of no particular importance to us. Note that the above behavior of the rate equation can be straightforwardly read off from the expression (8.20). The factors of $N^3$ and $M_p^{-4}$ are due to the decay being modeled as an effective three-body process. The dependence on $q$ then follows from dimensional grounds.

Equations (8.30) and (8.38) now describe the evolution of the condensate described by the Hamiltonian (8.3) in the Gaussian approximation, as long as higher order correlators of the fluctuations can be neglected. This we expect to hold for the majority of the collapse, until $\mathcal{O}(N)$ particles are ejected. Note that this in particular implies that we ignore the possibility of particles rescattering into the condensate, which we expect to give only a small correction for the above reason[4].

## 8.6 Solutions

Numerically, one may solve the collapse and evaporation equations (8.30) and (8.38) for generic initial conditions, drawing a complete picture of the behavior of the condensate in the variational approach. However, it turns out the equations possess a simple set of analytic solutions:

$$q(t) = q_i - vt \tag{8.39a}$$

$$N(t) = \sqrt{\frac{2v}{c}}\,\frac{(q_i - vt)^2}{\ell_P^2}\,. \tag{8.39b}$$

The parameter $v$ is fixed via the algebraic relation

$$\left(1-v^2\right)\left(\sqrt{c} - \left(\frac{3}{4}\right)^3\sqrt{v(1-v^2)}\right) = 0\,. \tag{8.40}$$

We find three solutions in the allowed range $0 \leq v \leq 1$; a $c$-independent solution $v = 1$ as well as the two $c$-dependent solutions[5]. On a side note, we observe that from Eq.(8.30), we can also infer the existence of the solution $\dot{q}(t) = -1$. This solution, however, will not correspond to a self-similar collapse. Let us also point to the curiosity that the two latter solutions are only real for sufficiently small $c$. At $c = c_{\text{crit}}$ both solutions disappear in a saddle-node bifurcation.

A remarkable feature of the solutions (8.39) is their self-similarity. The criticality condition $q \sim \ell_P\sqrt{N}$ is fulfilled throughout the collapse!

[4] In our derivation we did not restrict the momentum of the non-condensed particle. In particular, it could lie within the band of condensed particles. This can be improved by including an appropriate cut-off function. Its effect, however, will be only a renormalization of the numerical coefficient $c$.

[5] The corresponding values are given by $v = \frac{1}{\sqrt{3}}\cos\left(f(c)\right) \pm \sin\left(f(c)\right)$, where $f(c) = \frac{1}{3}\text{arccot}\left(\sqrt{\frac{27}{128\times 2^{1/3}c^2} - 1}^{-1}\right)$.

### 8.6.1 Stability

The self-similar behavior of the solutions (8.39) is of course only truly meaningful if the solutions are stable. As we will see, this is not the case for all three solutions. However, as long as the two $c$-dependent solutions exist, at least one of them presents an attractor.

In order to analyze the stability properties of the solutions (8.39), we decompose $N$ and $q$ as

$$q(t) = q_0(t) + \delta q(t)\,, \tag{8.41}$$

$$N(t) = \sqrt{\frac{2v}{c}}\frac{q^2(t)}{\ell_P^2} + \delta N(t)\,, \tag{8.42}$$

and linearize Eqs. (8.30) and (8.38) in $\delta q$ and $\delta N$. In addition, we perform the change of variables from $t$ to $x = -\log\frac{q_0}{q_i}$ and introduce the rescaled number perturbation $\delta\tilde{N} = \delta N \exp(x)$.

For $v = 1$, the linearized equations are particularly simple

$$\delta q'' = \delta q'\,, \tag{8.43}$$

$$\delta\tilde{N}' = -5\delta\tilde{N} - 2q_i\sqrt{\frac{2}{c}}\,\delta q'\,, \tag{8.44}$$

while in the other cases, we obtain

$$\delta q'' = -2\delta q' - \frac{2^{23/2}c^{3/2}}{3^6 v^{7/2} q_i}\delta\tilde{N}\,, \tag{8.45}$$

$$\delta\tilde{N}' = -5\delta\tilde{N} - 2q_i\sqrt{\frac{2v}{c}}\,\delta q'\,. \tag{8.46}$$

Primes denote derivatives with respect to $x$.

The eigenvalues of the stability matrix read

$$(-5, 0, 1)\ , \tag{8.47}$$

in the first case and

$$\left(0, -\frac{1}{2}\left(7 \pm \sqrt{\frac{2^{12}c - 3^8 v_{2,3}}{2^{12}c - 3^6 v_{2,3}}}\right)\right)\ , \tag{8.48}$$

in the latter. The expressions on the corresponding solutions for $v$ are rather lengthy. Important here is only that the eigenvalues are always negative for $v_2$, while for $v_3$ the larger one is positive for $c$ below some threshold

value. Henceforth, at least one of the two solutions is absolutely stable. The solution $v = 1$, on the other hand, possesses an unstable direction; under small perturbations, it flows towards the solution $v \approx 1 - 2.8c$. The scaling behavior therefore remains unaltered. The presence of the zero mode is due to translational invariance in the initial condition for $q$ and obviously does not influence the scaling.

Note that solutions with an unstable direction have attractive features nevertheless. As was shown in [Dvali et al., 2013], the existence of an instability in the Gross-Pitaevskii equation leads to generation of one-particle entanglement on a time scale logarithmic in the number of constituents. This could provide a first hint towards a fast scrambling behavior of black holes. Of course, once this happens, the solution itself is bound to become subject to corrections. This will be addressed in future studies.

## 8.7 Summary

Modeling black holes as Bose condensates of gravitons can allow for simple resolutions to many apparent problems. In particular, since the evaporation is modeled as dynamics of a bound state, the process is completely unitary. Moreover, the appearance of light modes could provide explanations for properties such as the black hole entropy, their quantumness properties, and possibly fast scrambling.

In this chapter, we have developed a toy model for Hawking evaporation in the context of the Bose condensate picture for black holes. To this end, we have constructed a Hamiltonian that captures essential ingredients to the underlying physics of black hole evaporation, while at the same time being stripped down from some of the complications that arise in Einstein gravity. In particular, we have focused on a single degree of freedom and have turned off processes that violate number conservation. We have introduced the Schwinger-Keldysh formalism for nonequilibrium dynamics of Bose condensates and derived the Keldysh action that describes a collapsing and evaporating condensate.

We have then chosen a variational approach to solve the ensuing equations of motion, using the number of condensed particles $N$ and the width of the condensate $q$ as variational parameters. The resultant action takes on the intuitive form of the motion of relativistic particle in an effective $N$-dependent potential. In comparison with existing results in the literature, we have identified the corrections due to the relativistic dispersion relation.

We have discovered a set of scaling solutions to the equations along which the particle number is related to the width via $N \sim q^2$, reminiscent of the

behavior for black holes. Moreover, the solutions have interesting stability properties. Depending on the coefficient of the dissipative contributions, there may be one, two or zero absolutely stable solutions. At a critical value, two of these solutions become complex in a tangent bifurcation. This can have interesting consequences for the existence of light Bogoliubov excitations. Moreover, the presence of unstable directions could be related to the fast generation of entanglement.

Further improvements of the toy model are in line to better the understanding of the processes in GR. This comprises the inclusion of particle number violating vertices, the generalization to non-vanishing helicity, and, in hand, the implementation of longitudinal modes that are responsible for the gravitational potential.

# Chapter 9

# RG Flows in Scalar O(N) Models with Shift Symmetry

## 9.1 Introduction

Theories of scalar fields with derivative interactions have received considerable interest in the recent past. They arise in a multitude of areas in physics, e.g. as linear and nonlinear sigma models [Gell-Mann and Lévy, 1960] in particle physics or condensed matter physics, as models for interactions of longitudinal directions in massive spin-1 or spin-2 theories [Chanowitz and Gaillard, 1985] or as alternatives to potential driven inflation or dark energy (e.g. [Armendariz-Picon et al., 2001, Nicolis et al., 2009]). In these contexts, they are usually considered to be low energy effective theories, valid below a certain energy scale. At high energies, they violate perturbative unitarity and are in need of an ultraviolet (UV) completion.

Derivatively interacting scalar fields may also serve as prototype models for theories of quantum gravity. Einstein gravity, as a quantum theory of a massless spin-2 particle, is not (perturbatively) renormalizable and appears to violate unitarity at Planckian energies ($\sqrt{s} \gtrsim M_p$, with the Planck mass $M_p$). However, this apparent violation of unitarity may in fact be cured by the formation of black holes. Similarly, derivatively coupled scalar fields are argued to exhibit features of self-completeness through formation of field configurations with a large number of quanta in high energy processes [Dvali et al., 2011b]. The driving mechanism for this so-called *classicalization* relies on the energy dependence of the leading interaction vertices.

An interesting subclass of theories are those of the form

$$\mathcal{L} = \Lambda^4 \, V\left(\frac{X}{\Lambda^4}\right) , \tag{9.1}$$

where $X = \partial_\mu\phi\partial^\mu\phi$ is the kinetic operator and $\Lambda$ is a scale that defines the strength of the first interactions at tree level.

Like in gravity, the given couplings do not *run* at the perturbative level. This is simple to see. Any loop that contributes to a given $k$-point amplitude, will contain at least $k+2$ inverse powers of $\Lambda$. Therefore, the extra mass dimensions have to be eaten up by appropriate powers of momenta; any logarithmic term is accompanied by at least an additional factor of momentum squared. Thus, running can only exist for higher derivative operators[1].

In the context of gravity, it has been shown that nevertheless, the renormalization group flow is nontrivial and may allow for an ultraviolet fixed point (FP). While there are arguments in gravity that such a fixed point can in fact never be observed because it is shielded by the formation of black holes [Dvali et al., 2011a], it is not clear that similar arguments can be continued through to derivatively coupled scalar theories[2]. Since one is looking at an ultraviolet fixed point, all higher dimensional operators can in principle be important, depending of course on their scaling dimension at a non-Gaussian FP. It is per se not clear whether the existence of the FP can be proven for a generic truncation. In other words, taking into account more terms may not only lead to a shift in the position of the FP, but could spoil its existence.

In absence of a definite answer to this question, assume that a fixed point is found for a given truncation, and also assume that it will survive the extension of the truncation. What is the physical meaning of the fixed point, in light of the above obstruction to the running of couplings in the perturbative regime? Can the existence of shielding mechanisms somehow be extracted from the renormalization group treatment? And how can one relate the physical momentum scale to the RG scale? In this chapter, we will set the preliminaries to address these questions. We will derive a set of flow equations for a subclass of shift symmetric scalar theories and show that, similar to the results of asymptotic safety, fixed points of the renormalization group flow exist for simple truncations.

We will work in the framework of the functional renormalization group (FRG) (occasionally also referred to as the exact renormalization group) [Wetterich, 1993a]. The FRG provides a renormalization group equation for the effective action $\Gamma$, the Legendre transform of the logarithm of the partition function, and generating functional of the one-particle irreducible vertices. In Euclidean spacetime, and focusing for simplicity on a single

[1] Of course, there will still be divergences that require a counterterm of the form $X^{k/2}$. These, however, are purely polynomial.

[2] The arguments for the shielding of the UV fixed point usually rely on some form of Thorne's hoop conjecture [Thorne, 1972]. While the spirit of classicalization is very similar, the arguments are not as strong.

scalar degree of freedom, we obtain

$$\Gamma[\phi] = -W[J] + \phi J\,, \tag{9.2}$$

where $exp(-W[J])$ is the generating functional and $\phi \equiv \delta W[J]/\delta J$, as usual. We may introduce a scale dependence into the effective action through the modification

$$e^{-W[J]} \to e^{-W_k[J]} = \int \mathcal{D}\phi e^{-(S_k + \mathcal{R}_k[\phi] - J\phi)}\,, \tag{9.3}$$

The function $\mathcal{R}_k[\phi]$ is the regulator that limits the integration in the functional integral to modes with momentum $|p| > k$. In other words, it is a quadratic functional of $\phi$ that serves to suppress fluctuations of long wavelength modes. In usual cases, it corresponds to a $k$ and $p$-dependent mass $m_k(p)$ with the properties $m_k \to 0$ for $p^2/k^2 \to \infty$ and $m_k \to \infty$ for $p^2/k^2 \to 0$.

Inserting Eq.(9.3) into Eq.(9.2) yields the definition of the *effective average action* [Wetterich, 1993a]

$$\Gamma_k[\phi] = -W_k[J] + \phi J\,. \tag{9.4}$$

We obtain the flow equation for $\Gamma_k[\phi]$ by differentiating both sides of Eq.(9.4) with respect to $k$. Using the definition (9.3), we have

$$\partial_k W_k[J] = e^{-W_k[J]} \int_p \partial_k \mathcal{R}_k \left[\frac{\delta}{\delta J(p)}\right] e^{W_k[J]}\,. \tag{9.5}$$

Introducing $R_k(p^2)$ via $\mathcal{R}_k = \phi(p) R_k(p^2) \phi(p)$ this can be rewritten as

$$\partial_k W_k[J] = -\int_p \frac{\partial_k R_k}{\Gamma_k''[\phi]} - \partial_k \mathcal{R}_k[\phi]\,. \tag{9.6}$$

The flow equation is then obtained by defining $\Gamma_k^{\rm av}[\phi] = \Gamma_k[\phi] - \mathcal{R}_k[\phi]$ and reads

$$\partial_k \Gamma_k^{\rm av}[\phi] = \int_p \frac{\partial_k R_k[\phi]}{\mathcal{R}_k[\phi] + \Gamma_k^{\rm av\,\prime\prime}[\phi]}\,. \tag{9.7}$$

In principle, Eq.(9.7) is a partial differential equation that can be solved. In practice, of course, this is virtually impossible. One therefore usually projects the equation onto expressions for $\phi$-independent coupling constants. Since this space is still infinite dimensional, one considers suitable truncations, where all but a finite number of couplings is set to zero.

In general, the choice of truncation has to be motivated using physical input, and, in the best case scenario, be validated through experimental data.

Note there are further subtleties in theories with the type of coupling considered above. For one, there is the question of well-definedness of the path integral quantization. The Hamiltonian of a theory that contains interactions with more than two derivatives inevitably includes terms that are at least trilinear in the canonical momenta. As a consequence, the integration over the canonical momenta in the path integral can in most cases not be performed exactly. Of course, one may *define* a partition function using Feynman's Lagrangian path integral. The physics described by this partition function, however, may even at tree level differ significantly from the physics described by the "bare" action.

Another point is the possible appearance of additional *ghost-like* poles in the full propagator due to higher derivative operators [Ostrogradski, 1850]. Higher derivative operators will be generated in any theory with derivative interactions, as follows already from a perturbative analysis. In the *effective field theory* regime, they are suppressed by powers of the cut-off; additional poles in the two-point function (possibly on a nontrivial background) will be above the scale where the effective field theory breaks down. Once one attempts to nonperturbatively renormalize a given theory, this can potentially change. A careful analysis of the pole structure of the exact propagator is in order.

### 9.1.1 The physics of the RG scale

Before we enter into actual calculations, we would like to remind the reader of the physical meaning of the RG-scale $k$. From the outset, $k$ denotes the scale above which all physics has been integrated out. Usually, one follows the RG-flow from some microscopic scale $k_{\rm UV}$ to an intermediate scale $k_0 \ll k_{\rm UV}$ s.t. at $k_0$, only the relevant couplings have residual dependence on the initial conditions chosen at $k_{\rm UV}$. For momentum scales $p \ll k_0$, one can then revert to the effective couplings to perform calculations. Note that this still includes the calculation of loops, and the corresponding running, only with a cut-off scale $k_0$.

At the same time, however, we may use the fact that crudely speaking, the external momentum enters loop diagrams like an IR-cutoff; a process at a given momentum $p$ is largely independent of the larger wavelengths. For concreteness, we consider the four-point interaction in a $\lambda\phi^4$ theory. Assume we have followed the RG flow down to the scale $k_0$, having obtained the corresponding coupling $\lambda_0 \ll 1$. In order to now calculate the strength of the four-point interaction[3] at some lower energy, we should take into account the

[3]The operators are here defined in an expansion around the Gaussian fixed point.

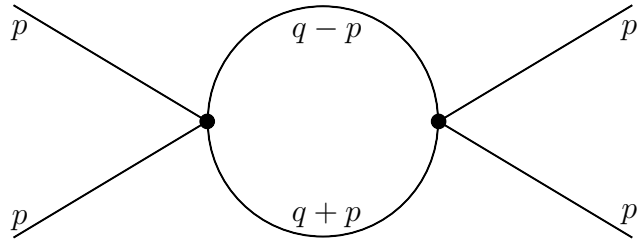


Figure 9.1: The one-loop diagram contributing to the renormalization of the four-point interaction in four-scalar theories.

corresponding loop corrections; at one loop, the relevant diagram is drawn in Fig. 9.1 and, for external momentum of order $p$, reads in four dimensions

$$\mathcal{A}_4 \sim \lambda_0^2 \int_0^{k_0} d^4q \frac{1}{(q+p)^2 + i\epsilon} \frac{1}{(q-p)^2 + i\epsilon} \sim \lambda_0^2 \log\left(\frac{p^2}{k_0^2}\right) . \tag{9.8}$$

The external momentum thus effectively suppresses contributions from low loop momenta.

This implies that we could have read the strength of the effective coupling constant straight from the RG flow. The physical coupling $\lambda_0(p)$ approximately agrees with the coupling $\lambda_p$ that we would have obtained had we followed the RG flow[4] down to the scale $p$. This hence allows for a simple identification of the RG scale with the external momentum at which a given coupling is evaluated. Obviously this identification is only valid for couplings that actually depend on external momentum.

In case of an interaction of the form $(\partial\phi)^4$, the story is quite similar. The corresponding diagram is given by

$$\mathcal{A}_4 \sim \lambda_0^2 \frac{p^4}{k_0^8} \int_0^{k_0} d^4q \frac{[(q+p)^\mu (q-p)_\mu]}{(q+p)^2 + i\epsilon} \frac{[(q+p)^\nu (q-p)_\nu]}{(q-p)^2 + i\epsilon} , \tag{9.9}$$

which now contains quartic, quadratic and logarithmic contributions from the cutoff. From dimensional grounds, we see that the latter contain additional powers of momenta and thus correspond to different classes of operators. Focusing on the quartic contribution, which is UV-dominated and hence independent of the IR cutoff, we obtain

$$\mathcal{A}_4 \sim \lambda_0^2 \frac{p^4}{k_0^4} . \tag{9.10}$$

[4]Of course the RG flow takes infinitely many more diagrams into account. However, at weak coupling, and sufficiently small energy ranges s.t. the logarithm in Eq. (9.8) does not become large, the difference is small.

We note the same momentum dependence as the tree level contribution. If we instead followed the RG flow down to the scale $p$, we would have obtained $\mathcal{A}_4 \sim \lambda_p$. Equating the two tells us that, to lowest order,

$$\frac{d\lambda_p}{d\log p} \sim 4\lambda_p\,, \tag{9.11}$$

which corresponds to the "trivial" running due to the momentum dependence of the coupling. If the scale identification works in the same way, no significant deviation from this behavior should be observed in the weak coupling regime.

## 9.2 Scalar O(N) model with shift symmetry

We now consider a set of $N$ real scalar fields $\phi_i$ in a $d$-dimensional theory with an $O(N)$ symmetry

$$\phi_i \to O_{ij}\phi_j \tag{9.12}$$

and a shift symmetry

$$\phi_i \to \phi_i + c_i, \tag{9.13}$$

where the $c_i$ are independent of space-time coordinates. The simplest Lorentz scalar that is invariant under both internal symmetries is given by the collective kinetic term

$$X = \frac{1}{2}\partial_\mu\phi_i\partial^\mu\phi_i, \tag{9.14}$$

where sums over repeated indices are to be understood. If the scalar field has canonical scaling dimension $[\phi_j] = \frac{d-2}{2}$, the invariant $X$ has $[X] = d$. Higher order combinations such as

$$Y = \frac{1}{2}(\Box\phi_j)^2 \tag{9.15}$$

are of dimension $d+2$ and higher.

We are interested in the form of the most general effective action $\Gamma[\phi]$ that is consistent with the symmetries (9.12) and (9.13). If $\Gamma[\phi]$ is also assumed to be local one can write it as

$$\Gamma[\phi] = \int d^dx\,\mathcal{L}(X, Y, \ldots) \tag{9.16}$$

where the ellipses stand for all possible other scalar combinations of arbitrary order in the fields. We may characterize $\Gamma[\phi]$ through an expansion in $\phi$. To lowest order this reads

$$\Gamma[\phi] = \Gamma_0 + \int_q \frac{1}{2}\phi(-q)P(q)\phi(q) + \mathcal{O}(\phi^4), \tag{9.17}$$

where $P(q)$ is the inverse propagator for vanishing expectation value $\phi_j(p) = 0$. The global shift symmetry implies $P(0) = 0$. Note that in general terms from many invariants $X$, $Y$ etc. contribute to $P(q)$ and that it may be important for the consistency of the theory to take all of them into account. In particular, taking into account only the contribution of $X$ and $Y$ one would have

$$P(q) = c_1 q^2 + c_2 q^4, \tag{9.18}$$

which appears as problematic since it contains ghost-like excitations. This is only a problem of an approximation, however, if the full function $P(q)$ has physical properties. For a causal and unitary theory, $G(q) = P(q)^{-1}$ is expected to have a spectral representation with all poles and branch cuts on the real frequency axis[5].

## 9.3 Flow equation

We begin our analysis by considering a truncation of the effective average action $\Gamma_k[\phi]$ limited to a generic function of $X$. Already at this level we will be able to investigate many interesting features of the FRG flow in these kind of theories. We therefore consider the truncation with a "potential" type term only,

$$\Gamma_k[\phi] = \int d^d x V_k(X). \tag{9.19}$$

Although rather simple, this is nevertheless a nontrivial theory with propagating modes since $X$ as defined in (9.14) contains derivative terms.

In order to project the general flow equation for $\Gamma_k[\phi]$ onto one for $V_k(X)$ we choose the following background configuration

$$\bar{\phi}_1 = \varphi_0 \cos(px) \tag{9.20}$$
$$\bar{\phi}_2 = \varphi_0 \sin(px) \tag{9.21}$$
$$\bar{\phi}_3 = ... = \bar{\phi}_N = 0. \tag{9.22}$$

This implies $X = X_0 = \frac{1}{2} p^2 \varphi_0^2 = \text{const}$. Denoting by $\delta\phi_j$ small fluctuations around said background, $\phi_j = \bar{\phi}_j + \delta\phi_j$, we obtain for the part of the flowing

[5]There are also arguments that the higher derivative operators that are generated at the quadratic level are all redundant and can be removed through appropriate field redefinitions [Anselmi, 2003].

action that is quadratic in $\delta\phi_j$,

$$\Gamma_{k,2} = \int d^dx \left[ V_k'(X_0)\frac{1}{2}(\partial_\mu \delta\phi_j)^2 + \frac{1}{2}V_k''(X_0)X_0\left(-\sin(px)\hat{p}^\mu\partial_\mu\delta\phi_1 + \cos(px)\hat{p}^\mu\partial_\mu\delta\phi_2\right)^2\right], \quad (9.23)$$

where $\hat{p}^\mu = \frac{p^\mu}{\sqrt{p^2}}$.

We can now evaluate (9.23) in Fourier space, which yields a rather lengthy expression. However, we wish to project onto a flow equation for the effective "potential" $V_k(X)$. It is therefore clear that contributions will only arise from terms containing equal powers of $p$ and $\phi_0$. This corresponds to taking the double scaling limit $p \to 0$, $\phi_0 \to \infty$ while keeping $X = \frac{1}{2}p^2\phi_0^2$ fixed and leaves us with

$$\Gamma_{k,2} = \int \frac{d^dq}{(2\pi)^d}\frac{1}{2}\phi_i(-q)\left[V_k'(X_0)q^2\delta_{ij} + 2X_0V''X_0(\hat{p}\cdot q)^2\delta_{i2}\delta_{j2}\right]\phi_j(q)\,. \quad (9.24)$$

We choose now an infrared regulator term that respects both the $O(N)$ and global shift symmetry,

$$\begin{aligned}\Delta S_k &= \int d^dx\frac{1}{2}\partial_\mu\phi_j Z_k r(-\partial^2/k^2)\partial^\mu\phi_j \\ &= \int \frac{d^dq}{(2\pi)^d}\frac{1}{2}\phi_j(-q)q^2 Z_k r(q^2/k^2)\phi_j(q), \end{aligned} \quad (9.25)$$

where $Z_k$ is a positive function of $k$ that will be specified below and $r(z)$ is a dimensionless real function that decays monotonically for large $z$. We normalize it by $r(0) = 1$. In principle there is quite some freedom in the precise choice of this function but for concreteness we concentrate here on the class of functions

$$r(q^2/k^2) = \frac{1}{\left(1+\frac{q^2}{c\,k^2}\right)^c}, \quad (9.26)$$

where $c \geq 1$ is some real parameter. Note in particular that

$$\lim_{c\to\infty} r(q^2/k^2) = \exp(-q^2/k^2). \quad (9.27)$$

The flow equation for the effective potential $V_k(X)$ reads (with $t = \ln k$)

$$\begin{aligned}\partial_t V_k(X)\big|_X =& \frac{1}{2}\int \frac{d^dq}{(2\pi)^d}\left(\frac{q^2\partial_t Z_k r(q^2/k^2)}{V_k'(X)q^2 + 2XV_k''(X)(\hat{p}\cdot q)^2 + q^2 Z_k r(q^2/k^2)}\right.\\ &\left. + \frac{(N-1)q^2\partial_t Z_k r(q^2/k^2)}{V_k'(X)q^2 + q^2 Z_k r(q^2/k^2)}\right)\\ =& \frac{1}{2}k^d\left[f_0^d\left(\frac{V_k'(X)}{Z_k}, \frac{2XV_k''(X)}{Z_k}; \eta\right) + (N-1)f_0^d\left(\frac{V_k'(X)}{Z_k}, 0; \eta\right)\right],\end{aligned} \tag{9.28}$$

where

$$f_0^d(a,b;\eta) = \frac{(d-1)v_{d-1}}{(2\pi)^d}\int_0^\pi d\theta \sin^{d-2}\theta \int_0^\infty dz\, z^{\frac{d-2}{2}} \frac{-zr'(z) - \frac{1}{2}\eta r(z)}{a + b\cos^2\theta + r(z)} \tag{9.29}$$

is an integral function,

$$\eta = -\frac{\partial_t Z_k}{Z_k}, \tag{9.30}$$

denotes the anomalous dimension and

$$v_d = \frac{\pi^{d/2}}{\Gamma(1+d/2)} \tag{9.31}$$

is the volume of the $d$-dimensional unit sphere.

We now introduce the dimensionless and rescaled quantities

$$\tilde{X} = \frac{Z_k X}{k^d} \tag{9.32}$$

and

$$\tilde{V}_k(\tilde{X}) = \frac{V_k(X)}{k^d}, \tag{9.33}$$

and thus obtain the scaling form of the flow equation for the effective potential

$$\begin{aligned}\partial_t \tilde{V}_k(\tilde{X})\big|_{\tilde{X}} =& \left(\frac{\partial}{\partial X}\tilde{V}_k(\tilde{X})\right)\partial_t X\big|_{\tilde{X}} + \partial_t \tilde{V}_k(\tilde{X})\big|_X\\ =& (d+\eta)\tilde{X}\,\tilde{V}_k'(\tilde{X}) - d\,\tilde{V}_k(\tilde{X}) + \frac{1}{2}f_0^d\left(\tilde{V}_k'(\tilde{X}), 2\tilde{X}V_k''(\tilde{X}); \eta\right)\\ &+ \frac{1}{2}(N-1)f_0^d\left(\tilde{V}_k'(\tilde{X}), 0; \eta\right).\end{aligned} \tag{9.34}$$

This is the main result of this chapter[6].

[6]During the time of writing, [de Rham and Ribeiro, 2014] appeared, in which a somewhat similar expression was derived.

## 9.4 Taylor expansion

It is instructive to analyse the flow equation for $\tilde{V}_k(\tilde{X})$ in (9.34) in terms of a Taylor expansion, first. To this end we write

$$\tilde{V}_k(\tilde{X}) = v_0 + v_1\tilde{X} + \frac{1}{2}v_2\tilde{X}^2 + \frac{1}{3!}v_3\tilde{X}^3 + \dots \tag{9.35}$$

where the coefficients $v_n$ depend on the renormalization group scale $k$. By expanding both sides of (9.34) one obtains the following flow equations for the lowest coefficients

$$\begin{aligned}
\partial_t v_0 =& - d v_0 + \frac{1}{2} N f_0^d(v_1, 0; \eta), \\
\partial_t v_1 =& \eta\, v_1 - v_2 f_{0,1}^d(v_1, 0; \eta) - \frac{N}{2} v_2 f_{1,0}^d(v_1, 0; \eta), \\
\partial_t v_2 =& (d + 2\eta) v_2 + 2 v_2^2 f_{1,1}^d(v_1, 0; \eta) + \frac{N}{2} v_2^2 f_{2,0}^d(v_1, 0; \eta) + 2 v_2^2 f_{0,2}^d(v_1, 0; \eta) \\
& - \frac{N}{2} v_3 f_{1,0}^d(v_1, 0; \eta) - 2 v_3 f_{0,1}^d(v_1, 0; \eta), \\
\partial_t v_3 =& (2d + 3\eta) v_3 \\
& - v_2^3 \left( 4 f_{0,3}^d(v_1, 0; \eta) + 6 f_{1,2}^d(v_1, 0; \eta) + 3 f_{2,1}^d(v_1, 0; \eta) + \frac{N}{2} f_{3,0}^d(v_1, 0; \eta) \right) \\
& + 3 v_2 v_3 \left( 4 f_{0,2}^d(v_1, 0; \eta) + 3 f_{1,1}^d(v_1, 0; \eta) + \frac{N}{2} f_{2,0}^d(v_1, 0; \eta) \right).
\end{aligned} \tag{9.36}$$

The functions $f_{m,n}^d(a, b; \eta)$ defined in Eq. (9.29) are linear in $\eta$. We now choose $Z_k$ such that $v_1 = 1$ for all $k$. This fixes also the anomalous dimension $\eta$. We also define the abbreviations $f_{m,n}^d = f_{m,n}^d(1, 0; \eta) = \bar{f}_{m,n}^d - \hat{f}_{m,n}^d \eta$. The definitions are such that $\bar{f}_{m,n}^d$ and $\hat{f}_{m,n}^d$ are positive. This leads to the set of

equations

$$\begin{aligned}
\eta =& \frac{v_2\left(\bar{f}^d_{0,1}+\frac{N}{2}\bar{f}^d_{1,0}\right)}{1+v_2\left(\hat{f}^d_{0,1}+\frac{N}{2}\hat{f}^d_{1,0}\right)},\\
\partial_t v_2 =& (d+2\eta)v_2 + v_2^2\left(2\bar{f}^d_{1,1}+\frac{N}{2}\bar{f}^d_{2,0}+2\bar{f}^d_{0,2}\right) - v_2^2\eta\left(2\hat{f}^d_{1,1}+\frac{N}{2}\hat{f}^d_{2,0}+2\hat{f}^d_{0,2}\right)\\
&- v_3\left(\frac{N}{2}\bar{f}^d_{1,0}+2\bar{f}^d_{0,1}\right)+v_3\,\eta\left(\frac{N}{2}\hat{f}^d_{1,0}+2\hat{f}^d_{0,1}\right),\\
\partial_t v_3 =& (2d+3\eta)v_3 + 3v_2v_3\left(4\bar{f}^d_{0,2}+3\bar{f}^d_{1,1}+\frac{N}{2}\bar{f}^d_{2,0}\right)\\
&- 3v_2v_3\eta\left(4\hat{f}^d_{0,2}+3\hat{f}^d_{1,1}+\frac{N}{2}\hat{f}^d_{2,0}\right) - v_2^3\left(4\bar{f}^d_{0,3}+6\bar{f}^d_{1,2}+3\bar{f}^d_{2,1}+\frac{N}{2}\bar{f}^d_{3,0}\right)\\
&+ v_2^3\eta\left(4\hat{f}^d_{0,3}+6\hat{f}^d_{1,2}+3\hat{f}^d_{2,1}+\frac{N}{2}\hat{f}^d_{3,0}\right).
\end{aligned} \tag{9.37}$$

Let us for simplicity first consider the case in which $v_3 \equiv 0$ (and for a second ignore the fact that it is generated according to the last equation in (9.37)). The expression for the anomalous dimension remains unchanged, while the flow equation for $v_2$ reads

$$\partial_t v_2 = (d+2\eta)v_2 + v_2^2\left(2\bar{f}^d_{1,1}+\frac{N}{2}\bar{f}^d_{2,0}+2\bar{f}^d_{0,2}\right) - v_2^2\eta\left(2\hat{f}^d_{1,1}+\frac{N}{2}\hat{f}^d_{2,0}+2\hat{f}^d_{0,2}\right). \tag{9.38}$$

This equation admits two fixed points (FP) with $\partial_t v_2 = 0$. The first corresponds to the Gaussian one at $v_2 = 0$, while the other one is interacting and located at negative $v_2 = v_2^*$. In Fig. 9.2a, we plot $\partial_t v_2$ versus $v_2$ for $d = 4$ and two values of $N$, while Fig.9.2b shows the corresponding anomalous dimension. It is interesting to observe that for larger $N$, the nontrivial FP is pushed towards the perturbative regime. We may classify the fixed points according to their stability properties, given by the eigenvalues of the stability matrix, which is in this case of course just the coefficient of the linear term when expanded around the fixed point:

- $v_2 = 0$: IR attractive, UV repulsive.
- $v_2 = v_2^*$: IR repulsive, UV attractive.

We have thus uncovered a UV-attractive FP in the simplest truncation.

Let us at this point briefly comment on the scale identification mentioned in section 9.1.1. Deep inside the perturbative regime around the Gaussian

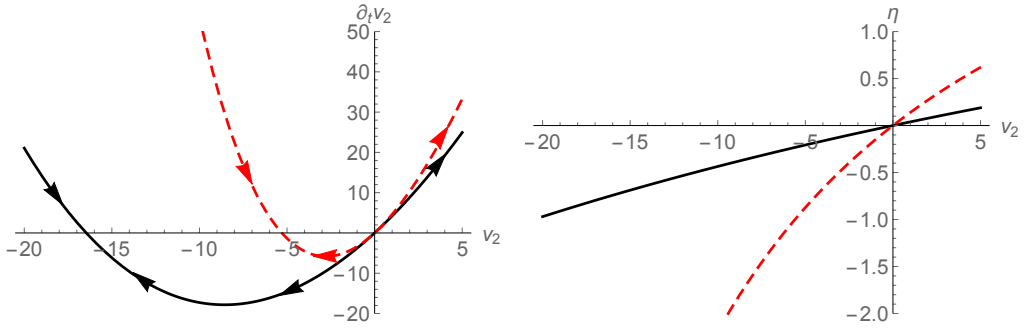


(a) (b)

Figure 9.2: (a): Flow equation $\partial_t v_2$ as a function of $v_2$ for $N = 1$ (black) and $N = 5$ (red, dashed). The arrows indicate the direction of the flow towards the UV. (b): Anomalous dimension $\eta$ as a function of $v_2$ for $N = 1$ (black) and $N = 5$ (red, dashed).

FP, we obtain $v_2(k) \sim v_2(0) \left(\frac{k}{k_0}\right)^4$, agreeing with our naive estimate. Once $v_2$ grows in magnitude (but is still less than one), we observe a deviation from this scaling due to the quadratic term in Eq.(9.38). Consequently, the scale identification is no longer straightforward. The physical understanding of this apparent mismatch will be one of the ultimate goals of our studies, but is beyond the scope of the present analysis. It will be subject of future work.

We now include the coupling $v_3$ in the analysis. Note that the right hand side of the last equation in (9.37) is linear in $v_3$ and one can therefore easily solve for the (unique) fixed point value $v_3^*$ where the flow vanishes, $\partial_t v_3 = 0$,

$$v_3^* = \frac{v_2^3 \left(4\bar{f}^d_{0,3} + 6\bar{f}^d_{1,2} + 3\bar{f}^d_{2,1} + \frac{N}{2}\bar{f}^d_{3,0}\right) - v_2^3\eta \left(4\hat{f}^d_{0,3} + 6\hat{f}^d_{1,2} + 3\hat{f}^d_{2,1} + \frac{N}{2}\hat{f}^d_{3,0}\right)}{2d + 3\eta + 3v_2 \left(4\bar{f}^d_{0,2} + 3\bar{f}^d_{1,1} + \frac{N}{2}\bar{f}^d_{2,0}\right) - 3v_2\eta \left(4\hat{f}^d_{0,2} + 3\hat{f}^d_{1,1} + \frac{N}{2}\hat{f}^d_{2,0}\right)}. \tag{9.39}$$

Using this expression together with the expression for the anomalous dimension in the second equation of (9.37) results in a closed expression for $\partial_t v_2$ in terms of a rational function of $v_2$.

We discover several fixed points. Besides the Gaussian FP, we find two more at negative $v_2$. We plot the fixed point value $v_3^*$ and the flow equation $\partial_t v_2$ as functions of $v_2$ in Fig. 9.3. Again, we note that in the $v_2$-direction, the fixed points for negative $v_2$ are UV attractive, while the Gaussian FP is IR attractive. The latter also holds in the direction of $v_3$. The FP at $v_2 = -9.09, v_3 = -308.78$ is IR attractive in the direction of $v_3$. On the other hand, we again find an FP that is UV attractive in either direction:

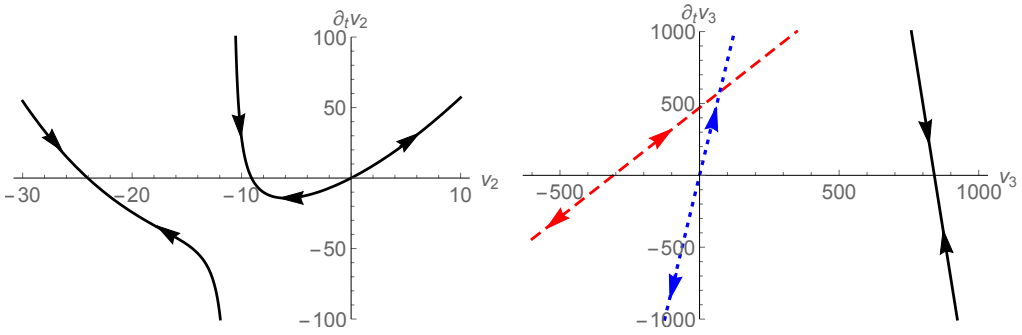


(a) (b)

Figure 9.3: (a): Flow equation $\partial_t v_2$ as a function of $v_2$ according to (9.37) with $v_3$ taken to be on its fixed point value. (b): Flow equation $\partial_t v_3$ as a function of $v_3$ according to (9.37) with $v_2$ taken on the fixed point values $v_2 = -24.05$ (black), $v_3 = -9.09$ (red, dashed) and $v_2 = 0$ (blue, dotted). In both panels, the arrows indicate the direction of the flow towards the UV.

the FP corresponding to $v_2 = -24.05, v_3 = 841.07$ (the black line in Fig. 9.3b).

In principle, this analysis can now be extended to arbitrarily high orders. Unfortunately, at the present time we cannot provide a general statement on the survival of a given FP when more couplings are taken into account. In this light, it would be of advantage to analyze the differential equation (9.34) for FP solutions without reverting to a Taylor expansion. While this is generically only possible numerically, we find that for particular forms of the regulator, the equation takes on a rather simple form. This is the subject of the following section.

## 9.5 A differential equation for a fixed point action

In this final section we make use of the curiosity that the functions $f_0^d$ in Eq.(9.29) may be integrated analytically if, instead of (9.26), one chooses the regulator to take the form

$$r(z) = \Theta(1 - z)\,. \tag{9.40}$$

It is known that the introduction of a non-differentiable regulator may lead to unphysical non-analytic features in the effective action [Wetterich, 1993a,b]. We will ignore this issue for now and enjoy the fact that for $d = 4$, the flow

equation takes on the closed form[7]

$$\partial_t V_k(X) = (4+\eta) X V_k'(X) - 4V_k(X) + (N-1)\frac{1}{2^6\pi^2}\frac{4-\eta}{1+V_k'(X)} + \frac{1}{2^6\pi^2}\frac{4-\eta}{XV_k''(X)}\left(-1+\sqrt{\frac{1+V_k'(X)+2XV_k''(X)}{1+V_k'(X)}}\right), \quad (9.41)$$

At a fixed point, the left hand side of this expression vanishes. Consequently, we obtain an ordinary differential equation for the effective action at the fixed point. Let us begin by confirming the existence of the free, Gaussian fixed point. Here, $V(X) = V_0 + X$ and $\eta = 0$, and thus

$$\partial_t V_k(X) = N\frac{1}{2^5\pi^2}\,. \quad (9.42)$$

This does not appear to vanish! So what went wrong? Nothing, in the end, since this only renormalizes the in our setup unobservable zero-point of the potential. What we learn is that our requirement for the left hand side of (9.41) to vanish is indeed a little too strict. Our differential equation for a generic non-Gaussian fixed point hence takes on the form

$$2^6\pi^2\frac{XV_k''}{4-\eta}\left[(4+\eta)XV_k' - 4V_k - \alpha\right] + \sqrt{\frac{1+V_k'+2XV_k''}{1+V_k'}} + (N-1)\frac{XV_k''}{1+V_k'} = 1\,. \quad (9.43)$$

where $\alpha$ is an $X$-independent constant that will be related to boundary conditions. Solving this equation for $V_k''$ yields

$$XV_k''(X) = 2\frac{\left(\frac{N}{1+V_k'(X)} + \frac{2^6\pi^2}{4-\eta}\left[(4+\eta)XV_k'(X) - 4V_k(X) - \alpha\right]\right)}{\left(\frac{N-1}{1+V_k'(X)} - \alpha + \frac{2^6\pi^2}{4-\eta}\left[(4+\eta)XV_k'(X) - 4V_k(X)\right]\right)^2}, \quad (9.44)$$

which, in the limit of large $N$, simplifies to

$$XV_k''(X) = 2\left(\frac{N}{1+V_k'(X)} + \frac{2^6\pi^2}{4-\eta}\left[(4+\eta)XV_k'(X) - 4V_k(X) - \alpha\right]\right)^{-1}. \quad (9.45)$$

Analytical solutions even to this equation are difficult to come by. Instead, one should resort to numerical methods to get a picture of the possible form of the action at a fixed point.

[7] Note that for simplicity we work in the convention $\Theta(0) = 1$.

Under the assumption that $V_k'(X) \to 0$ for large $X$, we find

$$V_k(X) \sim X^{\frac{4}{4+\eta}} \text{ for } X \gg 1\,, \tag{9.46}$$

which, in terms of physical quantities, would give at some RG-scale $\Lambda$

$$V_\Lambda(X) \sim \Lambda^{\frac{4\eta}{4+\eta}} X^{\frac{4}{4+\eta}}\,, \tag{9.47}$$

valid for $X \gg \Lambda$.

For a vanishing anomalous dimension, the above solution corresponds to the Gaussian fixed point and is valid for all $X$. It will be interesting to see whether Eqs.(9.41) or (9.45) admit physically viable solutions for nonzero anomalous dimension that are valid for all $X$.

While such solutions would automatically correspond to resummed nonlinearities, contributions from higher derivative operators are not taken into account. At this point it is not clear to what extent any fixed point can survive in a more general truncation. This will be subject of future studies.

## 9.6 Summary

In this chapter we have taken a first step towards the understanding of the renormalization group behavior of shift-symmetric scalar theories. To this end, we have derived a flow equation for the effective "potential" for scalar, $O(N)$ symmetric theories that are functions only of the kinetic term. We have shown that in a Taylor expansion, a variety of fixed points can be found. Of these, at least one proved to be UV-attractive.

In order to make more general statements on the existence of fixed points for an arbitrarily high order in the fields, we have given an exact differential equation for the fixed point potential under the assumption of a $\Theta$-function regulator. We have shown that in the limit of large $X$, this equation admits simple solutions.

Our analysis calls out to be extended in a number of directions. Most notably, we will extend the studies to operators with more derivatives per field. Moreover, we intend to make use of our results to provide a deeper understanding of the matching between renormalization group scale and physical momentum at least in these simple but nevertheless nontrivial theories. Solutions to this may shed light also on similar problems in asymptotic safety.

Finally, it will prove interesting to understand the relation of our results to the phenomenon of classicalization.

# Chapter 10

# Conclusions and Outlook

Within this dissertation, we have considered aspects of gravity and field theory on the shortest and longest scales.

The first part was dedicated to cosmology, in particular to the two phases of accelerated expansion. In the context of inflation, we considered a model that relies on the Higgs boson as the inflaton. While the most naive models of *Higgs inflation* are excluded due to the fact that the experimentally allowed values of the Higgs self-coupling are incompatible with slow-roll inflation, the introduction of a non-minimal coupling may resolve this. We have shown that a model in which the Higgs is coupled to the Einstein tensor can naturally provide for a gravitational wave spectrum compatible with the BICEP2 results. We further addressed the issues of strong coupling and quantum corrections in this model. We pointed out indications in favor of a stability of the model from quantum corrections.

Next, we focused on the recently started phase of accelerated expansion. We pointed out that in quintessential dark energy models that include the presence of an initial fifth force, the standard spherical collapse description of nonlinear structure formation is incorrect. Instead, we proposed a modified model that includes all important fifth force effects. We applied this to various scenarios to point out possible observational differences.

The part of the thesis on cosmology was concluded by studies of massive gravity. Generic interacting models of a massive graviton are plagued by ghost instabilities. Usually, these are due to the reemergence of the sixth polarization of the graviton as an additional degree of freedom. We pointed out how the appearance of this mode may be avoided. In particular, we constructed a theory of a massive spin-two degree of freedom that is ghost-free on the cubic level without relying on a nonlinear completion.

In the second part of this dissertation, we focused on issues in black hole physics. In a novel approach, black holes are modeled as Bose condensates

of gravitons that lie at a quantum critical point. This provides a quantum field theoretical description of black holes as bound states in which many apparent paradoxa of semiclassical black hole physics are resolved.

We worked out several peculiarities in this description. For one, we demonstrated how the presence of a quantum critical – or bifurcation – point can provide a natural explanation of considerable entanglement in the black hole quantum state. This could explain why the mean field description of a black hole in terms of a metric can break down even for $r_s \gg \ell_p$.

Moreover, we showed that black holes can be very efficient processors of information due to their instability towards collapse. We have introduced the concept of quantum breaking which measures the departure of the quantum mechanical evolution from a classical, mean field description. Essentially, quantum breaking measures the generation of one-particle entanglement. It therefore provides a first hint towards an explanation of the conjectured fast scrambling property of black holes.

Hawking evaporation in the quantum bound state description of black holes arises due to incoherent scattering of condensed gravitons and subsequent emission of on-shell gravitons. At the same time, the condensate coherently collapses. We have modeled this behavior in a simplified setup of a relativistic scalar field in which processes that violate number conservation are forbidden. We have proven the existence of scaling solutions, in which the number of condensed gravitons and the width of the bound state are related. We further discovered the appearance of a bifurcation along the collapse that could provide an explanation for the appearance of light modes.

The final part of the thesis focuses on the connection of non-Wilsonian approaches to UV-completion to more conservative attempts. To this regard, we considered the functional renormalization group flow in a theory of derivatively coupled scalar fields with an $O(N)$ symmetry. We derived the flow equation for the Lagrangian in case it is a function of the kinetic term only. Through solving this equation in a Taylor expansion, we have shown the existence of fixed points for the lowest order couplings. Furthermore, we derived an ordinary differential equation for the Lagrangian at the fixed point for the choice of a sharp regulator. A further aim was to understand subtle issues such as the mapping of the renormalization scale to physical energy scales. This is work in progress.

The contents of this thesis allow manifold ways of extension. Confirmation of the observation of gravitational waves would call for a better understanding of inflationary models in the regime of large field values. This could include addressing approximate shift symmetries in the ultraviolet as well as the understanding of contributions of nonperturbative, large action objects to the effective potential.

Our insights into nonlinear structure formation can be applied to almost all models that include fifth forces. Moreover, our methods can also be applied to models that go beyond the cold dark matter paradigm. For example, effects of nonvanishing pressure can be readily included in our approach.

The modeling of black holes as Bose condensates calls for further investigation on many scales. Issues include the origin of black hole entropy in Bogoliubov modes. So far, all prototype models relied on scalar fields. The inclusion of spin may shed light onto possible origins of the large number of light modes.

Our model of entanglement generation may be extended to chaotic models. While an instantaneous instability can readily explain the generation of one-particle entanglement, scrambling may require a persisting instability. Generalization of our results could provide valuable insight into the mechanism of thermalization in quantum theories.

The concepts of evaporating Bose condensates have so far only been applied to nonrelativistic systems. Our approach provides the first step to a generalization. Future directions include proofs of the independence of the results of the choice of variational ansatz and the inclusion of number-violating processes as well as the generalization to higher spins.

Finally, we propose to extend our analysis of the scalar $O(N)$ model with shift symmetry towards higher derivative interactions. This may provide valuable insights on the survival of fixed points if more UV-relevant directions are taken into account and could ultimately shed light on the physical viability of models of asymptotic safety.

# Appendix A

# Quantum Equivalence of Jordan and Einstein frame

In this appendix we will comment on the difference between Jordan and Einstein frame from a path integral perspective. We make the observation that from the Hamiltonian path integral point of view, both frames are equivalent as long as all Jacobians are properly carried along.

## A.1 Scalar field theory

For simplicity we begin our discussion with a theory of two scalar fields that contains the most important feature of gravity in the Jordan frame, namely the noncanonical kinetic term of one of the fields. The corresponding Lagrangian is given by

$$\mathcal{L} = \frac{1}{2}(\partial_\mu \phi_1)^2 + \frac{1}{2}\phi_1^2(\partial_\mu \phi_2)^2 - V(\phi_i)\,, \tag{A.1}$$

where our choice of the prefactor of $(\partial_\mu \phi_2)^2$ corresponds to a scale free action in Jordan frame. $V(\phi_i)$ contains all nonderivative contributions.

The first step in deriving the action path integral from the classical Lagrangian (A.1) is to write down the corresponding Hamiltonian. The canonical momenta are given by

$$\Pi_1 = \dot{\phi}_1\,, \;\; \Pi_2 = \phi_1^2 \dot{\phi}_2\,. \tag{A.2}$$

We see that the second relation is only invertible if $\phi_1$ is non-zero. In order to be able to perform the Legendre transform, we introduce a regulator $\epsilon$ s.t. $\phi_1^2(\partial_\mu \phi_2)^2 \to (\phi_1^2 + \epsilon^2)\,(\partial_\mu \phi_2)^2$. Consequently, we obtain the Hamiltonian

$$\mathcal{H} = \frac{1}{2}\Pi_1^2 + \frac{1}{2}\left(\nabla \phi_1\right)^2 + \frac{1}{2\left(\phi_1^2 + \epsilon^2\right)}\Pi_2^2 + \frac{1}{2}\left(\phi_1^2 + \epsilon^2\right)\left(\nabla \phi_2\right)^2 + V(\phi_i)\,. \tag{A.3}$$

The generating functional for the theory is defined by

$$Z[J] = \mathcal{N} \int \mathcal{D}\phi_i \mathcal{D}\Pi_j e^{i\int (\Pi_i \dot{\phi}_i - \mathcal{H} + J_i \phi_i)} \,. \tag{A.4}$$

The measure is defined in the usual way as, e.g., $\mathcal{D}\phi_i = \prod_k d\phi_k$, where the product is over all spacetime points. $\mathcal{N}$ is a normalization factor which we will never make explicit. The Hamiltonian (A.3) is quadratic in the momenta $\Pi_i$ and we may therefore perform the corresponding Gaussian integrals explicitly. The integral over $\Pi_1$ is completely straightforward and will, after completing the square, give rise to the term $\dot{\phi}_1^2$ in the exponent. The integral over $\Pi_2$, on the other hand, is slightly less trivial. Indeed, completion of the square now leads to

$$\Pi_2 \dot{\phi}_2 - \frac{1}{2\left(\phi_1^2 + \epsilon^2\right)} \Pi_2^2 = -\frac{1}{2\left(\phi_1^2 + \epsilon^2\right)} \left(\Pi_2 - \left(\phi_1^2 + \epsilon^2\right) \dot{\phi}_2\right)^2 + \frac{1}{2}\left(\phi_1^2 + \epsilon^2\right) \dot{\phi}_2^2 \,. \tag{A.5}$$

Therefore, integration over $\Pi_2$ gives rise to a functional determinant

$$d_\epsilon(\phi_1) \equiv \det\left[\left(\phi_1^2 + \epsilon^2\right)\right]^{\frac{1}{2}} \,, \tag{A.6}$$

where here and in the following, $\delta$-functions are suppressed and reintroduced when needed. Of course, this result could have equivalently been obtained through a corresponding redefinition of the canonical momentum $\Pi_2$. Note that the determinant cannot be absorbed into the overall normalization $\mathcal{N}$ since it is field dependent.

We obtain the functional integral

$$Z[J] = \mathcal{N} \int \mathcal{D}\phi_i d(\phi_1) e^{i\int (\mathcal{L} + J_i \phi_i)} \,. \tag{A.7}$$

The determinant $d_\epsilon(\phi_1)$ is a direct consequence of the noncanonical kinetic term and has to be taken into account [Unz, 1986][1]. We are presented with two possible options.

(i) Absorb the functional determinant into the measure of the path integral over $\phi_1$. In this case, however, our measure will explicitly depend on the regulator $\epsilon$, which we cannot send to zero without the measure becoming singular.

[1] Note that the argument of $d(\phi_1)$ is diagonal in position space. Reexponentiation of the determinant therefore yields an ultralocal contribution proportional to $\delta^{(4)}(0)$. Explicitly, we obtain

$$\det\left[i\left(\phi_1^2 + \epsilon^2\right)\right]^{\frac{1}{2}} = \exp\left(\frac{1}{2}\,\delta^{(4)}(0) \int \log\left[\left(\phi_1^2 + \epsilon^2\right)\right]\right) \,. \tag{A.8}$$

This term requires regularization. For example, in cut-off regularization, it is proportional to $\Lambda^4$, where $\Lambda$ is the ultraviolet cut-off.

(ii) Attempt a removal of the functional determinant through an appropriate field redefinition.

We shall here focus on the second option and remove the functional determinant through an appropriate redefinition of the field $\phi_2$. Requiring exact cancellation leads to

$$\frac{\delta\phi_2}{\delta\tilde{\phi}_2} = \left(\phi_1^2 + \epsilon^2\right)^{-\frac{1}{2}} , \tag{A.9}$$

and therefore

$$\phi_2 = \left(\phi_1^2 + \epsilon^2\right)^{-\frac{1}{2}} \tilde{\phi}_2 . \tag{A.10}$$

Obviously, this is nothing but the redefinition to canonically normalize the field $\phi_2$ in the original Lagrangian. We therefore see that the requirement that the action path integral follows from a Hamiltonian path integral without regulator dependent measures forces us to canonically normalize the fields in the original action.

For completeness we give the final expression for the generating functional after the field redefinition:

$$Z[J] = \mathcal{N} \int \mathcal{D}\phi_i e^{iS[\phi_i]} , \tag{A.11}$$

$$S[\phi_i] = \int \frac{1}{2}\left(1 + \frac{\phi_1^2}{\left(\phi_1^2+\epsilon^2\right)^2}\phi_2^2\right)(\partial_\mu\phi_1)^2 + \frac{1}{2}(\partial_\mu\phi_2)^2 - \frac{\phi_1}{\phi_1^2+\epsilon^2}\partial_\mu\phi_1\partial^\mu\phi_2\phi_2 \tag{A.12}$$

$$- V\left(\phi_1, \phi_2/\sqrt{\phi_1^2+\epsilon^2}\right) , \tag{A.13}$$

where we have dropped the tilde for notational simplicity.

Note that while it now appears that the kinetic terms of either field are not canonical, we may check through direct calculation that no determinant is generated if one rederives the path integral from (A.12). The corresponding terms are just derivative interactions.

At the same time, we note that the theory still has the strong coupling problem on a vanishing background for $\phi_1$ if the regulator $\epsilon$ is sent to zero.

## A.2 Gravity

Applying the previous results to GR is now straightforward. Of course, there are additional subtleties due to diffeomorphism invariance. Therefore, we will only give a sketchy derivation of the appropriate expressions. More detailed discussions of those subtleties can be found, for example, in [Henneaux and Teitelboim, 1992, Popov, 2001].

Let us consider the following action in the Jordan frame:

$$S_{\rm JF} = \int d^4x\sqrt{-g}\left[\frac{\phi^2}{2}R - \frac{1}{2}\left(\partial_\mu\phi\right)^2 - V(\phi)\right] , \tag{A.14}$$

where for simplicity we ignore couplings to matter, with the knowledge in mind that a generalization presents no conceptual issue.

The measure of the path integral is best derived in the ADM-formalism [Arnowitt et al., 1960, 2008]. We therefore split the metric into the spatial part $\gamma_{ij}$, the lapse $N_i$ and the shift $N$ according to[2]

$$\gamma_{ij} = g_{ij} , \tag{A.15}$$
$$N_i = g_{0i} , \tag{A.16}$$
$$N = \left(-g^{00}\right)^{-1/2} . \tag{A.17}$$

One defines the extrinsic curvature

$$K_{ij} = -\frac{1}{2N}\left(\dot{\gamma}_{ij} - 2\nabla_{(i}N_{j)}\right) , \tag{A.18}$$

where $\nabla$ is the covariant derivative w.r.t. the spatial metric $\gamma_{ij}$ and $(,)$ denotes symmetrization. Inserting the decomposition into the action (A.14), we obtain

$$\begin{aligned} S_{\rm JF} = \int d^4x \Bigg[ & \frac{\phi^2}{2}\Big\{ - \gamma_{ij}\partial_t\left[\sqrt{\gamma}\left(K^{ij} - K\gamma^{ij}\right)\right] + N\sqrt{\gamma}\left(R_\gamma + K^2 - K_{ij}^2\right) \\ & - 2N_i\sqrt{\gamma}\,\nabla_j\left(K^{ij} - K\gamma^{ij}\right) - 2\sqrt{\gamma}\,\nabla_i\left(\nabla_j N - K^{ij}N_j\right)\Big\} \\ & + \frac{\sqrt{\gamma}}{2N}\left(\dot{\phi} - N^i\nabla_i\phi\right)^2 - \frac{N\sqrt{\gamma}}{2}\left(\nabla_i\phi\right)^2 - N\sqrt{\gamma}\,V(\phi)\Bigg] , \end{aligned} \tag{A.19}$$

where $R_\gamma$ is the three-dimensional Ricci scalar and all tracing, raising and lowering operations are performed through appropriate applications of the spatial metric. After partial integration of the derivatives[3] acting on the

[2] For easier comparison to the original work, we work here using the metric signature $(-,+,+,+)$.

[3] Assuming asymptotically flat space, s.t. boundary terms may be neglected. Note that this does not change the conclusions below, but is only a matter of convenience.

extrinsic curvature, Eq. (A.19) becomes

$$S_{\mathrm{JF}} = \int d^4x \Bigg[ \frac{\phi^2}{2}\sqrt{\gamma}\, \Big\{ \dot{\gamma}_{ij} \left( K^{ij} - K\gamma^{ij} \right) + N \left( R_\gamma + K^2 - K_{ij}^2 \right) + 2\nabla_i N_j \left( K\gamma^{ij} - K^{ij} \right) \Big\} + \sqrt{\gamma} \Big\{ 2\phi K \left( \dot{\phi} - N^i \nabla_i \phi \right) - N\Delta\left(\phi^2\right) + \frac{1}{2N} \left( \dot{\phi} - N^i \nabla_i \phi \right)^2 - \frac{N}{2} \left( \nabla_i \phi \right)^2 - NV(\phi) \Big\} \Bigg] , \quad \text{(A.20)}$$

and allows us to straightforwardly read off the canonical momenta:

$$\pi^{ij} = \frac{\phi^2}{2}\sqrt{\gamma}\, \left( K\gamma^{ij} - K^{ij} \right) - \frac{\phi}{N}\sqrt{\gamma}\, \gamma^{ij} \left( \dot{\phi} - N^k \nabla_k \phi \right) , \quad \text{(A.21)}$$

$$\pi_\phi = \left( \dot{\phi} - N^i \nabla_i \phi + 2N\phi K \right) \frac{\sqrt{\gamma}}{N} . \quad \text{(A.22)}$$

Inversion (with appropriate regularization), insertion and the canonical redefinition $\pi_\phi \to \pi_\phi - \frac{2\phi\pi}{\phi^2+\epsilon^2}$ leads to the final action in ADM-form

$$S_{\mathrm{JF}} = \int d^4x \pi^{ij} \dot{\gamma}_{ij} + \pi_\phi \dot{\phi} + \frac{2\phi\pi}{\phi^2 + \epsilon^2} - N\mathcal{H} - N^i \mathcal{H}_i , \quad \text{(A.23)}$$

with

$$\mathcal{H} = - \frac{\phi^2 + \epsilon}{2}\sqrt{\gamma} R_\gamma + \frac{1}{\sqrt{\gamma}\left(\phi^2 + \epsilon^2\right)} \pi^{ij} \left( \gamma_{ik}\gamma_{jl} + \gamma_{il}\gamma_{jk} - \gamma_{ij}\gamma_{kl} \right) \pi^{kl} + \frac{1}{14\sqrt{\gamma}} \pi_\phi^2 + \frac{\sqrt{\gamma}}{2} \left( \nabla_i \phi \right)^2 + \sqrt{\gamma}\, V(\phi) + \sqrt{\gamma} \Delta \left( \phi^2 \right) , \quad \text{(A.24)}$$

$$\mathcal{H}_i = - 2\nabla^j \pi_{ij} + \left( \pi_\phi + \frac{2\phi\pi}{\phi^2 + \epsilon^2} \right) \nabla_i \phi , \quad \text{(A.25)}$$

From here, we can immediately read off the additional Jacobian factors that will enter the generating functional after integrating over the momenta. From the integration over $\pi^{ij}$, we obtain a factor of $\left(\phi^2 + \epsilon\right)^3$, while the integration over $\pi_\phi$ yields, apart from the metric determinant, only a numerical factor that can be absorbed into the overall normalization.

We are now in the exact same position as after Eq. (A.7). The corresponding redefinition that eliminates the Jacobian factor is

$$\gamma_{ij} = \frac{\phi^2 + \epsilon^2}{M_p^2} \tilde{\gamma}_{ij} , \quad \text{(A.26)}$$

where we have now introduced the Planck mass to keep track of the dimensions. However, in order to keep the covariance manifest, we should also redefine $N$ via $\tilde{N} = \frac{\sqrt{\phi^2+\epsilon}}{M_p} N$ ($N^i$ remains invariant under the corresponding rescaling). We thus obtain the full redefinition of the metric

$$g_{\mu\nu} = \frac{M_p^2}{\phi^2 + \epsilon^2} \tilde{g}_{\mu\nu} \,. \tag{A.27}$$

Not surprisingly, this corresponds to a Weyl rescaling. We are not yet done, though. The redefinition of $N$ has lead to an additional Jacobian determinant $\sim M_p/\sqrt{\phi^2+\epsilon^2}$, which we can only absorb if we also redefine the scalar field:

$$\frac{\delta\phi}{\delta\tilde{\phi}} = \frac{\sqrt{\phi^2+\epsilon^2}}{M_p} \,, \tag{A.28}$$

which integrates to

$$\phi = \frac{M_p}{2} \left( e^{\frac{\tilde{\phi}}{M_p}} - \frac{\epsilon^2}{M_p^2} e^{-\frac{\tilde{\phi}}{M_p}} \right) \tag{A.29}$$

This, however, is nothing but the redefinition of the scalar field to canonically normalize it after the Weyl rescaling. Henceforth, we have derived the Einstein frame action! After integration of all momenta, we obtain the generating functional

$$Z[J] = \int \mathcal{D}g_{\mu\nu} \mathcal{D}\tilde{\phi} e^{iS_{\rm EF}[g_{\mu\nu},\tilde{\phi}]} \,, \tag{A.30}$$

with

$$S_{\rm EF} = \int d^4x \sqrt{-g} \left[ \frac{M_p^2}{2} R - \frac{1}{2} \left( \partial_\mu \tilde{\phi} \right)^2 - U(\tilde{\phi}) \right] . \tag{A.31}$$

The potential $U(\tilde{\phi})$ is now a function of the Einstein frame field $\tilde{\phi}$:

$$U(\tilde{\phi}) = \frac{1}{\left( \phi^2 \left( \tilde{\phi} \right) + \epsilon \right)^2} V \left( \phi \left( \tilde{\phi} \right) \right) . \tag{A.32}$$

In particular, for $V(\phi) = \phi^k$ with $k \geq 4$, we can now take the limit $\epsilon \to 0$ and end up with a theory that we can happily quantize in the Feynman path integral.

# Bibliography


Georges Aad et al. Observation of a new particle in the search for the Standard Model Higgs boson with the ATLAS detector at the LHC. *Phys.Lett.*, B716:1–29, 2012. doi: 10.1016/j.physletb.2012.08.020.

L.R. Abramo, R.C. Batista, L. Liberato, and R. Rosenfeld. Structure formation in the presence of dark energy perturbations. *JCAP*, 0711:012, 2007. doi: 10.1088/1475-7516/2007/11/012.

Allan Adams, Nima Arkani-Hamed, Sergei Dubovsky, Alberto Nicolis, and Riccardo Rattazzi. Causality, analyticity and an IR obstruction to UV completion. *JHEP*, 0610:014, 2006. doi: 10.1088/1126-6708/2006/10/014.

P.A.R. Ade et al. Planck 2013 results. XXII. Constraints on inflation. 2013.

P.A.R. Ade et al. BICEP2 I: Detection Of B-mode Polarization at Degree Angular Scales. 2014a.

P.A.R. Ade et al. Detection of B-Mode Polarization at Degree Angular Scales by BICEP2. *Phys.Rev.Lett.*, 112:241101, 2014b. doi: 10.1103/PhysRevLett.112.241101.

Niayesh Afshordi, Matias Zaldarriaga, and Kazunori Kohri. On the stability of dark energy with mass-varying neutrinos. *Phys.Rev.*, D72:065024, 2005. doi: 10.1103/PhysRevD.72.065024.

Ahmed Almheiri, Donald Marolf, Joseph Polchinski, and James Sully. Black Holes: Complementarity or Firewalls? *JHEP*, 1302:062, 2013. doi: 10.1007/JHEP02(2013)062.

Alexander Altland and Fritz Haake. Quantum chaos and effective thermalization. *Physical Review Letters*, 108(7):073601, 2012.

L. Amendola. Coupled quintessence. *Phys. Rev. D*, page 043511, 2000.

Luca Amendola. Linear and non-linear perturbations in dark energy models. *Phys.Rev.*, D69:103524, 2004. doi: 10.1103/PhysRevD.69.103524.

Luca Amendola and Claudia Quercellini. Tracking and coupled dark energy as seen by WMAP. *Phys.Rev.*, D68:023514, 2003. doi: 10.1103/PhysRevD.68.023514.

Luca Amendola, Marco Baldi, and Christof Wetterich. Quintessence cosmologies with a growing matter component. *Phys.Rev.*, D78:023015, 2008. doi: 10.1103/PhysRevD.78.023015.

J. R. Anglin and A. Vardi. Dynamics of a two-mode bose-einstein condensate beyond mean-field theory. *Phys. Rev. A*, 64:013605, May 2001. doi: 10.1103/PhysRevA.64.013605. URL `http://link.aps.org/doi/10.1103/PhysRevA.64.013605`.

J. R. Anglin and W. H. Zurek. Decoherence of quantum fields: Pointer states and predictability. *Phys. Rev. D*, 53:7327–7335, June 1996. doi: 10.1103/PhysRevD.53.7327.

Christian Angrick and Matthias Bartelmann. Triaxial collapse and virialisation of dark-matter haloes. *Astron.Astrophys.*, 518:A38, 2010. doi: 10.1051/0004-6361/201014147.

Damiano Anselmi. Absence of higher derivatives in the renormalization of propagators in quantum field theories with infinitely many couplings. *Class.Quant.Grav.*, 20:2355–2378, 2003. doi: 10.1088/0264-9381/20/11/326.

Nima Arkani-Hamed, Savas Dimopoulos, and G.R. Dvali. The Hierarchy problem and new dimensions at a millimeter. *Phys.Lett.*, B429:263–272, 1998. doi: 10.1016/S0370-2693(98)00466-3.

Nima Arkani-Hamed, Howard Georgi, and Matthew D. Schwartz. Effective field theory for massive gravitons and gravity in theory space. *Annals Phys.*, 305:96–118, 2003. doi: 10.1016/S0003-4916(03)00068-X.

Nima Arkani-Hamed, Sergei Dubovsky, Alberto Nicolis, Enrico Trincherini, and Giovanni Villadoro. A Measure of de Sitter entropy and eternal inflation. *JHEP*, 0705:055, 2007. doi: 10.1088/1126-6708/2007/05/055.

C. Armendariz-Picon, Viatcheslav F. Mukhanov, and Paul J. Steinhardt. Essentials of k-essence. *Phys.Rev.*, D63:103510, 2001. doi: 10.1103/PhysRevD.63.103510.

Richard L. Arnowitt, Stanley Deser, and Charles W. Misner. Canonical variables for general relativity. *Phys.Rev.*, 117:1595–1602, 1960. doi: 10.1103/PhysRev.117.1595.

Richard L. Arnowitt, Stanley Deser, and Charles W. Misner. The Dynamics of general relativity. *Gen.Rel.Grav.*, 40:1997–2027, 2008. doi: 10.1007/s10714-008-0661-1.

Curtis Asplund, David Berenstein, and Diego Trancanelli. Evidence for fast thermalization in the plane-wave matrix model. *Phys.Rev.Lett.*, 107:171602, 2011. doi: 10.1103/PhysRevLett.107.171602.

Eugeny Babichev and Cédric Deffayet. An introduction to the Vainshtein mechanism. *Class.Quant.Grav.*, 30:184001, 2013. doi: 10.1088/0264-9381/30/18/184001.

Eugeny Babichev and Alessandro Fabbri. Instability of black holes in massive gravity. *Class.Quant.Grav.*, 30:152001, 2013. doi: 10.1088/0264-9381/30/15/152001.

Marco Baldi, Valeria Pettorino, Georg Robbers, and Volker Springel. Hydrodynamical N-body simulations of coupled dark energy cosmologies. *Mon.Not.Roy.Astron.Soc.*, 403:1684–1702, 2010. doi: 10.1111/j.1365-2966.2009.15987.x.

Tom Banks and Willy Fischler. A Model for high-energy scattering in quantum gravity. 1999.

Tom Banks, W. Fischler, S.H. Shenker, and Leonard Susskind. M theory as a matrix model: A Conjecture. *Phys.Rev.*, D55:5112–5128, 1997. doi: 10.1103/PhysRevD.55.5112.

Tom Banks, W. Fischler, Igor R. Klebanov, and Leonard Susskind. Schwarzschild black holes from matrix theory. *Phys.Rev.Lett.*, 80:226–229, 1998a. doi: 10.1103/PhysRevLett.80.226.

Tom Banks, W. Fischler, Igor R. Klebanov, and Leonard Susskind. Schwarzschild black holes in matrix theory. 2. *JHEP*, 9801:008, 1998b.

Jose L.F. Barbon and Javier M. Magan. Chaotic Fast Scrambling At Black Holes. *Phys.Rev.*, D84:106012, 2011. doi: 10.1103/PhysRevD.84.106012.

James M. Bardeen. Gauge Invariant Cosmological Perturbations. *Phys.Rev.*, D22:1882–1905, 1980. doi: 10.1103/PhysRevD.22.1882.

T. Barreiro, Edmund J. Copeland, and N.J. Nunes. Quintessence arising from exponential potentials. *Phys.Rev.*, D61:127301, 2000. doi: 10.1103/PhysRevD.61.127301.

Matthias Bartelmann, Michael Doran, and Christof Wetterich. Non-linear structure formation in cosmologies with early dark energy. *Astron.Astrophys.*, 454:27–36, 2006. doi: 10.1051/0004-6361:20053922.

Bruce A. Bassett, Shinji Tsujikawa, and David Wands. Inflation dynamics and reheating. *Rev.Mod.Phys.*, 78:537–589, 2006. doi: 10.1103/RevModPhys.78.537.

Sayandeb Basu and David Mattingly. Asymptotic Safety, Asymptotic Darkness, and the hoop conjecture in the extreme UV. *Phys.Rev.*, D82:124017, 2010. doi: 10.1103/PhysRevD.82.124017.

Rachel Bean, Eanna E. Flanagan, Istvan Laszlo, and Mark Trodden. Constraining Interactions in Cosmology's Dark Sector. *Phys.Rev.*, D78:123514, 2008. doi: 10.1103/PhysRevD.78.123514.

Niklas Beisert, Henriette Elvang, Daniel Z. Freedman, Michael Kiermaier, Alejandro Morales, et al. E7(7) constraints on counterterms in N=8 supergravity. *Phys.Lett.*, B694:265–271, 2010. doi: 10.1016/j.physletb.2010.09.069.

Jacob D. Bekenstein. Black holes and entropy. *Phys.Rev.*, D7:2333–2346, 1973. doi: 10.1103/PhysRevD.7.2333.

J.D. Bekenstein. Black holes and the second law. *Lett.Nuovo Cim.*, 4:737–740, 1972. doi: 10.1007/BF02757029.

Felix Berkhahn, Sophia Muller, Florian Niedermann, and Robert Schneider. Microscopic Picture of Non-Relativistic Classicalons. *JCAP*, 1308:028, 2013. doi: 10.1088/1475-7516/2013/08/028.

Z. Bern, J.J. Carrasco, Lance J. Dixon, H. Johansson, and R. Roiban. The Ultraviolet Behavior of N=8 Supergravity at Four Loops. *Phys.Rev.Lett.*, 103:081301, 2009. doi: 10.1103/PhysRevLett.103.081301.

Fedor L. Bezrukov and Mikhail Shaposhnikov. The Standard Model Higgs boson as the inflaton. *Phys.Lett.*, B659:703–706, 2008. doi: 10.1016/j.physletb.2007.11.072.

Neven Bilic, Robert J. Lindebaum, Gary B. Tupper, and Raoul D. Viollier. Nonlinear evolution of dark matter and dark energy in the Chaplygin-gas cosmology. *JCAP*, 0411:008, 2004. doi: 10.1088/1475-7516/2004/11/008.

G. D. Birkhoff and R. E. Langer. *Relativity and modern physics*. 1923.

Ole Eggers Bjaelde, Anthony W. Brookfield, Carsten van de Bruck, Steen Hannestad, David F. Mota, et al. Neutrino Dark Energy – Revisiting the Stability Issue. *JCAP*, 0801:026, 2008. doi: 10.1088/1475-7516/2008/01/026.

Christian G. Boehmer, Gabriela Caldera-Cabral, Ruth Lazkoz, and Roy Maartens. Dynamics of dark energy with a coupling to dark matter. *Phys.Rev.*, D78:023505, 2008. doi: 10.1103/PhysRevD.78.023505.

N.N. Bogoliubov. Kinetic equations. *Zhurnal Eksperimentalnoi i Teoreticheskoi Fiziki*, 16(8):691–702, 1946.

Nikolai Bogolyubov. On the theory of superfluidity. *J. Phys. (USSR)*, 11: 23, 1947.

B. Boisseau, Gilles Esposito-Farese, D. Polarski, and Alexei A. Starobinsky. Reconstruction of a scalar tensor theory of gravity in an accelerating universe. *Phys.Rev.Lett.*, 85:2236, 2000. doi: 10.1103/PhysRevLett.85.2236.

Max Born and HS Green. A general kinetic theory of liquids. i. the molecular distribution functions. *Proceedings of the Royal Society of London. Series A. Mathematical and Physical Sciences*, 188(1012):10–18, 1946.

S.N. Bose. Plancks gesetz und lichtquantenhypothese. *Zeitschrift für Physik*, 26(1):178–181, 1924. ISSN 0044-3328. doi: 10.1007/BF01327326. URL `http://dx.doi.org/10.1007/BF01327326`.

D.G. Boulware and Stanley Deser. Can gravitation have a finite range? *Phys.Rev.*, D6:3368–3382, 1972. doi: 10.1103/PhysRevD.6.3368.

Robert H. Brandenberger. Quantum Field Theory Methods and Inflationary Universe Models. *Rev.Mod.Phys.*, 57:1, 1985. doi: 10.1103/RevModPhys.57.1.

Anthony W. Brookfield, C. van de Bruck, D.F. Mota, and D. Tocchini-Valentini. Cosmology of mass-varying neutrinos driven by quintessence: theory and observations. *Phys.Rev.*, D73:083515, 2006a. doi: 10.1103/PhysRevD.73.083515,10.1103/PhysRevD.76.049901.

A.W. Brookfield, Carsten van de Bruck, D.F. Mota, and D. Tocchini-Valentini. Cosmology with massive neutrinos coupled to dark energy. *Phys.Rev.Lett.*, 96:061301, 2006b. doi: 10.1103/PhysRevLett.96.061301.

N. Brouzakis, N. Tetradis, and C. Wetterich. Neutrino Lumps in Quintessence Cosmology. *Phys.Lett.*, B665:131–134, 2008. doi: 10.1016/j.physletb.2008.05.068.

N. Brouzakis, A. Codello, N. Tetradis, and O. Zanusso. Quantum corrections in Galileon theories. 2013.

R. Brustein, G. Dvali, and G. Veneziano. A Bound on the effective gravitational coupling from semiclassical black holes. *JHEP*, 0910:085, 2009. doi: 10.1088/1126-6708/2009/10/085.

Ram Brustein and A.J.M. Medved. Restoring predictability in semiclassical gravitational collapse. *JHEP*, 1309:015, 2013a. doi: 10.1007/JHEP09(2013)015.

Ram Brustein and A.J.M. Medved. Semiclassical black holes expose forbidden charges and censor divergent densities. *JHEP*, 1309:108, 2013b. doi: 10.1007/JHEP09(2013)108.

Clare Burrage, Claudia de Rham, Lavinia Heisenberg, and Andrew J. Tolley. Chronology Protection in Galileon Models and Massive Gravity. *JCAP*, 1207:004, 2012. doi: 10.1088/1475-7516/2012/07/004.

Pasquale Calabrese and John L. Cardy. Evolution of entanglement entropy in one-dimensional systems. *J.Stat.Mech.*, 0504:P04010, 2005. doi: 10.1088/1742-5468/2005/04/P04010.

Pasquale Calabrese and John L. Cardy. Time-dependence of correlation functions following a quantum quench. *Phys.Rev.Lett.*, 96:136801, 2006. doi: 10.1103/PhysRevLett.96.136801.

John L. Cardy. Operator Content of Two-Dimensional Conformally Invariant Theories. *Nucl.Phys.*, B270:186–204, 1986. doi: 10.1016/0550-3213(86)90552-3.

L. D. Carr, Charles W. Clark, and W. P. Reinhardt. Stationary solutions of the one-dimensional nonlinear schrödinger equation. ii. case of attractive nonlinearity. *Phys. Rev. A*, 62:063611, Nov 2000. doi: 10.1103/PhysRevA.62.063611. URL `http://link.aps.org/doi/10.1103/PhysRevA.62.063611`.

Roberto Casadio and Fabio Scardigli. Horizon wave-function for single localized particles: GUP and quantum black hole decay. *Eur.Phys.J.*, C74: 2685, 2014. doi: 10.1140/epjc/s10052-013-2685-2.

Y. Castin and R. Dum. Low-temperature bose-einstein condensates in time-dependent traps: Beyond the $u(1)$ symmetry-breaking approach. *Phys. Rev. A*, 57:3008–3021, Apr 1998. doi: 10.1103/PhysRevA.57.3008. URL `http://link.aps.org/doi/10.1103/PhysRevA.57.3008`.

CERN. CERN Announces LHC Restart Schedule, June 2014. URL `http://press.web.cern.ch/press-releases/2014/06/cern-announces-lhc-restart-schedule`.

Michael S. Chanowitz and Mary K. Gaillard. The tev physics of strongly interacting w's and z's. *Nuclear Physics B*, 261(0):379 – 431, 1985. ISSN 0550-3213. doi: http://dx.doi.org/10.1016/0550-3213(85)90580-2. URL `http://www.sciencedirect.com/science/article/pii/0550321385905802`.

Serguei Chatrchyan et al. Observation of a new boson at a mass of 125 GeV with the CMS experiment at the LHC. *Phys.Lett.*, B716:30–61, 2012. doi: 10.1016/j.physletb.2012.08.021.

A. Codello, N. Tetradis, and O. Zanusso. The renormalization of fluctuating branes, the Galileon and asymptotic safety. *JHEP*, 1304:036, 2013. doi: 10.1007/JHEP04(2013)036.

Edmund J. Copeland, Andrew R Liddle, and David Wands. Exponential potentials and cosmological scaling solutions. *Phys.Rev.*, D57:4686–4690, 1998. doi: 10.1103/PhysRevD.57.4686.

Edmund J. Copeland, M. Sami, and Shinji Tsujikawa. Dynamics of dark energy. *Int.J.Mod.Phys.*, D15:1753–1936, 2006. doi: 10.1142/S021827180600942X.

Paolo Creminelli, Alberto Nicolis, Michele Papucci, and Enrico Trincherini. Ghosts in massive gravity. *JHEP*, 0509:003, 2005. doi: 10.1088/1126-6708/2005/09/003.

Paolo Creminelli, Guido D'Amico, Jorge Norena, Leonardo Senatore, and Filippo Vernizzi. Spherical collapse in quintessence models with zero speed of sound. *JCAP*, 1003:027, 2010. doi: 10.1088/1475-7516/2010/03/027.

F. Dalfovo, L.P. Pitaevskii, and S. Stringari. Bose–einstein condensates. In Jean-Pierre Françoise, Gregory L. Naber, and Tsou Sheung Tsun, editors, *Encyclopedia of Mathematical Physics*, pages 312 – 318. Academic Press, Oxford, 2006. ISBN 978-0-12-512666-3. doi: http://dx.doi.org/10.1016/B0-12-512666-2/00375-8. URL `http://www.sciencedirect.com/science/article/pii/B0125126662003758`.

Franco Dalfovo, Stefano Giorgini, Lev P. Pitaevskii, and Sandro Stringari. Theory of bose-einstein condensation in trapped gases. *Rev. Mod. Phys.*, 71:463–512, Apr 1999. doi: 10.1103/RevModPhys.71.463. URL `http://link.aps.org/doi/10.1103/RevModPhys.71.463`.

Iannis Dalianis and Fotis Farakos. Higher Derivative D-term Inflation in New-minimal Supergravity. 2014.

Antonio De Felice, A. Emir Gumrukcuoglu, and Shinji Mukohyama. Massive gravity: nonlinear instability of the homogeneous and isotropic universe. *Phys.Rev.Lett.*, 109:171101, 2012. doi: 10.1103/PhysRevLett.109.171101.

Paul de Fromont, Claudia de Rham, Lavinia Heisenberg, and Andrew Matas. Superluminality in the Bi- and Multi- Galileon. *JHEP*, 1307:067, 2013. doi: 10.1007/JHEP07(2013)067.

Tiberio de Paula Netto and Ilya L. Shapiro. One-loop divergences in the Galileon model. *Phys.Lett.*, B716:454–460, 2012. doi: 10.1016/j.physletb.2012.08.056.

Claudia de Rham. Massive Gravity. 2014.

Claudia de Rham and Raquel H. Ribeiro. Riding on irrelevant operators. 2014.

Claudia de Rham, Stefan Hofmann, Justin Khoury, and Andrew J. Tolley. Cascading Gravity and Degravitation. *JCAP*, 0802:011, 2008. doi: 10.1088/1475-7516/2008/02/011.

Claudia de Rham, Gregory Gabadadze, Lavinia Heisenberg, and David Pirtskhalava. Cosmic Acceleration and the Helicity-0 Graviton. *Phys.Rev.*, D83:103516, 2011a. doi: 10.1103/PhysRevD.83.103516.

Claudia de Rham, Gregory Gabadadze, and Andrew J. Tolley. Resummation of Massive Gravity. *Phys.Rev.Lett.*, 106:231101, 2011b. doi: 10.1103/PhysRevLett.106.231101.

Claudia de Rham, Gregory Gabadadze, and Andrew J. Tolley. Helicity Decomposition of Ghost-free Massive Gravity. *JHEP*, 1111:093, 2011c. doi: 10.1007/JHEP11(2011)093.

Claudia de Rham, Gregory Gabadadze, and Andrew J. Tolley. Ghost free Massive Gravity in the Stúckelberg language. *Phys.Lett.*, B711:190–195, 2012. doi: 10.1016/j.physletb.2012.03.081.

Claudia de Rham, Gregory Gabadadze, Lavinia Heisenberg, and David Pirtskhalava. Nonrenormalization and naturalness in a class of scalar-tensor theories. *Phys.Rev.*, D87(8):085017, 2013a. doi: 10.1103/PhysRevD.87.085017.

Claudia de Rham, Lavinia Heisenberg, and Raquel H. Ribeiro. Quantum Corrections in Massive Gravity. *Phys.Rev.*, D88:084058, 2013b. doi: 10.1103/PhysRevD.88.084058.

Cedric Deffayet and Jan-Willem Rombouts. Ghosts, strong coupling and accidental symmetries in massive gravity. *Phys.Rev.*, D72:044003, 2005. doi: 10.1103/PhysRevD.72.044003.

Cedric Deffayet, G.R. Dvali, Gregory Gabadadze, and Arkady I. Vainshtein. Nonperturbative continuity in graviton mass versus perturbative discontinuity. *Phys.Rev.*, D65:044026, 2002. doi: 10.1103/PhysRevD.65.044026.

Giuseppe Degrassi, Stefano Di Vita, Joan Elias-Miro, Jose R. Espinosa, Gian F. Giudice, et al. Higgs mass and vacuum stability in the Standard Model at NNLO. *JHEP*, 1208:098, 2012. doi: 10.1007/JHEP08(2012)098.

S. Deser and A. Waldron. Acausality of Massive Gravity. *Phys.Rev.Lett.*, 110(11):111101, 2013. doi: 10.1103/PhysRevLett.110.111101.

S. Deser, K. Izumi, Y.C. Ong, and A. Waldron. Massive Gravity Acausality Redux. *Phys.Lett.*, B726:544–548, 2013a. doi: 10.1016/j.physletb.2013.09.001.

S. Deser, K. Izumi, Y.C. Ong, and A. Waldron. Superluminal Propagation and Acausality of Nonlinear Massive Gravity. 2013b.

Stanley Deser. Selfinteraction and gauge invariance. *Gen.Rel.Grav.*, 1:9–18, 1970. doi: 10.1007/BF00759198.

Bryce S. DeWitt. Quantum theory of gravity. ii. the manifestly covariant theory. *Phys. Rev.*, 162:1195–1239, Oct 1967. doi: 10.1103/PhysRev.162.1195. URL `http://link.aps.org/doi/10.1103/PhysRev.162.1195`.

P.A.M. Dirac. *Lectures on Quantum Mechanics*. Belfer Graduate School of Science, monograph series. Dover Publications, 2001. ISBN 9780486417134. URL `http://books.google.de/books?id=GVwzb1rZW9kC`.

Michael Doran, Georg Robbers, and Christof Wetterich. Impact of three years of data from the Wilkinson Microwave Anisotropy Probe on cosmological models with dynamical dark energy. *Phys.Rev.*, D75:023003, 2007. doi: 10.1103/PhysRevD.75.023003.

S. Dubovsky, T. Gregoire, A. Nicolis, and R. Rattazzi. Null energy condition and superluminal propagation. *JHEP*, 0603:025, 2006. doi: 10.1088/1126-6708/2006/03/025.

R. A. Duine and H. T. Stoof. Explosion of a Collapsing Bose-Einstein Condensate. *Phys. Rev. Lett.*, 86:2204, March 2001. doi: 10.1103/PhysRevLett.86.2204.

R. A. Duine and H. T. Stoof. Stochastic dynamics of a trapped Bose-Einstein condensate. *Phys. Rev. A*, 65(1):013603, January 2002. doi: 10.1103/PhysRevA.65.013603.

Sourish Dutta and Irit Maor. Voids of dark energy. *Phys.Rev.*, D75:063507, 2007. doi: 10.1103/PhysRevD.75.063507.

Gia Dvali. Predictive Power of Strong Coupling in Theories with Large Distance Modified Gravity. *New J.Phys.*, 8:326, 2006. doi: 10.1088/1367-2630/8/12/326.

Gia Dvali. Classicalize or not to Classicalize? 2011.

Gia Dvali and Cesar Gomez. Self-Completeness of Einstein Gravity. 2010.

Gia Dvali and Cesar Gomez. Black Hole's Quantum N-Portrait. 2011.

Gia Dvali and Cesar Gomez. Black Holes as Critical Point of Quantum Phase Transition. 2012a.

Gia Dvali and Cesar Gomez. Landau-Ginzburg Limit of Black Hole's Quantum Portrait: Self Similarity and Critical Exponent. *Phys.Lett.*, B716: 240–242, 2012b. doi: 10.1016/j.physletb.2012.08.019.

Gia Dvali and Cesar Gomez. Black Hole Macro-Quantumness. 2012c.

Gia Dvali and Cesar Gomez. Black Hole's 1/N Hair. *Phys.Lett.*, B719:419–423, 2013a. doi: 10.1016/j.physletb.2013.01.020.

Gia Dvali and Cesar Gomez. Quantum Compositeness of Gravity: Black Holes, AdS and Inflation. 2013b.

Gia Dvali and Cesar Gomez. BICEP2 in Corpuscular Description of Inflation. 2014.

Gia Dvali, Stefan Hofmann, and Justin Khoury. Degravitation of the cosmological constant and graviton width. *Phys.Rev.*, D76:084006, 2007. doi: 10.1103/PhysRevD.76.084006.

Gia Dvali, Oriol Pujolas, and Michele Redi. Non Pauli-Fierz Massive Gravitons. *Phys.Rev.Lett.*, 101:171303, 2008. doi: 10.1103/PhysRevLett.101.171303.

Gia Dvali, Sarah Folkerts, and Cristiano Germani. Physics of Trans-Planckian Gravity. *Phys.Rev.*, D84:024039, 2011a. doi: 10.1103/PhysRevD.84.024039.

Gia Dvali, Gian F. Giudice, Cesar Gomez, and Alex Kehagias. UV-Completion by Classicalization. *JHEP*, 1108:108, 2011b. doi: 10.1007/JHEP08(2011)108.

Gia Dvali, Cesar Gomez, and Alex Kehagias. Classicalization of Gravitons and Goldstones. *JHEP*, 1111:070, 2011c. doi: 10.1007/JHEP11(2011)070.

Gia Dvali, Andre Franca, and Cesar Gomez. Road Signs for UV-Completion. 2012.

Gia Dvali, Daniel Flassig, Cesar Gomez, Alexander Pritzel, and Nico Wintergerst. Scrambling in the Black Hole Portrait. *Phys.Rev.*, D88(12):124041, 2013. doi: 10.1103/PhysRevD.88.124041.

G.R. Dvali, Gregory Gabadadze, and Massimo Porrati. 4-D gravity on a brane in 5-D Minkowski space. *Phys.Lett.*, B485:208–214, 2000. doi: 10.1016/S0370-2693(00)00669-9.

Douglas M. Eardley and Steven B. Giddings. Classical black hole production in high-energy collisions. *Phys.Rev.*, D66:044011, 2002. doi: 10.1103/PhysRevD.66.044011.

P. Ehrenfest. Bemerkung über die angenäherte gültigkeit der klassischen mechanik innerhalb der quantenmechanik. *Zeitschrift für Physik*, 45(7-8): 455–457, 1927. ISSN 0044-3328. doi: 10.1007/BF01329203. URL `http://dx.doi.org/10.1007/BF01329203`.

A. Einstein. Quantentheorie des einatomigen idealen gases. *Sitzungsberichte der Preussischen Akademie der Wissenschaften*, 1(3), 1925.

Albert Einstein. The Foundation of the General Theory of Relativity. *Annalen Phys.*, 49:769–822, 1916. doi: 10.1002/andp.200590044.

Sunu Engineer, Nissim Kanekar, and T. Padmanabhan. Nonlinear density evolution from an improved spherical collapse model. *Mon.Not.Roy.Astron.Soc.*, 314:279, 2000. doi: 10.1046/j.1365-8711.2000.03275.x.

Fotis Farakos, Cristiano Germani, Alex Kehagias, and Emmanuel N. Saridakis. A New Class of Four-Dimensional N=1 Supergravity with Nonminimal Derivative Couplings. *JHEP*, 1205:050, 2012. doi: 10.1007/JHEP05(2012)050.

Valerio Faraoni. Inflation and quintessence with nonminimal coupling. *Phys.Rev.*, D62:023504, 2000. doi: 10.1103/PhysRevD.62.023504.

Rob Fardon, Ann E. Nelson, and Neal Weiner. Dark energy from mass varying neutrinos. *JCAP*, 0410:005, 2004. doi: 10.1088/1475-7516/2004/10/005.

Pedro G. Ferreira and Michael Joyce. Cosmology with a primordial scaling field. *Phys.Rev.*, D58:023503, 1998. doi: 10.1103/PhysRevD.58.023503.

M. Fierz and W. Pauli. On relativistic wave equations for particles of arbitrary spin in an electromagnetic field. *Proc.Roy.Soc.Lond.*, A173:211–232, 1939. doi: 10.1098/rspa.1939.0140.

D. Flassig, A. Pritzel, and N. Wintergerst. Black Holes and Quantumness on Macroscopic Scales. *Phys.Rev.*, D87:084007, 2013. doi: 10.1103/PhysRevD.87.084007.

Stefan Floerchinger and Nico Wintergerst. On Renormalization Group Flows in Scalar O(N) models with Shift Symmetry, Work in Progress. 2014.

Valentino Foit, Sarah Folkerts, and Nico Wintergerst. Hawking evaporation in the Black Hole Portrait, Work in Progress. 2014.

Sarah Folkerts, Alexander Pritzel, and Nico Wintergerst. On ghosts in theories of self-interacting massive spin-2 particles. 2011.

Sarah Folkerts, Cristiano Germani, and Nico Wintergerst. Massive spin-2 theories. *Cosmology and Particle Physics beyond Standard Models: Ten Years of the SEENET-MTP Network*, pages 87–97, 2014.

Matthew J. Francis, Geraint F. Lewis, and Eric V. Linder. Halo Mass Functions in Early Dark Energy Cosmologies. *Mon.Not.Roy.Astron.Soc.Lett.*, 393:L31–L35, 2008. doi: 10.1111/j.1745-3933.2008.00592.x.

Marcel Froissart. Asymptotic behavior and subtractions in the Mandelstam representation. *Phys.Rev.*, 123:1053–1057, 1961. doi: 10.1103/PhysRev.123.1053.

G. Miele G. Mangano and V. Pettorino. Coupled quintessence and the coincidence problem. *Mod. Phys. Lett. A*, page 831, 2003.

M. Gell-Mann and M. Lévy. The axial vector current in beta decay. *Il Nuovo Cimento*, 16(4):705–726, 1960. ISSN 0029-6341. doi: 10.1007/BF02859738. URL `http://dx.doi.org/10.1007/BF02859738`.

Cristiano Germani. On the Covariant Galileon and a consistent self-accelerating Universe. *Phys.Rev.*, D86:104032, 2012a. doi: 10.1103/PhysRevD.86.104032.

Cristiano Germani. Spontaneous localization on a brane via a gravitational mechanism. *Phys.Rev.*, D85:055025, 2012b. doi: 10.1103/PhysRevD.85.055025.

Cristiano Germani. Slow Roll Inflation: A Somehow Different Perspective. *Rom.J.Phys.*, 57:841–848, 2012c.

Cristiano Germani and Alex Kehagias. Cosmological Perturbations in the New Higgs Inflation. *JCAP*, 1005:019, 2010a. doi: 10.1088/1475-7516/2010/05/019,10.1088/1475-7516/2010/06/E01.

Cristiano Germani and Alex Kehagias. New Model of Inflation with Non-minimal Derivative Coupling of Standard Model Higgs Boson to Gravity. *Phys.Rev.Lett.*, 105:011302, 2010b. doi: 10.1103/PhysRevLett.105.011302.

Cristiano Germani and Yuki Watanabe. UV-protected (Natural) Inflation: Primordial Fluctuations and non-Gaussian Features. *JCAP*, 1107:031, 2011. doi: 10.1088/1475-7516/2011/07/031,10.1088/1475-7516/2011/07/A01.

Cristiano Germani, Luca Martucci, and Parvin Moyassari. Introducing the Slotheon: a slow Galileon scalar field in curved space-time. *Phys.Rev.*, D85:103501, 2012. doi: 10.1103/PhysRevD.85.103501.

Cristiano Germani, Yuki Watanabe, and Nico Wintergerst. Self-unitarization of New Higgs Inflation and compatibility with Planck and BICEP2 data. 2014.

Steven B. Giddings. The gravitational S-matrix: Erice lectures. 2011.

Michael B. Green, Jorge G. Russo, and Pierre Vanhove. Ultraviolet properties of maximal supergravity. *Phys.Rev.Lett.*, 98:131602, 2007. doi: 10.1103/PhysRevLett.98.131602.

Lukas Gruending, Stefan Hofmann, Sophia Müller, and Tehseen Rug. Probing the Constituent Structure of Black Holes. 2014.

Andrei Gruzinov. All Fierz-Paulian massive gravity theories have ghosts or superluminal modes. 2011.

James E. Gunn and III Gott, J. Richard. On the Infall of Matter into Clusters of Galaxies and Some Effects on Their Evolution. *Astrophys.J.*, 176:1–19, 1972. doi: 10.1086/151605.

Alan H. Guth. The Inflationary Universe: A Possible Solution to the Horizon and Flatness Problems. *Phys.Rev.*, D23:347–356, 1981. doi: 10.1103/PhysRevD.23.347.

S.F. Hassan and Rachel A. Rosen. Confirmation of the Secondary Constraint and Absence of Ghost in Massive Gravity and Bimetric Gravity. *JHEP*, 1204:123, 2012a. doi: 10.1007/JHEP04(2012)123.

S.F. Hassan and Rachel A. Rosen. Resolving the Ghost Problem in non-Linear Massive Gravity. *Phys.Rev.Lett.*, 108:041101, 2012b. doi: 10.1103/PhysRevLett.108.041101.

Stephen W Hawking. *The large scale structure of space-time*, volume 1. Cambridge university press, 1973.

S.W. Hawking. Black hole explosions. *Nature*, 248:30–31, 1974. doi: 10.1038/248030a0.

S.W. Hawking. Particle Creation by Black Holes. *Commun.Math.Phys.*, 43:199–220, 1975. doi: 10.1007/BF02345020.

S.W. Hawking. Breakdown of Predictability in Gravitational Collapse. *Phys.Rev.*, D14:2460–2473, 1976. doi: 10.1103/PhysRevD.14.2460.

S.W. Hawking. Information loss in black holes. *Phys.Rev.*, D72:084013, 2005. doi: 10.1103/PhysRevD.72.084013.

Patrick Hayden and John Preskill. Black holes as mirrors: Quantum information in random subsystems. *JHEP*, 0709:120, 2007. doi: 10.1088/1126-6708/2007/09/120.

L. Henderson and V. Vedral. Classical, quantum and total correlations. *Journal of Physics A Mathematical General*, 34:6899–6905, September 2001. doi: 10.1088/0305-4470/34/35/315.

M. Henneaux and C. Teitelboim. *Quantization of Gauge Systems*. Princeton paperbacks. Princeton University Press, 1992. ISBN 9780691037691. URL `http://books.google.de/books?id=2FAuAKEKFyYC`.

Kurt Hinterbichler. Theoretical Aspects of Massive Gravity. *Rev.Mod.Phys.*, 84:671–710, 2012. doi: 10.1103/RevModPhys.84.671.

Kurt Hinterbichler. Ghost-Free Derivative Interactions for a Massive Graviton. *JHEP*, 1310:102, 2013. doi: 10.1007/JHEP10(2013)102.

Kurt Hinterbichler and Justin Khoury. Symmetron Fields: Screening Long-Range Forces Through Local Symmetry Restoration. *Phys.Rev.Lett.*, 104:231301, 2010. doi: 10.1103/PhysRevLett.104.231301.

Kurt Hinterbichler, Mark Trodden, and Daniel Wesley. Multi-field galileons and higher co-dimension branes. *Phys.Rev.*, D82:124018, 2010. doi: 10.1103/PhysRevD.82.124018.

Stefan Hofmann and Tehseen Rug. A Quantum Bound State Description of Black Holes. 2014.

J.C. Hwang. Cosmological perturbations in generalized gravity theories: Formulation. *Class.Quant.Grav.*, 7:1613–1631, 1990a. doi: 10.1088/0264-9381/7/9/013.

J.C. Hwang. Cosmological perturbations in generalized gravity theories: Solutions. *Phys.Rev.*, D42:2601–2606, 1990b. doi: 10.1103/PhysRevD.42.2601.

Jorg Tofte Jebsen. *Über die allgemeinen kugelsymmetrischen Lösungen der Einstein'schen Gravitationsgleichungen im Vakuum*. Almqvist & Wiksell, 1921.

Renata Kallosh. $E_{7(7)}$ Symmetry and Finiteness of N=8 Supergravity. *JHEP*, 1203:083, 2012. doi: 10.1007/JHEP03(2012)083.

Kohei Kamada, Tsutomu Kobayashi, Tomo Takahashi, Masahide Yamaguchi, and Jun'ichi Yokoyama. Generalized Higgs inflation. *Phys.Rev.*, D86:023504, 2012. doi: 10.1103/PhysRevD.86.023504.

Alex Kamenev. *Field theory of non-equilibrium systems*. Cambridge University Press, 2011.

R. Kanamoto, H. Saito, and M. Ueda. Quantum phase transition in one-dimensional Bose-Einstein condensates with attractive interactions. *Phys. Rev. A*, 67(1):013608, January 2003. doi: 10.1103/PhysRevA.67.013608.

Rina Kanamoto, Hiroki Saito, and Masahito Ueda. Quantum phase transition in one-dimensional bose-einstein condensates with attractive interactions. *Phys. Rev. A*, 67:013608, Jan 2003. doi: 10.1103/PhysRevA.67.013608. URL `http://link.aps.org/doi/10.1103/PhysRevA.67.013608`.

D. Kazanas. Dynamics of the Universe and Spontaneous Symmetry Breaking. *Astrophys.J.*, 241:L59–L63, 1980. doi: 10.1086/183361.

Alex Kehagias and Antonio Riotto. Remarks about the Tensor Mode Detection by the BICEP2 Collaboration and the Super-Planckian Excursions of the Inflaton Field. *Phys.Rev.*, D89:101301, 2014. doi: 10.1103/PhysRevD.89.101301.

Alex Kehagias, Azadeh Moradinezhad Dizgah, and Antonio Riotto. Comments on the Starobinsky Model of Inflation and its Descendants. *Phys.Rev.*, D89:043527, 2014. doi: 10.1103/PhysRevD.89.043527.

LV Keldysh. Diagram technique for nonequilibrium processes. *Sov. Phys. JETP*, 20(4):1018–1026, 1965.

Justin Khoury and Amanda Weltman. Chameleon cosmology. *Phys.Rev.*, D69:044026, 2004. doi: 10.1103/PhysRevD.69.044026.

John G Kirkwood. The statistical mechanical theory of transport processes i. general theory. *The Journal of Chemical Physics*, 14(3):180–201, 1946.

John G Kirkwood. The statistical mechanical theory of transport processes ii. transport in gases. *The Journal of Chemical Physics*, 15(1):72–76, 1947.

Tsutomu Kobayashi, Masahide Yamaguchi, and Jun'ichi Yokoyama. Generalized G-inflation: Inflation with the most general second-order field equations. *Prog.Theor.Phys.*, 126:511–529, 2011. doi: 10.1143/PTP.126.511.

Hideo Kodama and Misao Sasaki. Cosmological Perturbation Theory. *Prog.Theor.Phys.Suppl.*, 78:1–166, 1984. doi: 10.1143/PTPS.78.1.

Lev Kofman, Andrei D. Linde, and Alexei A. Starobinsky. Reheating after inflation. *Phys.Rev.Lett.*, 73:3195–3198, 1994. doi: 10.1103/PhysRevLett.73.3195.

Ian I. Kogan, Stavros Mouslopoulos, and Antonios Papazoglou. The m -¿ 0 limit for massive graviton in dS(4) and AdS(4): How to circumvent the van Dam-Veltman-Zakharov discontinuity. *Phys.Lett.*, B503:173–180, 2001. doi: 10.1016/S0370-2693(01)00209-X.

Zohar Komargodski and Adam Schwimmer. On Renormalization Group Flows in Four Dimensions. *JHEP*, 1112:099, 2011. doi: 10.1007/JHEP12(2011)099.

E. Komatsu et al. Seven-Year Wilkinson Microwave Anisotropy Probe (WMAP) Observations: Cosmological Interpretation. *Astrophys.J.Suppl.*, 192:18, 2011. doi: 10.1088/0067-0049/192/2/18.

Florian Kuhnel. Instability of certain bimetric and massive-gravity theories. *Phys.Rev.*, D88(6):064024, 2013. doi: 10.1103/PhysRevD.88.064024.

Marek Kuś, Fritz Haake, and Dominique Delande. Prebifurcation periodic ghost orbits in semiclassical quantization. *Phys. Rev. Lett.*, 71(14):2167, 1993.

G. La Vacca, J.R. Kristiansen, L.P.L. Colombo, R. Mainini, and S.A. Bonometto. Do WMAP data favor neutrino mass and a coupling between Cold Dark Matter and Dark Energy? *JCAP*, 0904:007, 2009. doi: 10.1088/1475-7516/2009/04/007.

Nima Lashkari, Douglas Stanford, Matthew Hastings, Tobias Osborne, and Patrick Hayden. Towards the Fast Scrambling Conjecture. *JHEP*, 1304:022, 2013. doi: 10.1007/JHEP04(2013)022.

T. D. Lee and C. N. Yang. Many-body problem in quantum mechanics and quantum statistical mechanics. *Phys. Rev.*, 105:1119–1120, Feb 1957. doi: 10.1103/PhysRev.105.1119. URL `http://link.aps.org/doi/10.1103/PhysRev.105.1119`.

T. D. Lee, Kerson Huang, and C. N. Yang. Eigenvalues and eigenfunctions of a bose system of hard spheres and its low-temperature properties. *Phys. Rev.*, 106:1135–1145, Jun 1957. doi: 10.1103/PhysRev.106.1135. URL `http://link.aps.org/doi/10.1103/PhysRev.106.1135`.

Andrei D. Linde. Phase Transitions in Gauge Theories and Cosmology. *Rept.Prog.Phys.*, 42:389, 1979. doi: 10.1088/0034-4885/42/3/001.

Andrei D. Linde. A New Inflationary Universe Scenario: A Possible Solution of the Horizon, Flatness, Homogeneity, Isotropy and Primordial Monopole Problems. *Phys.Lett.*, B108:389–393, 1982. doi: 10.1016/0370-2693(82)91219-9.

Andrei D. Linde. Chaotic Inflation. *Phys.Lett.*, B129:177–181, 1983. doi: 10.1016/0370-2693(83)90837-7.

Andrei D. Linde. The Inflationary Universe. *Rept.Prog.Phys.*, 47:925–986, 1984. doi: 10.1088/0034-4885/47/8/002.

Andrei D. Linde. Particle physics and inflationary cosmology. *Contemp.Concepts Phys.*, 5:1–362, 1990.

Markus A. Luty, Massimo Porrati, and Riccardo Rattazzi. Strong interactions and stability in the DGP model. *JHEP*, 0309:029, 2003a. doi: 10.1088/1126-6708/2003/09/029.

Markus A. Luty, Massimo Porrati, and Riccardo Rattazzi. Strong interactions and stability in the DGP model. *JHEP*, 0309:029, 2003b. doi: 10.1088/1126-6708/2003/09/029.

David H. Lyth. What would we learn by detecting a gravitational wave signal in the cosmic microwave background anisotropy? *Phys.Rev.Lett.*, 78:1861–1863, 1997. doi: 10.1103/PhysRevLett.78.1861.

David H. Lyth and Antonio Riotto. Particle physics models of inflation and the cosmological density perturbation. *Phys.Rept.*, 314:1–146, 1999. doi: 10.1016/S0370-1573(98)00128-8.

Chung-Pei Ma and Edmund Bertschinger. Cosmological perturbation theory in the synchronous and conformal Newtonian gauges. *Astrophys.J.*, 455: 7–25, 1995. doi: 10.1086/176550.

Andrea V. Maccio, Claudia Quercellini, Roberto Mainini, Luca Amendola, and Silvio A. Bonometto. N-body simulations for coupled dark energy: Halo mass function and density profiles. *Phys.Rev.*, D69:123516, 2004. doi: 10.1103/PhysRevD.69.123516.

R. Mainini, Andrea V. Maccio, S.A. Bonometto, and A. Klypin. Modeling dynamical dark energy. *Astrophys.J.*, 599:24–30, 2003. doi: 10.1086/379236.

Roberto Mainini and Silvio Bonometto. Mass functions in coupled Dark Energy models. *Phys.Rev.*, D74:043504, 2006. doi: 10.1103/PhysRevD.74.043504.

Juan Martin Maldacena. The Large N limit of superconformal field theories and supergravity. *Adv.Theor.Math.Phys.*, 2:231–252, 1998.

Juan Martin Maldacena. Non-Gaussian features of primordial fluctuations in single field inflationary models. *JHEP*, 0305:013, 2003a. doi: 10.1088/1126-6708/2003/05/013.

Juan Martin Maldacena. Eternal black holes in anti-de Sitter. *JHEP*, 0304: 021, 2003b. doi: 10.1088/1126-6708/2003/04/021.

Irit Maor and Ofer Lahav. On virialization with dark energy. *JCAP*, 0507: 003, 2005. doi: 10.1088/1475-7516/2005/07/003.

Sabino Matarrese, Carlo Baccigalupi, and Francesca Perrotta. Approaching lambda without fine - tuning. *Phys.Rev.*, D70:061301, 2004. doi: 10.1103/PhysRevD.70.061301.

Samir D. Mathur. The Fuzzball proposal for black holes: An Elementary review. *Fortsch.Phys.*, 53:793–827, 2005. doi: 10.1002/prop.200410203.

J. Michell. On the Means of Discovering the Distance, Magnitude, [...]. In a Letter to Henry Cavendish, Esq. F. R. S. and A. S. *Royal Society of London Philosophical Transactions Series I*, 74:35–57, 1784.

Charles W Misner and John Archibald Wheeler. *Gravitation*. Macmillan, 1973.

David F. Mota, Douglas J. Shaw, and Joseph Silk. On the Magnitude of Dark Energy Voids and Overdensities. *Astrophys.J.*, 675:29–48, 2008a. doi: 10.1086/524401.

D.F. Mota and C. van de Bruck. On the Spherical collapse model in dark energy cosmologies. *Astron.Astrophys.*, 421:71–81, 2004. doi: 10.1051/0004-6361:20041090.

D.F. Mota, V. Pettorino, G. Robbers, and C. Wetterich. Neutrino clustering in growing neutrino quintessence. *Phys.Lett.*, B663:160–164, 2008b. doi: 10.1016/j.physletb.2008.03.060.

V.F. Mukhanov. Physical foundations of cosmology. 2005. URL `http://books.google.de/books?id=1TXO7GmwZFgC`.

Viatcheslav F. Mukhanov and G. V. Chibisov. Quantum Fluctuation and Nonsingular Universe. (In Russian). *JETP Lett.*, 33:532–535, 1981.

Viatcheslav F. Mukhanov, H.A. Feldman, and Robert H. Brandenberger. Theory of cosmological perturbations. Part 1. Classical perturbations. Part 2. Quantum theory of perturbations. Part 3. Extensions. *Phys.Rept.*, 215: 203–333, 1992. doi: 10.1016/0370-1573(92)90044-Z.

Kazunori Nakayama and Fuminobu Takahashi. Higgs Chaotic Inflation and the Primordial B-mode Polarization Discovered by BICEP2. 2014.

Alberto Nicolis and Riccardo Rattazzi. Classical and quantum consistency of the DGP model. *JHEP*, 0406:059, 2004. doi: 10.1088/1126-6708/2004/06/059.

Alberto Nicolis, Riccardo Rattazzi, and Enrico Trincherini. The Galileon as a local modification of gravity. *Phys.Rev.*, D79:064036, 2009. doi: 10.1103/PhysRevD.79.064036.

Nobelprize.org. Nobel Media, Web. The 2011 Nobel Prize in Physics - Press Release, August 2011. URL `http://www.nobelprize.org/nobel_prizes/physics/laureates/2011/press.html`.

Nelson J. Nunes and D.F. Mota. Structure formation in inhomogeneous dark energy models. *Mon.Not.Roy.Astron.Soc.*, 368:751–758, 2006. doi: 10.1111/j.1365-2966.2006.10166.x.

V.I Ogievetsky and I.V Polubarinov. Interacting field of spin 2 and the einstein equations. *Annals of Physics*, 35(2):167 – 208, 1965. ISSN 0003-4916. doi: http://dx.doi.org/10.1016/0003-4916(65)90077-1. URL `http://www.sciencedirect.com/science/article/pii/0003491665900771`.

Keith A. Olive. Inflation. *Phys.Rept.*, 190:307–403, 1990. doi: 10.1016/0370-1573(90)90144-Q.

M Ostrogradski. Memoires sur les equations differentielles relatives au probleme des isoperimetres mem. ac. st. petersburg, vi series, vol. 4 385517; rp woodard. *Lect. Notes Phys*, 720:403–433, 1850.

F. Pace, J.-C. Waizmann, and M. Bartelmann. Spherical collapse model in dark energy cosmologies. 2010.

T. Padmanabhan. *Structure Formation in the Universe*. Cambridge University Press, 1993. ISBN 9780521424868. URL `http://books.google.de/books?id=44gA8634YrEC`.

Don N. Page. Average entropy of a subsystem. *Phys.Rev.Lett.*, 71:1291–1294, 1993a. doi: 10.1103/PhysRevLett.71.1291.

Don N. Page. Information in black hole radiation. *Phys.Rev.Lett.*, 71:3743–3746, 1993b. doi: 10.1103/PhysRevLett.71.3743.

J.A. Peacock. *Cosmological Physics*. Cambridge Astrophysics. Cambridge University Press, 1999. ISBN 9780521422703. URL `http://books.google.de/books?id=t8O-yylU0j0C`.

J.A. Peacock and S.J. Dodds. Nonlinear evolution of cosmological power spectra. *Mon.Not.Roy.Astron.Soc.*, 280:L19, 1996. doi: 10.1093/mnras/280.3.L19.

P. J. E. Peebles. The Gravitational Instability of the Universe. *Astrophys. J.* , 147:859, March 1967. doi: 10.1086/149077.

P.J.E. Peebles and Bharat Ratra. The Cosmological constant and dark energy. *Rev.Mod.Phys.*, 75:559–606, 2003. doi: 10.1103/RevModPhys.75.559.

Víctor M. Pérez-García, Humberto Michinel, J. I. Cirac, M. Lewenstein, and P. Zoller. Dynamics of bose-einstein condensates: Variational solutions of the gross-pitaevskii equations. *Phys. Rev. A*, 56:1424–1432, Aug 1997. doi: 10.1103/PhysRevA.56.1424. URL `http://link.aps.org/doi/10.1103/PhysRevA.56.1424`.

S. Perlmutter et al. Measurements of Omega and Lambda from 42 high redshift supernovae. *Astrophys.J.*, 517:565–586, 1999. doi: 10.1086/307221.

Francesca Perrotta and Carlo Baccigalupi. On the dark energy clustering properties. *Phys.Rev.*, D65:123505, 2002. doi: 10.1103/PhysRevD.65.123505.

Francesca Perrotta, Carlo Baccigalupi, and Sabino Matarrese. Extended quintessence. *Phys.Rev.*, D61:023507, 1999. doi: 10.1103/PhysRevD.61.023507.

Valeria Pettorino and Carlo Baccigalupi. Coupled and Extended Quintessence: theoretical differences and structure formation. *Phys.Rev.*, D77:103003, 2008. doi: 10.1103/PhysRevD.77.103003.

Valeria Pettorino, C. Baccigalupi, and F. Perrotta. Scaling solutions in scalar-tensor cosmologies. *JCAP*, 0512:003, 2005. doi: 10.1088/1475-7516/2005/12/003.

Valeria Pettorino, Nico Wintergerst, Luca Amendola, and Christof Wetterich. Neutrino lumps and the Cosmic Microwave Background. *Phys.Rev.*, D82:123001, 2010. doi: 10.1103/PhysRevD.82.123001.

Massimo Pietroni. Flowing with Time: a New Approach to Nonlinear Cosmological Perturbations. *JCAP*, 0810:036, 2008. doi: 10.1088/1475-7516/2008/10/036.

Joseph Polchinski. Renormalization and Effective Lagrangians. *Nucl.Phys.*, B231:269–295, 1984. doi: 10.1016/0550-3213(84)90287-6.

Viktor Nikolayevich Popov. *Functional integrals in quantum field theory and statistical physics*, volume 8. Springer, 2001.

M. Porrati. No van Dam-Veltman-Zakharov discontinuity in AdS space. *Phys.Lett.*, B498:92–96, 2001. doi: 10.1016/S0370-2693(00)01380-0.

W. H. Press. Long Wave Trains of Gravitational Waves from a Vibrating Black Hole. *Astrophys. J. Lett.* , 170:L105, December 1971. doi: 10.1086/180849.

William H. Press and Paul Schechter. Formation of galaxies and clusters of galaxies by selfsimilar gravitational condensation. *Astrophys.J.*, 187:425–438, 1974. doi: 10.1086/152650.

Lisa C. Qian, Michael L. Wall, Shaoliang Zhang, Zhengwei Zhou, and Han Pu. Bose-einstein condensates on a ring with periodic scattering length: Spontaneous symmetry breaking and entanglement. *Phys. Rev. A*, 77: 013611, Jan 2008. doi: 10.1103/PhysRevA.77.013611. URL `http://link.aps.org/doi/10.1103/PhysRevA.77.013611`.

Miguel Quartin, Mauricio O. Calvao, Sergio E. Joras, Ribamar R.R. Reis, and Ioav Waga. Dark Interactions and Cosmological Fine-Tuning. *JCAP*, 0805:007, 2008. doi: 10.1088/1475-7516/2008/05/007.

Lisa Randall and Raman Sundrum. A Large mass hierarchy from a small extra dimension. *Phys.Rev.Lett.*, 83:3370–3373, 1999. doi: 10.1103/PhysRevLett.83.3370.

Bharat Ratra and P.J.E. Peebles. Cosmological Consequences of a Rolling Homogeneous Scalar Field. *Phys.Rev.*, D37:3406, 1988. doi: 10.1103/PhysRevD.37.3406.

Alain Riazuelo and Jean-Philippe Uzan. Cosmological observations in scalar - tensor quintessence. *Phys.Rev.*, D66:023525, 2002. doi: 10.1103/PhysRevD.66.023525.

Adam G. Riess et al. Observational evidence from supernovae for an accelerating universe and a cosmological constant. *Astron.J.*, 116:1009–1038, 1998. doi: 10.1086/300499.

S. Sadeh, Y. Rephaeli, and J. Silk. Cluster abundances and S-Z power spectra: effects of non-Gaussianity and early dark energy. *Mon.Not.Roy.Astron.Soc.*, 380:637–645, 2007. doi: 10.1111/j.1365-2966.2007.12091.x.

K. Sato. First Order Phase Transition of a Vacuum and Expansion of the Universe. *Mon.Not.Roy.Astron.Soc.*, 195:467–479, 1981.

Julian Schwinger. Brownian motion of a quantum oscillator. *Journal of Mathematical Physics*, 2(3):407–432, 1961.

Yasuhiro Sekino and Leonard Susskind. Fast Scramblers. *JHEP*, 0810:065, 2008. doi: 10.1088/1126-6708/2008/10/065.

Assaf Shomer. A Pedagogical explanation for the non-renormalizability of gravity. 2007.

E. V. Shuryak. Metastable bose condensate made of atoms with attractive interaction. *Phys. Rev. A*, 54:3151–3154, Oct 1996. doi: 10.1103/PhysRevA.54.3151. URL http://link.aps.org/doi/10.1103/PhysRevA.54.3151.

T.H.R. Skyrme. A Nonlinear field theory. *Proc.Roy.Soc.Lond.*, A260:127–138, 1961. doi: 10.1098/rspa.1961.0018.

Alexei A. Starobinsky. Spectrum of relict gravitational radiation and the early state of the universe. *JETP Lett.*, 30:682–685, 1979.

Alexei A. Starobinsky. A New Type of Isotropic Cosmological Models Without Singularity. *Phys.Lett.*, B91:99–102, 1980. doi: 10.1016/0370-2693(80)90670-X.

H.T.C. Stoof. Macroscopic quantum tunneling of a bose condensate. *Journal of Statistical Physics*, 87(5-6):1353–1366, 1997. ISSN 0022-4715. doi: 10.1007/BF02181289. URL http://dx.doi.org/10.1007/BF02181289.

H.T.C. Stoof. Coherent versus incoherent dynamics during bose-einstein condensation in atomic gases. *Journal of Low Temperature Physics*, 114 (1-2):11–108, 1999. ISSN 0022-2291. doi: 10.1023/A:1021897703053. URL http://dx.doi.org/10.1023/A%3A1021897703053.

Sandro Stringari. Bose–einstein condensation in ultracold atomic gases. *Physics Letters A*, 347(1–3):150 – 156, 2005. ISSN 0375-9601. doi: http://dx.doi.org/10.1016/j.physleta.2005.09.051. URL http://www.sciencedirect.com/science/article/pii/S0375960105015197. Einstein Special Issue Special Issue in celebration of this year's World of Physics and the centenary of Einstein's annus mirabilis Einstein Special Issue.

Andrew Strominger. Les Houches lectures on black holes. 1994.

Andrew Strominger and Cumrun Vafa. Microscopic origin of the Bekenstein-Hawking entropy. *Phys.Lett.*, B379:99–104, 1996. doi: 10.1016/0370-2693(96)00345-0.

Leonard Susskind. Addendum to Fast Scramblers. 2011.

Leonard Susskind, Larus Thorlacius, and John Uglum. The Stretched horizon and black hole complementarity. *Phys.Rev.*, D48:3743–3761, 1993. doi: 10.1103/PhysRevD.48.3743.

Gerard 't Hooft. Naturalness, chiral symmetry, and spontaneous chiral symmetry breaking. *NATO Sci.Ser.B*, 59:135, 1980.

Gerard 't Hooft. On the Quantum Structure of a Black Hole. *Nucl.Phys.*, B256:727, 1985. doi: 10.1016/0550-3213(85)90418-3.

Gerard 't Hooft. Graviton Dominance in Ultrahigh-Energy Scattering. *Phys.Lett.*, B198:61–63, 1987. doi: 10.1016/0370-2693(87)90159-6.

Ryo Takahashi and Morimitsu Tanimoto. Speed of sound in the mass varying neutrinos scenario. *JHEP*, 0605:021, 2006. doi: 10.1088/1126-6708/2006/05/021.

Gianmassimo Tasinato, Kazuya Koyama, and Gustavo Niz. Vector instabilities and self-acceleration in the decoupling limit of massive gravity. *Phys.Rev.*, D87(6):064029, 2013. doi: 10.1103/PhysRevD.87.064029.

K. S. Thorne. *Nonspherical Gravitational Collapse–A Short Review*, page 231. 1972.

Shinji Tsujikawa. Observational tests of inflation with a field derivative coupling to gravity. *Phys.Rev.*, D85:083518, 2012. doi: 10.1103/PhysRevD.85.083518.

Ron K. Unz. Path Integration and the Functional Measure. *Nuovo Cim.*, A92:397–426, 1986. doi: 10.1007/BF02730500.

Jean-Philippe Uzan. Cosmological scaling solutions of nonminimally coupled scalar fields. *Phys.Rev.*, D59:123510, 1999. doi: 10.1103/PhysRevD.59.123510.

A.I. Vainshtein. To the problem of nonvanishing gravitation mass. *Phys.Lett.*, B39:393–394, 1972. doi: 10.1016/0370-2693(72)90147-5.

H. van Dam and M.J.G. Veltman. Massive and massless Yang-Mills and gravitational fields. *Nucl.Phys.*, B22:397–411, 1970. doi: 10.1016/0550-3213(70)90416-5.

P. Van Nieuwenhuizen. On ghost-free tensor lagrangians and linearized gravitation. *Nucl.Phys.*, B60:478–492, 1973. doi: 10.1016/0550-3213(73)90194-6.

G. Veneziano. Quantum hair and the string-black hole correspondence. *Class.Quant.Grav.*, 30:092001, 2013. doi: 10.1088/0264-9381/30/9/092001.

Erik P. Verlinde. On the holographic principle in a radiation dominated universe. 2000.

G. Vidal, J. I. Latorre, E. Rico, and A. Kitaev. Entanglement in quantum critical phenomena. *Phys. Rev. Lett.*, 90:227902, Jun 2003. doi: 10.1103/PhysRevLett.90.227902. URL `http://link.aps.org/doi/10.1103/PhysRevLett.90.227902`.

CV Vishveshwara. Scattering of gravitational radiation by a schwarzschild black-hole. 1970.

Robert M. Wald. The thermodynamics of black holes. *Living Rev.Rel.*, 4:6, 2001.

Bin Wang, Jiadong Zang, Chi-Yong Lin, Elcio Abdalla, and S. Micheletti. Interacting Dark Energy and Dark Matter: Observational Constraints from Cosmological Parameters. *Nucl.Phys.*, B778:69–84, 2007. doi: 10.1016/j.nuclphysb.2007.04.037.

Li-Min Wang and Paul J. Steinhardt. Cluster abundance constraints on quintessence models. *Astrophys.J.*, 508:483–490, 1998. doi: 10.1086/306436.

Peng Wang. Virialization in dark energy cosmology. *Astrophys.J.*, 640:18–21, 2006. doi: 10.1086/500074.

S. Weinberg. Ultraviolet divergences in quantum theories of gravitation. In S. W. Hawking and W. Israel, editors, *General Relativity: An Einstein centenary survey*, pages 790–831, 1979.

Steven Weinberg. Photons and Gravitons in s Matrix Theory: Derivation of Charge Conservation and Equality of Gravitational and Inertial Mass. *Phys.Rev.*, 135:B1049–B1056, 1964. doi: 10.1103/PhysRev.135.B1049.

Steven Weinberg. Photons and gravitons in perturbation theory: Derivation of Maxwell's and Einstein's equations. *Phys.Rev.*, 138:B988–B1002, 1965. doi: 10.1103/PhysRev.138.B988.

Steven Weinberg. Critical Phenomena for Field Theorists. 1976.

Steven Weinberg. The Cosmological Constant Problem. *Rev.Mod.Phys.*, 61:1–23, 1989. doi: 10.1103/RevModPhys.61.1.

C. Wetterich. Cosmology and the Fate of Dilatation Symmetry. *Nucl.Phys.*, B302:668, 1988. doi: 10.1016/0550-3213(88)90193-9.

C. Wetterich. Growing neutrinos and cosmological selection. *Phys.Lett.*, B655:201–208, 2007. doi: 10.1016/j.physletb.2007.08.060.

Christof Wetterich. Exact evolution equation for the effective potential. *Phys.Lett.*, B301:90–94, 1993a. doi: 10.1016/0370-2693(93)90726-X.

Christof Wetterich. The average action for scalar fields near phase transitions. *Zeitschrift für Physik C Particles and Fields*, 57(3):451–469, 1993b. ISSN 0170-9739. doi: 10.1007/BF01474340. URL `http://dx.doi.org/10.1007/BF01474340`.

Christof Wetterich. The Cosmon model for an asymptotically vanishing time dependent cosmological 'constant'. *Astron.Astrophys.*, 301:321–328, 1995.

Christof Wetterich. Phenomenological parameterization of quintessence. *Phys.Lett.*, B594:17–22, 2004. doi: 10.1016/j.physletb.2004.05.008.

K.G. Wilson and John B. Kogut. The Renormalization group and the epsilon expansion. *Phys.Rept.*, 12:75–200, 1974. doi: 10.1016/0370-1573(74)90023-4.

N. Wintergerst, V. Pettorino, D.F. Mota, and C. Wetterich. Very large scale structures in growing neutrino quintessence. *Phys.Rev.*, D81:063525, 2010. doi: 10.1103/PhysRevD.81.063525.

Nico Wintergerst. Structure formation on very large scales in growing neutrino quintessence. Master's thesis, Heidelberg, Univ., Dipl., 2009, 2009. Zsfassung in dt. Sprache.

Nico Wintergerst. Evaporation of relativistic scalar field condensates. 2014.

Nico Wintergerst and Valeria Pettorino. Clarifying spherical collapse in coupled dark energy cosmologies. *Phys.Rev.*, D82:103516, 2010. doi: 10.1103/PhysRevD.82.103516.

Edward Witten. Baryons in the 1/N Expansion. *Nucl.Phys.*, B160:57, 1979. doi: 10.1016/0550-3213(79)90232-3.

Edward Witten. Anti-de Sitter space and holography. *Adv.Theor.Math.Phys.*, 2:253–291, 1998.

M.-F. Yang. Ground-state fidelity in one-dimensional gapless models. *Phys. Rev. B*, 76(18):180403, November 2007. doi: 10.1103/PhysRevB.76.180403.

Jacques Yvon. *La théorie statistique des fluides et l'équation d'état*, volume 203. Hermann & cie, 1935.

V.I. Zakharov. Linearized gravitation theory and the graviton mass. *JETP Lett.*, 12:312, 1970.

A.B. Zamolodchikov. Irreversibility of the Flux of the Renormalization Group in a 2D Field Theory. *JETP Lett.*, 43:730–732, 1986.

P. Zanardi and N. Paunković. Ground state overlap and quantum phase transitions. *Phys. Rev. E*, 74(3):031123, September 2006. doi: 10.1103/PhysRevE.74.031123.

W. H. Zurek. Decoherence, einselection, and the quantum origins of the classical. *Reviews of Modern Physics*, 75:715–775, May 2003. doi: 10.1103/RevModPhys.75.715.

Wojciech Hubert Zurek and Juan Pablo Paz. Decoherence, chaos, and the second law. *Physical Review Letters*, 72(16):2508–2511, 1994.

# Acknowledgements

My first and foremost thanks go to Gia Dvali, who has been an outstanding mentor over the past years. I am grateful for his support and guidance, for the long discussions in which he shared his deep understanding of theoretical physics, but also for the freedom that he granted me to pursue all those topics that sprang to my mind.

I wish to thank Stefan Hofmann for agreeing to be the co-examiner of this thesis, for his constant advice, and for countless inspiring discussions, on physics and everything else. I am still looking forward to writing that paper for JoH.

I am grateful to Dieter Lüst and Jochen Weller for being part of my PhD committee.

I am greatly indebted to my collaborators from whom I have learned almost everything I know about physics: Luca Amendola, Gia Dvali, Daniel Flassig, Stefan Flörchinger, Valentino Foit, Sarah Folkerts, Cristiano Germani, César Gómez, David Mota, Valeria Pettorino, Alex Pritzel, Yuki Watanabe and Christof Wetterich have shaped this work through innumerous discussions and inspiring insights. None of this would have been possible without them. In particular, I would like to thank Christof for making possible all the visits to Heidelberg, and David for hosting me in Oslo.

My great colleagues that have accompanied me over the years at the Arnold-Sommerfeld Center, Lasma, Fedor, Oscar, Matthias, Daniel, André, Tino, Sarah, Cri, Lukas, Alex G., Tobias, Alberto, Andrei, Claudius, Nina, Sophia, Korbi, Mischa, Alex, Tehseen, Constantin, Yuki and many others have made my time at the LMU truly enjoyable. Thanks for all the lunches, the coffees, the Frisbee sessions, but of course also for all the stimulating conversations.

I especially thank Daniel, Alex and Tehseen for reading and improving large parts of this thesis.

At the Arnold-Sommerfeld Center, Gabi and Herta have provided continuous help to maneuver through all possible administrative and bureaucratic labyrinths.

A special word of gratitude is due to the people that have supported me in the form of reference letters and recommendations. Thank you, Gia, Cesar, Stefan, David and Christof!

A major shoutout to my friends and flatmates, Toni, Quaschtl, Daniel, Lammo, Norbert, Matze, Janine, Philipp, Laura, Gustl, Richard, Mona, Chris, Markus and all those that I have forgotten for turning Munich into a very special place, and for providing all the indispensable distractions from work and physics. I am incredibly lucky to have met all of you.

I have thoroughly enjoyed every single of the countless hours that I spent with my teammates from PSV Wikinger München, and I am grateful for having been part of that lot. Particularly, I thank my referee partner Steven for heaps of fun times on and off the field.

My deepest gratitude goes to my family. Without their endless support, I would have never even made it close to this point. My parents have always been there for me in every possible way, and no words capture how indebted I am to them. I wish to thank my sister Anne, my brother Jakob, my grandparents Sigrid and Werner, my grandma Liesel and all the rest of my awesome family for always standing by my side.

The final lines of this thesis are dedicated to my amazing girlfriend Paulina. For her constant encouragement and unlimited support, for her loyalty and friendship, and for continuously reminding me of what is truly important in life, I wish to thank her with all my heart. I can't wait to see what the future holds in line for us.